

**THERAPEUTIC APPLICATIONS OF CERAMIDE LIPIDS FOR
APOPTOSIS INDUCTION**

by

JENNIFER A. SHABBITS

B.Sc. (Biochemistry), Simon Fraser University, 1997

A THESIS SUBMITTED IN PARTIAL FULFILLMENT OF THE REQUIREMENTS
FOR THE DEGREE OF

DOCTOR OF PHILOSOPHY
(Pharmaceutical Sciences)

in

THE FACULTY OF GRADUATE STUDIES

Faculty of Pharmaceutical Sciences
Department of Pharmaceutics and Biopharmaceutics

We accept this thesis as conforming to the required standard

THE UNIVERSITY OF BRITISH COLUMBIA

April, 2003

© Jennifer A. Shabbits, 2003

In presenting this thesis in partial fulfilment of the requirements for an advanced degree at the University of British Columbia, I agree that the Library shall make it freely available for reference and study. I further agree that permission for extensive copying of this thesis for scholarly purposes may be granted by the head of my department or by his or her representatives. It is understood that copying or publication of this thesis for financial gain shall not be allowed without my written permission.

Department of Pharmaceutical Sciences

The University of British Columbia
Vancouver, Canada

Date April 16/03

ABSTRACT

The emerging role of ceramide lipids in apoptosis and an increased understanding of their involvement in multidrug resistance (MDR) has revealed new opportunities for manipulating ceramide levels in order to achieve specific therapeutic objectives. The research presented in this thesis focused on the relationship between ceramide, MDR and apoptosis. Direct and indirect approaches for modulating intracellular ceramide levels were investigated in an attempt to chemosensitize MDR tumors and induce apoptosis.

Inhibition of pro-apoptotic ceramide conversion to its non-cytotoxic glucosylceramide metabolite was shown to sensitize two human MDR breast cancer cell lines to the cytotoxic effects of tubulin-binding chemotherapy drugs. Enhanced sensitization was correlated with increased ceramide, suggesting that therapeutic manipulations aimed at increasing endogenous ceramide should promote apoptosis.

On the basis of these results, the feasibility of delivering therapeutic amounts of exogenous ceramides to cells was then investigated. After evaluating different chain length ceramides it was determined that synthetic C₆-ceramide was internalized and cytotoxic to cells whereas naturally occurring C₁₆-ceramide was neither internalized nor cytotoxic. This difference established the importance of intracellular delivery as a prerequisite to apoptosis induction by exogenous ceramides. Liposome-based delivery systems were then introduced in an attempt to overcome the limitations associated with intracellular delivery of natural ceramide. Physically stable liposomes containing up to 50 mole percent C₁₆-ceramide in the lipid bilayer were successfully formulated. These liposomes were internalized by J774 macrophage cells *in vitro* and induced apoptosis with similar potency to free C₆-ceramide.

In order to translate this encouraging data to an *in vivo* model it was first necessary to evaluate the behavior of these liposomes in the circulation. Pharmacokinetic studies demonstrated *in vivo* stability over 24 hours following iv bolus administration. The antitumor activity of these liposomes was then evaluated in the J774 ascites tumor model. Optimal antitumor activity was observed following intraperitoneal administration of C₁₆-ceramide liposomes on days 1, 5, and 9. This corresponded to a statistically significant increase in animal survival of 43.5% over non-ceramide control liposomes. Taken together, this research provides evidence for the rational design of ceramide-based liposomes as a novel approach for cancer chemotherapy.

TABLE OF CONTENTS

ABSTRACT	ii
TABLE OF CONTENTS	iv
LIST OF FIGURES	viii
LIST OF TABLES	xii
LIST OF ABBREVIATIONS	xiii
ACKNOWLEDGEMENTS	xvii
DEDICATION	xviii
 CHAPTER 1: INTRODUCTION	 1
1.1 THE MULTIDRUG RESISTANCE PHENOMENON	1
1.1.1 Overview of Multidrug Resistance in Cancer and Clinical Significance	1
1.1.2 Mechanisms of MDR	2
1.1.2.1 Transport-based MDR	3
1.1.2.2 Enzyme-related MDR	6
1.1.2.3 Tumor microenvironment	7
1.1.2.4 Alterations in apoptosis pathways	8
1.1.2.5 Alterations in ceramide metabolism	10
1.2 MODULATION OF MULTIDRUG RESISTANCE	11
1.2.1 MDR Modulation by Drug Transport Inhibitors	12
1.2.2 Apoptosis Pathways	15
1.2.2.1 Apoptosis induction and execution via the death receptor (extrinsic) pathway	18
1.2.2.2 Apoptosis induction and execution via the mitochondrial (intrinsic) pathway	19
1.2.2.3 The degradation phase of apoptosis: common effector caspases	21
1.2.3 MDR Modulation Strategies Related to Apoptosis Pathways	21
1.2.3.1 Downregulation of anti-apoptotic signals to chemosensitize tumors	21
1.2.3.2 Upregulation of pro-apoptotic signals	23
1.2.3.3 Modulation of ceramide metabolism	23
1.3 CERAMIDE LIPIDS AS INTRACELLULAR SIGNALING MOLECULES	24
1.3.1 Structure and Metabolism of Ceramide Lipids	25
1.3.2 Biological Targets of Ceramide Lipids and their Role in Apoptosis	28
1.3.3 Ceramide Signaling via Lipid Rafts	32
1.4 LIPOSOMAL DRUG DELIVERY SYSTEMS	33
1.4.1 Review of Liposomes	34
1.4.1.1 Liposome preparation and classification	36
1.4.1.2 Lipid composition	39
1.4.1.3 Lipid polymorphism	45

1.4.2	Liposomes as Drug Carriers	47
1.4.2.1	Passive encapsulation	47
1.4.2.2	Active encapsulation	49
1.4.3	Drug Delivery Approaches to MDR Modulation	50
1.4.3.1	Application of liposomes to MDR reversal	50
1.4.3.2	Application of liposomes to the delivery of bioactive lipids	53
1.5	THESIS OBJECTIVES AND HYPOTHESIS	53
CHAPTER 2: THE ROLE OF 1-PHENYL-2-DECANOYLAMINO-3-MORPHOLINO-1-PROPANOL (PDMP) AND P-GLYCOPROTEIN IN MODULATING CERAMIDE-MEDIATED SENSITIVITY OF HUMAN BREAST CANCER CELLS TO TUBULIN-BINDING ANTICANCER DRUGS		55
2.1	Introduction and Rationale	55
2.2	Hypothesis	56
2.3	Materials and Methods	57
2.3.1	Materials	57
2.3.2	Cell lines and culture	58
2.3.3	Evaluation of cell surface Pgp expression by flow cytometry	58
2.3.4	Evaluation of intracellular Pgp expression by fluorescence microscopy	59
2.3.5	MTT cytotoxicity assays	60
2.3.6	[³ H]Taxol [®] uptake studies	60
2.3.7	Cell radiolabeling and lipid extraction	61
2.3.8	Lipid detection by thin layer chromatography (TLC)	62
2.3.9	Statistical analysis	62
2.4	Results	62
2.4.1	Chemosensitization effects of PDMP in human breast cancer cells	62
2.4.2	Influence of exogenous C ₆ -ceramide on PDMP-induced chemosensitization	72
2.4.3	Effect of Pgp inhibition on PDMP-induced chemosensitization	72
2.4.4	Correlation of chemosensitization effects with glucosylceramide levels	73
2.5	Discussion	77
CHAPTER 3: INTRACELLULAR DELIVERY OF EXOGENOUS CERAMIDE LIPIDS INDUCES APOPTOSIS IN VITRO		82
3.1	Introduction and Rationale	82
3.2	Hypothesis	83
3.3	Materials and Methods	83
3.3.1	Materials	83
3.3.2	Cell lines and culture	84
3.3.3	MTT cytotoxicity assays	84
3.3.4	Lipid uptake studies	84
3.3.5	Spectrophotometric protein quantitation	85
3.3.6	Preparation of liposomes	86

3.3.7	Lactose trapping	87
3.3.8	Cryo-transmission electron microscopy	87
3.4	Results	88
3.4.1	The effect of ceramide acyl chain length on <i>in vitro</i> cytotoxicity in MDA435/LCC6 cells	88
3.4.2	Correlation of MTT cytotoxicity results with ceramide uptake	90
3.4.3	Formulation and cytotoxicity of C ₆ -ceramide containing liposomes in MDA435/LCC6 cells	92
3.4.4	Formulation and cytotoxicity of C ₁₆ -ceramide containing liposomes in MDA435/LCC6 cells	95
3.4.5	Cytotoxicity of free and liposomal ceramide in J774 murine macrophage cells	105
3.5	Discussion	112

CHAPTER 4: DEVELOPMENT OF AN IN VITRO EXCHANGE ASSAY TO ACCURATELY PREDICT THE LIPID AND DRUG RETENTION PROPERTIES OF LIPOSOME-BASED DELIVERY SYSTEMS 118

4.1	Introduction and Rationale	118
4.2	Hypothesis	121
4.3	Materials and Methods	121
4.3.1	Materials	121
4.3.2	Preparation of donor large unilamellar vesicles (LUVs)	122
4.3.3	Preparation of acceptor multilamellar vesicles (MLVs)	122
4.3.4	Separation of LUV and MLV populations	123
4.3.5	Liposomal encapsulation of doxorubicin	124
4.3.6	Liposomal encapsulation of verapamil	124
4.3.7	Ceramide lipid/drug release from liposomes using dialysis assays	125
4.3.8	Ceramide lipid/drug release from liposomes using the MLV-based exchange assay	125
4.3.9	<i>In vivo</i> ceramide lipid/drug release	126
4.4	Results	126
4.4.1	Design of the MLV-based exchange assay procedure	126
4.4.2	Separation of control and ceramide-containing donor LUV and acceptor MLV populations	128
4.4.3	Evaluation of C ₆ -ceramide retention using conventional <i>in vitro</i> dialysis assays	130
4.4.4	Evaluation of C ₆ -ceramide retention following i.v. bolus administration	130
4.4.5	Evaluation of C ₆ -ceramide retention using the MLV-based <i>in vitro</i> assay	133
4.4.6	Evaluation of C ₁₆ -ceramide retention using the MLV-based <i>in vitro</i> assay	136
4.4.7	Evaluation of the MLV-based assay as a measure of liposomally encapsulated conventional drug release	136

4.5	Discussion	142
CHAPTER 5: PHARMACOKINETIC EVALUATION AND ANTITUMOR ACTIVITY OF HIGH CERAMIDE CONTENT LIPOSOMES		145
5.1	Introduction and Rationale	145
5.2	Hypothesis	146
5.3	Materials and Methods	146
5.3.1	Materials	146
5.3.2	Cell line and culture	146
5.3.3	Preparation of liposomes	147
5.3.4	Pharmacokinetic analysis of control and ceramide liposomes	147
5.3.5	Establishment of the J774 ascites tumor model	148
5.3.6	Evaluation of antitumor activity	150
5.3.7	Statistical analysis	150
5.4	Results	150
5.4.1	Pharmacokinetic analysis of control and ceramide liposomes following i.v. bolus administration	150
5.4.2	Evaluation of antitumor activity of ceramide liposomes in the J774 ascites tumor model	154
5.5	Discussion	159
CHAPTER 6: SUMMARY OF RESULTS AND FUTURE DIRECTIONS		163
REFERENCES		170

LIST OF FIGURES

Figure 1.1	A schematic illustration of apoptosis pathways highlighting the inter-relationships between key apoptotic proteins	17
Figure 1.2	The chemical structures of a natural and synthetic ceramide lipid	25
Figure 1.3	Sphingolipid metabolic pathways illustrating the various routes of ceramide synthesis and breakdown	27
Figure 1.4	A schematic illustration of a hypothetical multifunctional liposome	34
Figure 1.5	An illustration of spontaneous bilayer formation upon hydration of amphipathic lipids in an aqueous buffer	37
Figure 1.6	Schematic illustrations and scanning electron micrographs of the three main liposome classes	38
Figure 1.7	The general structure of a phospholipid depicting some commonly occurring headgroups and fatty acid moieties	40
Figure 1.8	The chemical structures of cholesterol and cholesteryl hemisuccinate lipids	43
Figure 1.9	A schematic illustration of a pegylated liposome showing the chemical structure of polyethylene glycol derivatized phosphatidylethanolamine (PEG-PE)	44
Figure 1.10	Drug distribution following active and passive encapsulation for hydrophobic and hydrophilic drugs	48
Figure 2.1	Cell surface P-glycoprotein expression in wild-type and multidrug resistant MCF7 and MDA435/LCC6 breast cancer cells as shown by flow cytometry	65
Figure 2.2	Fluorescence microscopy images of wild-type and multidrug resistant MCF7 and MDA435/LCC6 cells following two-step staining with mouse anti-human Pgp C219 primary and goat anti-mouse IgG FITC secondary antibodies	66
Figure 2.3	The effect of 5 μ M PDMP on Taxol [®] and vincristine cytotoxicity in wild-type and multidrug resistant MCF7 cells	68
Figure 2.4	The effect of 5 μ M PDMP on Taxol [®] and vincristine cytotoxicity in wild-type and multidrug resistant MDA435/LCC6 cells	69

Figure 2.5	Accumulation of [³ H]Taxol [®] in wild-type and multidrug resistant MCF7 and MDA435/LCC6 cells	71
Figure 2.6	A model to explain the influence of Pgp on ceramide metabolism in the context of chemosensitization	81
Figure 3.1	Cytotoxicity of various acyl chain length free ceramide lipids on wild-type and <i>mdr-1</i> gene transfected MDA435/LCC6 human breast cancer cells	89
Figure 3.2	Cellular uptake of free C ₆ - and C ₁₆ -ceramide by wild-type and <i>mdr-1</i> gene transfected MDA435/LCC6 cells	91
Figure 3.3	Mean liposome vesicle diameter for C ₆ -cer/DSPC/Chol (45:10:45) and DSPC/Chol (55:45) liposomes as determined by quasi-elastic light scattering	93
Figure 3.4	Cytotoxicity of control and C ₆ -ceramide liposomes on wild-type and <i>mdr-1</i> gene transfected MDA435/LCC6 human breast cancer cells	94
Figure 3.5	Cellular uptake of [³ H]CHE liposome and [¹⁴ C]C ₆ -ceramide radiolabels by wild-type and <i>mdr-1</i> gene transfected MDA435/LCC6 human breast cancer cells	96
Figure 3.6	Mean liposome vesicle diameter for C ₁₆ -cer/DSPC/Chol (15:40:45) containing liposomes as determined by quasi-elastic light scattering	99
Figure 3.7	Cytotoxicity of C ₁₆ -cer/DSPC/Chol (15:40:45) and control DSPC/Chol (55:45) liposomes on wild-type and <i>mdr-1</i> gene transfected MDA435/LCC6 human breast cancer cells	100
Figure 3.8	Cellular uptake of C ₁₆ -cer/DSPC/Chol (15:40:45) liposomes by wild-type and <i>mdr-1</i> gene transfected MDA435/LCC6 cells	101
Figure 3.9	Mean liposome vesicle diameter for C ₁₆ -cer/CHEMS (50:50) and control DPPC/CHEMS (50:50) liposomes as determined by quasi-elastic light scattering	103
Figure 3.10	Cryo-transmission electron micrographs of DPPC/CHEMS/PEG ₂₀₀₀ -DSPE (49.5:49.5:1) and C ₁₆ -cer/CHEMS/PEG ₂₀₀₀ -DSPE (49.5:49.5:1) liposomes	104
Figure 3.11	Cytotoxicity of C ₁₆ -cer/CHEMS and DPPC/CHEMS liposomes on wild-type and <i>mdr-1</i> gene transfected MDA435/LCC6 human breast cancer cells	106

Figure 3.12	Cellular uptake of C ₁₆ -cer/CHEMS (50:50) liposomes by wild-type and <i>mdr-1</i> gene transfected MDA435/LCC6 cells	107
Figure 3.13	Cytotoxicity of various acyl chain length free ceramide lipids on J774 murine macrophage cells	109
Figure 3.14	Cytotoxicity of C ₁₆ -cer/CHEMS and DPPC/CHEMS liposomes on J774 cells	110
Figure 3.15	Cellular uptake of [³ H]CHE and [¹⁴ C]C ₁₆ -ceramide labeled C ₁₆ -cer/CHEMS liposomes by J774 cells	111
Figure 4.1	A schematic illustration of the <i>in vitro</i> MLV-based assay	127
Figure 4.2	Profile of C ₆ -ceramide release from C ₆ -cer/DSPC/Chol/PEG ₂₀₀₀ -DSPE (15:10:40:5) donor LUVs following dialysis against HBS or HBS + 30% FBS for 24 hours at 37°C	131
Figure 4.3	Circulation profile of C ₆ -ceramide and bulk liposomal lipid following i.v. bolus administration of C ₆ -cer/DSPC/Chol/PEG ₂₀₀₀ -DSPE (15:10:40:5) liposomes to female Balb/c mice	132
Figure 4.4	Profile of C ₆ -ceramide release from C ₆ -cer/DSPC/Chol/PEG ₂₀₀₀ -DSPE (15:10:40:5) donor LUVs using the MLV-based exchange assay	134
Figure 4.5	Profile of C ₁₆ -ceramide release from C ₁₆ -cer/CHEMS (50:50) donor LUVs using the MLV-based exchange assay	137
Figure 4.6	Release profiles of doxorubicin and verapamil from liposomes as measured by dialysis assays, the <i>in vitro</i> MLV-based assay, or from plasma collected following i.v. bolus liposome administration	141
Figure 5.1	Correlation plots comparing observed and predicted log plasma concentration versus time graphs for control and ceramide liposomes modeled using a one-compartment, i.v. bolus dosing model in WinNonlin 1.1.	149
Figure 5.2	Plasma elimination profile of control (DPPC/CHEMS/PEG ₂₀₀₀ -DSPE, 47.5/47.5/5) and ceramide-based (C ₁₆ -cer/CHEMS/PEG ₂₀₀₀ -DSPE, 47.5/47.5/5) liposomes following i.v. bolus administration to female Balb/c mice	152
Figure 5.3	Evaluation of antitumor activity of C ₁₆ -cer/CHEMS/PEG ₂₀₀₀ -DSPE (47.5:47.5:5) versus DPPC/CHEMS/PEG ₂₀₀₀ -DSPE (47.5:47.5:5)	

	liposomes administered i.v. on days 1, 5, and 9 in the J774 ascites tumor model	156
Figure 5.4	Evaluation of antitumor activity of C ₁₆ -cer/CHEMS/PEG ₂₀₀₀ -DSPE (47.5:47.5:5) versus DPPC/CHEMS/PEG ₂₀₀₀ -DSPE (47.5:47.5:5) liposomes administered i.p. on day 1 in the J774 ascites tumor model	157
Figure 5.5	Evaluation of antitumor activity of C ₁₆ -cer/CHEMS/PEG ₂₀₀₀ -DSPE (47.5:47.5:5) versus DPPC/CHEMS/PEG ₂₀₀₀ -DSPE (47.5:47.5:5) liposomes administered i.p. on days 1, 5, and 9 in the J774 ascites tumor model	158

LIST OF TABLES

Table 1.1	Anticancer drugs and drug classes typically associated with the MDR phenomenon	2
Table 1.2	Major mechanisms of multidrug resistance	3
Table 1.3	Third-generation MDR modulators	14
Table 1.4	Molecular shape of various lipids and their associated structures	45
Table 2.1	The effect of 5 μ M PDMP, 1 μ g/ml Valspodar and 2 μ M C ₆ -ceramide on anticancer drug cytotoxicity in wild-type and multidrug resistant MCF7 and MDA435/LCC6 breast cancer cells	64
Table 2.2	The effect of Pgp blockade on the degree of PDMP-induced chemosensitization in MCF7/AdrR and MDA435/LCC6 ^{MDR1} cells as measured by a sensitization ratio	74
Table 2.3	Incorporation of [³ H]palmitic acid into ceramide and glucosylceramide of treated and control MCF7 cells	76
Table 3.1	Cytotoxicity of various acyl chain length free ceramide lipids in wild-type and resistant MDA435/LCC6 human breast cancer cells	90
Table 3.2	Summary table describing various C ₁₆ -ceramide containing liposome formulations attempted and their respective characteristics	98
Table 4.1	Separation of empty [³ H]-LUV donor and [¹⁴ C]-MLV acceptor vesicles by centrifugation	129
Table 4.2	Correlation coefficient (r) and coefficient of determination (r ²) for ceramide lipid, doxorubicin or verapamil release from liposomes as measured by the dialysis and MLV-based assays relative to actual <i>in vivo</i> results	135
Table 4.3	Separation of doxorubicin or verapamil-loaded [³ H]-LUV donor and [¹⁴ C]-MLV acceptor populations by centrifugation	140
Table 5.1	Summary of plasma pharmacokinetic parameters for control and C ₁₆ -ceramide containing liposomes following i.v. bolus administration at a dose of 100 mg/kg total lipid	153

LIST OF ABBREVIATIONS

5FU	5-Fluorouracil
ABC	ATP-binding cassette
Abs	Absorbance
ADR	Adriamycin
AIC	Akaike Information Criterion
AIF	Apoptosis inducing factor
ANOVA	Analysis of variance
Apaf-1	Apoptotic protease activating factor-1
Ara-C	Cytosine arabinoside
AS-ODN	Antisense oligonucleotide
ATP	Adenosine triphosphate
AUC	Area under the curve
BSA	Bovine serum albumin
C ₁₀ -cer	N-decanoyl-D-erythrosphingosine
C ₁₄ -cer	N-myristoyl-D-erythrosphingosine
C ₁₆ -cer	N-palmitoyl-D-erythrosphingosine
C ₂ -cer	N-acetoyl-D-erythrosphingosine
C ₆ -cer	N-hexanoyl-D-erythrosphingosine
C ₈ -cer	N-octanoyl-D-erythrosphingosine
C _{max}	Peak plasma concentration achieved
CAD	Caspase-activated DNase
CAPK	Ceramide activated protein kinase
CAPP	Ceramide activated protein phosphatase
Cer	Ceramide
CHE	Cholesteryl hexadecyl ether
CHEMS	Cholesteryl hemisuccinate
Chol	Cholesterol
CL	Plasma clearance
CO ₂	Carbon dioxide
Cryo-TEM	Cryo-transmission electron microscopy

CsA	Cyclosporin A
Cyt c	Cytochrome c
Da	Daltons
DABCO	1,4-Diazobicyclo-(2,2,2)octane
DAPI	4',6-Diamidino-2-phenylindole
dATP	Deoxyadenosine triphosphate
DD	Death domain
DED	Death effector domain
DDF	DNA fragmentation factor
dH ₂ O	Demineralized water
Diablo	Direct IAP binding protein with low pI
DISC	Death-inducing signaling complex
DMEM	Dulbecco's modified eagle's medium
DOPE	Dioleoylphosphatidylethanolamine
DOTAP	1,2-Dioleoyl-3-trimethylammonium propane
DPM	Disintegrations per minute
DPPC	Dipalmitoylphosphatidylcholine
DSPC	Disteroylphosphatidylcholine
EDTA	Ethylenediaminetetraacetic acid
EPC	Egg phosphatidylcholine
FBS	Fetal bovine serum
FITC	Fluorescein isothiocyanate
GCS	Glucosylceramide synthase
GlcCer	Glycosylceramide
GSH	Glutathione
GSL	Glycosphingolipid
GST	Glutathione-S-transferase
HBS	Hepes buffered saline
i.p.	Intraperitoneal
i.v.	Intravenous
IAP	Inhibitors of apoptosis

IC ₂₀	Concentration required to achieve 20% cell kill
IC ₅₀	Concentration required to achieve 50% cell kill
ILS	Increase in lifespan
J774	Murine-derived macrophage cell line
kDa	Kilodaltons
KSR	Kinase suppressor of Ras
LUV	Large unilamellar vesicle
MCF7	Human breast carcinoma, sensitive (wild-type)
MCF7/AdrR	Human breast carcinoma, MDR (selected for adriamycin resistance)
MDA435/LCC6	Human breast carcinoma, sensitive (wild-type)
MDA435/LCC6 ^{MDR1}	Human breast carcinoma, MDR (transfected with <i>mdr-1</i>)
MDR	Multidrug resistance
<i>mdr-1</i>	Multidrug resistance gene encoding P-glycoprotein
MLV	Multilamellar vesicle
MRP	Multidrug resistance associated protein
MTT	3-(4,5-dimethylthiazol-2-yl)-2,5-diphenyl tetrazolium bromide
NOE	N-oleoylethanolamine
PARP	Poly ADP ribose polymerase
PBS	Phosphate buffered saline
PBSB	PBS + 0.1% BSA
PBSBT	PBSB + 0.5% Tween-20
PC	Phosphatidylcholine
PDMP	1-Phenyl-2-decanoylamino-3-morpholino-1-propanol
PPMP	1-Phenyl-2-hexanoylamino-3-morpholino-1-propanol
PE	Phosphatidylethanolamine
PEG	Polyethylene glycol
Pgp	P-glycoprotein
PI	Phosphatidylinositol
PKB	Protein kinase B
PKC	Protein kinase C

PP1	Protein phosphatase 1
PP2A	Protein phosphatase 2A
PPMP	1-Phenyl-2-hexadecanoylamino-3-morpholino-1-propanol
PPPP	1-phenyl-2- hexadecanoylamino-3-pyrrolidino-1-propanol
PS	Phosphatidylserine
PSC 833	Cyclosporin D analog (Valspodar)
PT	Permeability transition
RES	Reticuloendothelial system
ROS	Reactive oxygen species
S1P	Sphingosine-1-phosphate
SAPK	Stress activated protein kinase
SD	Standard deviation
SEM	Standard error of the mean
SM	Sphingomyelin
Smac	Second mitochondria-derived activation of caspases
SMase	Sphingomyelinase
SR	Sensitization ratio
SUV	Small unilamellar vesicle
$t_{1/2}$	Plasma elimination half-life
TNF	Tumor necrosis factor
TNF-R	TNF receptor
TRAIL	TNF-related apoptosis inducing ligand
TRAIL-R	TRAIL receptor
V_d	Volume of distribution
XIAP	X-linked inhibitor of apoptosis

ACKNOWLEDGEMENTS

First and foremost I am grateful to my supervisor Lawrence for his constant support and guidance, for helping me to become a scientist, and for also allowing me to become a teacher.

I am also grateful to Marcel for creating such a unique and special lab environment. I feel very lucky to have been a part of such a wonderful research family.

Thank you to the members of A.T. past for passing on your words of wisdom and for proving that there really is an end!

Thank you to the members of A.T. present for creating such a great environment for work (and lots of play!). From lunches at the GGW to Drag Queen night at the Odessey, you made it fun to come to work.

Thank you also to my family for giving me a lifetime of love and support, and for always encouraging me to do my best.

And last but not least, thank you to Mike - my husband and best friend - for your unwavering love and understanding, and for always believing that one day this thesis would finally be complete.

DEDICATION

To my family.

CHAPTER 1

INTRODUCTION

1.1 THE MULTIDRUG RESISTANCE PHENOMENON

Multidrug resistance (MDR) is a major obstacle to the effective treatment of cancer. Despite vast improvements in our understanding of the mechanisms of drug resistance, the ability to modulate MDR has been complicated by the fact that many human tumors simultaneously exhibit multiple resistance mechanisms. This section provides an overview of MDR and its major mechanisms, and introduces the rationale underlying the studies described in this thesis to utilize ceramide manipulations to sensitize tumors to chemotherapy.

1.1.1 Overview of Multidrug Resistance in Cancer and Clinical Significance

Each year approximately 1.5 million new cases of cancer are reported in North America (1). While many of these will respond favorably to initial treatment with conventional chemotherapeutic regimens, the ultimate success in achieving long-term tumor regression or cures is frequently limited by the development of drug resistance. Drug resistant cancers are either inherently untreatable (intrinsic resistance), or they have progressed to develop resistance to a wide variety of anticancer agents over the course of treatment due to selection pressures caused by repeated drug administration (acquired resistance). The term multidrug resistance is used to describe the ability of tumor cells exposed to a single cytotoxic agent to develop resistance to a broad range of structurally and functionally unrelated drugs. Table 1.1 lists some anticancer drugs and their classes that are typically associated with MDR.

Table 1.1
Anticancer Drugs and Drug Classes Typically Associated with the MDR Phenomenon

<i>Anthracyclines</i>	<i>Taxanes</i>	<i>Vinca Alkaloids</i>	<i>Epipodophyllotoxins</i>	<i>Other</i>
Doxorubicin	Paclitaxel	Vincristine	Etoposide	Tamoxifen
Daunorubicin	Docetaxel	Vinblastine	Teniposide	Mitomycin
Epirubicin		Vinorelbine		Dactinomycin
Idarubicin				
Mitoxantrone				

The clinical significance of this phenomenon is highlighted by estimations that up to one-third of all new cases of cancer each year in North America will eventually exhibit characteristics consistent with MDR. Clearly then, the development of systems which successfully modulate drug resistance *in vivo* will be invaluable in treating patients with previously non-responsive tumors.

1.1.2 Mechanisms of MDR

There are numerous mechanisms that contribute to the MDR phenomenon. The classical mechanism is decreased intracellular drug accumulation caused by drug efflux protein pumps that are often overexpressed in MDR tumors. Although drug transport is the best characterized resistance mechanism studied to date, several other mechanisms are also known to be involved. For example, increased DNA repair and alterations at the level of drug target enzymes have been implicated in drug resistance. In addition, specific features of the tumor microenvironment have been shown to contribute to resistance in many cell types. Since most chemotherapy approaches ultimately elicit their effects via apoptosis (programmed cell death), alterations at the level of apoptosis control provide yet another mechanism by which drug resistance may occur. The various classes

of cellular mechanisms that have been shown to contribute to MDR, which are summarized in Table 1.2, are briefly described below.

Table 1.2
Major Mechanisms of Multidrug Resistance

Drug Transport Based	Enzyme Related	Tumor Microenvironment	Apoptosis Control
Pgp	↑ DNA Repair	Vasculature-related	Bcl-2 family
MRP1	↑ GSH Conjugation	Hypoxia	p53
	Altered Topoisomerases	↓ pH	IAP
			Ceramide

1.1.2.1 Transport-based MDR

Two members of the ATP-Binding Cassette (ABC) superfamily of membrane transport ATPases, P-glycoprotein (Pgp) and multidrug resistance-associated protein (MRP1), have been shown to act as primary mediators of intracellular drug transport-based MDR. When overexpressed in malignant cells they serve to actively efflux anticancer drugs out of cells, resulting in reduced cellular drug accumulation and decreased cytotoxicity (2). Their involvement in MDR has been corroborated by observations that the extent of drug resistance correlates with the amount of Pgp and/or MRP1 expression (3), and introduction of these proteins into previously non-resistant tumor cells via gene transfection confers the MDR phenotype (4, 5).

P-Glycoprotein

The most well characterized mechanism of transport-based MDR involves the ABC family member Pgp, a 170 kDa transmembrane protein encoded by the *mdr-1* gene (6, 7). P-glycoprotein is tandemly duplicated with two homologous halves, each of which spans the membrane 6 times and contains an ATP binding domain (8). It is

believed that drugs which bind to Pgp are actively effluxed out of the cell via the transmembrane portion of the protein, utilizing the energy supplied by Pgp-controlled ATP hydrolysis. Several mechanisms have been put forward to explain this transport function of Pgp. The "flippase" model postulates that Pgp encounters xenobiotics in the inner leaflet of the plasma membrane and flips the agents to the outer leaflet where they diffuse into the extracellular space (9). In the "hydrophobic vacuum cleaner" model proposed by Gottesman and Pastan (10) it is suggested that Pgp interacts directly with substrates in the plasma membrane via specific drug binding domains and pumps them out of the cell in an energy-dependent manner. Substrates for Pgp comprise a broad spectrum of agents including anthracyclines, vinca alkaloids, epipodophyllotoxins and taxanes.

P-glycoprotein is expressed in many healthy tissues such as the liver, kidney, colon, small intestine and in specialized endothelial cells of the brain (reviewed in (11)). The identification of Pgp in normal tissues led to the establishment of its role as a protective mechanism in the transport and excretion of xenobiotics. In particular, the observation that Pgp is expressed in the brain suggests a role in the blood-brain barrier to prevent the permeation of drugs into the central nervous system. Whereas Pgp fulfills critical functions in transport processes involved in normal physiology, overexpression of this protein in tumor cells results in reduced intracellular accumulation of anticancer agents to sub-therapeutic levels through increased drug efflux. Direct evidence of Pgp-mediated drug transport came from initial studies employing partially purified membrane vesicles in which it was demonstrated that vesicles prepared from resistant cells were more capable of binding and transporting radiolabeled vinblastine than those prepared

from sensitive cells (12). Overexpression of Pgp in many tumors has since been correlated with poor response to anticancer drug therapy and subsequent shorter survival in many clinical studies (13). In particular, a large study of patients with acute non-lymphoblastic leukemia revealed a strong correlation between Pgp detection at the time of diagnosis and a lower rate of complete regression after intensive chemotherapy, in addition to shorter patient survival (14). Similar correlations have been made for sarcomas (15) and neuroblastoma (16). Although Pgp is implicated in a number of multidrug resistant phenotypes, it does not completely explain the MDR phenomenon.

Multidrug Resistance-Associated Protein (MRP)

In the early 1990's another ABC family member, called the multidrug resistance-associated protein (MRP1), was found to confer multidrug resistance through altered drug transport. This protein was first identified in a drug resistant lung cancer cell line that was found not to overexpress Pgp (17). Multidrug resistance-associated protein is a 190 kDa transmembrane glycoprotein that contains 17 potential membrane-spanning domains (18). It requires reduced cellular glutathione (GSH) for its function as a drug efflux pump (19), since it primarily transports drugs as glutathione or glucuronic acid conjugates (20). As with Pgp, MRP1 is expressed in normal human tissues such as muscle, lung, spleen and gall bladder (21), where it is believed to play a role in the excretion of organic anion drug conjugates. Overexpression of MRP1 has been observed in a number of human tumors exhibiting the MDR phenotype, including lung cancer (22) and leukemias (23), and its overexpression is frequently correlated with poor clinical outcome (24, 25).

1.1.2.2 Enzyme-related MDR

DNA Repair Enzymes

Generally speaking, cell death via apoptosis (discussed in detail in Section 1.2.2) occurs when cellular damage exceeds the capacity of internal repair mechanisms. Since DNA is the primary target of many anticancer drugs, increased activity of DNA repair mechanisms reduces drug-induced damage and cytotoxicity. For example, upregulation of enzymes involved in the nucleotide excision repair pathway remove platinum-DNA adducts caused by cisplatin treatment and thus constitute a major cause of cisplatin resistance (26, 27). Increased activity of the O⁶-alkyl-guanine transferase enzyme removes O⁶-methylguanine, a common product of treatment with alkylating agents, which leads to resistance to this class of chemotherapeutic agents (28, 29). Other examples of MDR mediated by DNA repair enzymes include increased repair of single strand DNA breaks and early onset of DNA repair (reviewed in (30)).

Glutathione S-Transferase (GST)

Glutathione mediated detoxification pathways play an important role in eliminating chemotherapeutic agents from the body. Glutathione S-transferase is an enzyme system that conjugates reduced glutathione to organic molecules in order to produce polar compounds that are readily excretable. These enzymes are important in the biotransformation and detoxification of many anticancer agents. Overexpression of GST enzymes and increased intracellular levels of GSH, both of which contribute to the drug resistance by promoting anticancer drug inactivation and elimination, have been noted in many resistant cell lines (31, 32).

Topoisomerase Activity

DNA topoisomerases are enzymes that catalyze changes in DNA topology required for replication to occur. They act by causing either transient single (topoisomerase I) or double (topoisomerase II) strand breaks that facilitate DNA strand unwinding (33). Under physiological conditions these covalent enzyme-DNA cleavage complexes are short-lived intermediates that are well tolerated by the cell. Many anticancer agents (doxorubicin, etoposide, teniposide) exert their effects by stabilizing the DNA-enzyme complex, thus preventing DNA re-ligation from occurring. The resulting strand breaks then trigger apoptosis. Resistance to chemotherapy drugs acting in this manner can arise when the activity or quantity of these enzymes is reduced or when the enzyme is mutated to disfavor drug binding.

1.1.2.3 Tumor microenvironment

Features of the tumor microenvironment can also contribute to MDR. Vasculature structure, vascular distribution and blood flow in malignant tumors are intrinsically different from those in normal tissues (34), and this can lead to decreased delivery of cytotoxic agents to the tumor site. The growth of blood vessels in tumors is irregular and the vasculature is often poorly formed and disorganized (35). Furthermore, the extracellular environment exhibits increased interstitial fluid pressure due to higher vascular permeability and the absence of a functional lymphatic system (36). These factors all contribute to decreased drug access to tumor cells and can lead to tumor regions which are oxygen deficient and nutrient deprived. The nutritional state of cells is known to directly influence the cellular uptake, metabolism and toxicity of some anticancer drugs (37). Nutrient deprived cells tend to proliferate slowly and the increased

presence of non-cycling cells renders tumors resistant to drugs that act via anti-proliferative mechanisms. Hypoxic cells produce lactic acid, which creates an acidic tumor environment that further inhibits cell proliferation. This has been suggested to confer a resistance mechanism for drug- and radiation-based therapies that are most active against rapidly dividing cells (34). An acidic tumor environment has also been suggested to confer a resistance mechanism for weak base drugs such as doxorubicin, whose cellular uptake is dependent on ionization state (38).

1.1.2.4 Alterations in apoptosis pathways

Chemotherapeutic agents are generally believed to elicit their cytotoxic effects through the process of apoptosis, a form of programmed cell death (39, 40). The decision as to whether a cell undergoes apoptosis or continues to progress through the cell cycle is dependent upon the interplay between a complex set of genes and proteins that interact to regulate cell cycle progression. Drug resistance can emerge if cells alter the expression of proteins that regulate the propagation of signals arising from cellular insults such as chemotherapy to protect against apoptosis. While the apoptotic pathway is still not completely understood, several proteins are known to be important regulators of this process.

Bcl-2 Family

The process of cellular apoptosis is regulated in part by the Bcl-2 family of proteins. Most notably, apoptosis is stimulated by expression of pro-apoptotic Bax and Bak, and is inhibited by expression of anti-apoptotic Bcl-2. Whether or not apoptosis occurs is regulated by hetero- and homodimerization of the Bax, Bak and Bcl-2 proteins. Overexpression of Bcl-2 or downregulation of Bax or Bak (all of which result in

increased Bcl-2 homodimer formation) has been correlated with decreased sensitivity to a wide range of chemotherapeutic agents and the emergence of resistance (41, 42). The mechanism by which this occurs will become apparent in Section 1.2.3 where mitochondria-regulated apoptosis is discussed. In addition, the apoptosis antagonists Bcl-X_L and Mcl-1 are also emerging as potential contributors to the MDR phenomenon. Overexpression of Bcl-X_L has been demonstrated to confer a multidrug resistance phenotype in some cancers (43, 44); however, the role of Mcl-1 in drug resistance is less clear.

p53 Tumor Suppressor

The tumor suppressor gene p53 appears to play a significant role in tumorigenesis, and several studies have found that p53 mutation correlates with aggressive tumor growth and recurrence (45). Its importance in cancer is highlighted by the fact that it is mutated in more than fifty percent of all human tumors (46). DNA damage, hypoxia, activation of oncogenes or loss of function of other tumor suppressor genes result in p53 accumulation (47), which either triggers cell cycle arrest in G₁ so that the damage may be repaired or, if the extent of damage is deemed too great, it will direct the cell to undergo apoptosis (48). The integrity of this cellular defense mechanism is crucial for maintenance of an intact genome and, therefore, p53 is often referred to as the “guardian of the genome” (49, 50). Consequently, loss of p53 function, either through direct mutation of the p53 gene itself or via regulators of p53 function, results in disregulated cell growth, the accumulation of mutations and promotes genetic instability—all of which may contribute to MDR.

Inhibitor of Apoptosis (IAP) Family

Inhibitors of apoptosis proteins (IAPs) are a family of proteins that were first discovered in baculoviruses as apoptosis suppressors (51). Six IAP relatives have been identified in humans (reviewed in (52)). The mechanism used by IAPs to inhibit cell death is unclear, although there is evidence to suggest that several of the IAPs bind to pro-caspases and prevent them from being activated (53, 54) (described in Section 1.2.2). The ratio of caspases to IAPs likely determines whether a cell undergoes apoptosis, and alterations in this ratio may contribute to MDR. The IAP *survivin* is highly expressed in various malignant tissues and has been correlated with poor clinical outcome in some cases (reviewed in (55)). Overexpression of *X-linked IAP (XIAP)* has been associated with drug resistance in various pre-clinical animal models and was found to have adverse prognostic significance for patients with acute myeloid leukemias (56).

1.1.2.5 Alterations in Ceramide Metabolism

The sphingolipid breakdown product *ceramide* has recently become the subject of considerable interest as an intracellular signaling molecule. The mechanisms of ceramide generation and its intracellular effects are discussed in detail in Section 1.3; the focus of this section will be on the specific relationship between ceramide lipids and MDR.

Ceramide is recognized as a mediator of apoptosis and as a co-ordinator of cellular responses to stress (57). Intracellular ceramide levels have been shown to increase following exposure to many chemotherapy drugs (reviewed in (58)) and ionizing radiation (59), and cells subsequently exhibit morphologies typical of apoptosis (50, 60). Several studies have demonstrated that alterations in ceramide metabolism, whereby intracellular ceramide levels decrease and cells accumulate the non-apoptotic ceramide

metabolite *glucosylceramide* (GlcCer), contribute to the development of multidrug resistance (61-65). In this scenario, although intracellular ceramide is generated by chemotherapeutic agents or other stimuli, apoptosis-inducing threshold levels of ceramide are not achieved due to its rapid conversion to GlcCer. Indeed, a number of drug resistant cancer cell lines show higher levels of GlcCer than their drug sensitive counterparts (61), and analysis of clinical tumor specimens from patients who failed conventional chemotherapy revealed higher GlcCer levels than samples taken from those patients who responded well to treatment (66). The level of activity of the glucosylceramide synthase (GCS) enzyme, which converts ceramide to GlcCer, is believed to be responsible for this aspect of the MDR phenotype. This was demonstrated by retroviral transfection of GCS into drug sensitive MCF7 human breast cancer cells. The resulting MCF7/GCS cell line expressed an 11-fold higher level of GCS, which correlated to an 11-fold increase in resistance to doxorubicin (67). Lipid metabolism studies further demonstrated that exposure of these cells to the cytokine TNF- α , which is known to generate intracellular ceramide, caused an increase in ceramide in the drug sensitive MCF7 cells and an increase in GlcCer in the MCF7/GCS cells. These findings suggest that increases in GCS activity and the resulting accumulation of intracellular GlcCer are important to the development of drug resistance in cancer cells.

1.2 MODULATION OF MULTIDRUG RESISTANCE

The complex nature of the MDR-related drug transport, drug metabolism and apoptosis pathways described above have presented researchers and clinicians with many

potential targets to pursue in an effort to promote and/or restore apoptosis signaling in resistant cells. Some of these strategies are described in the following section.

1.2.1 MDR Modulation by Drug Transport Inhibitors

Identification of the molecular basis for MDR and studies of the effects of Pgp on anticancer drugs resulted in the identification of the first generation of agents that could reverse or modulate MDR *in vitro* by directly inhibiting the drug efflux activity of Pgp. These modulators included pharmaceutical agents such as the calcium channel blocker verapamil (68), the calmodulin inhibitor prochlorperazine (69), and the immunosuppressant cyclosporin A (70, 71). This chemosensitization approach involved co-administration of the MDR modulator with an anticancer drug in an attempt to block Pgp-mediated anticancer drug efflux and increase intracellular anticancer drug accumulation. Although these first-generation modulating agents demonstrated potent MDR reversal activity when combined with anticancer agents *in vitro*, the doses required to achieve plasma concentrations adequate to reverse MDR *in vivo* (both pre-clinically and clinically) resulted in significant toxicities arising from the modulators' inherent pharmacological activities (72). For example, whereas a 2-6 μM plasma verapamil concentration is required to modulate MDR, the plasma concentration at which cardiovascular effects are observed is within the range of 0.4-1.2 μM (73). These complications highlighted the need to develop modulating agents with lower inherent toxicity and increased potency, and through these efforts a second-generation of MDR modulators was discovered.

Second-generation modulating agents largely comprised stereoisomers or structural analogs of the first generation drugs. These included dexverapamil and PSC 833 (Valspodar), a non-immunosuppressive analog of cyclosporin A. Dexverapamil was shown to reverse MDR to a degree equivalent to verapamil but without cardiovascular toxicities in several animal models (74). The use of Valspodar has resulted in considerable improvements in antitumor activity in ascites and solid MDR tumor models (reviewed in (75)), and is the modulating agent in the most advanced stage of development. Phase III clinical trials combining Valspodar with various anticancer agents have been conducted and improved responses to chemotherapy have been observed (76-79). Generally speaking, however, co-administration of the second generation modulators with anticancer drugs results in exacerbated anticancer drug toxicity due to altered anticancer drug pharmacokinetic and biodistribution properties (reviewed in (80)). This has been attributed to the blockade of Pgp and other membrane transporters in non-tumor tissues, and the resulting increase in anticancer drug exposure of healthy tissues has necessitated dose reduction in many studies (81), potentially compromising therapy via reduced tumor accumulation of the anticancer agent. Examples of such pharmacokinetic interactions include an 8-fold increase in plasma area under the curve (AUC) for the anticancer drug daunorubicin when combined with verapamil in rats (82), and an 8-fold increase in liver, kidney and intestinal vincristine accumulation was observed in mice following co-administration of verapamil and vincristine (83). Co-administration of Valspodar with doxorubicin in mice was shown to result in a 2-fold increase in C_{max} and a 10-fold increase in AUC, which was associated with increased toxicity (84). These complications have given rise to third-generation

modulating agents that have since been developed in an attempt to avoid such pharmacokinetic interactions.

Third-generation modulating agents with increased Pgp specificity have been largely designed through combinatorial chemistry approaches. This was done in anticipation of improved therapeutic response and reduced toxicity compared to first- and second-generation modulators. They are highly potent and can reverse MDR at extremely low concentrations, typically in the nanomolar range. Some examples of third-generation modulating agents are presented in Table 1.3. Although these newer agents appear to be active against their targets and well tolerated in combination with anticancer drugs, it remains to be seen whether they will be sufficient to achieve therapeutically effective MDR reversal in the clinic. The lack of specificity for action on tumor Pgp remains an inherent disadvantage, and alternative methods to improve the selectivity of MDR modulation at the tumor site may offer a significant advantage.

Table 1.3

Third-Generation MDR Modulators

Agent	Target	Company	Stage	Notes of Interest	Refs
LY335979	PGP	Eli Lilly	Phase I	<ul style="list-style-type: none"> latent modulating activity does not alter the PK of doxorubicin or etoposide 	(85)
XR9576	PGP	Xenova	Phase I , II	<ul style="list-style-type: none"> does not alter the PK of Taxol[®] no increase in toxicity of co-administered anticancer drugs 	(86, 87)
OC144-093	PGP	Ontogen	Phase I	<ul style="list-style-type: none"> no increase in toxicity of co-administered doxorubicin or paclitaxel 	(88)
GF120918	PGP	Glaxo	Phase I	<ul style="list-style-type: none"> no increase in toxicity of co-administered doxorubicin increases doxorubicinol levels 	(89, 90)
VX710 (Biricodar)	PGP & MRP	Vertex	Phase I , II	<ul style="list-style-type: none"> allows potentially efficacious plasma concentrations of paclitaxel to be achieved at lower doses 	(91-93)

1.2.2 Apoptosis Pathways

Although MDR is a multifactorial phenomenon, a lack of cellular apoptosis is the ultimate result regardless of the mechanism(s) involved. It will therefore be instructive to review the key pathways involved in the apoptotic response in order to understand how MDR modulation strategies may be designed to overcome biochemical alterations that lead to reduced apoptosis.

Apoptosis is an important cellular process that serves to maintain normal tissue homeostasis by regulating a delicate balance between cell death and cell proliferation. Apoptosis is characterized by blebbing of the plasma membrane, externalization of the membrane lipid phosphatidylserine (PS), nuclear condensation, DNA cleavage into approximately 200 base-pair fragments and the formation of apoptotic bodies that contain self-enclosed fragments of the nucleus surrounded by cytoplasm and a cell membrane. Since the plasma membrane remains intact, the process of apoptosis does not trigger an inflammatory response and cells are rapidly engulfed by phagocytic cells such as macrophages. These features stand in contrast to the characteristics of necrosis, the prevailing form of cell death resulting from a non-specific injury such as blunt trauma, exposure to a toxin, or a loss of blood supply. In necrosis, cells undergo swelling and eventual rupture, and the release of cytoplasmic contents then triggers a pronounced inflammatory response (94).

The apoptotic process can be divided into three major phases. During the induction phase cells receive and process diverse external stimuli which are integrated by the cell and a decision whether or not to commit to apoptosis is made. If the signals warrant apoptosis, cells enter the execution phase, during which the apoptotic pathways

become activated. Two basic pathways define the execution phase of apoptosis – the death receptor pathway (also known as the extrinsic pathway), and the mitochondrial pathway (often referred to as the intrinsic pathway), which are described in detail below. Apoptosis culminates with the degradation phase, in which the hallmarks of apoptosis become evident.

Many of the biochemical and morphological features typical of apoptosis result from the selective proteolytic cleavage of cellular proteins mediated by a family of proteins known as caspases (cysteine proteases with specificity for aspartate residues: cysteine aspartate-specific proteases). They are synthesized as dormant pro-enzymes that require proteolytic processing to become active (95-97). Caspases may cleave and activate other caspase family members or they may act on non-caspase targets, including proteins of the DNA repair system such as poly ADP ribose polymerase (PARP), and cytoskeletal and structural proteins such as laminin B1 and β -actin (94, 98).

Although diverse stimuli can initiate apoptosis, common biochemical and morphological alterations are observed in the degradative phase, independent of the initial stimulus. This suggests that the apoptotic signals ultimately converge on common effector pathways prior to degradation. A schematic illustration of the apoptosis machinery and processes that will be discussed in this section is presented in Figure 1.1.

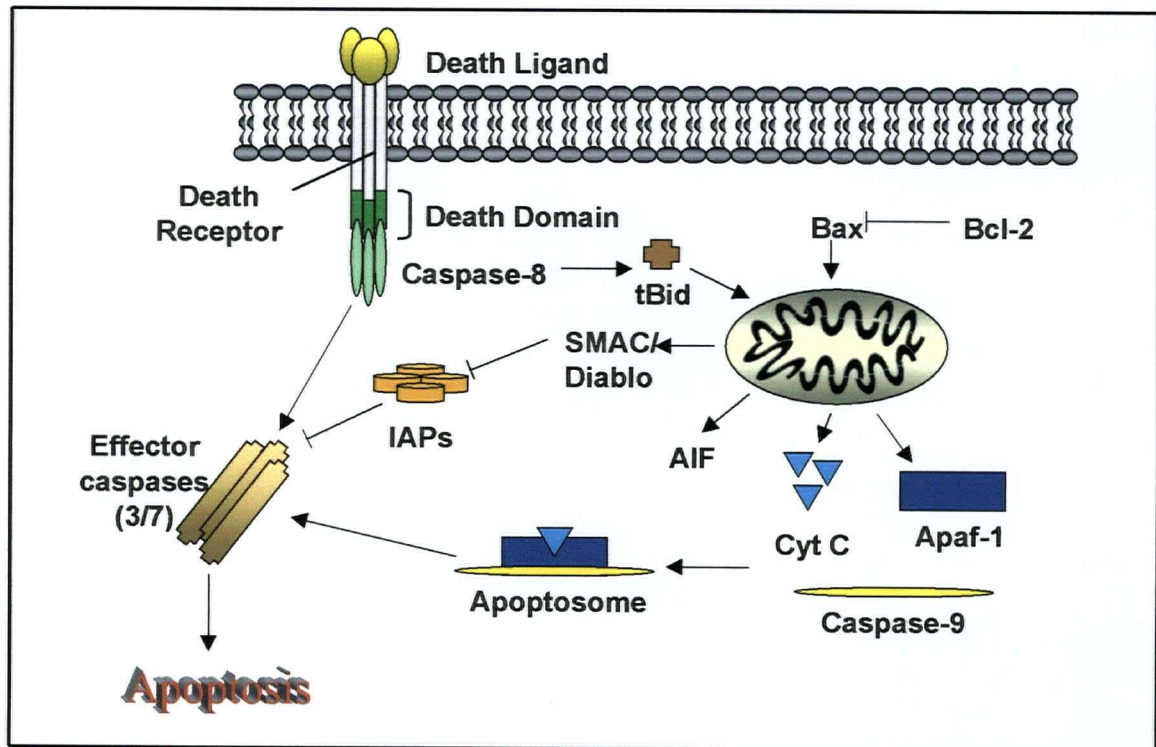


Figure 1.1 A schematic illustration of apoptosis pathways highlighting the inter-relationships between key apoptotic proteins (adapted from Herr *et al.*, (99)). Abbreviations used: IAP, inhibitor of apoptosis; SMAC/Diablo, second mitochondria-derived activation of caspases/direct IAP binding protein with low pI; AIF, apoptosis inducing factor; cyt c, cytochrome c; Apaf-1, apoptotic protease activating factor-1.

1.2.2.1 Apoptosis induction and execution via the death receptor (extrinsic) pathway

Apoptosis signaling through the death receptor pathway is typically initiated by cytokine binding to cell-surface receptors, of which members of the tumor necrosis factor (TNF) receptor superfamily are understood in the greatest detail. This family of receptors includes the Fas (CD95/Apo-1) receptor which binds Fas ligand (Fas-L), the TNF receptor (TNF-R, p55) which binds the TNF α ligand, and the TRAIL (TNF-related apoptosis inducing ligand) receptor (TRAIL-R) which binds the TRAIL ligand (94). The Fas/Fas-L system is the most well characterized and will be described here to illustrate the intracellular cascade of events in the death receptor mediated pathway.

Activation of death receptors leads to apoptosis through a cascade of protein-protein interactions. The cytoplasmic domain of the Fas receptor contains an interaction motif known as the death domain (DD). Binding of Fas-L to the Fas receptor causes trimerization of the DDs, which in turn initiates the recruitment of adaptor molecules such as FADD (Fas-associated protein with death domain; also known as MORT-1) (100). FADD molecules interact with the receptor via common DDs at one end, while the other end of FADD molecules contains death effector domains (DEDs) that interact with DEDs in pro-caspase-8 molecules. The complex of Fas-L/Fas-R, FADD and pro-caspase-8 forms the death-inducing signaling complex (DISC). Once assembled, the DISC triggers the rapid self-activation of caspase-8. Activated caspase-8 can then act via two different mechanisms: in so called Type I cells caspase-8 directly activates the effector caspases-3, -6 and -9 (101). In Type II cells, however, the amount of caspase-8 that is generated is not sufficient to activate effector caspases and apoptosis instead proceeds through an amplification cascade involving mitochondrial dysfunction. This is

initiated by caspase-8 induced cleavage of the cytoplasmic protein Bid, whose C-terminal fragment (tBid) translocates to the mitochondria to activate the mitochondrial pathway of apoptosis (97).

1.2.2.2 Apoptosis induction and execution via the mitochondrial (intrinsic) pathway

In contrast to the death receptor pathway, which is activated by a relatively small number of structurally related ligands, the mitochondrial pathway can be induced by a wide variety of unrelated agents, including UV and gamma irradiation, chemotherapeutic drugs, reactive oxygen species (ROS) and environmental stresses such as growth factor withdrawal or heat. Apoptosis signaling through the mitochondrial pathway is initiated by release of cytochrome c from the inner mitochondrial membrane space.

Several models have been proposed to explain the process by which mitochondrial outer membrane permeability occurs and cytochrome c release occurs (95, 102). One theory depends on the phenomenon known as the mitochondrial permeability transition (PT) and the formation of a PT pore. The PT pore is a non-selective channel that forms at contact sites between the inner and outer mitochondrial membranes. Opening of the PT pore can be triggered by physiological effectors such as Ca^{2+} , ROS or changes in pH, and this results in a sudden increase in the permeability of the inner mitochondrial membrane to molecules with a molecular weight of less than 1.5 kDa. The PT event results in loss of mitochondrial membrane potential, osmotic swelling of the matrix and ultimate disruption of the outer membrane (103). An alternative theory relies on the translocation of proteins/molecules to the mitochondria and the formation of pores large enough for the passage of soluble proteins such as cytochrome c. Proposed pore-forming molecules include ceramide lipids (104-106) and the pro-apoptotic Bcl-2 family

members Bax and Bak, whose transcription is upregulated by activated p53 in response to DNA damage (94). Bax and Bak are believed to translocate from the cytoplasm to the outer mitochondrial membrane, possibly mediated by the tBid protein generated via the death receptor pathway, where they oligomerize to form pores that mediate cytochrome c release (reviewed in (95, 102)). To relate these events to the phenomenon of MDR, anti-apoptotic Bcl-2 proteins have been demonstrated to inhibit Bax translocation to the mitochondria, thus preventing cytochrome c release and subsequent apoptosis activation. Whether or not apoptosis proceeds is regulated by a delicate balance between these pro- and anti-apoptotic Bcl-2 family members. Thus, overexpression of the Bcl-2 protein can tip the balance in favour of cell survival despite the presence of apoptotic initiating stimuli such as anticancer drugs.

Once in the cytoplasm, cytochrome c facilitates assembly of the “apoptosome” by binding Apaf-1 (apoptotic protease activating factor-1) and ATP or dATP. The apoptosome activates pro-caspase-9 (107), which in turn activates caspase-3 (108). Other molecules that are released from the mitochondria include apoptosis inducing factor (AIF) (109), which is believed to translocate to the nucleus where it induces caspase-independent DNA fragmentation (110) and may also directly activate caspase-3 (111), and SMAC/Diablo (second mitochondria-derived activator of caspases/direct IAP binding protein with low pI), which is believed to displace XIAP from pro-caspase-9, permitting its activation (112). In this scenario MDR can arise if overexpression of XIAP renders SMAC/Diablo unable to facilitate the activation of caspase-9.

1.2.2.3 The degradation phase of apoptosis – common effector caspases

Activation of both the death receptor and mitochondrial pathways culminate with activation of caspase-3 which, along with caspase-6 and -9, form the common effector caspases (113). These caspases are responsible for cleavage of a variety of protein substrates that disable critical cellular processes and break down structural components of the cell. These include activation of a DNA fragmentation factor (DFF) which is responsible for internucleosomal DNA cleavage (114), activation of CAD (caspase-activated DNase), cleavage of nuclear lamins involved in chromatin condensation and nuclear shrinkage, cleavage of cytoskeletal proteins such as actin, which leads to cell fragmentation and plasma membrane blebbing (111), and ultimate cell death.

1.2.3 MDR Modulation Strategies Related to Apoptosis Pathways

An increased understanding of the proteins and pathways involved in apoptosis signaling, combined with evidence that many anticancer agents induce their cytotoxic effects via apoptosis (39, 40), has spawned great interest in developing approaches to chemosensitize tumors by altering apoptosis regulation. Some of these strategies are described below.

1.2.3.1 Downregulation of anti-apoptotic signals to chemosensitize tumors

Pre-clinical and clinical trials are currently underway to evaluate the effectiveness of antisense oligonucleotide (AS-ODN) technologies directed against various anti-apoptotic proteins in sensitizing MDR tumors. The most common approach to increase apoptotic susceptibility has been to down-regulate expression of apoptosis antagonists

using AS-ODN that block mRNA expression of the targeted protein in a nucleotide sequence specific manner. To date, the Bcl-2 family of proteins has received the most attention in this regard. Numerous studies have investigated the effect of Bcl-2 AS-ODN on drug sensitivity and several clear examples of true chemosensitization have been documented (115-117). A pre-clinical study in mice bearing Bcl-2 overexpressing human B-cell lymphoma showed complete cures in all mice following treatment with Bcl-2 antisense + low dose cyclophosphamide (118). Clinical trials with Genasense™ (Genta Inc.) Bcl-2 antisense are currently underway to investigate its effectiveness in combination with several different anticancer drugs. Preliminary phase I trial data in patients with relapsed and refractory lymphoma showed *in vivo* decreases in Bcl-2 protein levels and some antitumor activity (115). A phase I/II clinical study investigating Genasense™ + dacarbazine showed several antitumor responses in patients with resistant malignant melanoma (119). Although still in the pre-clinical stages of testing, similar approaches are aimed at downregulating IAP family members using antisense gene therapy strategies. For example, downregulation of XIAP has been shown to induce apoptosis in chemoresistant ovarian cancer cells (120). Anti-survivin antisense was able to downregulate survivin levels, which corresponded to complete chemosensitization of acute lymphoblastic leukemia cells to doxorubicin (121), and complete eradication of tumors derived from mouse thymic lymphoid tumors was observed in response to survivin antisense therapy (122).

1.2.3.2 Upregulation of pro-apoptotic signals

Gene therapy approaches to introduce the normal p53 gene back into tumor cells in which it has been mutated have been investigated, and efficacy has been observed in tissue culture and animal models (123, 124).

On the basis of observations that decreases in intracellular ceramide levels via conversion to GlcCer result in reduced apoptosis and the emergence of drug resistance, efforts to raise intracellular levels of pro-apoptotic ceramide by exogenous administration of the lipid or its sphingomyelin (SM) precursor have been explored. Addition of exogenous cell-permeable ceramide lipid enhanced the activity of paclitaxel in a human T-cell leukemia cell line (125). Co-administration of SM with the anticancer drug 5-fluorouracil (5FU) resulted in significant tumor growth inhibition in an HT29 human colonic tumor xenograft mouse model (126). Follow-up work by this group demonstrated similar antitumor activity of SM in combination with both 5FU and irinotecan using other models of colon cancer (127). These results have been attributed to the enhancement of apoptotic cell death by increasing the intracellular pool of SM that is available for conversion to pro-apoptotic ceramide.

1.2.3.3 Modulation of ceramide metabolism

The identification of GCS activity and GlcCer levels as markers for drug resistant tumors provided a new avenue for therapies directed at overcoming MDR. A number of studies have demonstrated that inhibition of GlcCer synthesis results in MDR circumvention. Liu *et al.* demonstrated that downregulation of GCS activity in doxorubicin resistant MCF7/AdrR cells by transfection with GCS antisense resulted in a 30% reduction in GCS activity, which was correlated with a 28-fold increase in

doxorubicin sensitivity (128). Other approaches have used GlcCer analogs such as 1-phenyl-2-decanoylamino-3-morpholino-1-propanol (PDMP) (129-131), a specific inhibitor of GCS. Combined treatment of sub-lethal concentrations of PDMP with Taxol[®] or vincristine fully sensitized resistant neuroblastoma cells to the cytotoxic effects of these agents (132). Research presented in Chapter 2 extends this observation to human breast cancer cell lines and proposes an additional role for Pgp in this response (133). Both PDMP and its analog 1-phenyl-2-hexadecanoylamino-3-pyrrolidino-1-propanol (PPPP) showed preferential killing of three MDR human carcinoma cell lines (134). In another approach, cytotoxicity of the novel synthetic retinoid fenretinide was found to be enhanced by modulators of ceramide metabolism such as dihydrosphingosine (safingol) and 1-phenyl-2-hexadecanoylamino-3-morpholino-1-propanol (PPMP), and synergistic relationships were observed in neuroblastoma, lung, melanoma, prostate, colon and pancreatic cancer cell lines (135). Furthermore, pharmacologic suppression of acid ceramidase by N-oleoylethanolamine (NOE) restored ceramide accumulation and sensitivity to cytokine-induced apoptosis in fibroblasts (136), and was demonstrated to increase endogenous ceramide levels and trigger apoptosis in resistant, metastatic colon cancer cells (137).

1.3 CERAMIDE LIPIDS AS INTRACELLULAR SIGNALING MOLECULES

From the preceding sections it is apparent that ceramide lipids are of particular therapeutic interest because of their role in apoptosis induction and their involvement in both the emergence and circumvention of MDR. These observations prompted the work discussed in this thesis, in which specific strategies to modulate ceramide levels in favour

of apoptosis were investigated. Before describing this work, however, it will be instructive to review the general biology of ceramide lipids.

1.3.1 Structure and Metabolism of Ceramide Lipids

Ceramides comprise a group of cellular lipids characterized by a sphingosine base linked to a variable length fatty acid by means of an amide linkage (Figure 1.2). Ceramides are typically classified based on the length of the fatty acid moiety. Natural ceramides isolated from mammalian membranes have acyl chain lengths that typically vary from 16 to 24 carbon atoms (C_{16} - C_{24} -ceramide) (138, 139). These are generally regarded as long-chain or endogenous ceramides and are among the most hydrophobic lipids in nature. They are found ubiquitously in the stratum corneum (140) where they have a central role in maintaining the water impermeability of the skin.

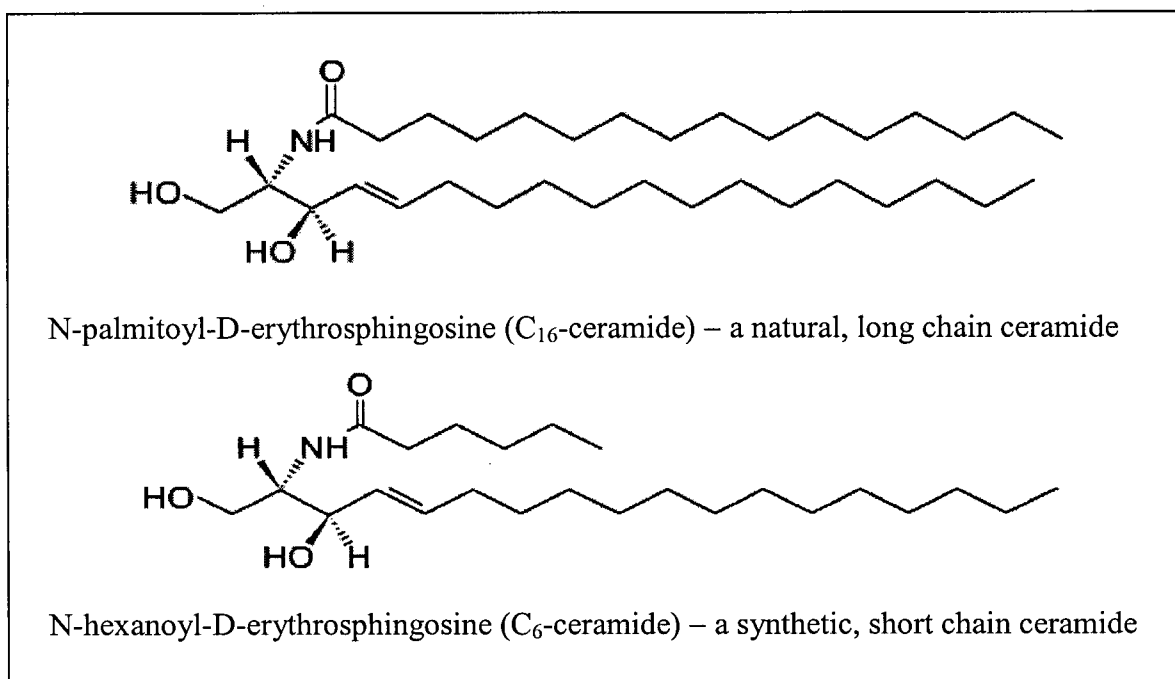


Figure 1.2 The chemical structures of a natural and synthetic ceramide lipid. Both C_6 - and C_{16} -ceramide were extensively used in this thesis.

Ceramide constitutes the hydrophobic backbone of all the complex sphingolipids such as sphingomyelin, cerebroside and gangliosides. Consequently, it has a central role in sphingolipid metabolism (Figure 1.3). Ceramide homeostasis is controlled by several inter-related pathways that regulate its synthesis and metabolism. Ceramide synthesis via the multi-step *de novo* synthetic pathway begins with the condensation of serine and palmitoyl-CoA by serine palmitoyltransferase to form 3-ketosphinganine, which is subsequently reduced to sphinganine. The addition of an amide-linked fatty acid by dihydroceramide synthase yields dihydroceramide. A desaturase enzyme introduces the 4-*trans* double bond to produce ceramide. These reactions take place on the cytosolic surface of the endoplasmic reticulum. Alternatively, ceramide may be generated by activation of intracellular sphingomyelinase (SMase) enzymes that catalyze the hydrolysis of the membrane lipid sphingomyelin to ceramide and phosphocholine. Several isoforms of SMase have been identified to date and these are distinguished by pH optima and subcellular localization (141, 142). Acid SMase (aSMase) is localized in endosomes and lysosomes (143) and possibly caveolae (144), and displays a pH optimum of 4.5. A secreted form of aSMase has also been identified (145). There also exist several neutral SMases (nSMase) (144, 146) located in the plasma membrane, cytosol, endoplasmic reticulum and nuclear membranes. Activation of aSMase versus nSMase occurs differently in response to different stimuli (147). An alkaline SMase has been identified in intestinal cells (148), although it is believed to function specifically in the metabolic degradation of dietary sphingomyelin and does not appear to have a major role in cell signaling.

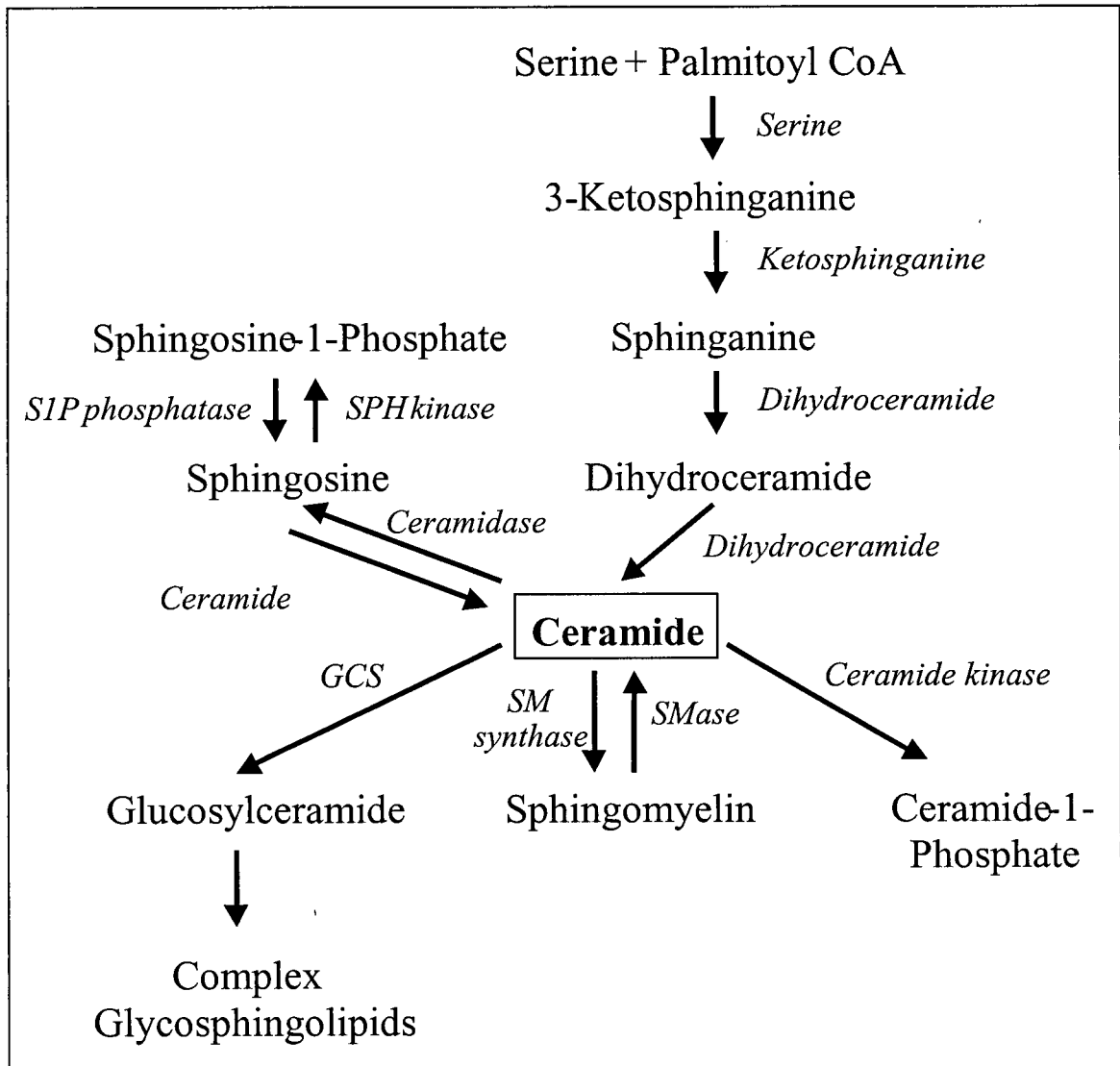


Figure 1.3 Sphingolipid metabolic pathways illustrating the various routes of ceramide synthesis and breakdown. Abbreviations used: SM, sphingomyelin; SMase, sphingomyelinase; GCS, glucosylceramide synthase; SPH, sphingosine; SIP, sphingosine-1-phosphate

Ceramide breakdown proceeds primarily through the action of ceramidase enzymes that catabolize ceramide to sphingosine. Three classes of mammalian ceramidases have been identified and are again classified according to their subcellular localization and pH optima. Acid ceramidase is lysosomal (149), neutral ceramidase is mitochondrial (150), and alkaline ceramidase is found in the Golgi and endoplasmic reticulum (151). Sphingosine, in turn, can be converted to sphingosine-1-phosphate (S1P) via sphingosine-1-kinase. Sphingosine-1-phosphate is also emerging as an important regulator of apoptosis. It mediates proliferation and mitogenesis and tends to oppose the pro-apoptotic effects of ceramide. In this regard the ceramide/S1P-rheostat model proposes that the balance between intracellular ceramide and S1P levels determines cell fate (152). Alternatively, ceramide may be metabolized to GlcCer, as described previously, which serves as a precursor to numerous glycolipids and gangliosides.

1.3.2 Biological Targets of Ceramide Lipids and their Role in Apoptosis

Although ceramide lipids were once believed to play a primarily structural role in cellular membranes, it has become increasingly apparent that they also have important roles as regulators of cell function. In particular, the role for ceramide in mediating growth suppression and apoptosis has received significant attention. The production of ceramide is associated with numerous stress stimuli and thus, generation of ceramide has been suggested to be a universal feature of apoptosis. Several lines of evidence support this contention. Among these are observations that many cytokines (153-155) and environmental stresses (59, 156) known to initiate apoptosis induce rapid endogenous ceramide generation. Ionizing radiation and cytosine arabinoside (Ara-C) also elicit their

apoptotic effects through generation of intracellular ceramide via SM hydrolysis. The Fas receptor pathway may be responsible for aSMase-generated ceramide (157), and this mechanism has been shown to mediate doxorubicin-induced apoptosis (158). Acid SMase deficient mice are resistant to radiation (159) and Fas-induced apoptosis (160), the latter of which could be restored by addition of exogenous C₁₆-ceramide. On the basis of correlations between apoptosis and changes in intracellular ceramide levels, it has been suggested that C₁₆-ceramide in particular functions as the endogenous second messenger in apoptosis (161). The chemotherapeutic agents paclitaxel, etoposide and the vinca alkaloids also elicit their apoptotic effects in part by ceramide generated via the de novo pathway (58), which can be blocked by the ceramide synthesis inhibitor fumonisins B1 (162). Moreover, treatment of tumor cells with ceramidase inhibitors increases endogenous ceramide levels and results in apoptosis (137). The addition of exogenous, cell-permeable ceramides has also been shown to induce apoptosis in many cell lines (153, 154, 157). These effects are very specific, as the metabolic precursor dihydroceramide, which differs only in the lack of 4-5 trans double bond, does not induce apoptosis although its uptake and metabolism are similar to that of ceramide (163). In addition, the examples of MDR reversal achieved by modulating endogenous ceramide levels previously described further support an important role for ceramide in apoptosis induction. The production of ceramide is thus emerging as an important component of apoptosis, and many mediators of apoptosis described in previous sections have been demonstrated to be both regulators of ceramide generation and downstream targets of ceramide action.

Ceramide presumably exerts its effects through direct molecular interactions with specific target molecules that, in turn, activate further signaling cascades. However, the exact nature of these targets and details of the downstream signaling events are not fully understood. Several direct targets have been identified, however, including phosphatases, proteases and kinases. Ceramide is known to activate serine/threonine phosphatases of the protein phosphatase-1 and -2A (PP1 and PP2A) families, which are collectively termed CAPP (ceramide activated protein phosphatases). Activation of CAPP promotes growth suppression via dephosphorylation of the pro-growth cellular regulators PKC α , PKB, Bcl-2 and the retinoblastoma protein Rb (164, 165). Ceramide is also known to activate ceramide activated protein kinase (CAPK; also known as KSR - kinase suppressor of Ras) which phosphorylates Raf-1 and in turn activates the MAP kinase pathway. This pathway culminates with inactivation of PKB, whose kinase activity maintains the pro-apoptotic Bcl-2 family member Bad in the inactive form. Therefore, ceramide mediated inactivation of PKB promotes Bad-triggered cell death (166). Endosomal/lysosomal cathepsin D has also been identified as a ceramide binding protein, and it is believed that ceramide produced in this compartment induces release of the protease into the cytosol where it initiates a proteolytic cascade leading to apoptosis (167, 168).

Although changes in endogenous levels of ceramide are observed in response to apoptosis-inducing agents and have been shown to precede the onset of typical hallmarks of apoptosis (57), the exact mechanism(s) of ceramide-induced apoptosis remain enigmatic. Recent studies are pointing toward the mitochondria as an important mediator of ceramide-induced apoptosis. This is perhaps not surprising, given the central role of

mitochondria in regulating apoptosis signaling cascades. Caspase-8 activation has been shown to trigger the formation of ceramide (94, 169), which in turn activates the PARP-cleaving protease caspase-3 (170). The activation of aSMase by Fas and TNF α receptor ligation, both of which contain death domain regions that activate caspases, provide yet another link between caspases, ceramide and apoptosis (166). Ceramide has been shown to exert direct effects on isolated mitochondria and intact cells through the generation of ROS and induction of cytochrome c release (104), possibly via pore formation in mitochondrial membranes (105, 106). Such pore formation is consistent with the molecular geometry of natural ceramide lipids, which will be described in Section 1.4.1.3. The activation of caspases-9 and -3 by cytochrome c provides a link between ceramide signaling and execution caspases (171). The identification of components of sphingolipid signaling pathways such as sphingomyelin, ceramide and ceramide synthase within mitochondrial membranes further suggests the existence of a mitochondrial pathway of ceramide metabolism that may regulate apoptosis (172). Support for this comes from a study in which bacterial nSMase was targeted to different cellular compartments, including the plasma membrane, cytoplasm, mitochondria, Golgi, endoplasmic reticulum and nucleus. While ceramide levels were shown to increase in all compartments, only mitochondrial ceramide accumulation caused apoptosis (173), suggesting a role for endogenous mitochondrial ceramide in apoptosis. Overexpression of anti-apoptotic proteins such as Bcl-2 or Bcl-xL inhibit cell death but do not affect upstream ceramide generation, indicating that elevated ceramide is not simply a consequence of cell collapse (174).

1.3.3. Ceramide Signaling via Lipid Rafts

In addition to the ceramide targets described above, emerging evidence has begun to suggest that some of the effects of ceramide are mediated by its unique biophysical properties. The polar head group, amide linkage and hydroxyl groups of the sphingosine and fatty acid chains enable ceramide lipids to act as both donors and acceptors of hydrogen bonds. This gives them the capacity to form extensive hydrogen bonds in the phospholipid bilayer. Consequently, a relatively new focus of ceramide-mediated apoptosis involves the formation of ceramide signaling platforms.

The plasma membrane is largely composed of cholesterol and sphingomyelin, the latter of which is almost exclusively localized to the cytoplasmic leaflet. Hydrogen bond formation and hydrophobic van der Waals interactions mediate a tight association between the sterol ring of membrane associated cholesterol and the sphingomyelin pool. This results in a lateral segregation of these lipids into gel-like regions of tightly packed sphingolipids called rafts, which “float” in the liquid-crystalline phospholipid portion of the cell membrane (175). These membrane rafts are believed to act as specific sites for ceramide generation in response to various agonists and stress signals. For example, Fas receptor stimulation was shown to result in translocation of aSMase to the extracellular leaflet of the cell membrane (176, 177) where it mediates hydrolysis of sphingomyelin to ceramide within lipid rafts. Ceramide itself has been shown to self-aggregate into microdomains (178, 179) which are capable of fusing into larger macrodomains known as platforms (180). One possible mechanism for the biological action of ceramide is through changes in membrane structure and organization via formation of these platforms, which may serve to cluster and activate ligand-bound receptors in a process

known as capping (176, 181). In support of this theory, Cremesti *et al.* demonstrated that addition of exogenous C₁₆-ceramide to soluble Fas ligand promoted receptor crosslinking (capping) and subsequent apoptosis (177). The formation of ceramide signaling platforms is likely involved in other signaling cascades, and may provide an explanation for ceramides' pleiotropic intracellular effects.

Since ceramide lipids appear to be important in the context of apoptosis and multidrug resistance, the focus of this thesis was to better understand the role of ceramide in MDR and to identify ways in which these lipids could be directly introduced into tumor cells to induce apoptosis in a therapeutic setting. Given that ceramides are naturally occurring lipids, liposome-based delivery systems were investigated as delivery vehicles to efficiently introduce ceramides into tumor cells. The following section describes the preparation and properties of liposomes in this context.

1.4 LIPOSOMAL DRUG DELIVERY SYSTEMS

Liposomes were first described by Bangham and colleagues who observed that spherical membrane vesicles spontaneously formed upon hydration of dried lipids in aqueous solutions (182). Liposomes were initially developed as model membrane systems to evaluate the structural and functional roles of lipids in biological membranes (183). However, they were later developed for use as delivery vehicles for conventional drugs, and are more recently evolving as carriers of bioactive lipids.

1.4.1 Review of Liposomes

Over the past several decades liposomes have progressed from conventional phospholipid/cholesterol-based first-generation formulations, to second-generation sterically stabilized systems, to the more recent third-generation multifunctional liposomes that may incorporate multiple small molecule compounds, nucleic acids and bioactive lipid components (illustrated in Figure 1.4). These modifications have allowed for the production of liposomes with increased stability and longevity in the circulation, as well as enhanced

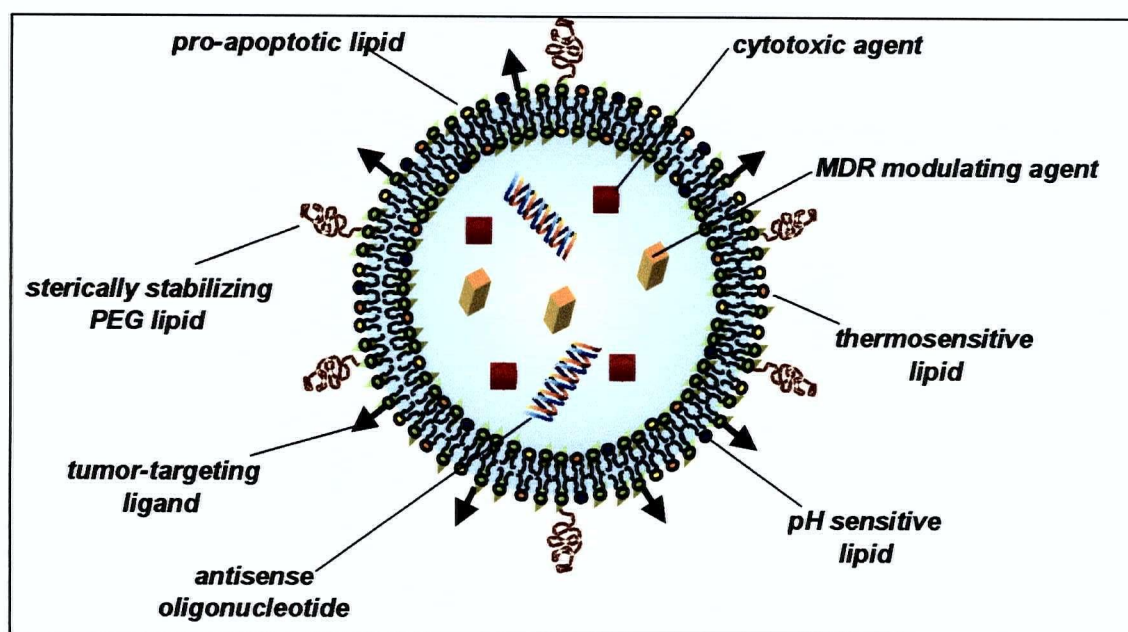


Figure 1.4 A schematic illustration of a hypothetical multifunctional liposome incorporating agents directed against multiple intracellular targets.

active targeting capabilities and controlled drug release properties triggered by pH (184, 185) or temperature (186).

Many liposome formulations have been developed as effective carriers for the delivery of anticancer drugs (187-193), antimicrobial agents (194-196), genes (197) and antisense oligonucleotides (118, 198-200). Some of these formulations have already been approved for human use, and others are in various stages of clinical trials (reviewed in (201)). The therapeutic advantage of liposome-based drug delivery systems can be attributed to two main characteristics. First, liposome encapsulation mediates changes in drug circulation lifetimes and tissue distribution characteristics whereby these parameters are dictated by the liposomal carrier rather than the drug itself. For example, a drug such as doxorubicin, which exhibits rapid elimination from the plasma compartment following administration in its free form can remain in the circulation in excess of 24 hours when encapsulated in a sterically stabilized liposome. The second and perhaps most unique feature of liposome-based drug delivery systems stems from their use in enhancing drug accumulation at disease sites, which leads to a selective accumulation of drug in diseased versus healthy tissues. This process, termed passive targeting because it occurs in the absence of specific targeting ligands, is mediated by the natural process of extravasation and preferential accumulation of liposomes at sites of inflammation (202), infection (203) and tumor growth (204, 205). Whereas the permeability of normal vasculature structure is tightly controlled, the specific example of passive tumor accumulation is achieved because the tumor microvasculature is typically discontinuous and contains fenestrations varying between 100-780 nm in diameter (206). This allows liposomes to extravasate into the tumor tissue to provide locally concentrated drug delivery. Such tumor-specific

accumulation offers the additional advantage of decreasing drug accumulation in non-target tissues, thereby reducing drug-associated toxicities in healthy tissues.

1.4.1.1 Liposome preparation and classification

When most amphipathic phospholipids are dispersed in an aqueous buffer they spontaneously form bilayers (Figure 1.5). Hydration of a dried lipid film produces bilayer structures arranged in concentric rings called multilamellar vesicles (MLVs). Multilamellar vesicles are of limited value for pharmaceutical applications due to their heterogenous diameter range (1-10 microns) and rapid elimination from the plasma following *in vivo* administration (207). However, the size and lamellarity of MLVs can be modified by sonication, reverse-phase evaporation or extrusion techniques (208, 209). The most versatile and frequently utilized method involves extruding MLVs through polycarbonate filters under high pressures of an inert gas. This produces a homogenous population of large unilamellar vesicles (LUVs) of well-defined size that may be controlled by filter pore size (50-400 nm range). Large unilamellar vesicles are the most suitable for pharmaceutical applications due to their stability in the circulation and optimal passive targeting properties. Small unilamellar vesicles (SUV) in the 25-50 nm range can be prepared by sonication but are generally unstable due to the high radius of curvature of the membranes, making them unsuitable for pharmaceutical applications. Figure 1.6 depicts these three classes of liposomes. Both MLVs and LUVs were used in this research, and the extrusion procedure, which is described in detail in Chapter 3, was used for the preparation of all LUVs.

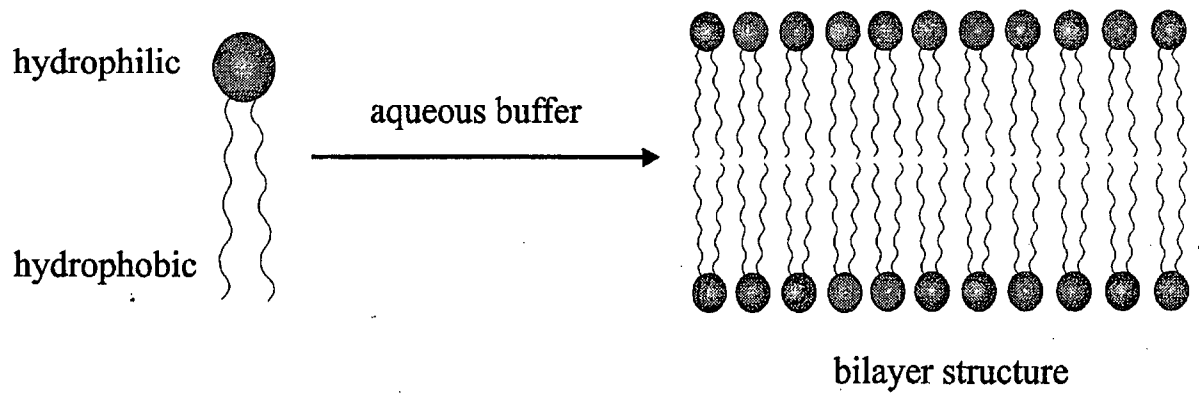


Figure 1.5 An illustration of spontaneous bilayer formation upon hydration of amphipathic lipids in an aqueous buffer.

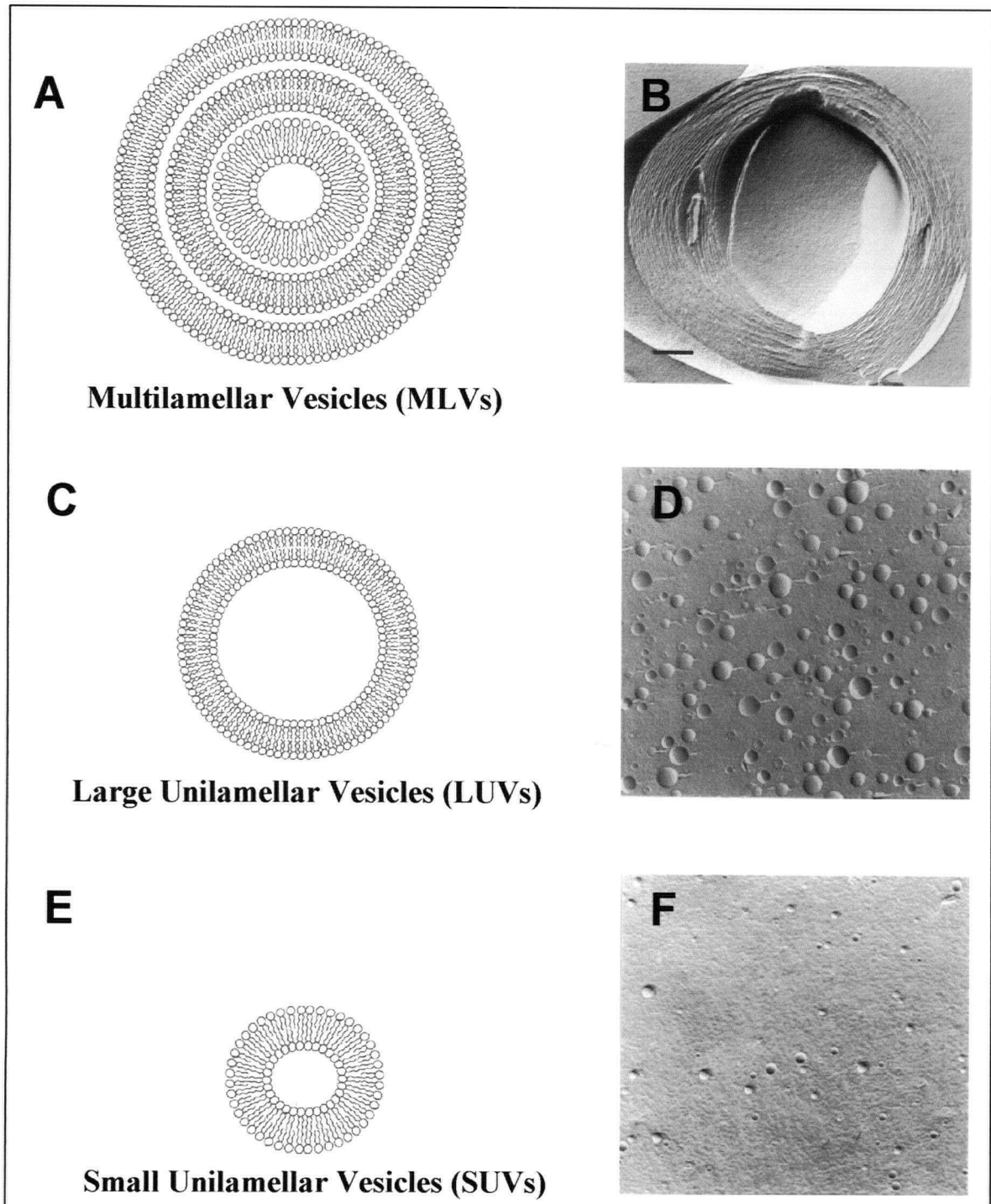


Figure 1.6 Schematic illustrations and scanning electron micrographs of the three main liposome classes: multilamellar vesicles (MLVs, A and B); large unilamellar vesicles (LUVs, C and D); small unilamellar vesicles (SUVs, E and F). The bar in the lower left of image B represents 200 nm. Adapted from Ostro and Cullis, 1989 (210).

1.4.2.1 Lipid Composition

Phospholipids

Phospholipids are a class of amphipathic lipids that form one of the major components of physiological membranes and synthetic liposomes. Although phosphatidylcholine (PC) is the most abundant phospholipid in nature, other naturally occurring phospholipids include phosphatidylethanolamine (PE), phosphatidylserine (PS) and phosphatidylinositol (PI). Phosphatidylcholine is the phospholipid predominantly used in the research presented in this thesis. A generic phospholipid with commonly occurring headgroups and fatty acid moieties is illustrated in Figure 1.7. This illustration depicts the hydrophilic phosphate-containing head group and hydrophobic acyl chains esterified to a glycerol backbone. The distinct properties of each phospholipid are determined both by the nature of the head group and the composition of the acyl chains. Different head groups give rise to phospholipids which may be anionic (PS, PI) or neutral (PC, PE) at physiological pH. Naturally occurring cationic lipids are extremely rare. However, cationic lipids such as 1,2-dioleoyl-3-trimethylammonium propane (DOTAP) have been synthesized for use in gene therapy studies in which the cationic lipids are complexed with DNA (211, 212). Variability of the acyl chains arises from alterations in the hydrocarbon length and the degree of saturation. The acyl chain length of phospholipids comprising physiological membranes typically ranges from 12-24 carbon atoms, and both mono- and polyunsaturated acyl chains are common in nature.

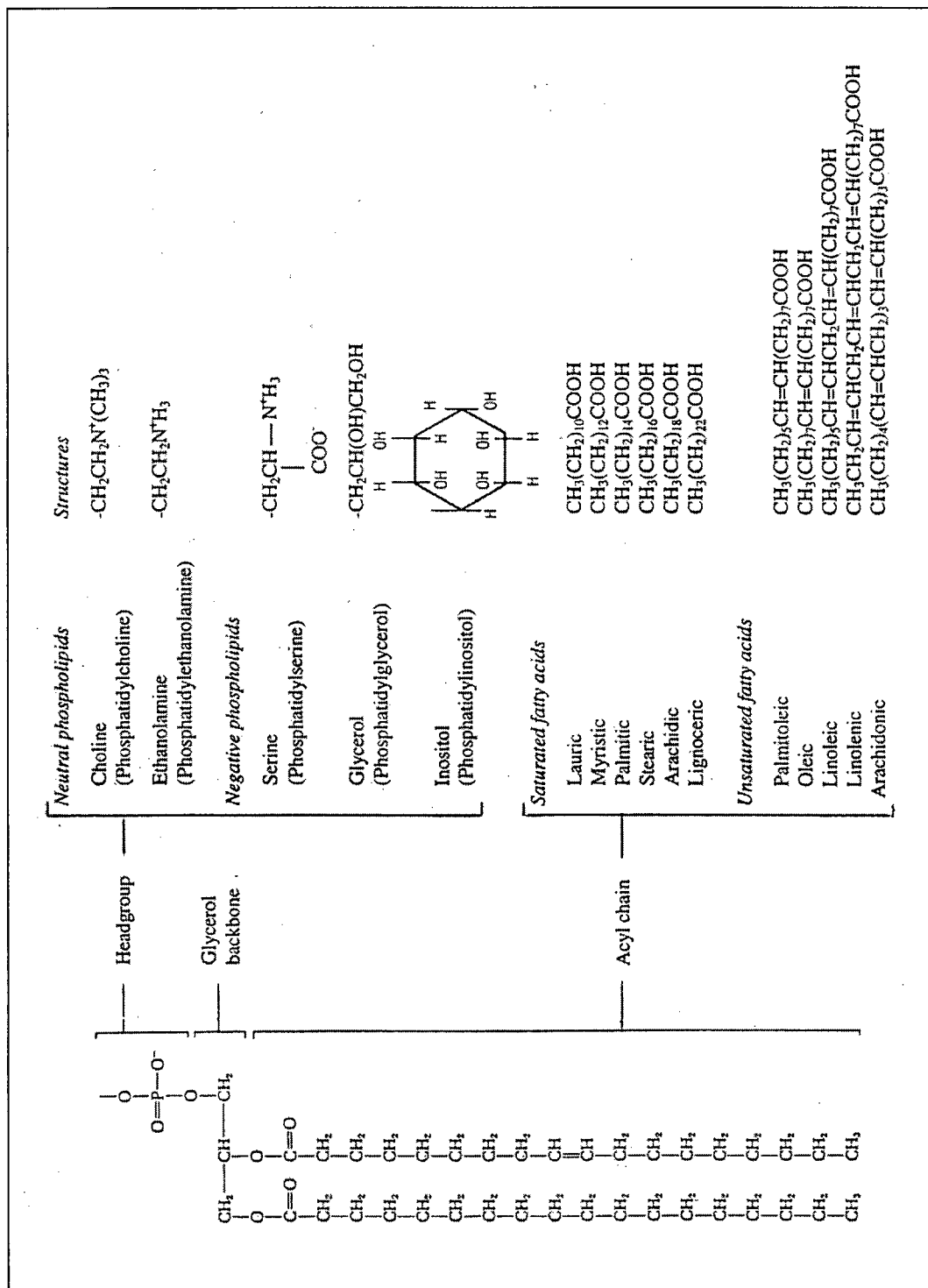


Figure 1.7 The general structure of a phospholipid depicting some commonly occurring headgroups and fatty acid moieties.

Cholesterol

Cholesterol is a neutral, amphipathic lipid that is commonly found in physiological membranes. Its planar ring structure allows it to intercalate between phospholipids in the bilayer, where the hydrophobic steroid ring can interact with phospholipid acyl chains via hydrophobic and van der Waals interactions. The hydroxyl group of cholesterol makes this otherwise hydrophobic molecule amphipathic and mediates hydrogen bond formation between the polar head groups of neighboring phospholipids and the aqueous environment. The rigidifying effect of incorporating planar cholesterol into liposomes can be used to advantage in stabilizing liposome bilayers against lipoprotein-liposome interactions (213). The interaction of liposomes *in vivo* involves the binding of plasma proteins and lipoproteins, which dictates the subsequent interaction with the major elimination mechanism for liposomes – the reticuloendothelial system (RES). Liposome interactions with lipoproteins often result in extensive lipid exchange from the liposome bilayer into lipoproteins, which may result in the ultimate dissolution of the liposome. However, it was demonstrated that liposomes containing >30 mole percent cholesterol in the membrane were able to avoid lipoprotein-mediated liposome destabilization. The presence of cholesterol also makes it more difficult for proteins to penetrate and disrupt the membrane structure (214-216) and results in reduced liposome opsonization and removal via phagocytic cells of the RES.

The cholesterol derivative *cholesteryl hemisuccinate* (CHEMS) contains a succinate head group that is negatively charged at physiological pH and is therefore more polar than the single hydroxyl head group of cholesterol. However, in an acidic environment (pH<5.8) CHEMS becomes charge neutralized (protonated). This alters its

overall lipid geometry (described below), which has implications for liposome destabilization that can be exploited to achieve triggered drug release (217, 218). The chemical structures of cholesterol and CHEMS, both of which were used in this thesis, are shown in Figure 1.8.

Polyethylene glycol-modified lipids

Polyethylene glycol (PEG) is a flexible, hydrophilic polymer consisting of repeating units of ethylene glycol ($\text{CH}_2\text{-CH}_2\text{-O}$)_n that is often chemically conjugated to the headgroup of PE, which serves as a lipid anchor (Figure 1.9). Incorporation of PEG-PE into liposome bilayers gives rise to “sterically stabilized” liposomes that demonstrate greatly improved liposome stability in the circulation (219, 220). Much like cholesterol, the ability of PEG to prolong liposome circulation longevity is believed to involve reduced interaction with lipoproteins and decreased serum protein binding to the liposome surface. Whereas this was achieved through a rigidifying effect of the membrane by cholesterol, PEG acts through reduced recognition by cells of the RES. Polyethylene glycol acts as a steric barrier that inhibits the close approach of plasma proteins that would otherwise mark non-PEGylated vesicles for elimination through the stimulation of phagocytic macrophages (221-224). It has also been speculated that the PEG coating may reduce cellular uptake directly, so that even in the presence of bound plasma proteins the PEG coating will inhibit receptor mediated binding at the level of the macrophage (225). Sterically stabilized liposomes containing PEG₂₀₀₀-DSPE were used for all *in vivo* studies in this thesis.

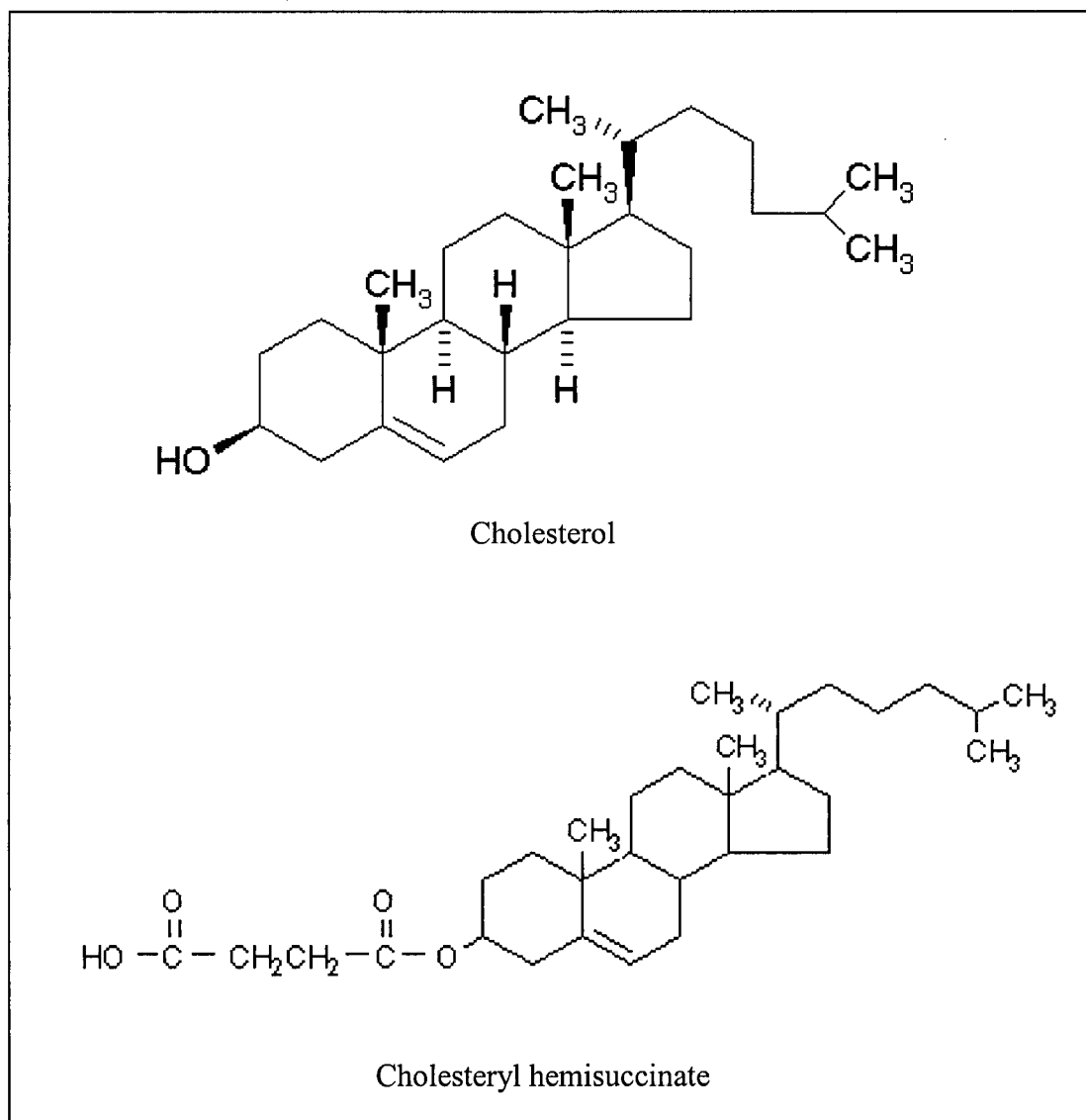


Figure 1.8 Chemical structures of cholesterol and cholesteryl hemisuccinate lipids.

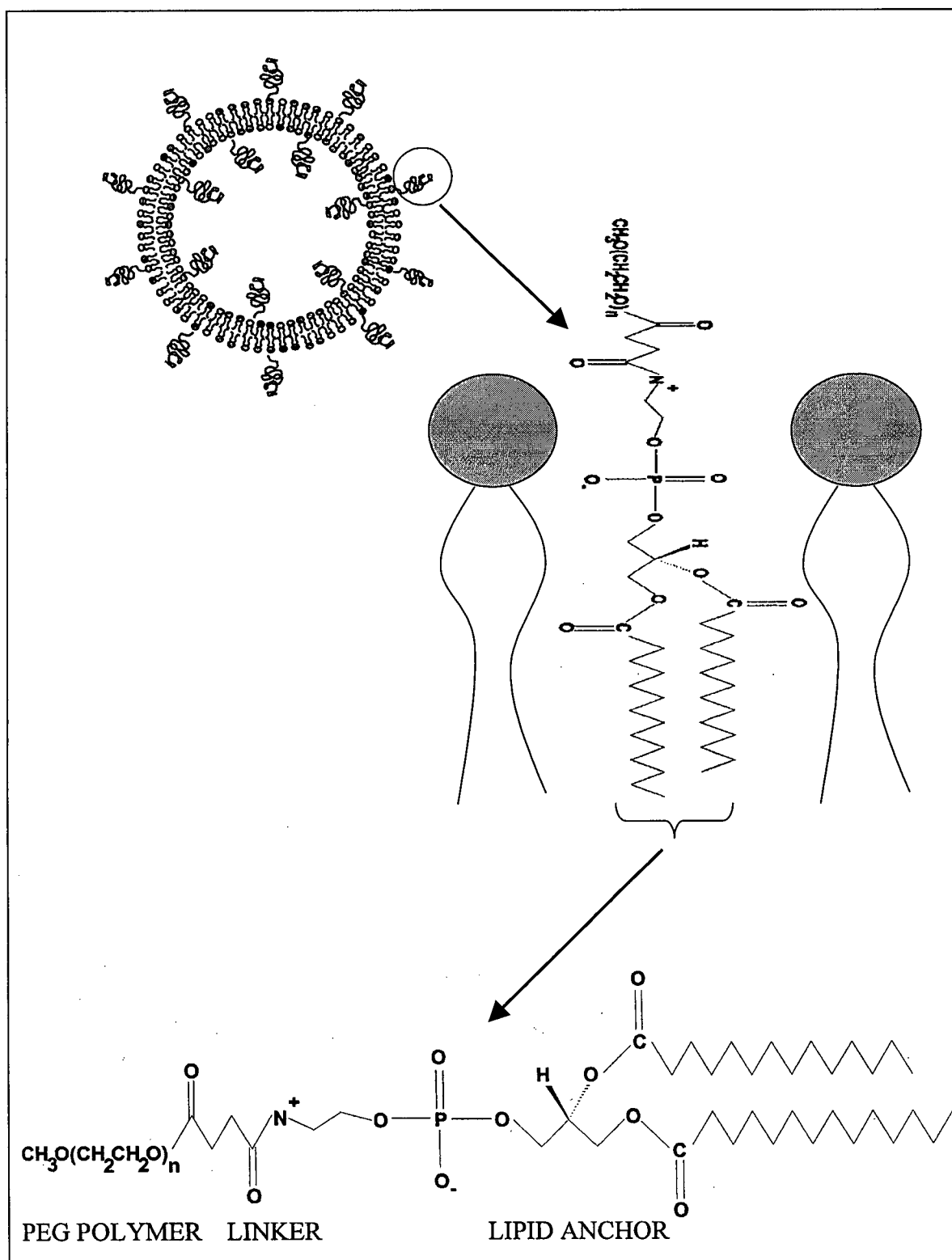

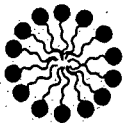

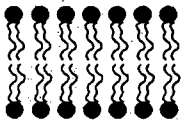

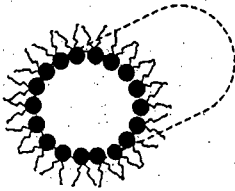


Figure 1.9 A schematic illustration of a pegylated liposome showing the chemical structure of polyethylene glycol derivatized phosphatidylethanolamine (PEG-PE).

1.4.1.2 Lipid polymorphism

One factor to consider when designing liposomes is the molecular shape of the individual lipid components. In particular, the size and shape of the polar head group in relation to the hydrophobic acyl chains is important, as this largely dictates the type of lipid structure that is formed in an aqueous environment (226). The ability of lipids to adopt structures other than a bilayer has been described as lipid polymorphism. Table 1.4 illustrates the three main classes of lipid geometries and their respective phase behaviours upon dispersion in an aqueous environment.

Table 1.4
Molecular Shape of Various Lipids and their Associated Structures
(adapted from Cullis *et al.*, 1996 (226))

Lipid	Molecular Shape	Structure
Lysophospholipids Detergents PEG-conjugated lipids Short-chain ceramides	 Inverted Cone	 Micelle
Phosphatidylcholine Phosphatidylserine Sphingomyelin Cholesteryl hemisuccinate (neutral pH) Short-chain ceramides	 Cylinder	 Bilayer
Phosphatidylethanolamine Cholesteryl hemisuccinate (acidic pH) Long-chain ceramides	 Cone	 Hexagonal (HII)

The large cross-sectional area of the polar head groups of lipids such as lysolipids and detergents relative to their single acyl chain gives rise to an inverted cone geometry that confers a tendency for these lipids to form micellar structures in an aqueous environment. Many phospholipids have a cylindrical geometry in which the cross-sectional area of the polar head group and non-polar acyl chains is approximately equal. These lipids spontaneously arrange into stable bilayers in an aqueous environment. When the cross-sectional area of the headgroup is small relative to that of the acyl chains the lipid takes on a cone-shaped geometry. This confers a tendency to spontaneously form hexagonal phase (H_{II}) or inverted micelle structures, and this particular organization is involved in membrane destabilization and fusion. Natural (long-chain) ceramide lipids, which are a primary focus of this thesis, fall into this latter category of molecular shape due to the small head group relative to the long fatty acyl tails (227). This limits the extent to which they can be stably incorporated into liposome bilayers. Cholesteryl hemisuccinate is a bilayer forming lipid at physiological pH (negatively charged polar head group) but charge neutralization of the head group upon protonation at low pH causes the molecular geometry to change from that of a cylinder to a cone, and the lipid therefore forms inverted micellar structures in an acidic environment. This causes liposome destabilization and forms the basis of pH sensitive liposomes, which have been described for the intracellular delivery of liposome encapsulated drugs and macromolecules (218). Cholesteryl hemisuccinate can be used to stabilize the bilayer structure of non-bilayer forming lipids such as DOPE, and the work presented in Chapter 3 of this thesis extends this application to the stabilization of natural ceramide lipid in ceramide-containing liposome bilayers.

1.4.2 Liposomes as Drug Carriers

Liposome-based drug delivery systems typically consist of a drug or small molecule compound encapsulated either in the aqueous vesicle core or partitioned into the lipid bilayer of liposomes. There are two basic strategies for encapsulating drugs within liposomes. Entrapment of either hydrophilic or lipophilic drugs may be achieved during the vesicle formation process (passive trapping) or by loading amphipathic drugs into pre-formed liposomes in response to a transmembrane pH gradient (active trapping). The drug distribution patterns for these encapsulation procedures are illustrated in Figure 1.10. The passive loading procedure was used to encapsulate [^{14}C]lactose for trapped volume studies described in Chapter 3, and is the method by which the ceramide-containing liposomes described in Chapters 3-5 were prepared. Most conventional anticancer drugs are currently encapsulated using procedures based on the active loading technique. The active loading procedure was used to encapsulate doxorubicin and verapamil for the drug release studies presented in Chapter 4.

1.4.2.1 Passive encapsulation

Passive encapsulation of hydrophobic drugs involves including the compound in the original lipid mixture prior to hydration. The antifungal agent Amphotericin B is one example of a drug that is encapsulated in this manner (228). The encapsulation efficiency of this technique depends on the capacity of the lipid bilayer to solubilize the drug while maintaining its vesicular structure. Although trapping efficiencies approaching 100% can be obtained, drugs of this class often exhibit appreciable exchange rates into other membranes and the drug rapidly leaves the liposome carrier *in vivo* (228).

This phenomenon is addressed by the development of a lipid/drug exchange assay that forms the basis of Chapter 4.

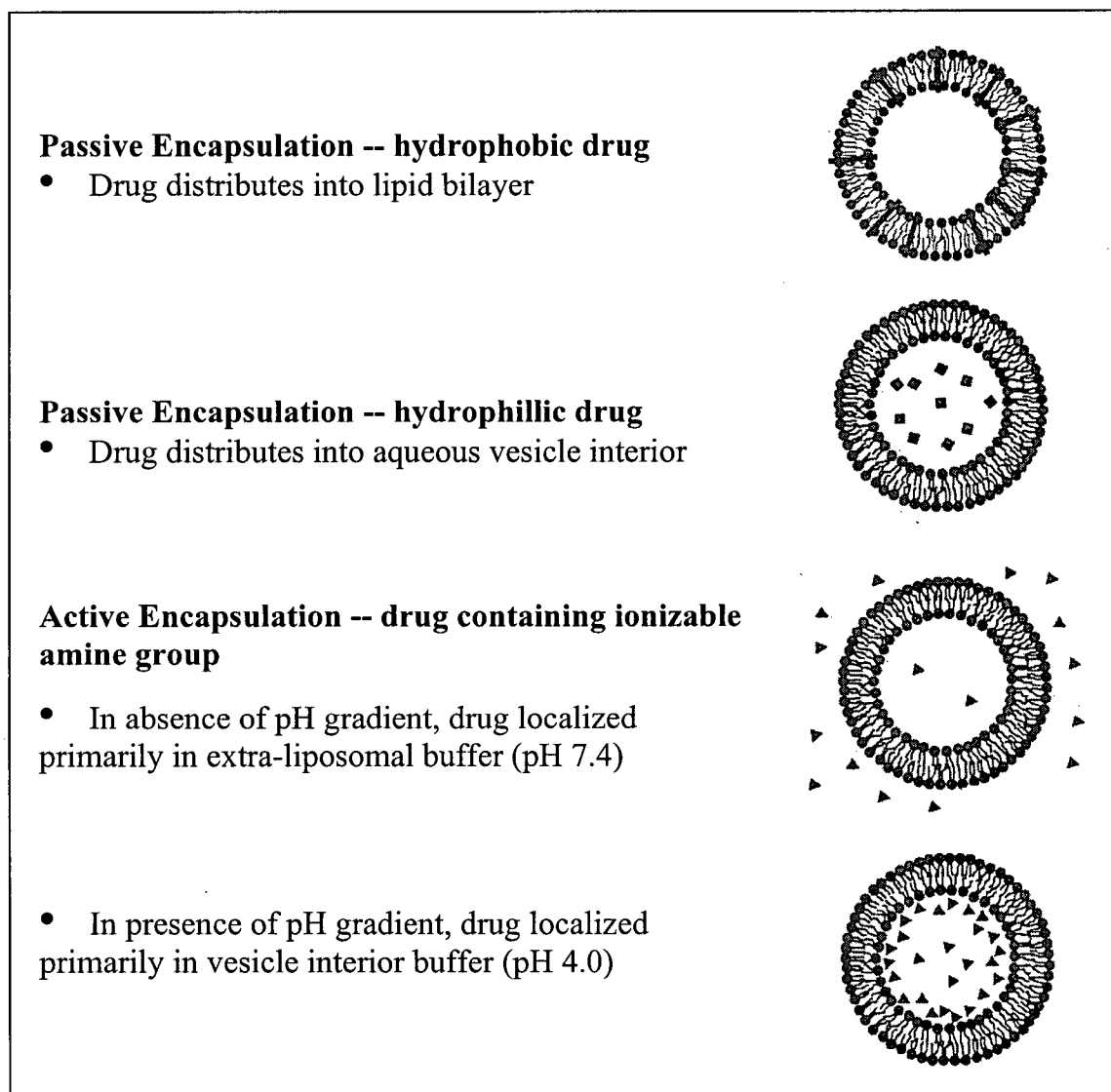


Figure 1.10 Drug distribution following active and passive encapsulation for hydrophobic and hydrophilic drugs

Passive encapsulation of hydrophilic agents involves dissolving the drug in the aqueous buffer used to hydrate the lipid film. The encapsulation efficiency of this method, therefore, depends on the internal aqueous volume of the liposome. The trapped volume of LUVs, which typically range from 1-10 $\mu\text{l}/\mu\text{mole}$ lipid, can result in encapsulation efficiencies in excess of 50% (229). The retention of hydrophilic drugs trapped in this manner depends on the nature of both the drug and the lipid membrane, as well as the concentration of liposomes during hydration and extrusion. Drugs that possess some degree of lipophilic character, such as doxorubicin, exhibit more rapid release than membrane impermeable drugs (230). Lipid bilayers composed of long-chain, saturated phospholipids and cholesterol can also improve drug retention by decreasing membrane permeability.

1.4.2.2 Active encapsulation

Active loading procedures are designed to load drug into the interior of pre-formed liposomes exhibiting a transmembrane proton gradient (inside acidic). Drugs that are encapsulated by this method are typically lipophilic cations with ionizable amine groups, such as doxorubicin. In the neutral, extra-liposomal environment the drug is predominantly uncharged and can readily diffuse across the liposome bilayer when added to the liposome suspension. However, the drug is readily protonated upon reaching the acidic vesicle interior and becomes effectively trapped, as the charged species is significantly less membrane permeable. Since many drugs are lipophilic weak base amines, this mechanism of active loading has widespread applications (231). Although encapsulation efficiencies approaching 100% can be achieved with active loading procedures, the drug retention properties vary considerably and are dependent on the

membrane permeability properties of the drug and the ability of the liposome formulation to maintain the proton gradient (232).

1.4.3 Drug Delivery Approaches to MDR Modulation

Despite the fact that we now know more than ever about the various mechanisms that contribute to MDR, the fact remains that relatively small advances have been made to circumvent MDR and improve the clinical response of refractory tumors. Some of the growing evidence to suggest that liposomes are capable of providing many of the features that will likely be useful in improving the treatment of MDR tumors is presented below.

1.4.3.1 Application of liposomes to MDR reversal

Liposomes can be applied to the treatment of MDR tumors using three basic approaches: (1) using liposomes as carriers of anticancer drugs in order to increase tumor-specific drug delivery, (2) combining potent conventional MDR modulators with liposomal anticancer drugs in order to reduce adverse drug/modulator pharmacokinetic interactions, and (3) incorporating MDR modulators into the liposome bilayer or encapsulated within the liposome core for tumor-specific MDR reversal.

The advantages achieved by applying liposomes to MDR reversal strategies stem primarily from their ability to passively accumulate in solid tumors due to the increased permeability of tumor blood vessels relative to the vascular lining of healthy tissues (233). This allows for increased selectivity of anticancer drug delivery to the tumor site and reduced drug accumulation and toxicities in healthy tissues, which can provide tumor associated drug levels that are up to 10-fold higher than achievable with conventional aqueous anticancer drug formulations (205, 234). This increase in tumor drug exposure

has been shown to partially overcome drug resistance in MDR tumors, leading to enhanced antitumor activity independent of additional agents aimed at blocking molecular mediators of MDR (81, 235). This presumably reflects the effects of mass-action driven improved intra-tumor drug accumulation that arises from elevated drug concentrations in the tumor interstitial space. While the increased dose intensity and selective tumor delivery afforded by liposomes improves the treatment of MDR tumors, this in itself is not sufficient to completely overcome resistance (236).

An exciting recent advance in liposomal anticancer drug delivery concerns the use of triggered drug release to dramatically increase the bioavailability of encapsulated agents specifically at the tumor site. This technology utilizes thermosensitive liposomes from which drug release can be dramatically increased by selective mild heating of tumors to 41-42°C (186). This causes rapid exposure of tumor tissue to high concentrations of anticancer drug and has been shown to cause complete regression of human xenograft solid tumors, which was not observed following treatment with conventional liposomal carriers (237, 238). It will be particularly interesting to see whether this technology can further enhance the treatment of MDR tumors by virtue of significant increases in tumor drug exposure.

As an alternative approach, co-administration of MDR modulators with liposomal anticancer drugs was investigated in an attempt to alleviate the complications associated with altered Pgp function in healthy tissues by virtue of selective drug delivery to tumor tissue. It was found that co-administration of the Pgp inhibitor Valspodar with liposomal doxorubicin eliminated the adverse pharmacokinetic interactions observed upon Valspodar administration in combination with free doxorubicin (84). This approach

allowed for the ability to deliver full dose chemotherapy in combination with Valspodar and resulted in full chemosensitization and marked tumor regression in MDR solid tumors (81). This improved therapeutic index was attributed to the selective accumulation of doxorubicin in tumor tissue so that anticancer drug toxicity associated with Pgp blockade in healthy tissues was minimized. In addition, the use of liposomes to selectively deliver anticancer drugs to solid tumors should minimize non-selective action of other chemosensitization approaches in healthy tissues, thus providing increased specificity of MDR modulation effects for tumor cells.

Given the inability of current MDR modulating agents to differentiate between tumor and non-tumor Pgp, one particularly attractive application of liposome technology would be to encapsulate the modulating agent itself in a liposome-based delivery system. Since liposomes have a natural tendency to accumulate at tumor sites, such a system would enable the modulator to induce tumor-specific Pgp blockade, further minimizing the adverse toxicities of co-administered anticancer agents on healthy tissues. This would have the added benefit of increased versatility whereby a single liposome-based MDR modulator could be co-administered with any number of anticancer drugs in their free form, or perhaps even as co-encapsulated agents. Liposome encapsulation of MDR modulators has indeed been investigated, but to date the modulating agents have not proven to be amenable to formulation into stable, systemically viable liposomes. Although MDR modulating agents such as verapamil, prochlorperazine, cyclosporin A and the proprietary Pgp inhibitor OC144-093 can be efficiently encapsulated into liposomes, their high membrane permeabilities and rapid leakage following systemic administration has limited development in this area.

1.4.3.2 Application of liposomes to the delivery of bioactive lipids

Although liposome-based drug delivery has primarily focused on delivery of encapsulated drugs as described above, they are more recently being explored as drug delivery vehicles for bioactive lipids that form part the liposome bilayer itself. For example, liposomes containing phosphatidylserine (PS) in the bilayer have been demonstrated to induce selective thrombosis after binding to VCAM-1 in endothelial cells (239, 240). The work contained in Chapters 3-5 of this thesis was aimed at extending this application of liposomes to include liposome-based intracellular delivery of pro-apoptotic ceramide lipids in order to achieve chemosensitization and tumor cell death.

1.5 THESIS OBJECTIVES AND HYPOTHESIS

The apparent involvement of ceramide lipids in both apoptosis and multidrug resistance suggests that therapeutic approaches aimed at modulating ceramide, by increasing intracellular ceramide levels and/or by decreasing ceramide metabolism, should provide enhanced activity against both sensitive and MDR tumors. Consequently, the research contained in this thesis was designed to evaluate the therapeutic application of ceramide lipids within this context. The following four specific objectives were designed to test the overall hypothesis that **therapeutic manipulations aimed at increasing intracellular ceramide levels will result in apoptosis:**

Specific Objective 1: to investigate the effect of inhibiting ceramide metabolism on the sensitivity of multidrug resistant tumor cell lines to conventional chemotherapeutic agents

Specific Objective 2: to investigate the relationship between ceramide acyl chain length, intracellular delivery and apoptosis induction using exogenously applied ceramide lipids in vitro, and to determine whether these parameters could be enhanced by formulating ceramide into liposomal carriers

Specific Objective 3: to develop an in vitro exchange assay that allows the in vivo drug/lipid retention properties of liposomal systems to be predicted

Specific Objective 4: to characterize the in vivo pharmacokinetics and antitumor activity of ceramide-based liposomes

The experiments designed to test these specific objectives and the results that were obtained are presented in Chapters 2-5. The summarizing discussion presented in Chapter 6 outlines the overall conclusions drawn from these studies, and highlights areas of particular interest for potential future research.

CHAPTER 2

ROLE OF 1-PHENYL-2-DECANOYLAMINO-3-MORPHOLINO-1-PROPANOL (PDMP) AND P-GLYCOPROTEIN IN MODULATING CERAMIDE-MEDIATED SENSITIVITY OF HUMAN BREAST CANCER CELLS TO TUBULIN-BINDING ANTICANCER DRUGS*

2.1 INTRODUCTION AND RATIONALE

As described in Chapter 1, overexpression of the drug efflux pump Pgp has long been regarded as a major cause of MDR in a number of human malignancies. Multidrug resistance reversal agents often act by blocking Pgp's drug efflux activity, thereby increasing intracellular drug levels and inducing cell death. However, as more has been learned about Pgp its functional role has expanded to include activity as a drug flippase and phospholipid translocator (241), and it has been shown to transport short-chain fluorescent analogues of SM and GlcCer across membranes (242). In addition, Pgp may play a role in regulating some caspase-dependent apoptotic pathways, a function completely independent of its drug/lipid transport properties (243). In light of these expanding roles it is possible that Pgp may also be involved in regulating ceramide-based apoptosis and metabolism. As discussed in Chapter 1, although ceramide is a pro-apoptotic lipid its GlcCer metabolite is not. Thus, conversion of ceramide to GlcCer by the GCS enzyme is one mechanism by which cells can lower intracellular ceramide levels and avoid apoptosis. The correlation between ceramide, GlcCer and MDR suggests that inhibiting ceramide glycosylation should keep intracellular levels of the pro-apoptotic

*Adapted from: JA Shabbits and LD Mayer (2002). *P-glycoprotein modulates ceramide-mediated sensitivity of human breast cancer cells to tubulin-binding anticancer drugs*. *Molecular Cancer Therapeutics*, 1: 205-213.

lipid elevated, making it a potential approach for inducing apoptosis and circumventing MDR.

1-phenyl-2-decanoylamino-3-morpholino-1-propanol (PDMP) is a well-known inhibitor of the GCS enzyme that has been shown to decrease GlcCer production and promote ceramide accumulation (130). Previous work has shown that PDMP sensitizes murine neuroblastoma cells to treatment with microtubule-affecting cytostatics (132). The research presented in this chapter describes experiments designed to evaluate PDMP-mediated chemosensitization in two human breast cancer cell lines. Based on results obtained in early studies, the involvement of Pgp in ceramide-mediated cell death and chemosensitivity was also investigated. Cells which overexpress both Pgp and GCS, having developed resistance through drug selection, versus cells that were transfected with the *mdr-1* gene and thus overexpress only Pgp, were specifically compared in order to investigate whether Pgp-based transport plays a specific role in ceramide-mediated chemosensitization and apoptosis.

2.2 HYPOTHESIS

The hypothesis underlying the research presented in this chapter is that the inhibition of ceramide metabolism to GlcCer by PDMP will increase endogenous ceramide levels and sensitize multidrug resistant cells to co-administered conventional chemotherapeutic agents.

2.3 MATERIALS AND METHODS

2.3.1 Materials

Dulbecco's Modified Eagle's Medium (DMEM), RPMI 1640 Medium (RPMI) and Hank's Balanced Salt Solution (Hank's) were obtained from Stem Cell Technologies (Vancouver, BC, Canada). Fetal bovine serum was obtained from Hyclone (Logan, UT). L-glutamine and trypsin-EDTA were purchased from Gibco BRL (Life Technologies, Burlington, ON, Canada). Eppendorf tubes were obtained from VWR (West Chester, PA). Formaldehyde was from Polysciences (Warrington, PA). Tween-20, DABCO anti-fade, goat serum and all chemicals were obtained from the Sigma Chemical Company (St. Louis, MO), unless otherwise indicated. MTT reagent was purchased from Sigma-Aldrich Canada (Oakville, ON, Canada). Human IgG was from ICN (ImmunoBiologicals, Lisle, IL). Mouse isotype control-PE (Phycoerythrin), mouse anti-human Pgp-PE and goat anti-mouse IgG-FITC antibodies were obtained from BD Biosciences (Mississauga, ON, Canada). DAPI stain was from Molecular Probes (Eugene, OR). The C219 primary antibody was from Signet Laboratories (Dedham, MA). Microtitre (96-well) Falcon[®] plates and culture flasks were obtained from Becton Dickinson (Franklin Lakes, NJ). Taxol[®] was obtained from Bristol-Myers Squibb (Montreal, QC, Canada). Vincristine sulfate, cisplatin and doxorubicin-HCl were obtained from Faulding (Canada) Inc. (Vaudreuil, QC, Canada). PDMP and glucosylceramide (Gaucher's spleen) were from Matreya Inc. (Pleasant Gap, PA). C₆- and C₁₆-ceramide lipids were from Avanti Polar Lipids (Alabaster, AL). Valspodar was from Novartis (Dorval, QC, Canada). [³H]Taxol[®] was from Moravek Biochemicals Inc. (Brea, CA). [³H]palmitic acid was from NEN (Boston, MA). Pico-fluor 40 scintillation

cocktail was purchased from Packard Biosciences (Groningen, The Netherlands). Silica gel G chromatography plates were from Analtech (Newark, DE).

2.3.2 Cell Lines and Culture

The MDA435/LCC6 and MDA435/LCC6^{MDR1} human estrogen receptor negative breast cancer cells were a generous gift from Dr. Robert Clarke, Georgetown University, Washington, D.C. The MCF7 human estrogen receptor positive breast adenocarcinoma cells were obtained from the American Type Tissue Collection (ATCC; Rockville, MD). The adriamycin resistant MCF7/AdrR cells were obtained from Dr. Gerald Batist at the Lady Davis Research Institute (Montreal, QC, Canada). All cell lines were grown as adherent monolayer cultures in 25-cm² Falcon[®] flasks in DMEM (MDA435/LCC6 cells) or RPMI 1640 (MCF7 cells) culture medium supplemented with 10% fetal bovine serum and 1% L-glutamine. Cells were maintained at 37°C in humidified air with 5% CO₂ and were sub-cultured weekly using 0.25% Trypsin with 1 mM EDTA.

2.3.3 Evaluation of Cell Surface Pgp Expression by Flow Cytometry

Cells were harvested with 0.25% Trypsin + 1 mM EDTA, counted with trypan blue and the concentration was adjusted to 10⁷ cells/ml. Aliquots of 10⁶ cells per cell line were resuspended in 0.1 ml PBS + 0.1% BSA (PBSB) + 20% human serum and incubated on ice for 15 minutes. Cells were incubated with anti-human Pgp-PE (Phycoerythrin) or isotype control-PE for 45 minutes on ice, washed three times with PBSB and analyzed by flow cytometry using the EPICS Elite^{ESP} flow cytometer (Beckman-Coulter, Miami, FL).

2.3.4 Evaluation of Intracellular Pgp Expression by Fluorescence Microscopy

Cells were harvested with 0.25% Trypsin + 1 mM EDTA, counted with trypan blue, and 6×10^6 cells of each cell type were placed in 1.7 ml Eppendorf tubes. After centrifugation at 7000 rpm for 15 seconds the pellets were resuspended in 0.3 ml 2% formaldehyde in PBS and left to incubate at room temperature for 30 minutes for fixation. In order to increase cell permeability, 1% Tween-20 was added for the last 15 minutes of fixation. Fixed cells were centrifuged at 11,000 rpm for 25 seconds and the pellets were resuspended in 0.1 ml PBSB followed by two washes with 1 ml PBS + 0.1% BSA + 0.5% Tween-20 (PBSBT). Pellets were resuspended in 0.75 ml blocking reagent containing PBSBT + 100 µg/ml human IgG + 20% normal human serum. Samples were placed at 4°C overnight for blocking and then equally distributed to three Eppendorf tubes. Aliquot A was used as an autofluorescence control, aliquot B to control for non-specific staining by exposure to secondary antibody only, and aliquot C for the two-step staining procedure. Mouse anti-human Pgp (C219) primary antibody was added to sample C at 1 µg/ml and incubated at room temperature for 2 hours. All cells were washed twice with 1 ml PBSBT and once with PBSB, centrifuged at 11,000 rpm for 25 seconds and resuspended in 0.25 ml PBSBT + 20% goat serum. Goat anti-mouse IgG-FITC secondary antibody was added to samples B and C, incubated at room temperature for 1 hour and washed twice with PBSBT. All samples were then washed with 1 ml PBSB, centrifuged and the pellets resuspended in 0.3 ml PBSB + 0.1 µg/ml DAPI. Cells were spun onto glass slides, dried for 10 minutes at room temperature and mounted in 10 µl of 2.5% DABCO anti-fade in 90% glycerol. All images were acquired with a Leica DC 100 fluorescence microscope (Leica Microsystems (Canada), Richmond Hill, ON,

Canada) and Image Database V4.01 software for 9 seconds. Images were later processed with Adobe Photoshop® 4.0 in an identical manner.

2.3.5 MTT Cytotoxicity Assays

Cells were counted and seeded into 96-well microtiter Falcon® plates at 2×10^3 cells/well in 0.1 ml complete medium. The perimeter wells of the 96-well plates were not used and contained 0.2 ml sterile water. After 24 hours at 37°C the medium was replaced with 0.2 ml of fresh medium containing Taxol®, vincristine sulfate, cisplatin or doxorubicin with or without PDMP, C₆-ceramide or Valspodar at the concentrations specified for each experiment. After 72 hours the cell viability was assessed using a conventional 3-(4,5-dimethylthiazol-2-yl)-2,5-diphenyl tetrazolium bromide (MTT) dye reduction assay. Fifty microlitres of 5 mg/ml MTT reagent in PBS was added to each well. Viable cells with active mitochondria reduce the MTT to an insoluble purple formazan precipitate that is solubilized by the subsequent addition of 150 µl dimethyl sulfoxide. The formazan dye was measured spectrophotometrically (570 nm) using an MRX microplate reader (Dynex Technologies Inc., Chantilly, VA). All assays were performed in triplicate. The cytotoxic effect of each treatment was expressed as percent cell viability relative to untreated control cells (% control) and was defined as: $[(\text{Abs}_{570} \text{ treated cells}) / \text{Abs}_{570} \text{ untreated cells}] \times 100$.

2.3.6 [³H]Taxol® Uptake Studies

Cells were seeded into 6-well Falcon® plates at 1.5×10^6 cells/ml in 2 ml complete medium. After 24 hours at 37°C the old medium was aspirated and cells were incubated

with 2 ml complete medium containing the indicated concentrations of Taxol[®] + 0.25 μ Ci/ml [³H]Taxol[®] in the absence or presence of 5 μ M PDMP for the times indicated. Culture medium was then removed and cells were washed twice with 0.2 ml ice-cold PBS. Cells were harvested by scraping into 0.5 ml PBS and radioactivity was measured by liquid scintillation counting. An aliquot was obtained for cell counting by trypan blue exclusion. Uptake was expressed as picograms [³H]Taxol[®]/10⁶ cells and was corrected for binding using controls incubated at 4°C.

2.3.7 Cell Radiolabeling and Lipid Extraction

Cells were seeded into 75-cm² Falcon[®] flasks in complete medium and grown to ~70% confluence. Plating medium was replaced by 15 ml complete medium containing 1.0 μ Ci/ml [³H]palmitic acid with or without 5 μ M PDMP and/or 1 μ g/ml Valspodar for 24 hours. Cells were washed twice with ice-cold Hank's medium and harvested by scraping into 2.5 ml ice-cold methanol containing 2% acetic acid. The collected cells were transferred to glass vials with teflon-lined screw caps. Lipids were extracted from the methanol layer by adding equal volumes of water and chloroform, vortexing and centrifuging at 3000 rpm for 5 minutes. The lipid-containing lower, organic phase was collected into pre-weighed tubes. Three 10 μ l aliquots were removed for scintillation counting to determine the total amount of radiolabeled lipid. The remaining organic phase was dried under a stream of nitrogen and tubes were re-weighed to determine the total mass of extracted lipid.

2.3.8 Lipid Detection by Thin Layer Chromatography (TLC)

The dried lipid film was dissolved in chloroform/methanol (2:1) and 300 µg total lipid was spotted onto silica gel G TLC plates. Plates were developed in chloroform/acetic acid (90:10) for ceramide separation and chloroform/methanol/ammonium hydroxide (70:20:4) for GlcCer separation. Commercial C₁₆-ceramide and GlcCer standards were co-chromatographed. Chromatography plates were visualized with iodine vapor and spots corresponding to ceramide or GlcCer were scraped into scintillation vials for quantitation by liquid scintillation counting. The radioactivity of the selected spots was expressed as a percentage of the total amount of radiolabeled lipid extracted from the cells.

2.3.9 Statistical Analysis

Statistical analysis was performed using one way analysis of variance (ANOVA) followed by Student-Newman-Keuls analysis with InStat Version 3.0 for Windows (GraphPad Software, Inc., San Diego, CA). Mean differences with a *p* value <0.05 were considered statistically significant.

2.4 RESULTS

2.4.1 Chemosensitization Effects of PDMP in Human Breast Cancer Cells

MTT cytotoxicity studies comparing the chemosensitivity of wild-type cell lines to their drug resistant counterparts demonstrated the presence of statistically significant resistance to Taxol[®], vincristine and doxorubicin in both the MCF7/AdrR and MDA435/LCC6^{MDR1} cell lines (Table 2.1). However, resistance to cisplatin did not reach

statistical significance for either cell line ($p=0.66$ and $p=0.23$ for the MCF7/AdrR and MDA435/LCC6^{MDR1} cell lines, respectively). Flow cytometry studies using the fluorescent Pgp-PE antibody demonstrated that cell-surface Pgp was overexpressed in both of the resistant cell lines relative to wild-type. The fluorescence intensity of the MCF7/AdrR cell line was 9.5 times greater than wild-type, and that of the MDA435/LCC6^{MDR1} cell line was 6.8 times greater than wild-type (Figure 2.1). Immunofluorescence studies using a 2-step staining procedure employing the C219 anti-Pgp primary antibody and an IgG-FITC secondary antibody demonstrated that Pgp was intracellularly distributed and not solely localized to the plasma membrane (Figure 2.2). Low level background staining of the primary antibody was observed in the wild-type cells, as was low level non-specific staining with the FITC secondary antibody controls. However, the anti-Pgp staining in the MDR cells was increased and aggregates of high intensity fluorescence were observed, which is indicative of intracellularly distributed Pgp.

Table 2.1

The Effect of 5 μ M PDMP, 1 μ g/ml Valspodar and 2 μ M C₆-Ceramide on Anticancer Drug Cytotoxicity in Wild-Type and Multidrug Resistant MCF7 and MDA435/LCC6 Breast Cancer Cells

Cell Line	IC ₅₀ ^a \pm SEM			
	Taxol [®]	Vincristine	Doxorubicin	Cisplatin
MCF7	12.52 \pm 3.64 nM	0.76 \pm 0.18 nM	0.17 \pm 0.06 μ M	33.99 \pm 3.29 μ M
MCF7 + PDMP	12.08 \pm 0.11 nM	0.77 \pm 0.16 nM	0.18 \pm 0.07 μ M	34.38 \pm 4.55 μ M
MCF7/AdrR	3.24 \pm 0.06 μ M ^b	11.02 \pm 2.16 μ M ^b	0.34 \pm 0.12 μ M ^b	27.57 \pm 9.08 μ M
MCF7/AdrR + PDMP	0.50 \pm 0.20 μ M ^c	1.82 \pm 0.16 μ M ^c	0.34 \pm 0.12 μ M	28.75 \pm 12.52 μ M
MCF7/AdrR + Valspodar	60.77 \pm 4.20 nM	33.93 \pm 0.38 nM	N/D ^e	N/D
MCF7/AdrR + Valspodar + PDMP	30.40 \pm 2.27 nM ^d	17.26 \pm 14.14 nM ^d	N/D	N/D
MCF7/AdrR + PDMP + C ₆ -Cer	0.68 \pm 0.08 μ M	1.48 \pm 0.01 μ M	N/D	N/D
MDA435/LCC6	1.81 \pm 1.37 nM	0.22 \pm 0.02 nM	0.25 \pm 0.14 μ M	10.17 \pm 3.57 μ M
MDA435/LCC6 + PDMP	1.27 \pm 1.06 nM	0.18 \pm 0.02 nM	0.23 \pm 0.16 μ M	9.95 \pm 5.02 μ M
MDA435/LCC6 ^{MDR1}	30.01 \pm 4.13 nM ^b	39.25 \pm 7.90 nM ^b	3.87 \pm 1.57 μ M ^b	14.25 \pm 1.06 μ M
MDA435/ LCC6 ^{MDR1} + PDMP	2.21 \pm 1.14 nM ^c	1.04 \pm 0.40 nM ^c	3.41 \pm 1.51 μ M	14.25 \pm 1.06 μ M
MDA435/ LCC6 ^{MDR1} + Valspodar	0.05 \pm 0.04 nM	0.61 \pm 0.47 nM	N/D	N/D
MDA435/ LCC6 ^{MDR1} + Valspodar + PDMP	0.05 \pm 0.04 nM	0.52 \pm 0.37 nM	N/D	N/D
MDA435/LCC6 ^{MDR1} + PDMP + C ₆ -Cer	2.40 \pm 1.97 nM	1.18 \pm 0.38 nM	N/D	N/D

^a Cells were incubated with increasing drug concentrations \pm 5 μ M PDMP, 1 μ g/ml Valspodar and/or 2 μ M C₆-ceramide over 72 hours, after which cell viability was analyzed by the MTT assay. The IC₅₀ value was taken as the anticancer drug concentration that inhibits cell growth by 50% relative to untreated control cells.

^b Statistically different from wild-type (p<0.05)

^c Statistically different from resistant cells in the absence of PDMP (p<0.05)

^d Statistically different from resistant cells + 1 μ g/ml Valspodar in the absence of PDMP (p<0.05)

^e Not determined

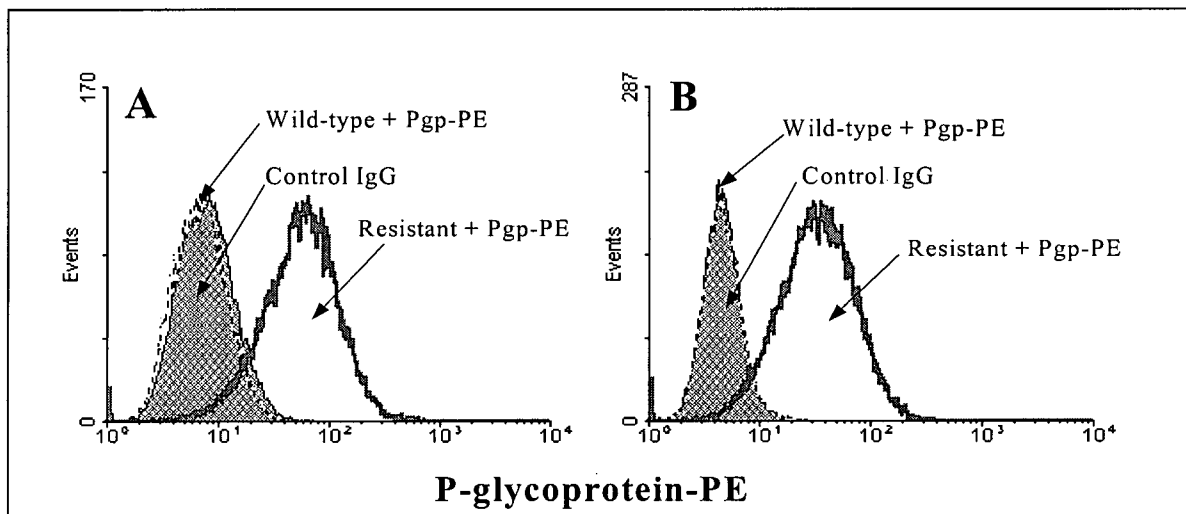


Figure 2.1 Cell-surface P-glycoprotein expression as measured by flow cytometry, demonstrating 9.5 times greater Pgp expression in multidrug resistant MCF7 cells compared to wild-type (A) and 6.8 times greater Pgp expression in multidrug resistant MDA435/LCC6 cells compared to wild-type (B) as shown by flow cytometry. Cells were stained with mouse isotype control-PE (Phycoerythrin) or mouse anti-human Pgp-PE antibody and analyzed by flow cytometry using the EPICS Elite^{ESP} flow cytometer (Beckman-Coulter, Miami, FL).

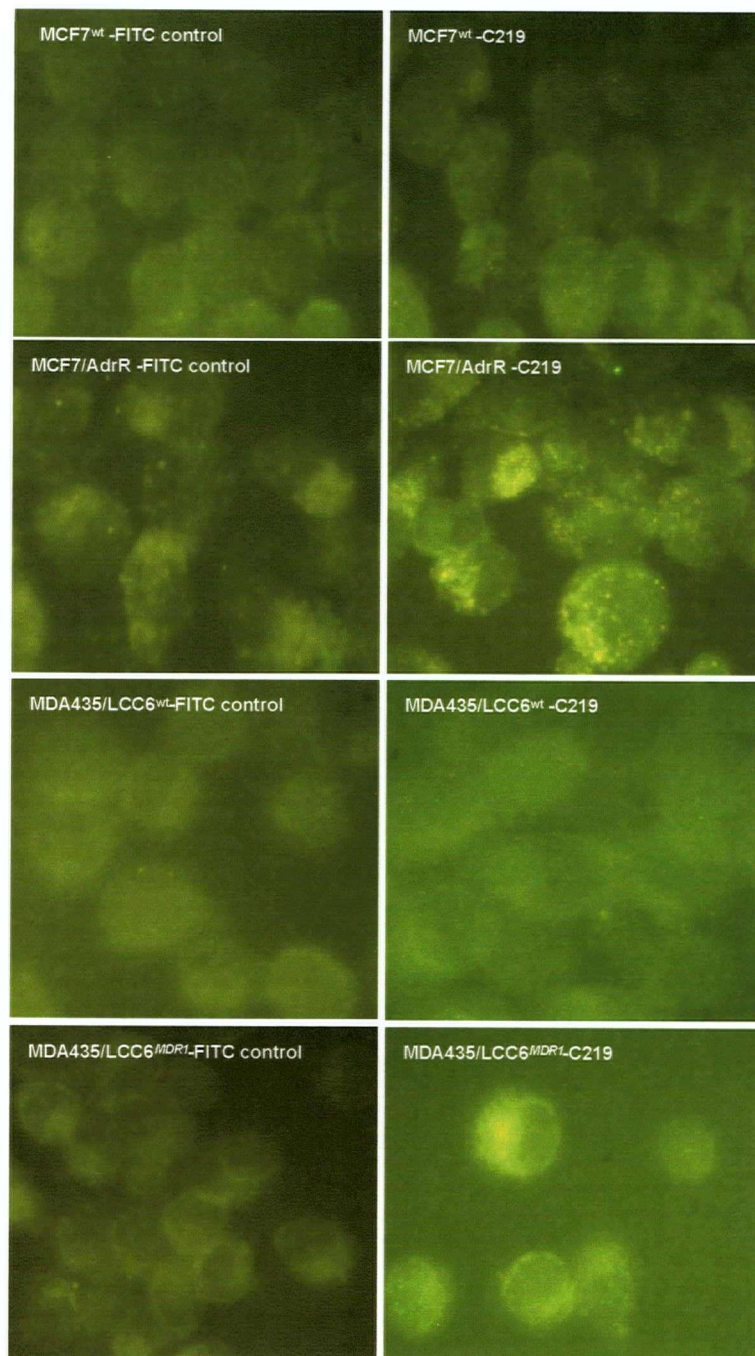


Figure 2.2 Fluorescence microscopy images of intracellular Pgp staining in wild-type and multidrug resistant MCF7 and MDA435/LCC6 cells following two-step staining with mouse anti-human Pgp C219 primary and goat anti-mouse IgG FITC secondary antibodies. Images were acquired with a Leica DC 100 fluorescence microscope (Leica Microsystems (Canada), Richmond Hill, ON, Canada) and later processed with Adobe Photoshop 4.0 in an identical manner.

As described in Chapter 1, there are numerous mechanisms that are known to contribute to the MDR phenomenon. In order to investigate the specific involvement of ceramide production and metabolism, the ability of PDMP to sensitize the resistant cell lines to conventional chemotherapeutic agents by virtue of inhibition of ceramide metabolism to GlcCer was investigated. Cells were exposed to increasing concentrations of anticancer drug in the absence or presence of a non-toxic (5 μ M) concentration of PDMP. Chemosensitization was evaluated by comparing the anticancer drug IC₅₀ values (concentration of drug required to inhibit cell growth by 50% relative to untreated controls) in the presence and absence of PDMP, and a decrease in IC₅₀ value toward that of the wild-type counterpart was indicative of chemosensitization. PDMP induced statistically significant chemosensitization of both resistant cell lines to the cytotoxic effects of Taxol[®] and vincristine. In the MCF7/AdrR cell line, PDMP decreased the Taxol[®] IC₅₀ from $3.24 \pm 0.06 \mu\text{M}$ to $0.50 \pm 0.20 \mu\text{M}$ and the vincristine IC₅₀ from $11.02 \pm 2.16 \mu\text{M}$ to $1.82 \pm 0.16 \mu\text{M}$ (Figure 2.3 and Table 2.1). In the MDA435/LCC6^{MDR1} cell line PDMP decreased the Taxol[®] IC₅₀ from $30.01 \pm 4.13 \text{ nM}$ to $2.21 \pm 1.14 \text{ nM}$ and the vincristine IC₅₀ from $39.25 \pm 7.90 \text{ nM}$ to $1.04 \pm 0.40 \text{ nM}$ (Figure 2.4 and Table 2.1). PDMP had no effect on the IC₅₀ values for the wild-type counterparts of either cell line (Table 2.1). Interestingly, PDMP did not sensitize the resistant cells to the cytotoxic effects of the non-tubulin binding drugs doxorubicin or cisplatin (Table 2.1). The presence of a PDMP-induced chemosensitization effect in the *mdr-1* transfected MDA435/LCC6^{MDR1} cell line was surprising since these cells are not

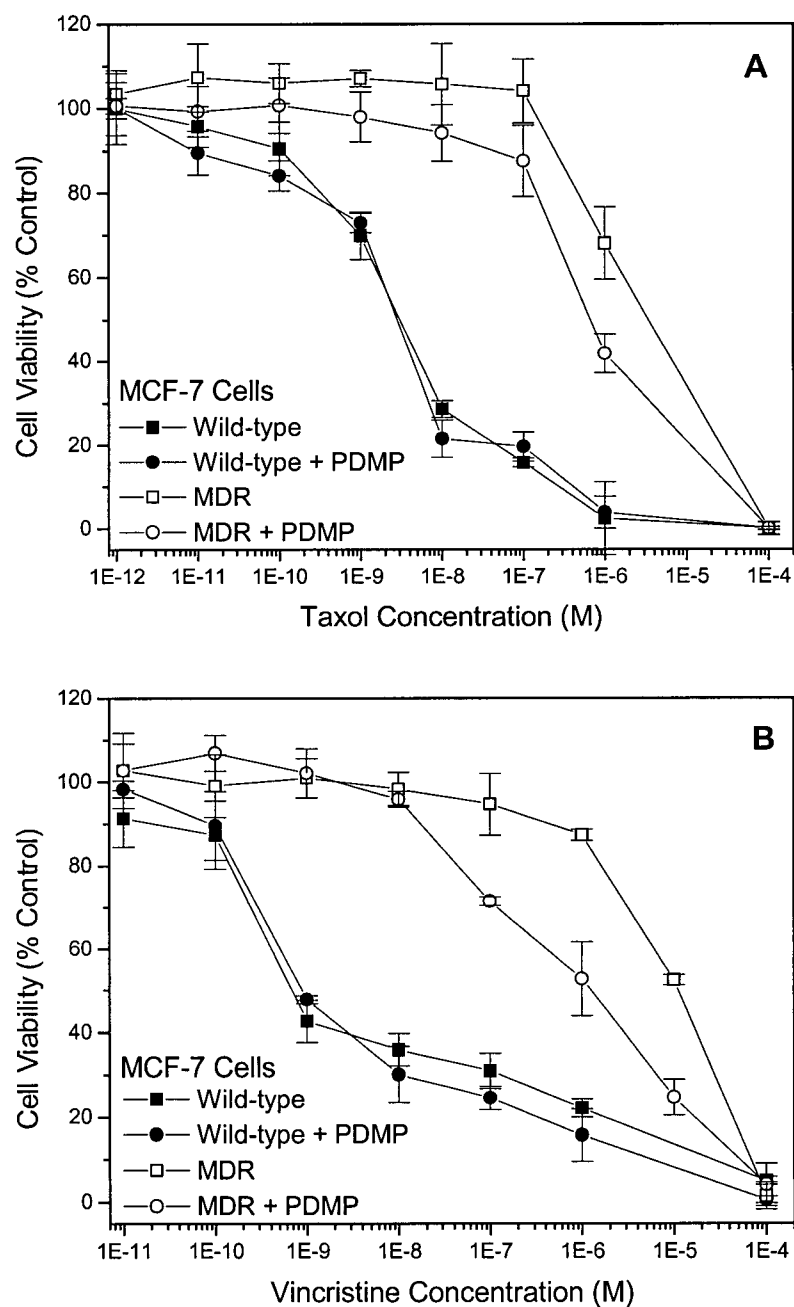


Figure 2.3 Effect of 5 μ M PDMP on Taxol[®] (A) and vincristine (B) cytotoxicity in wild-type and multidrug resistant MCF7 cells. Cells were incubated with the indicated anticancer drug concentrations \pm PDMP for 72 hours and cell viability was measured using the MTT assay. Each value represents the mean from at least three independent experiments; bars, SD.

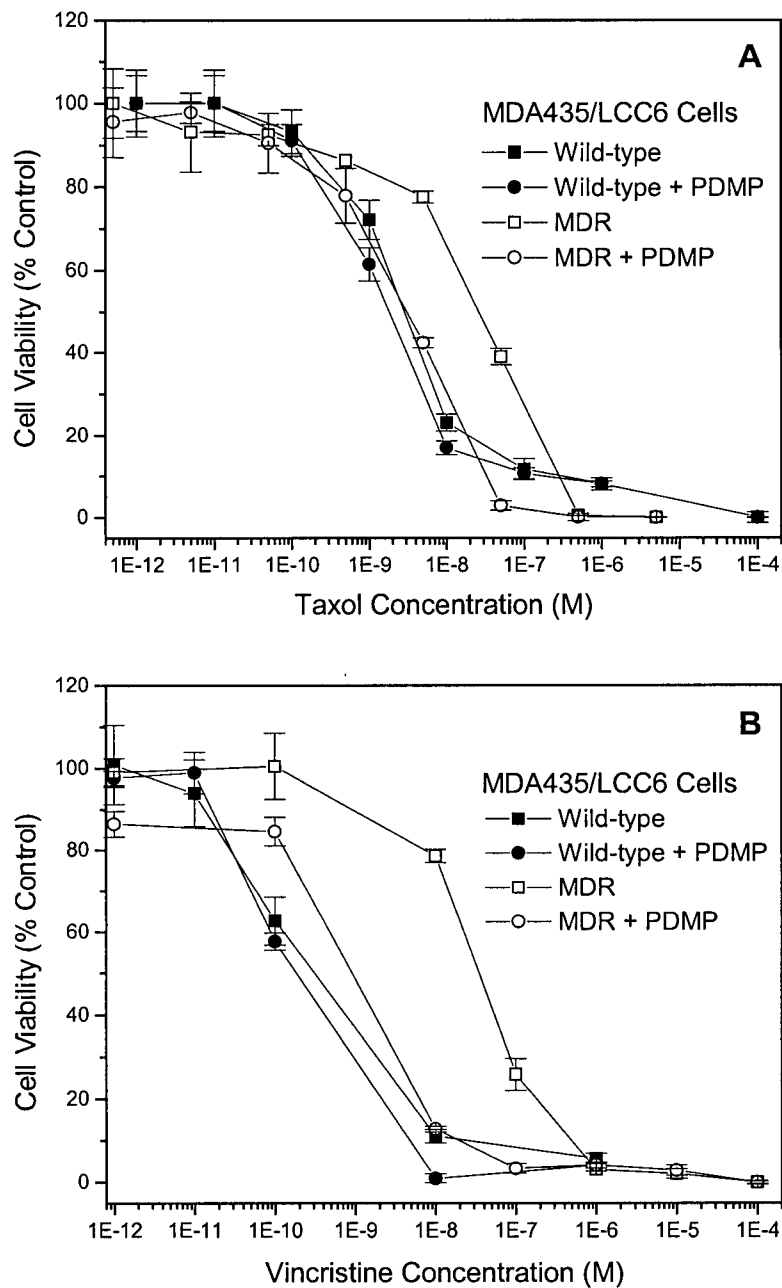


Figure 2.4 Effect of 5 μ M PDMP on Taxol[®] (A) and vincristine (B) cytotoxicity in wild-type and multidrug resistant MDA435/LCC6 cells. Cells were incubated with the indicated anticancer drug concentrations \pm PDMP for 72 hours and cell viability was measured using the MTT assay. Each value represents the mean from at least three independent experiments; bars, SD.

known to overexpress GCS. The observed PDMP effect in these cells therefore suggested an additional involvement of Pgp in ceramide-mediated resistance.

In order to demonstrate that the chemosensitization effect was not simply due to PDMP-induced alterations in cellular drug uptake, cells were incubated with 10 nM (MDA435/LCC6 cells) or 500 nM (MCF7 cells) Taxol[®] + 0.25 μ Ci/ml [³H]Taxol[®] for 1 and 4 hours in the absence and presence of 5 μ M PDMP. The presence of PDMP did not affect cellular drug accumulation, since the percent accumulation of total [³H]Taxol[®] after 1 and 4 hours was the same in the presence and absence of PDMP (Figure 2.5). Although the IC₅₀ values for the wild-type and resistant counterparts of each cell line are different, cells were incubated with the same Taxol[®] concentration so that direct comparisons between uptake levels in the wild-type versus MDR cells could be made. A Taxol[®] concentration intermediate between the respective IC₅₀ values was chosen. The results show increased Taxol[®] accumulation in both wild-type cell lines compared to their MDR counterparts, which is consistent with Pgp overexpression. Specifically, Taxol[®] accumulation was 2.5-3-fold greater in the MCF7^{wt} cells compared to MCF7/AdrR cells, and was approximately 4-fold greater in MDA435/LCC6^{wt} cells compared to MDA435/LCC6^{MDR1} cells.

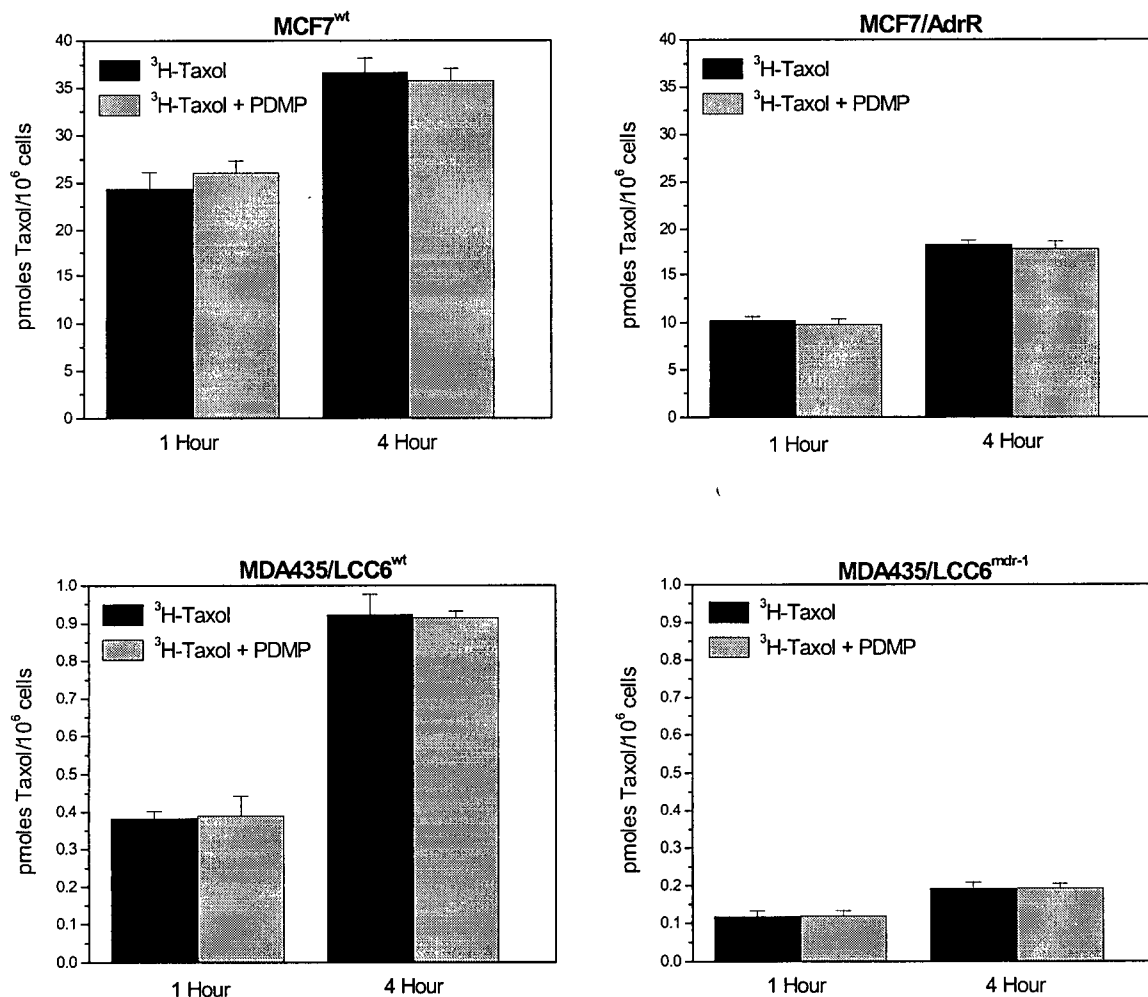


Figure 2.5 Accumulation of [³H]Taxol[®] in wild-type and multidrug resistant MCF7 and MDA435/LCC6 cells. MCF7 cells were incubated with 500 nM Taxol[®] + 0.25 μ Ci/ml [³H]Taxol[®] and MDA435/LCC6 cells with 10 nM Taxol[®] + 0.25 μ Ci/ml [³H]Taxol[®] in the presence and absence of 5 μ M PDMP for the times indicated. Culture medium was removed and cells were washed twice with ice-cold PBS. Cells were harvested by scraping into PBS and radioactivity was measured by liquid scintillation counting. Uptake is expressed as picograms Taxol[®]/10⁶ cells and was corrected for binding using controls incubated at 4°C. Each value represents the mean from three experiments; bars, SD.

2.4.2 Influence of Exogenous C₆-ceramide on PDMP-Induced Chemosensitization

Based on studies to date, PDMP-induced chemosensitization effects are presumably attributed to increased intracellular ceramide accumulation as its metabolism to GlcCer is blocked. On this basis it was speculated that the addition of exogenous short-chain ceramide, which is itself cytotoxic (244), may further enhance this chemosensitization effect. In order to test this, cytotoxicity experiments with the various anticancer drugs were repeated in the presence of 2 μ M C₆-ceramide. This ceramide concentration reflected the approximate IC₂₀ (20% reduction of cell growth), which would provide ceramide exposure without causing high cell death by itself. Combined treatment with Taxol[®] or vincristine plus PDMP and ceramide did not enhance chemosensitivity beyond that achieved by exposure to Taxol[®] or vincristine with PDMP in the absence of exogenous ceramide (Table 2.1).

2.4.3 Effect of Pgp Inhibition on PDMP-Induced Chemosensitization

In order to determine whether Pgp was involved in mediating the PDMP-induced effect, the cytotoxicity experiments were repeated in the presence of 1 μ g/ml Valspodar, a potent Pgp inhibitor. Side-by-side cytotoxicity experiments were conducted in order to assess the degree of PDMP-induced shift in Taxol[®]/vincristine IC₅₀ values compared to the degree of PDMP-induced shift in the Taxol[®]/vincristine + 1 μ g/ml Valspodar IC₅₀ values. Although Valspodar itself induces Taxol[®] and vincristine chemosensitization by virtue of Pgp blockade, the focus of this experiment was to measure the degree of any further chemosensitization upon subsequent addition of PDMP. The PDMP effect in the

presence or absence of Valspodar was expressed as a sensitization ratio (SR), which was calculated as:

$$\text{SR} = (\text{Drug IC}_{50} \text{ treatment} - \text{PDMP}) / (\text{Drug IC}_{50} \text{ treatment} + \text{PDMP})$$

In the MCF7/AdrR cell line the presence of Pgp blockade induced by Valspodar treatment resulted in a 3-fold decrease in the SR for both Taxol[®] (SR = 6.5 without and SR = 2.0 with Valspodar) and vincristine (SR = 6.1 without and SR = 2.0 with Valspodar). In the MDA435/LCC6^{MDR1} cell line, treatment with Valspodar eliminated the sensitization ratio completely (SR = 1.0) for both Taxol[®] and vincristine (Table 2.2). The diminished PDMP effect in the presence of Pgp blockade further supported a role for Pgp in the regulation of ceramide metabolism to GlcCer, and indicated that Pgp function was related to the PDMP response. Valspodar had no effect on the chemosensitivity of the wild-type, non-Pgp expressing cell lines.

2.4.4 Correlation of Chemosensitization Effects with Glucosylceramide Levels

In order to correlate the observed chemosensitization effects with changes in intracellular lipids, baseline and treatment-induced ceramide and GlcCer levels in wild-type and MDR cells were analyzed by TLC. GlcCer levels were approximately equal in the wild-type MDA435/LCC6 and the *mdr-1* gene transfected MDA435/LCC6^{MDR1} cells (1.52 ± 0.21 and 1.54 ± 0.09 percent total [³H]lipid, respectively), which is consistent with lack of GCS overexpression in this cell line. By contrast, GlcCer was elevated 2-fold in the drug-selected MCF7/AdrR cells compared to wild-type cells (Table 2.3). Elevated GlcCer in this cell line is consistent with previous reports (61, 62), and confirmed that GCS is overexpressed in these cells. Treatment of the MCF7/AdrR cells

Table 2.2

The Effect of Pgp Blockade on the Degree of PDMP-Induced Chemosensitization in MCF7/AdrR and MDA435/LCC6^{MDR1} Cells as Measured by a Sensitization Ratio

	Sensitization Ratio (SR)^{a,b}	
	Taxol[®]	Vincristine
MCF7/AdrR ± 5µM PDMP	6.48	6.07
MCF7/AdrR + 1µg/ml Valspodar ± 5µM PDMP	2.00	1.97
MDA435/LCC6 ^{MDR1} ± 5µM PDMP	13.57	37.74
MDA435/LCC6 ^{MDR1} + 1µg/ml Valspodar ± 5µM PDMP	1.11	1.16

^a Cells were incubated with increasing Taxol[®] or vincristine concentrations ± 5 µM PDMP with and without 1 µg/ml Valspodar for 72 hours. Cell viability was analyzed using the MTT assay.

^b SR = (Drug IC₅₀ treatment – PDMP)/(Drug IC₅₀ treatment + PDMP) using the IC₅₀ values presented in Table 2.1.

with 5 μ M PDMP reduced GlcCer to levels comparable to the wild-type counterpart, indicating that PDMP indeed inhibits GlcCer formation. This decrease in GlcCer was correlated with a 1.7-fold increase in pro-apoptotic ceramide, which provides the basis for PDMP-induced chemosensitization. Treatment with PDMP did not alter GlcCer levels in the MCF7 wild-type cells.

Treatment with 1 μ g/ml Valspodar increased ceramide production by approximately 4-fold and GlcCer production by approximately 1.5 fold in the MCF7/AdrR cells. This was expected based on previous demonstration that Valspodar does elevate intracellular ceramide (245). Because these cells overexpress GCS, it would be expected that much of the ceramide formed in response to Valspodar would be converted to GlcCer. Combined treatment with Valspodar + PDMP returned GlcCer back to wild-type levels but increased ceramide a further 1.5-fold. This supports the finding that PDMP-induced chemosensitization was still observed in the presence of Pgp blockade, although to a lesser degree.

Table 2.3

Incorporation of [³H]Palmitic Acid into Ceramide and Glucosylceramide of Treated and Control MCF7 Cells

Lipid	Percent [³ H]lipid ± SD ^a					
	MCF7-wt	MCF7-wt + PDMP	MCF7/AdrR	MCF7/AdrR + PDMP	MCF7/AdrR + Valspodar	MCF7/AdrR + Valspodar + PDMP
Cer	0.54 ± 0.09	0.25 ± 0.01	0.21 ± 0.03	0.35 ± 0.05 ^b	0.86 ± 0.01	1.33 ± 0.08 ^c
GlcCer	1.19 ± 0.07	1.16 ± 0.18	2.19 ± 0.15	1.32 ± 0.12 ^b	3.02 ± 0.35	1.16 ± 0.09 ^c

^a Cells were incubated with 1.0 µCi/ml [³H]palmitic acid in complete medium for 24 hours, washed and harvested by scraping. Total lipids were extracted using equal volumes of methanol-2% acetic acid/chloroform/water. The radioactivity of total extracted lipids was measured by scintillation counting. Lipids were spotted onto TLC plates and developed in chloroform/acetic acid (90:10) for ceramide or chloroform/methanol/ammonium hydroxide (70:20:4) for GlcCer. Lipid spots corresponding to co-chromatographed standards were scraped into scintillation vials for quantitation by liquid scintillation counting. The lipid amounts presented are expressed as a percentage of the total tritiated lipid extracted from the cells.

^b Statistically different from MCF7/AdrR in the absence of 5µM PDMP (p<0.05)

^c Statistically different from MCF7/AdrR + 1 µg/ml Valspodar in the absence of 5µM PDMP (p<0.05)

2.5 DISCUSSION

The emerging role of ceramide as an intracellular signaling molecule involved in mediating apoptosis and MDR suggests that the ability to modulate ceramide metabolism should provide a new avenue by which drug sensitivity in MDR cells may be increased. The small molecule PDMP is a competitive inhibitor of the GCS enzyme that blocks the conversion of pro-apoptotic ceramide to non-cytotoxic GlcCer at doses which are non-toxic to cells. It has previously been demonstrated that PDMP sensitizes murine neuroblastoma cells to Taxol[®] and vincristine (132). The results presented in this chapter extend the study of PDMP-induced chemosensitization to two human breast cancer cell lines. The chemosensitization effects of PDMP-altered ceramide metabolism in resistant MCF7/AdrR and MDA435/LCC6^{MDR1} cell lines, which were developed for resistance by drug selection and *mdr-1* gene transfection, respectively, were compared. The rationale for choosing these cell lines was based on the fact that although both lines overexpress Pgp, the transfected MDA435/LCC6^{MDR1} cell line does not exhibit elevated GCS whereas GCS expression in the MCF7/AdrR cells is increased. Consequently, these differences allowed for the differentiation of sensitization effects associated with ceramide metabolism versus Pgp transport.

A non-toxic dose of PDMP was found to induce significant chemosensitization to Taxol[®] and vincristine in both of the resistant breast cancer cell lines under investigation. Interestingly, chemosensitization was not observed with the non-tubulin binding drugs doxorubicin or cisplatin. Since Taxol[®] and vincristine have both been demonstrated to induce ceramide formation in cancer cells (174, 246), it might initially seem that the PDMP effect was simply due to inhibition of the metabolism of pro-apoptotic ceramide

induced by the cytotoxic drugs to non-apoptotic GlcCer. However, if this were the case one would expect to see PDMP-induced sensitization in the GCS overexpressing MCF7/AdrR cells only. Similar to wild-type MDA435/LCC6 cells, which are not affected by PDMP, the MDA435/LCC6^{MDR1} cells do not display elevated GCS yet PDMP still induced a chemosensitization response. The commonality between the MCF7/AdrR and MDA435/LCC6^{MDR1} cell lines, however, is elevated Pgp expression, and this led to the investigation of a possible role for Pgp in ceramide signaling. This was further supported by the fact that PDMP had no effect on the chemosensitivity of non-Pgp expressing wild-type MCF7 or MDA435/LCC6 cells. The fact that the PDMP-induced effect is specific for tubulin-binding drugs is itself interesting, and suggests that intracellular transport mechanisms/microtubule assembly may be involved in the processes of ceramide signaling and/or metabolism.

In order to rule out the possibility that PDMP modulated chemosensitivity via non-specific alterations in cellular drug uptake the accumulation of radiolabeled Taxol[®] in the presence and absence of PDMP was measured. PDMP had no effect on the cellular uptake of Taxol[®]. Consequently, chemosensitization in the MDR cell lines was not attributable to increased intracellular anticancer drug concentrations.

In order to assess whether the combination of PDMP plus exogenous ceramide would further enhance the PDMP-induced chemosensitization effect the cytotoxicity assays were repeated in the presence of 2 μ M C₆-ceramide. Since this is a cell-permeable ceramide, it readily and rapidly distributes to various membranes within the cell. The observation that combination treatment with Taxol[®] or vincristine plus PDMP and ceramide did not further enhance chemosensitivity may be explained by the fact that

short-chain, cell-permeable ceramides can readily distribute to numerous intracellular locations due to their relatively hydrophilic nature. It has been reported that short-chain ceramides can be glycosylated (247). However, GCS is specifically localized to the cytoplasmic face of the Golgi (248, 249). Therefore, a significant proportion of exogenously added ceramide would be expected to localize in GCS-poor regions. Consequently, addition of PDMP may not significantly impact overall ceramide-induced apoptosis because the pool(s) of ceramide being modulated by PDMP are small relative to the overall amount of ceramide that is distributed throughout the cell.

The specific involvement of Pgp in ceramide-mediated apoptosis was examined by evaluating the chemosensitization effect of PDMP in the presence of 1 $\mu\text{g/ml}$ Valspodar, a potent Pgp inhibitor. Interestingly, under conditions of Pgp blockade the PDMP effect was no longer observed in the MDA435/LCC6^{MDR1} cells, and was decreased 3-fold in the MCF7/AdrR cells. This suggested that Pgp function is involved in regulating ceramide metabolism to GlcCer.

Figure 2.6 provides an illustration of the proposed relationship between Pgp, GlcCer and PDMP that is consistent with these observations. The presence of intracellularly distributed Pgp has been demonstrated by a number of groups (250-254), and was confirmed in the two MDR cell lines under investigation by fluorescence microscopy studies. Functional Pgp activity has been previously demonstrated in the Golgi of multidrug resistant cells, including the same MCF7/AdrR cell line used in these studies (251, 252). It has also been shown that Pgp can mediate the translocation of GlcCer from the cytoplasmic face of the Golgi to the lumen where further processing to higher glycosphingolipid species is known to occur (255-257). Wild-type (drug

sensitive) cells do not overexpress Pgp or GCS so exposure of these cells to anticancer agents results in increased intracellular ceramide and subsequent apoptosis. The negligible chemosensitizing effects of PDMP in these cells is attributed to the fact that relatively little ceramide is metabolized to GlcCer, and an equilibrium exists between ceramide and GlcCer that is generated. Resistant cells that overexpress Pgp are capable of translocating GlcCer across the Golgi membrane. In these cells the loss of GlcCer from the cytoplasmic face of the Golgi provides a driving force for further ceramide to GlcCer conversion. Continuous removal of GlcCer by Pgp removes the negative feedback control on the GCS enzyme and promotes further ceramide metabolism. This could explain why a PDMP-induced chemosensitization effect was observed in the MDA435/LCC6^{MDR1} cells even though they do not display elevated GlcCer. The loss of sensitization in the presence of Valspodar further supports this theory.

In the case of the MCF7/AdrR cells that additionally overexpress GCS, ceramide generated by anticancer drug exposure is rapidly converted to GlcCer before apoptosis pathways can be activated. Chemosensitization was observed in these cells because PDMP inhibits the conversion of ceramide to GlcCer. When PDMP is co-incubated with Valspodar the Pgp-mediated translocation of GlcCer across the Golgi should be blocked. This causes a relative accumulation of GlcCer on the cytoplasmic face of the Golgi, which in turn reduces the ceramide to GlcCer conversion via negative feedback. In this case PDMP is still acting as an inhibitor of the GCS enzyme, but the PDMP effect is diminished due to GlcCer product feedback inhibition.

Taken together, the research contained in this chapter provides an increased understanding of the relationship between ceramide, ceramide metabolism and Pgp in the

context of multidrug resistance and chemosensitization. These observations suggest that therapeutic approaches aimed at increasing intracellular endogenous ceramide levels should enhance apoptosis. Based on these results, the focus of the research presented in Chapter 3 was to investigate the utility of exogenously applied ceramide lipids in achieving this goal.

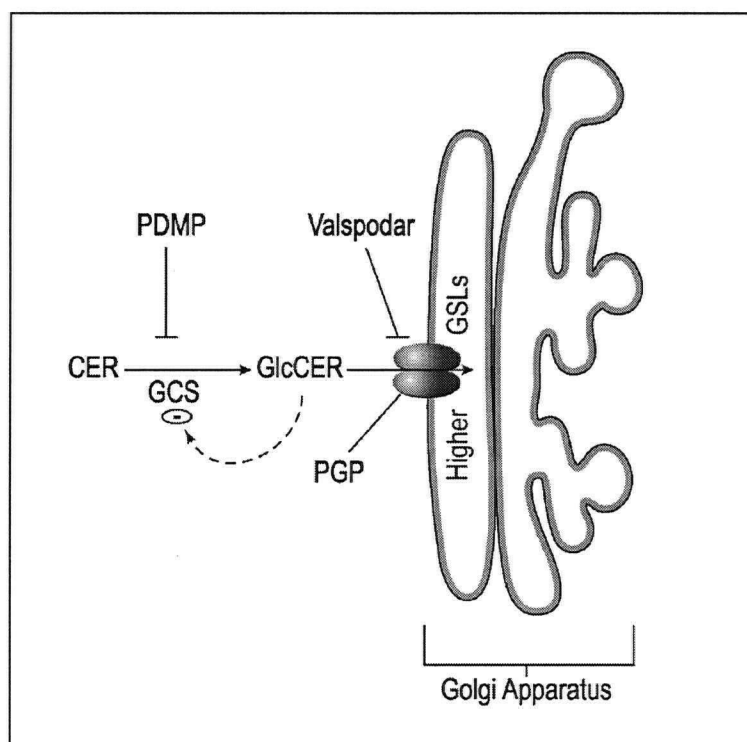


Figure 2.6 A model to explain the influence of Pgp on ceramide metabolism in the context of chemosensitization. Wild-type cells that do not overexpress Pgp or the GCS enzyme do not display PDMP-induced chemosensitization because very little ceramide is converted to glucosylceramide. Multidrug resistant cells that do overexpress Pgp, however, may translocate newly-formed GlcCer across the Golgi membrane. This provides a driving force for further Cer to GlcCer conversion and reduces negative feedback on the GCS enzyme. Inhibition of Pgp promotes GlcCer accumulation in the cytoplasm and reduces GlcCer formation via negative feedback, which in turn reduces PDMP-induced chemosensitization. Abbreviations used: cer, ceramide; GCS, glucosylceramide synthase; GlcCer, glucosylceramide; GSL, glycosphingolipid.

CHAPTER 3

INTRACELLULAR DELIVERY OF EXOGENOUS CERAMIDE LIPIDS INDUCES APOPTOSIS IN VITRO*

3.1 INTRODUCTION AND RATIONALE

The role of ceramide as a mediator of apoptosis has attracted significant recent attention. Although the specific mechanisms have not been fully defined, the evidence presented in Chapter 1 suggests its direct involvement in regulating cell death. Much of the research on ceramide to date has been aimed at elucidating the mechanism(s) by which it mediates apoptosis and other intracellular effects, and observations made during these studies suggest that stimuli which result in increased intracellular ceramide levels have pro-apoptotic effects. Furthermore, the documented involvement of ceramide in MDR, combined with the chemosensitization results presented in Chapter 2, suggest its therapeutic potential. Therefore, the objectives of the research presented in this chapter were to initially investigate the cellular uptake and cytotoxicity of various chain length synthetic ceramide lipids in order to identify therapeutically active exogenous ceramides, and subsequently to enhance these effects by formulating ceramide into liposome-based delivery systems in an effort to improve intracellular delivery and therefore pro-apoptotic activity.

*Adapted from: JA Shabbits and LD Mayer (2003). *Intracellular delivery of ceramide lipids via liposomes enhances apoptosis in vitro*. *Biochemica et biophysica acta* 78474: 1-9.

3.2 HYPOTHESIS

The hypothesis underlying the research presented in this chapter is that intracellular delivery of exogenous ceramide lipids can be used to induce apoptosis *in vitro*.

3.3 MATERIALS AND METHODS

3.3.1 Materials

All phospholipids and ceramides were obtained from Avanti Polar Lipids (Alabaster, AL). Cholesterol, cholesteryl hemisuccinate and MTT reagent were obtained from Sigma-Aldrich Canada (Oakville, ON, Canada). [^3H]cholesteryl hexadecyl ether (CHE) was purchased from Perkin Elmer (Boston, MA). [^{14}C]C₆- and [^{14}C]C₁₆-ceramide were purchased from American Radiolabeled Chemicals (St. Louis, MO). Dulbecco's Modified Eagle's Medium (DMEM) and Hank's Balanced Salt Solution (without pH indicator; Hank's) were obtained from Stem Cell Technologies (Vancouver, BC, Canada). Fetal bovine serum was purchased from Hyclone (Logan, UT). L-glutamine and trypsin-EDTA were obtained from Gibco BRL (Burlington, ON, Canada). The Micro BCA Protein Assay kit was purchased from Pierce (Rockford, IL). Tissue culture flasks, incubation plates and cell scrapers were obtained from Falcon[®] (Becton Dickinson, Franklin Lakes, NJ). Nucleopore[®] polycarbonate extrusion filters were obtained from Whatman Inc. (Clifton, NJ). Liposomes were prepared using an extrusion apparatus (Lipex Biomembranes, Vancouver, BC, Canada). [^{14}C]lactose and Sephadex G-50 chromatography beads were purchased from the Sigma Chemical Company (St.

Louis, MO). Pico-fluor 40 scintillation cocktail was purchased from Packard Biosciences (Groningen, The Netherlands).

3.3.2 Cell Lines and Culture

The wild-type and *mdr-1* gene transfected MDA435/LCC6 human breast cancer cell lines described in Chapter 2 were used for these studies. The J774 murine macrophage cells also used in these studies were obtained from ATCC (Rockville, MD). Cells were cultured and prepared as described in Chapter 2 with the exception of J774 cells, which were harvested by gentle scraping rather than with trypsin-EDTA.

3.3.3 MTT Cytotoxicity Assays

MTT cytotoxicity assays were performed as previously described in Chapter 2. Free ceramide was diluted from ethanol stocks into complete medium and added to cells in 0.2 ml to achieve the desired final concentration. The C₁₆-ceramide stock was kept warm, diluted into warm medium prior to addition to the cells and remained in solution at all times at the concentrations used in these studies. When the cytotoxicity of ceramide-containing liposome formulations was investigated, calculations were based specifically on the concentration of ceramide added to each well. Control (non-ceramide) formulations were calculated on the basis of total lipid.

3.3.4 Lipid Uptake Studies

Cell suspensions were diluted 1:1 with trypan blue, counted with a hemocytometer and seeded into 6-well Falcon® plates at 2.5×10^5 cells/well in 2 ml

complete medium. The cells were allowed to adhere for 24 hours at 37°C, after which the medium was aspirated and replaced with 1 ml complete medium. Free ceramide was diluted from ethanol stocks into 1 ml complete medium as previously described and added to each well to give the desired final concentration of 1 μ M C₆-ceramide (corresponds to IC₂₀ value) or 50 μ M C₁₆-ceramide. [¹⁴C]ceramide was incorporated at 0.1 μ Ci/nmole for each ceramide lipid to facilitate quantitation. Cells were incubated with the treatments for 1, 4 and 24 hours at 37°C. The incubation medium was then aspirated and cells were washed twice with 2 ml Hank's. Cells were gently scraped into 0.5 ml Hank's and collected into glass scintillation vials using glass pipettes. Each well was rinsed with an additional 0.5 ml Hank's to remove residual cells. An aliquot of cells was removed for protein quantification and the remainder were counted for radioactivity by scintillation counting. Uptake was expressed as pmoles ceramide/ μ g protein and was corrected for binding using controls incubated at 4°C.

3.3.5 Spectrophotometric Protein Quantitation

The protein content of each cell aliquot was determined using the Pierce micro BCA protein assay according to the method included with the assay kit. Briefly, a standard curve was prepared using the supplied purified bovine serum albumin (BSA) diluted in distilled water (dH₂O) to a final volume of 0.5 ml. Samples were prepared using 5 μ l cell suspension + 495 μ l dH₂O. Micro BCA reagents A, B and C were added in the specified ratios. All samples and standards were prepared in glass test tubes, which were heated in a 65°C waterbath for 1 hour and cooled to room temperature. The absorbance at 562 nm of each sample was read against a dH₂O reference. The protein

concentration for each cell sample was determined using a standard curve prepared from the known BSA samples.

3.3.6 Preparation of Liposomes

Lipids were weighed into individual test tubes and dissolved in 1 mL of chloroform (DPPC, DSPC, CHEMS, Chol), ethanol (C₆-ceramide) or chloroform:methanol (2:1, v/v; C₁₆-ceramide). C₁₆-ceramide required brief heating at 65°C to achieve complete dissolution. Appropriate volumes of each lipid were transferred to a single tube in order to achieve the desired ratio of each lipid component. All lipid ratios indicated in this research are on a mole:mole basis unless otherwise indicated. [³H]CHE was incorporated at 1 µCi/mg lipid as a non-exchangeable, non-metabolizable lipid marker (258) to facilitate liposome quantitation. For the preparation of ceramide-containing liposomes, [¹⁴C]C₆-ceramide or [¹⁴C]C₁₆-ceramide was incorporated into the formulation at 0.5 µCi/mg ceramide. The mixtures were evaporated with vortexing and heating under a stream of nitrogen gas and subjected to vacuum drying for a minimum of 4 hours to produce a homogenous lipid film. The lipid film was hydrated in 1 ml of warm Hepes buffered saline (HBS; 20 mM Hepes/150 mM NaCl; pH 7.4) with vortexing. Homogenously sized liposomes were then produced following a 10 cycle extrusion through three stacked 100 nm polycarbonate filters at 65°C for non-ceramide formulations and 95°C for ceramide formulations, using an extrusion apparatus. The resulting mean liposome diameter obtained following extrusion was approximately 100 nm as determined by quasi-elastic light scattering using the Nicomp 270 submicron

particle sizer model 370/270 (209, 229). Liposome and ceramide concentrations were determined by liquid scintillation counting.

3.3.7 Lactose Trapping

In order to determine the liposome trapped volume, [³H]CHE labeled lipid films were prepared as described above and hydrated in HBS (pH 7.4) containing [¹⁴C]lactose at a concentration of 0.23 μ Ci [¹⁴C]lactose/mg lipid. Following extrusion and sizing, the sample was passed down a Sephadex G-50 column equilibrated with HBS. Trapped volume was determined by the following equation:

$$\text{Trapped Volume} = (A/B) / (C/D)$$

where A = [¹⁴C]lactose dpm eluted from the Sephadex G-50 HBS column

B = [¹⁴C]lactose dpm of initial suspension prior to extrusion/ μ l

C = [³H]CHE dpm lipid eluted from the Sephadex G-50 HBS column

D = specific activity of lipid stock (dpm/ μ mole total lipid)

3.3.8 Cryo-Transmission Electron Microscopy

Control and ceramide-containing liposomes were analyzed by cryo-transmission electron microscopy (cryo-TEM) performed in the laboratory of Dr. Katarina Edwards in Uppsala, Sweden. The method employed and interpretation of liposome images have been previously described by that group (259). Briefly, liposome samples were diluted to 10 mM and transferred onto a copper grid containing a holey polymer film in a climate controlled chamber. The samples were blotted to form a thin film, vitrified by submersion in liquid ethane and transferred into the microscope at -165°C for analysis.

3.4 RESULTS

3.4.1 Effect of Ceramide Acyl Chain Length on *In Vitro* Cytotoxicity in MDA435/LCC6 Human Breast Cancer Cells

The cytotoxic activity of free, exogenous ceramides with increasing acyl chain length was evaluated by incubating the MDA435/LCC6 and MDA435/LCC6^{MDR1} cells with free C₂-, C₆-, C₈-, C₁₀-, C₁₄-, or C₁₆-ceramide over a range of 0-100 μ M final ceramide concentration. Both the wild-type and MDR cell lines were investigated in order to determine whether therapeutic strategies based on exogenous ceramide administration might be equally effective against sensitive and resistant tumor cells. The 72 hour MTT cytotoxicity results shown in Figure 3.1 demonstrate that cytotoxic activity is affected by ceramide acyl chain length, with the C₆- and C₈-ceramides being the most potent. This may be explained by the cell-permeability characteristics of the various ceramides. In order to be active, the exogenous ceramide must transfer from the tissue culture medium in which it is dispersed, cross the plasma membrane of the cell and exchange into cellular membranes from which it can interact with its intracellular target(s). The C₂-ceramide, having the shortest acyl chain and therefore being the most hydrophilic, likely remains dispersed in the tissue culture media and does not readily exchange into cell membranes. This is consistent with the observed IC₅₀ values of 74 μ M and 79 μ M for the wild-type and MDR cell lines, respectively (Table 3.1). The C₆- and C₈-ceramides were the most cytotoxic, with IC₅₀ values in the 3-14 μ M range, likely due to their highly cell-permeable nature. As the chain length increased to C₁₀-, C₁₄- and C₁₆-ceramide the hydrophobic nature also increased. This would be expected to decrease the water solubility of the lipids and may reduce availability to intracellular membranes. Accordingly, IC₅₀ values of 45 μ M for C₁₀-ceramide and greater than 100 μ M for C₁₄-

and C₁₆-ceramides were obtained. These results led to the identification of C₆-ceramide as the most potent exogenous ceramide form.

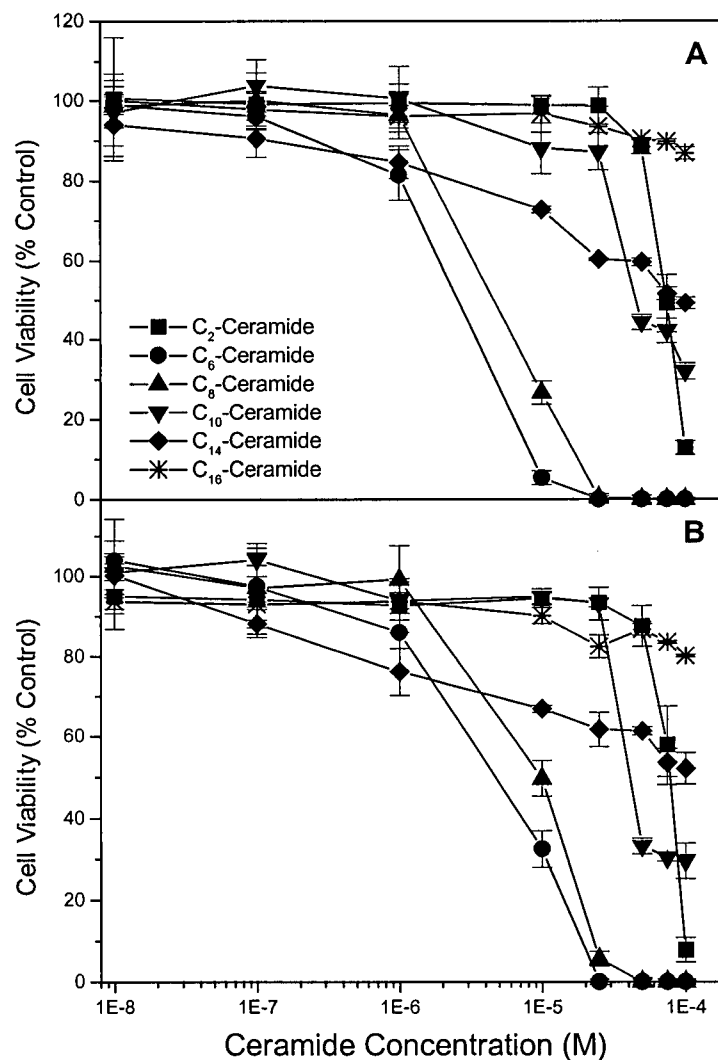


Figure 3.1 Cytotoxicity of various acyl chain length free ceramide lipids on wild-type (A) and *mdr-1* gene transfected (B) MDA435/LCC6 human breast cancer cells. Cells were incubated with the indicated ceramide concentrations for 72 hours and cell viability was measured using the MTT assay. Each value represents the mean from three independent experiments conducted in triplicate; bars, SD.

Table 3.1**Cytotoxicity of Various Acyl Chain Length Free Ceramide Lipids in Wild-type and Resistant MDA435/LCC6 Human Breast Cancer Cells**

Cell Line	IC ₅₀ ^a ± SEM (μM)					
	C ₂ -Cer	C ₆ -Cer	C ₈ -Cer	C ₁₀ -Cer	C ₁₄ -Cer	C ₁₆ -Cer
Wild-type	73.60±7.92	2.71±0.69	7.00±3.25	44.10±2.69	>100	>100
Resistant	79.20±6.04	5.67±0.70	13.95±2.19	46.00±1.39	>100	>100

^aCells were incubated with increasing concentrations of free ceramide lipids of varying acyl chain length over 72 hours and cell viability was measured using the MTT assay. The IC₅₀ value was taken as the ceramide concentration that inhibits cell growth by 50% relative to untreated control cells.

3.4.2 Correlation of MTT Cytotoxicity Results with Ceramide Uptake

In order to examine whether acyl chain length determines ceramide cytotoxicity because of differences in cell-permeability, cellular uptake studies using radioactive C₆- and C₁₆-ceramides were conducted. Figure 3.2 shows that in both the wild-type and resistant cell lines the [¹⁴C]C₆-ceramide levels steadily increased to 7 pmol ceramide/μg protein over the 24 hour incubation period while [¹⁴C]C₁₆-ceramide levels remained under 2 pmol ceramide/μg protein over 24 hours, which correlates with its lack of cytotoxic effect.

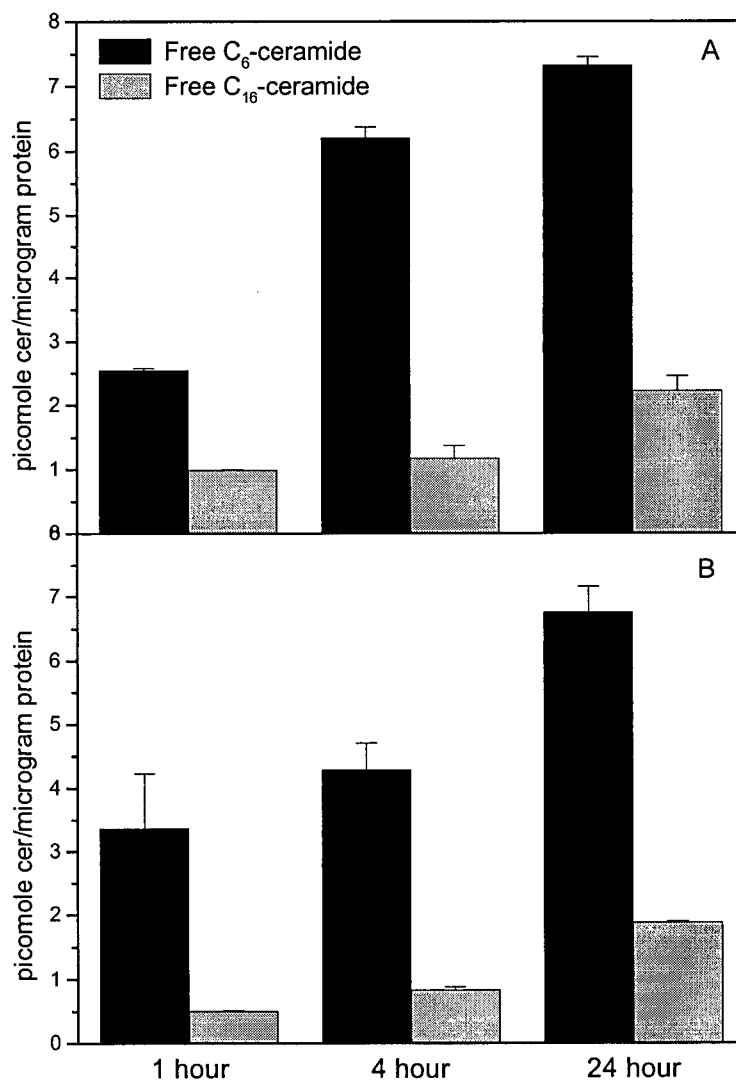


Figure 3.2 Cellular uptake of free C₆- and C₁₆-ceramide by wild-type (A) and *mdr-1* gene transfected MDA435/LCC6 cells (B). Cells were incubated with 1 μ M C₆-ceramide or 50 μ M C₁₆-ceramide for the times indicated. [¹⁴C]C₆- or [¹⁴C]C₁₆-ceramide was added at 0.1 μ Ci/nmole ceramide for quantitation by scintillation counting. Cellular protein was measured spectrophotometrically (Abs 562 nm) using the micro BCA protein assay kit. Uptake is expressed as pmoles ceramide/ μ g protein and was corrected for binding using controls incubated at 4°C. Data are averaged means from two independent experiments conducted in triplicate; bars, SD.

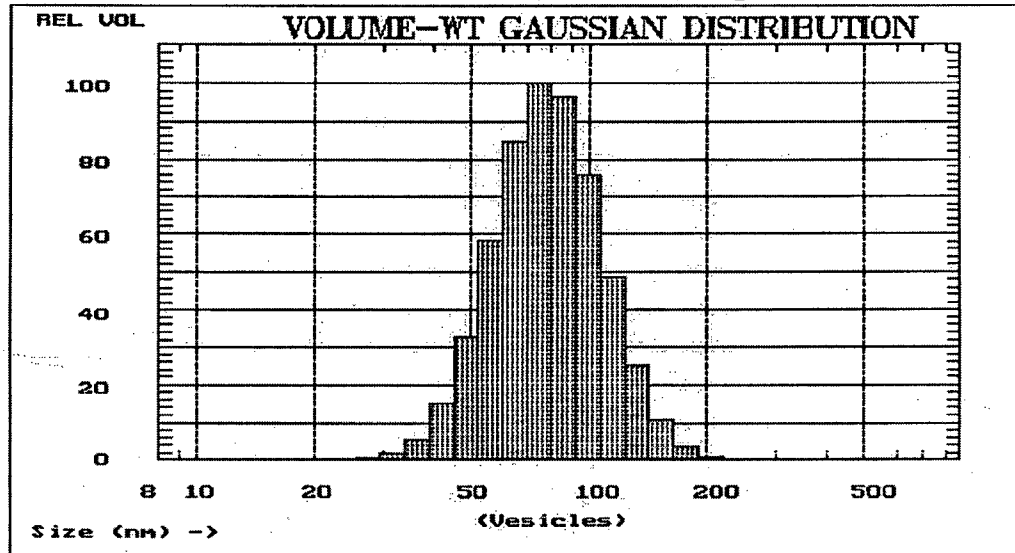
These results highlighted the importance of intracellular ceramide delivery in order to obtain the intended apoptotic response. Given its role as a bioactive lipid with dose-dependent cytotoxic activity, formulation of C₆-ceramide into liposomes was investigated in order to facilitate the delivery of large amounts of this cytotoxic ceramide lipid to cells by virtue of the drug delivery characteristics of liposomes described in Chapter 1.

3.4.3 Formulation and Cytotoxicity of C₆-Ceramide Containing Liposomes

Liposomes containing up to 45 mole percent C₆-ceramide were successfully formulated into conventional DSPC/Chol liposomes with an overall composition of C₆-cer/DSPC/Chol (45:10:45). These liposomes displayed a mean diameter of 82.7 nm with a standard deviation of 31.8% (Figure 3.3) as measured by quasi-elastic light scattering using a Nicomp 270 submicron particle sizer model 370/270. Attempts to increase the level of ceramide incorporation beyond 45 mole percent resulted in difficulties hydrating the lipid film due to the formation of lipid aggregates. Control (non-ceramide) liposomes composed of DSPC/Chol (55:45), which have been extensively characterized in previous literature (208, 260), displayed a mean diameter of 101.2 nm with a standard deviation of 22% (Figure 3.3).

Following successful formulation of C₆-ceramide into liposomes, the *in vitro* cytotoxicity of this formulation was then evaluated. Figure 3.4 demonstrates that C₆-ceramide liposomes were cytotoxic to cells *in vitro*, with IC₅₀ values of $15.5 \pm 2.6 \mu\text{M}$ and $19.9 \pm 4.72 \mu\text{M}$ for wild-type and *mdr-1* gene transfected MDA435/LCC6 cells, respectively. The cytotoxicity was ceramide-specific, as control liposomes composed of

A: C₆-cer/DSPC/Chol (45:10:45) Liposomes



B: DSPC/Chol (55:45) Liposomes

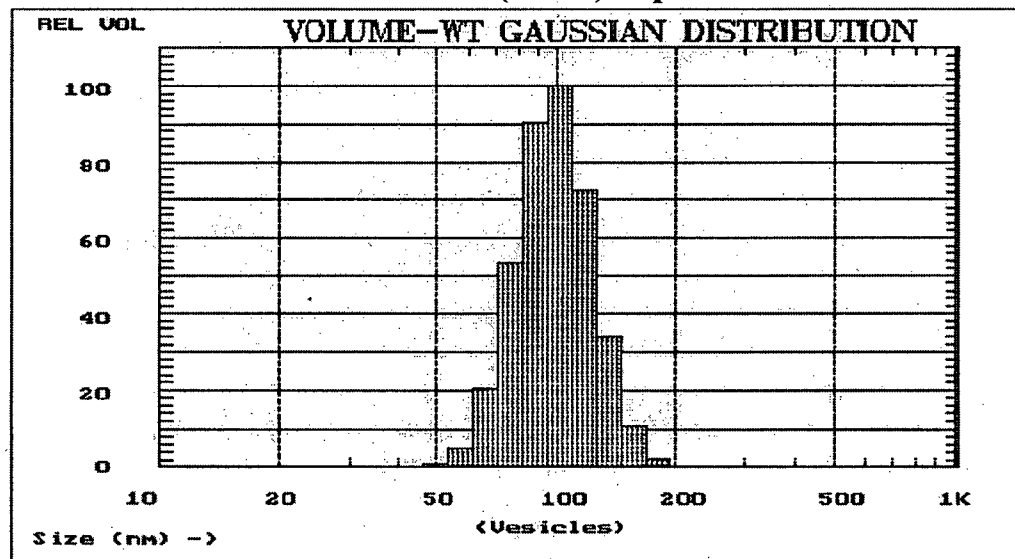


Figure 3.3 Mean liposome diameters of 82.7 ± 26.3 nm for C₆-cer/DSPC/Chol (45:10:45; A) and 101.2 ± 22.3 nm for DSPC/Chol (55:45; B) liposomes as determined by quasi-elastic light scattering using a Nicomp 270 submicron particle sizer model 370/270. Hepes buffered saline pH 7.4 was used for sample dilution.

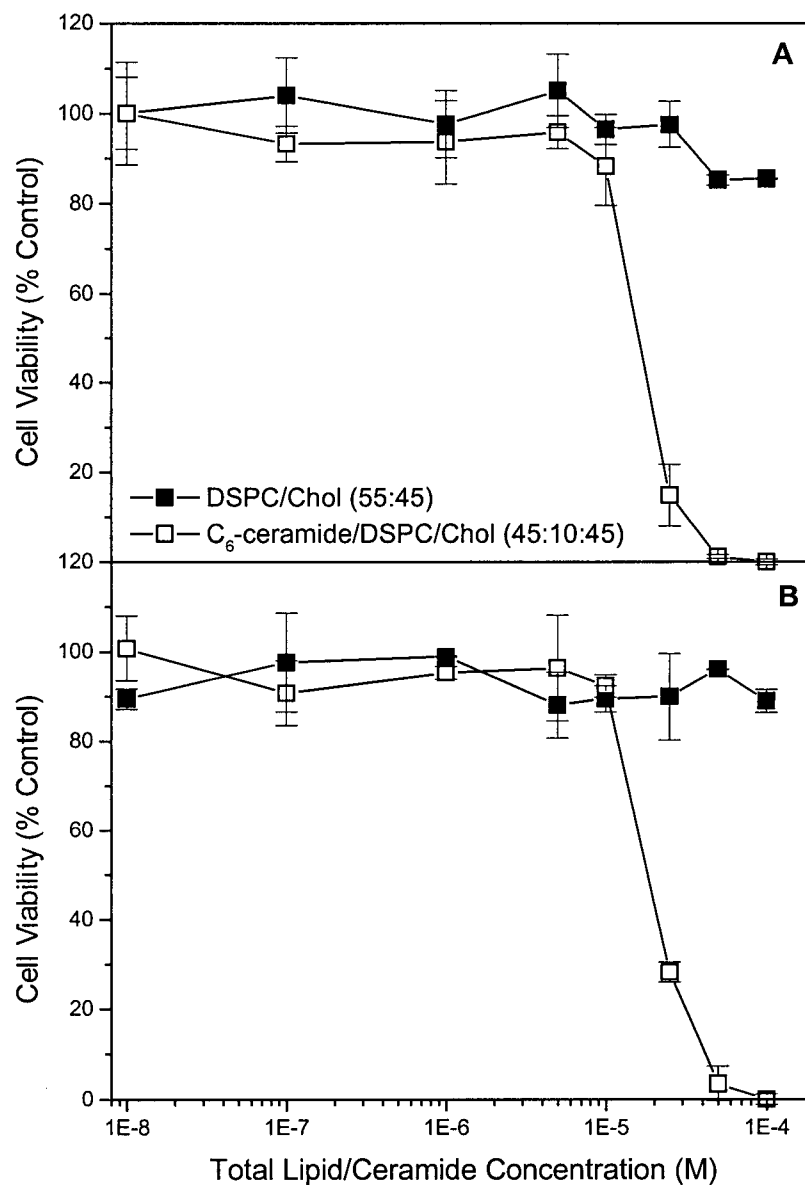


Figure 3.4 Cytotoxicity of control and C₆-ceramide liposomes on wild-type (A) and *mdr-1* gene transfected (B) MDA435/LCC6 human breast cancer cells. Cells were incubated with the indicated ceramide or total lipid concentrations for 72 hours and cell viability was measured using the MTT assay. Each value represents the mean from three independent experiments conducted in triplicate; bars, SD.

DSPC/Chol (55:45) displayed no activity (IC_{50} values $>100 \mu M$). The ceramide based cytotoxicity results were then correlated with cellular lipid uptake, which was expressed as a percent of the total radioactivity added in order to allow for direct comparisons to be made between the ceramide lipid and bulk liposomal lipid. The results in Figure 3.5 indicate that the [^{14}C]C₆-ceramide component of the liposomes was taken up by the tumor cells and 80% internalization was approached after 24 hours, whereas less than 10% of the [3H]CHE liposome label was cell-associated after 24 hours. These results suggest that the C₆-ceramide is being delivered not via liposomes, but rather by exchange of free ceramide lipid from the liposome bilayer into cellular membranes in a manner similar to that following addition of free C₆-ceramide.

3.4.4 Formulation and Cytotoxicity of C₁₆-Ceramide Containing Liposomes

The uptake results presented in Figure 3.5 indicate that the incorporation of C₆-ceramide into liposomes did not afford any increased activity over free C₆-ceramide. This lack of enhanced activity was attributed to the amphipathic nature of the short-chain ceramide, which appeared to have sufficient hydrophilicity to allow it to exchange from the liposomal carrier into the cellular membrane pool. Due to the reduced stability of C₆-ceramide in the liposome bilayer upon exposure to cellular membranes, the long-chain C₁₆-ceramide, which showed no cytotoxic activity in its free form, became an attractive alternate ceramide lipid for liposomal formulation. This was investigated on the basis that the more hydrophobic C₁₆-ceramide would be more likely to remain associated with its liposomal carrier during delivery. Furthermore, C₁₆-ceramide is a more physiologically relevant ceramide given that increases in endogenous C₁₆-ceramide

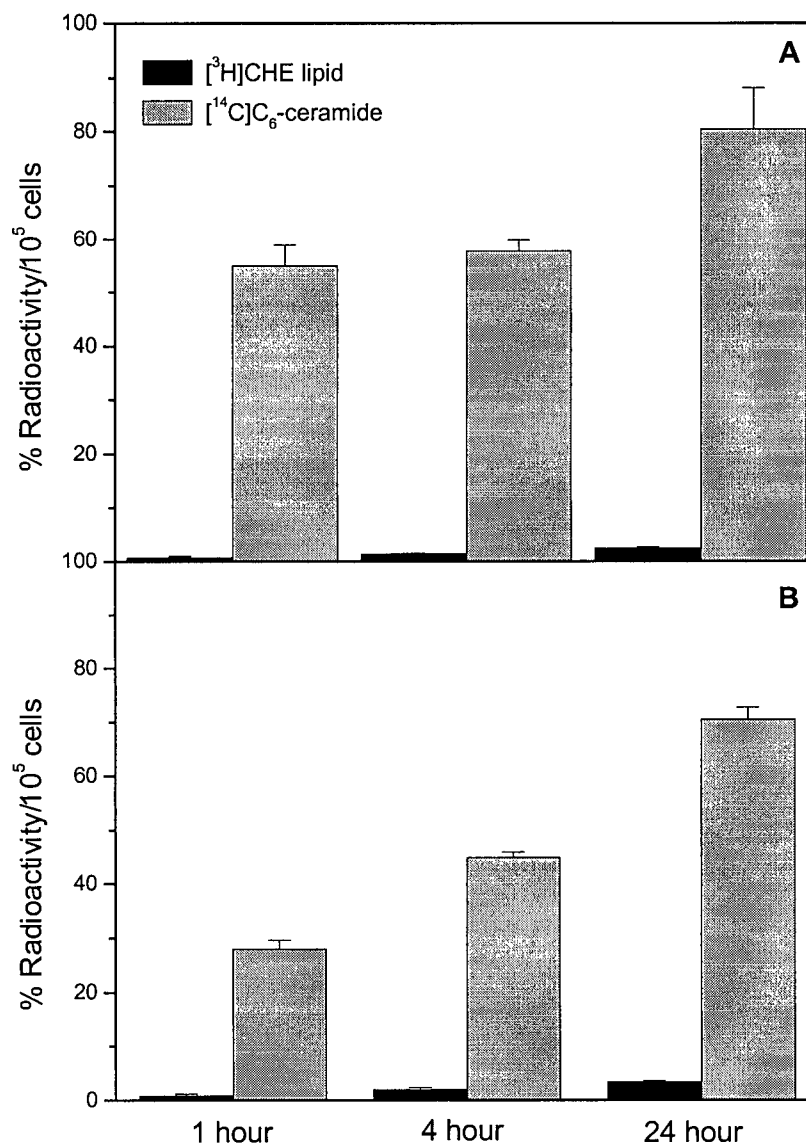


Figure 3.5 Cellular uptake of [³H]CHE liposome and [¹⁴C]C₆-ceramide radiolabels by wild-type (A) and mdr-1 gene transfected (B) MDA435/LCC6 human breast cancer cells. Cells were incubated with a liposome concentration corresponding to 1 μ M C₆-ceramide. Lipids were quantified by liquid scintillation counting. Uptake is expressed as a percentage of the total radioactivity added (corrected for binding with controls at 4°C) to allow for direct comparisons between liposomal and ceramide lipid to be made. Data are averaged means from two independent experiments conducted in triplicate; bars, SD.

accumulation have observed during apoptosis (161). Subsequent internalization of the ceramide-containing liposome should overcome the cell permeability limitations of free C₁₆-ceramide, thereby improving its *in vitro* activity.

The physico-chemical properties of C₁₆-ceramide described in Chapter 1 presented difficulties for liposome formulation. Several different lipid compositions and mole percentages were evaluated in an attempt to identify formulations that allowed C₁₆-ceramide to be successfully incorporated into the liposome bilayer, as well as to identify the maximum extent of ceramide incorporation (Table 3.2). It was not possible to incorporate C₁₆-ceramide into stable, unilamellar vesicles at mole percentages greater than 15%. Liposomes composed of C₁₆-cer/DSPC/Chol (15:40:45) were successfully prepared and displayed a mean diameter of 121.9 nm with a standard deviation of 43.6% (Figure 3.6). Evaluation of the *in vitro* cytotoxicity of C₁₆-ceramide liposomes in the MDA435/LCC6 cells showed that these formulations displayed activity that was comparable to control (non-ceramide) DSPC/Chol (55:45) liposomes (Figure 3.7). This lack of cytotoxicity was correlated with cellular uptake studies, which indicated that neither the ceramide-lipid nor the liposomal carrier was internalized after 24 hours (Figure 3.8). Therefore, the inability of liposomes to enhance the cytotoxicity of C₁₆-ceramide appeared to be attributed to lack of internalization of the liposomes by the MDA435/LCC6 cells. This was perhaps not surprising, since neutral (uncharged) liposomes do not readily interact with tumor cells and are not internalized in the absence of a targeting ligand. Therefore, the liposome formulation was modified to include a

Table 3.2**Summary Table Describing Various C₁₆-Ceramide Containing Liposome Formulations Attempted and their Respective Characteristics**

Lipid Composition^a (mole:mole)	Mole % C₁₆-Cer	Formulation Characteristics
C ₁₆ -cer/DSPC/Chol (15:40:45)	15	hydrates well and extrudes with >80% efficiency
C ₁₆ -cer/DSPC/Chol (20:35:45)	20	lipid film difficult to hydrate; lipid aggregates
C ₁₆ -cer/DSPC/Chol (20:50:30)	20	lipid film difficult to hydrate; lipid aggregates
C ₁₆ -cer/DSPC/Chol (20:50:30)	20	lipid film difficult to hydrate; lipid aggregates
C ₁₆ -cer/DPPC/Chol (15:40:45)	15	hydrates well and extrudes with >80% efficiency
C ₁₆ -cer/DPPC/Chol (20:35:45)	20	lipid film difficult to hydrate; lipid aggregates
C ₁₆ -cer/Chol (50:50)	50	lipid film difficult to hydrate; lipid aggregates
C ₁₆ -cer/CHEMS (50:50)	50	hydrates well and extrudes with >80% efficiency at concentrations ≤ 20 mg/ml total lipid
C ₁₆ -cer/DPG/PEG ₃₅₀ -DSPE (30:30:40)	30	hydrates well and extrudes but non-uniform, tri- modal liposome size distribution with aggregates

^aLiposomes of all compositions were prepared in HBS pH 7.4 buffer using the extrusion method of vesicle formation with 100 nm polycarbonate filters.

C₁₆-cer/DSPC/Chol (15:40:45) Liposomes

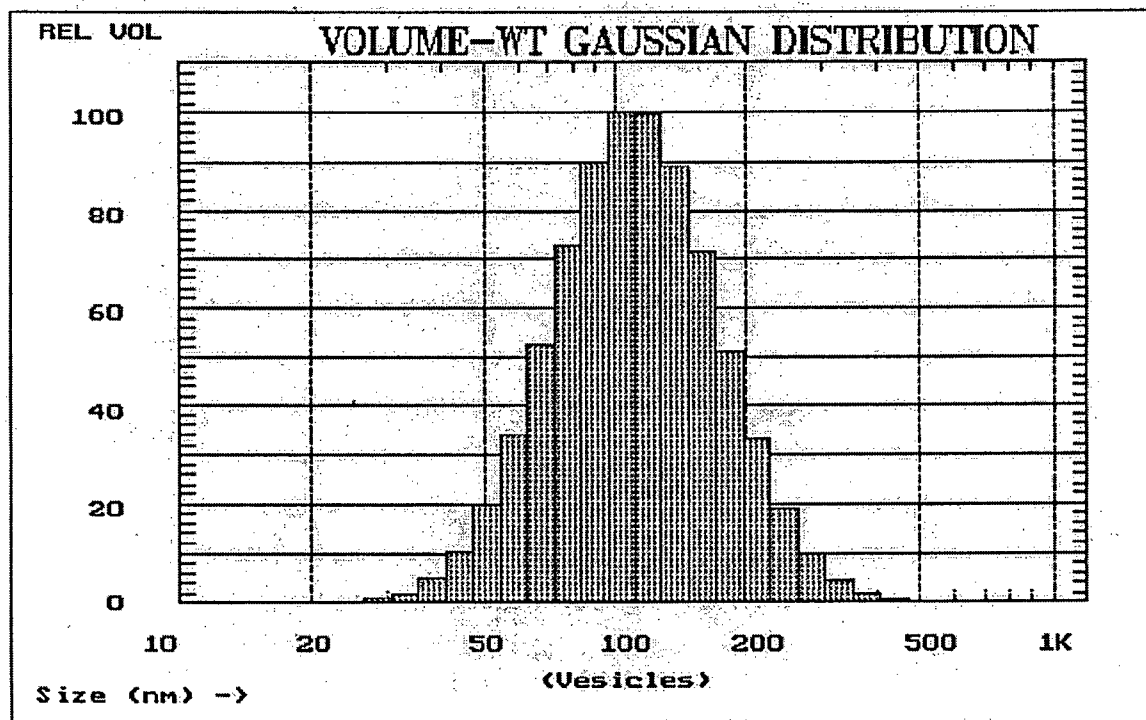


Figure 3.6 Mean liposome vesicle diameter of 121.9 ± 53.2 nm for C₁₆-cer/DSPC/Chol (15:40:45) liposomes as determined by quasi-elastic light scattering using a Nicomp 270 submicron particle sizer model 370/270. Hepes buffered saline pH 7.4 was used for sample dilution.

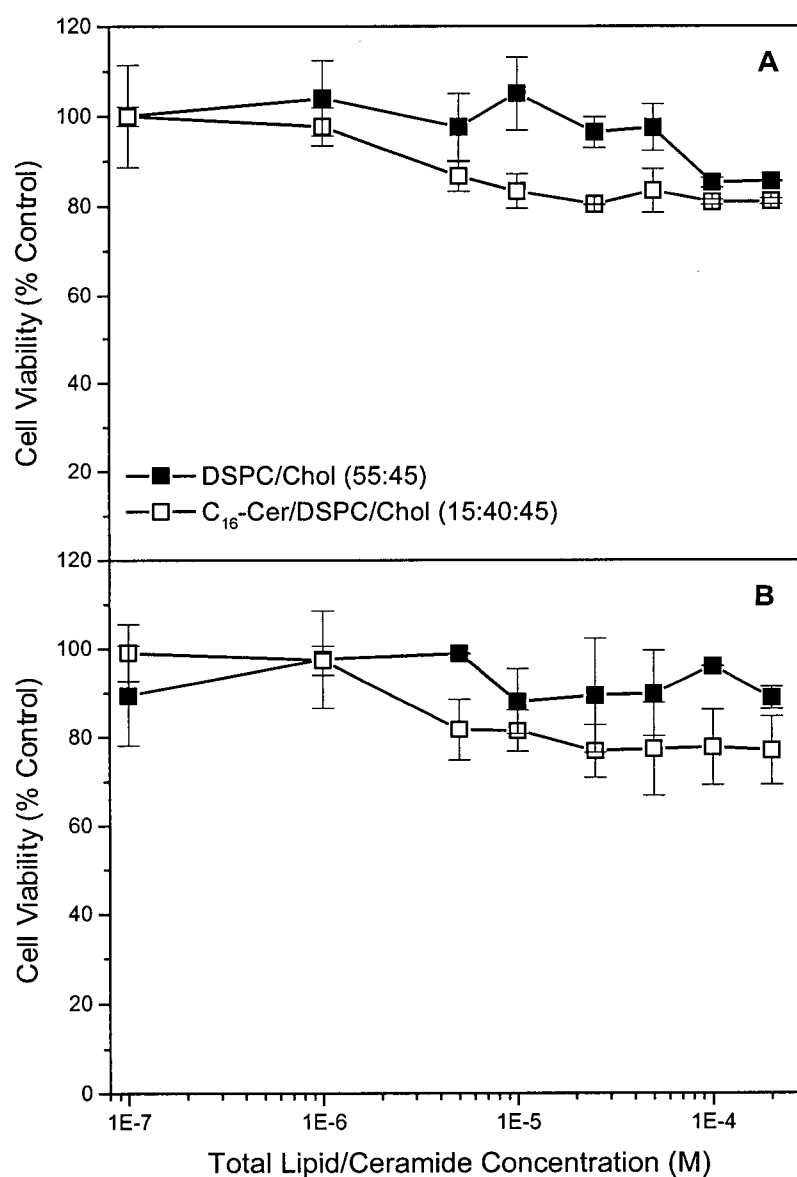


Figure 3.7 Cytotoxicity of C₁₆-cer/DSPC/Chol (15:40:45) and control DSPC/Chol (55:45) liposomes on wild-type (A) and *mdr-1* gene transfected (B) MDA435/LCC6 human breast cancer cells. Cells were incubated with the indicated ceramide or total lipid concentrations for 72 hours and cell viability was measured using the MTT assay. Each value represents the mean from three independent experiments conducted in triplicate; bars, SD.

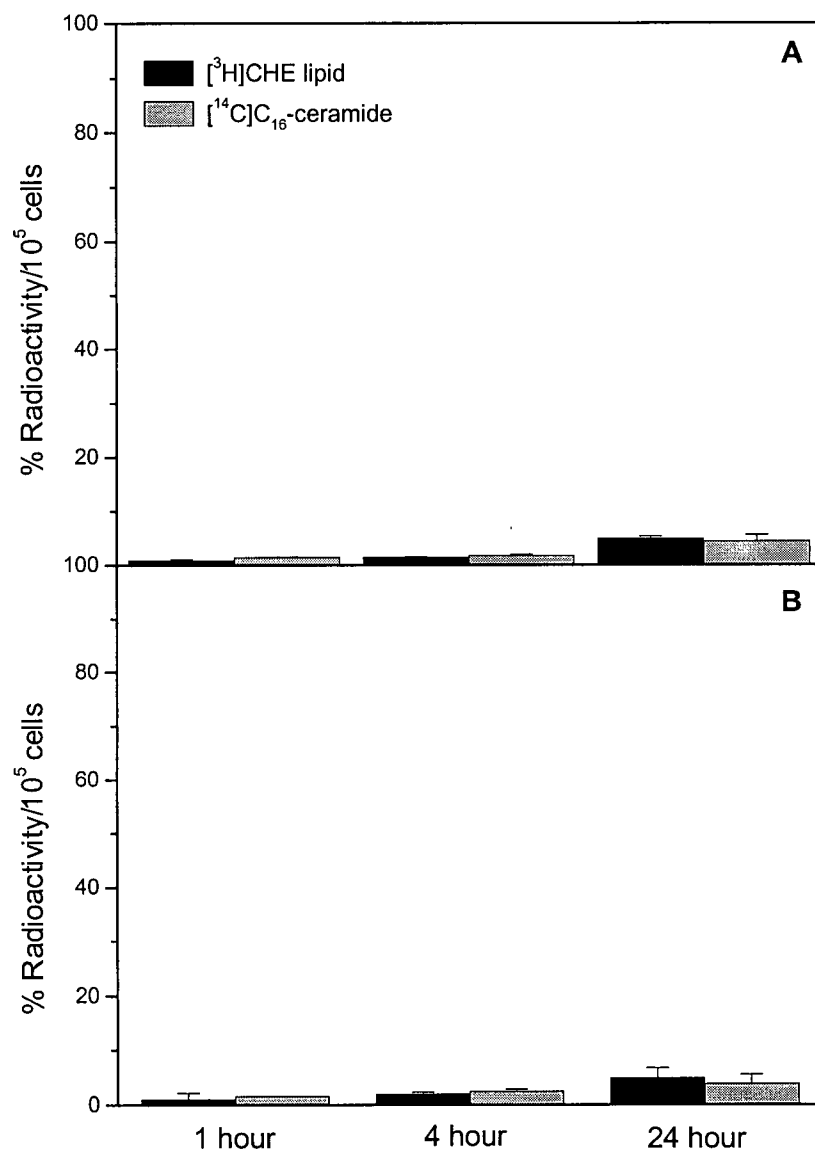


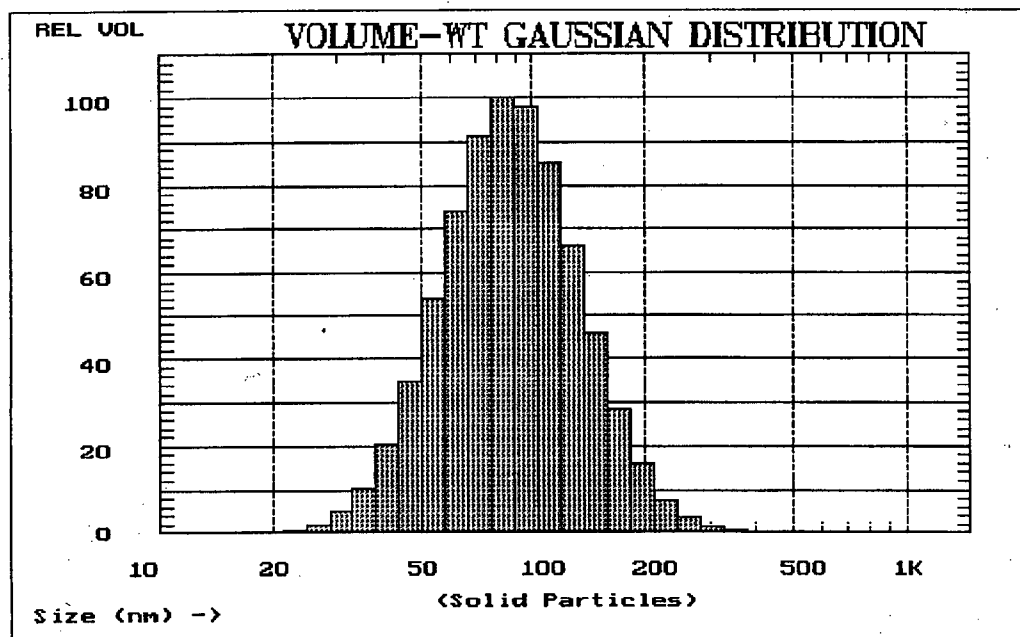
Figure 3.8 Cellular uptake of C₁₆-cer/DSPC/Chol (15:40:45) liposomes by wild-type (A) and *mdr-1* gene transfected (B) MDA435/LCC6 cells. Uptake of [³H]CHE bulk liposomal lipid and [¹⁴C]C₁₆-ceramide are expressed as a percent of the total radioactivity added, normalized to 10⁵ cells. Data are averaged means from two independent experiments conducted in triplicate; bars, SD.

negatively charged lipid in an attempt to increase the interaction of the liposomes with the target cells.

To accomplish this goal the cholesterol component of the formulation was replaced by the acidic cholesterol ester *cholesteryl hemisuccinate* (CHEMS). Using this lipid, C₁₆-ceramide could be incorporated into CHEMS containing liposomes at 50 mole percent, for a final lipid composition of C₁₆-cer/CHEMS (50:50; Table 3.2). The increase in ceramide incorporation was attributed to the molecular geometry of CHEMS, as described in Chapter 1. These liposomes displayed a mean diameter of 95.2 nm with a standard deviation of 42.6% (Figure 3.9).

Liposomes composed of high content C₁₆-ceramide have not been previously described in the literature. Therefore, cryo-TEM images were obtained in order to further characterize the size and shape of these novel vesicles. Control liposomes composed of DPPC/CHEMS (50:50) were also evaluated. The non-ceramide lipid of the control liposomes in this case was changed from DSPC to DPPC to more closely match the 16 carbon acyl chain length of the ceramide. Control liposomes displayed a mean diameter of 97.2 nm with a standard deviation of 27.3% as measured by quasi-elastic light scattering (Figure 3.9). The representative cryo-EM micrographs in Figure 3.10 show that both the control and ceramide-based liposomes are spherical vesicles with an average diameter in the range of 100 nm, which confirms the quasi-elastic light scattering data. The images also indicate that the ceramide-based liposomes are uniform, primarily unilamellar vesicles. A small amount (1 mole percent) of the steric stabilizer PEG₂₀₀₀-

A: C₁₆-cer/CHEMS (50:50) Liposomes



B: DPPC/CHEMS (50:50) Liposomes

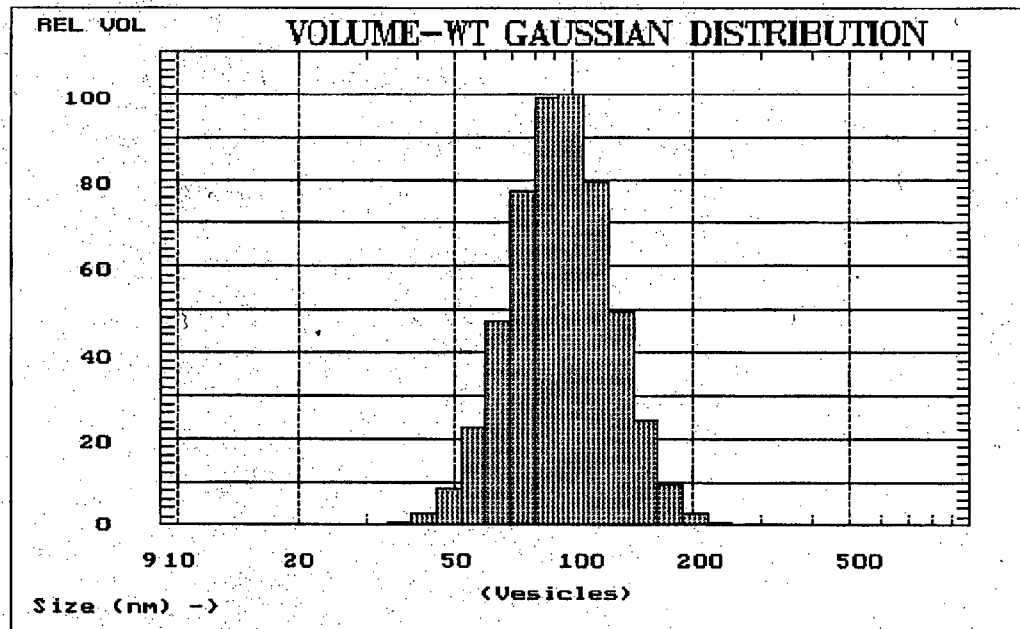


Figure 3.9 Mean liposome vesicle diameter of 95.2 ± 40.5 nm for C₁₆-cer/CHEMS (50:50) (A) and 97.2 ± 28.5 nm for control DPPC/CHEMS (50:50) (B) liposomes as determined by quasi-elastic light scattering using a Nicomp 270 submicron particle sizer model 370/270. Hepes buffered saline pH 7.4 was used for sample dilution.

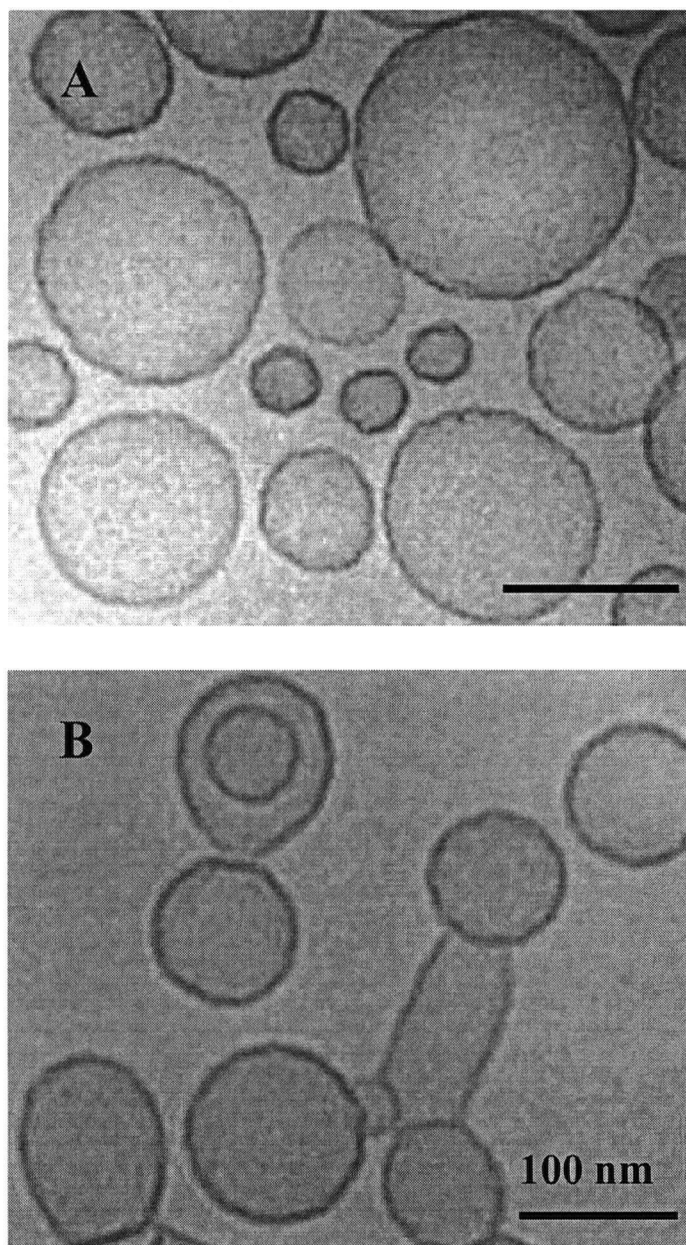


Figure 3.10 Cryo-transmission electron micrographs of DPPC/CHEMS/PEG₂₀₀₀-DSPE (49.5:49.5:1; A) and C₁₆-cer/CHEMS/PEG₂₀₀₀-DSPE (49.5:49.5:1; B) liposomes. The bar in each image represents 100 nm.

DSPE was incorporated into these formulations to prevent liposome aggregation during transport. The DPPC/CHEMS and C₁₆-cer/CHEMS formulations were also characterized on the basis of trapped volume, which provides a measure of the internal aqueous volume of the lipid vesicles. Control (DPPC/CHEMS) and ceramide (C₁₆-cer/CHEMS) liposomes were determined to have trapped volumes of $1.81 \pm 0.03 \mu\text{l}/\mu\text{mole}$ total lipid and $1.64 \pm 0.07 \mu\text{l}/\mu\text{mole}$ total lipid, respectively. These results are consistent with previously published results for other phospholipid/cholesterol liposome formulations (261). Evaluation of the *in vitro* cytotoxicity of C₁₆-cer/CHEMS liposomes demonstrated a modest increase in activity over the C₁₆-cer/DSPC/Chol formulation; however, the IC₅₀ value remained greater than 100 μM (Figure 3.11). The slight improvement in activity was not attributable to the negative charge of the CHEMS lipid, as control liposomes composed of DPPC/CHEMS (50:50) showed no activity at all. The cytotoxicity was correlated with a modest increase in cellular uptake ($\sim 16\%$ ceramide uptake at 24 hours for the C₁₆-cer/CHEMS formulation versus $\sim 4.5\%$ ceramide uptake at 24 hours for the C₁₆-cer/DSPC/Chol formulation; Figure 3.12). However, overall liposome internalization remained low.

3.4.5 Cytotoxicity of Free and Liposomal Ceramide in J774 Murine Macrophage Cells

The modest improvement in activity afforded by the C₁₆-cer/CHEMS liposomes gave a preliminary indication that liposomal delivery of C₁₆-ceramide may be effective if efficient intracellular delivery could be achieved. In order to demonstrate this from a proof-of-principle perspective, the J774 murine macrophage cell line was investigated as a new target cell population. This cell line has been demonstrated to internalize

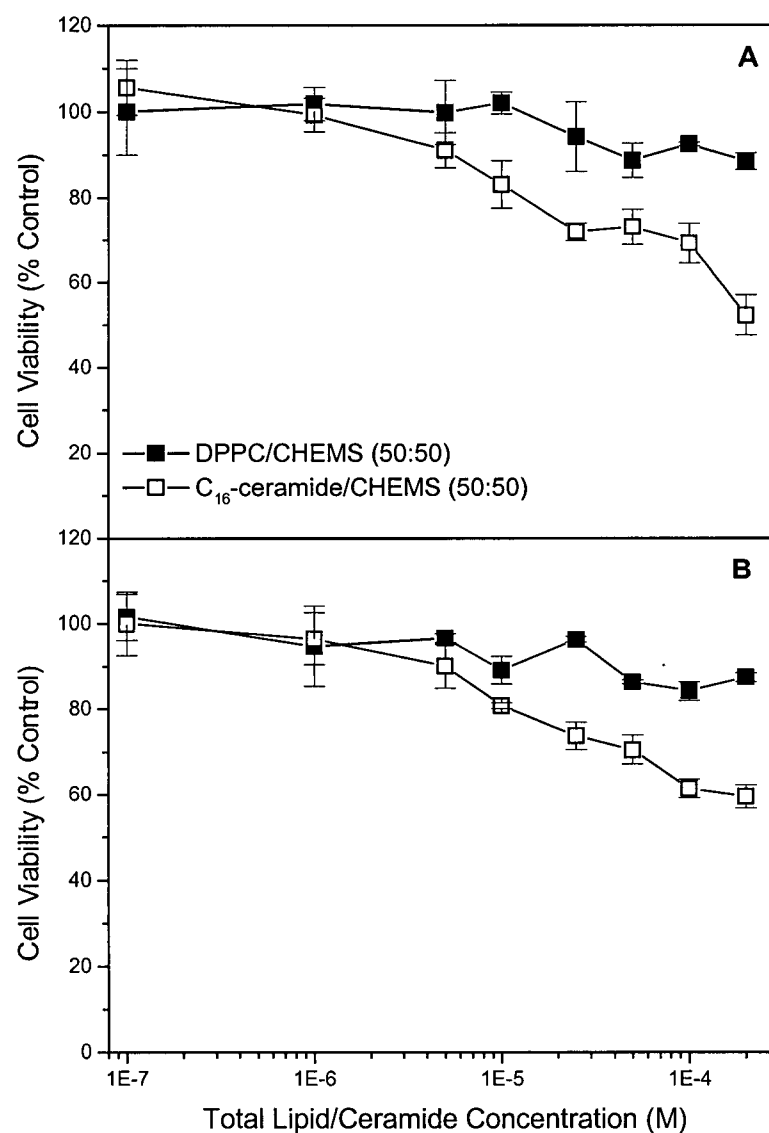


Figure 3.11 Cytotoxicity of C₁₆-cer/CHEMS (50:50) and DPPC/CHEMS (50:50) liposomes on wild-type (A) and *mdr-1* gene transfected (B) MDA435/LCC6 human breast cancer cells. Cells were incubated with the indicated ceramide or total lipid concentrations for 72 hours and cell viability was measured using the MTT assay. Each value represents the mean from three independent experiments conducted in triplicate; bars, SD.

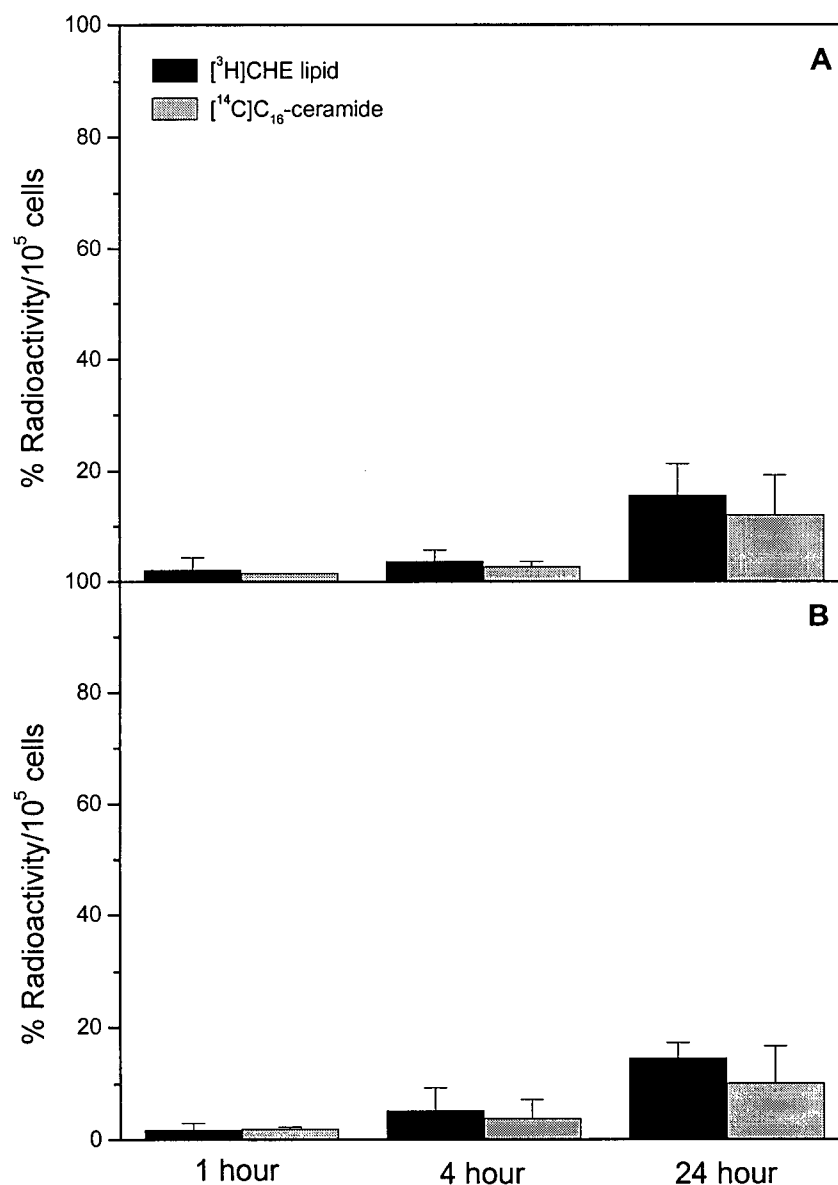


Figure 3.12 Cellular uptake of C₁₆-cer/CHEMS (50:50) liposomes by wild-type (A) and mdr-1 gene transfected (B) MDA435/LCC6 cells. Uptake of [³H]CHE bulk liposomal lipid and [¹⁴C]C₁₆-ceramide are expressed as a percent of the total radioactivity added, normalized to 10⁵ cells. Uptake is expressed as a percentage of the total radioactivity added (corrected for binding with controls at 4°C) in order to allow for direct comparisons between liposomal and ceramide lipid to be made. Data are averaged means from two independent experiments conducted in triplicate; bars, SD.

liposomes via the endocytic pathway (224), and should therefore facilitate intracellular delivery of the liposomes to an organelle (endosomes) where pro-apoptotic ceramide is known to be endogenously generated by sMases (159, 160, 262).

Before investigating the effect of ceramide-containing liposomes on J774 cells it was first necessary to examine whether free ceramide lipids displayed similar cytotoxicity against the J774 cells as was observed in the MDA435/LCC6 cells. The results in Figure 3.13 confirmed that the same trend of free ceramide cytotoxicity was observed, with the short-chain C₆- and C₈-ceramides being the most active (IC₅₀ values of 14.4 μ M for both) and C₁₆-ceramide showing no activity.

Evaluation of the *in vitro* cytotoxicity of C₁₆-ceramide liposomes in the J774 cell line demonstrated that C₁₆-cer/CHEMS liposomes dramatically improved the cytotoxicity of C₁₆-ceramide in these cells (Figure 3.14). Specifically, while the IC₅₀ value of C₁₆-ceramide when exogenously applied to J774 cells in its free form was well in excess of 100 μ M, its formulation into and delivery via CHEMS liposomes decreased the IC₅₀ to 36.1 μ M, bringing it into the range of cytotoxicity observed with free C₆-ceramide (14.4 μ M). This cytotoxic effect was ceramide-specific and was not attributed to the CHEMS lipid, as control DPPC/CHEMS (50:50) liposomes were non-cytotoxic (Figure 3.14). Cellular uptake studies indicated that both the liposome and the ceramide components were internalized, as was evidenced by uptake of the [³H]CHE and [¹⁴C]C₁₆-ceramide labels, which both approached 50% after 24 hours (Figure 3.15). This indicated that under these conditions the C₁₆-ceramide lipid was being delivered specifically by the liposomal carrier rather than by passive lipid exchange, as was previously the case for C₆-ceramide liposomes.

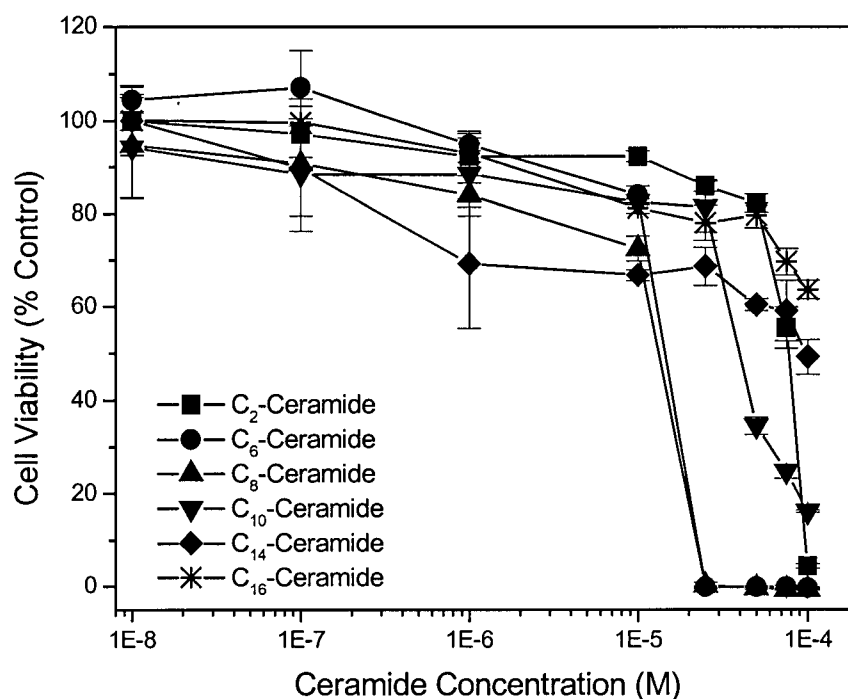


Figure 3.13 Cytotoxicity of various acyl chain length free ceramide lipids on J774 murine macrophage cells. Cells were incubated with the indicated ceramide concentrations for 72 hours and cell viability was measured using the MTT assay. Each value represents the mean from three independent experiments conducted in triplicate; bars, SD.

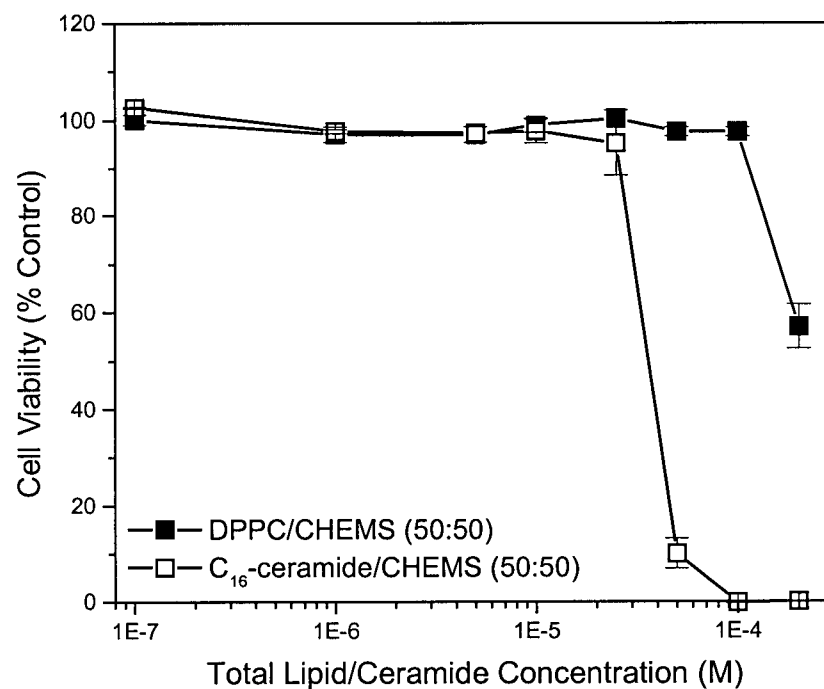


Figure 3.14 Cytotoxicity of C₁₆-cer/CHEMS and DPPC/CHEMS liposomes on J774 cells. Cells were incubated with the indicated ceramide or total lipid concentrations for 72 hours and cell viability was measured using the MTT assay. Each value represents the mean from three independent experiments conducted in triplicate; bars, SD.

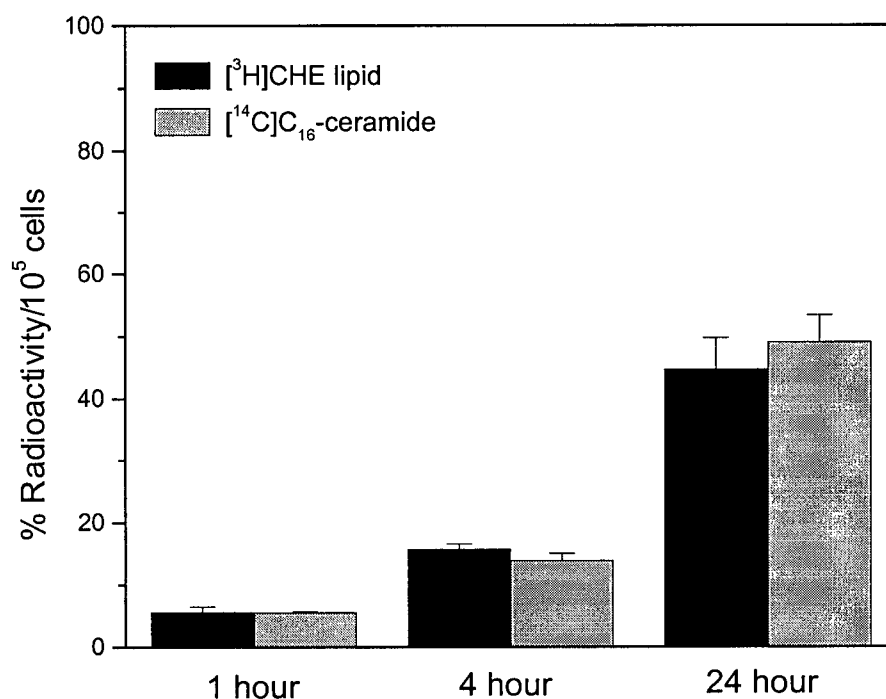


Figure 3.15 Cellular uptake of C_{16} -cer/CHEMS liposomes by J774 cells. Uptake is expressed as a percentage of the total radioactivity added (corrected for binding with controls at 4°C) in order to allow for direct comparisons between liposomal and ceramide lipid to be made. Data are averaged means from two independent experiments conducted in triplicate; bars, SD.

3.5 DISCUSSION

The field of sphingolipid biology is rapidly evolving, with great emphasis on ceramide lipids in particular as mediators of diverse biological effects. Research involving the relationship between ceramide lipids and apoptosis has received considerable interest from both mechanistic (105, 106, 176, 177, 263) and therapeutic (58, 264) perspectives. Therapeutic approaches based on the modulation of intracellular ceramide levels *in vitro* is not a novel concept *per se*. The direct addition of exogenous, cell-permeable ceramides has been shown to induce apoptosis in many cell lines. Research based on this approach has largely focused on the C₆-ceramide form due to its ease of solubility and therefore delivery in aqueous media. However, studies investigating exogenous application of the more physiologically relevant long-chain ceramides such as C₁₆-ceramide have been limited by difficulties with the poor solubility of natural ceramide in aqueous media and its reduced cell permeability characteristics. Therefore, the experimental objective of this chapter was to investigate the pro-apoptotic characteristics of free exogenous ceramides with respect to acyl chain length, and to then employ liposome-based delivery systems to enhance this activity through improved intracellular delivery.

Initial studies examined the effect of different acyl chain length synthetic ceramides on *in vitro* cytotoxicity using the wild-type and *mdr-1* gene transfected MDA435/LCC6 cell lines. A relationship between acyl chain length and cytotoxicity was observed, with short-chain C₆-ceramide being most active (IC₅₀ values in the 3-6 μ M range) and the longer chain C₁₆-ceramide being least active (IC₅₀ values well in excess of 100 μ M). The finding of potent activity of C₆-ceramide is consistent with other research

in this field (265-267). As well, the minimal cytotoxicity observed with C₂-ceramide is supported by work by Payne *et al.* (268) who found the cytotoxicity of C₂-ceramide equivalent to control treatment in primary placental trophoblasts as measured by MTT assays. O'Byrne *et al.* also failed to observe apoptosis in response to C₂-ceramide exposure (269). This is not always the case, however, as other research has shown potent cytotoxicity with C₂-ceramide, suggesting that its pro-apoptotic effects may be cell-line specific (270).

It is encouraging to note that there was very little difference in the sensitivity of wild-type versus resistant cell lines to the effects of ceramide. This suggests that ceramide-based therapies may be equally effective in the treatment of sensitive and MDR tumors that overexpress Pgp.

The observed differences in cytotoxicity related to acyl chain length were correlated with the relative uptake of radioactive [¹⁴C]C₆- and [¹⁴C]C₁₆-ceramide lipids. These results demonstrated that short-chain ceramide uptake was more than 3-fold greater than that of long-chain ceramide (7 pmol cer/μg protein versus 2 pmol cer/μg protein), implicating ceramide cell-permeability characteristics as an important determinant of cytotoxicity. This highlights the importance of achieving intracellular delivery as a pre-requisite to ceramide-mediated apoptosis. The benefits of liposome-based delivery systems presented in Chapter 1, combined with the emerging role of ceramide as a bioactive lipid, led to the novel concept of incorporating ceramide lipids into liposome bilayers.

The intrinsic activity of C₆-ceramide identified it as the initial candidate for formulation into ceramide-based liposomes. Homogenous, primarily unilamellar vesicles

of approximately 100 nm average diameter containing up to 45 mole percent C₆-ceramide in the liposome bilayer were successfully prepared. These liposomes demonstrated potent cytotoxic activity in both the wild-type and resistant MDA435/LCC6 cell lines, with IC₅₀ values less than 20 μM whereas control (non-ceramide) liposomes were inactive. However, cellular uptake studies revealed that the cytotoxicity was due to exchange of the short-chain ceramide lipid from the liposome bilayer rather than through delivery by the liposome carrier. Thus, liposomal formulation of C₆-ceramide offered no delivery advantage over free C₆-ceramide. Because of this reduced C₆-ceramide stability in the bilayer, the longer chain and more physiologically relevant C₁₆-ceramide became an attractive alternative. Since the lack of activity of free C₁₆-ceramide was attributed to poor intracellular delivery, it was speculated that its formulation into a liposomal delivery system may be sufficient to overcome this obstacle.

The physico-chemical properties of C₁₆-ceramide described in Chapter 1 presented significant formulation challenges and prevented proper hydration and dispersion of the lipid film when incorporated into DSPC/Chol-based liposomes above 15 mole percent. This observation is consistent with those of Holopainen *et al.* who observed extensive aggregation upon incorporation of high ceramide levels into MLVs designed to evaluate the biophysical effects of ceramide on lipid bilayers (271). Interestingly, despite the successful incorporation of 15 mole percent C₁₆-ceramide into C₁₆-cer/DSPC/Chol (15:40:45) liposomes, this formulation showed no activity when incubated with cells *in vitro* and the ceramide IC₅₀ value remained greater than 100 μM. This was attributed to a lack of liposome internalization by the target cells. Consistent with the postulation that C₆-ceramide exchanged from the bilayer because of its short

acyl chain length, the longer chain (more hydrophobic) C₁₆-ceramide did not appear to exchange from the liposome bilayer. However, since the liposomes were not internalized by the MDA435/LCC6 cells the ceramide component of the bilayer could not reach its intracellular target(s).

Limited cellular uptake of liposomes is not uncommon for uncharged liposome formulations in the absence of specific targeting ligands. Therefore, the next step was to modify the liposome formulation in an attempt to increase association with the target cells. Cholesteryl hemisuccinate was chosen for this purpose on the basis of three specific attributes. First, as discussed in Chapter 1, this lipid has been successfully combined with the non-bilayer forming (H_{II} phase) lipid dioleoylphosphatidylethanolamine (DOPE) to stabilize its presence in liposome bilayers. Since C₁₆-ceramide has similar shape-related properties to DOPE the objective was to extend the application of CHEMS to the stabilization of long-chain ceramide in bilayers. Second, the presence of electrostatic interactions due to the negatively charged CHEMS should cause the liposomes to interact more strongly with the cell surface and this may promote liposome internalization. Third, CHEMS is a pH sensitive lipid that, when protonated at pH ~5.5, triggers liposome destabilization and should promote ceramide lipid release in endosomes, where pro-apoptotic ceramide is known to be produced via aSMase. Based on this rationale, C₁₆-ceramide incorporation into CHEMS containing liposomes was investigated. Indeed, C₁₆-ceramide could be formulated into stable liposomes at up to 50 mole percent (C₁₆-cer/CHEMS, 50:50), which represented a substantial improvement over the non-CHEMS based formulations in which the maximum level of ceramide incorporation was 15 mole percent. Characterization of

these liposomes by quasi-elastic light scattering and cryo-TEM revealed uniform, primarily unilamellar, spherical vesicles of approximately 100 nm diameter. Trapped volume studies were consistent with those for conventional liposomes composed of phospholipids and cholesterol. Control liposomes composed of DPPC/CHEMS (50:50) were prepared in order to match the acyl chain length of the C₁₆-ceramide component. Cytotoxicity studies showed a modest improvement in activity of C₁₆-cer/CHEMS liposomes over C₁₆-cer/DSPC/Chol formulations; however, the IC₅₀ value remained above 100 μ M. Cellular uptake studies revealed that the presence of CHEMS only enhanced liposome internalization by the MDA435/LCC6 cells to a small degree. Nevertheless, these results gave a preliminary indication that exogenous C₁₆-ceramide may show activity if the objective of efficient intracellular delivery could be met. Since modifications at the level of the liposome formulation were not sufficient to enhance liposome internalization, attention was turned to the target cell population.

In order to evaluate the effectiveness of liposome-based delivery of C₁₆-ceramide from a proof-of-principle perspective the J774 murine macrophage cell line, which has been previously demonstrated to internalize liposomes via endocytosis, was introduced. Cytotoxicity studies using free ceramide lipids confirmed that the J774 cells were affected by exogenous ceramides in a similar manner to the MDA435/LCC6 cells. Evaluation of the C₁₆-cer/CHEMS liposomes in J774 cells showed enhanced cytotoxicity over both free C₁₆-ceramide and C₁₆-cer/DSPC/Chol formulations. Specifically, whereas the IC₅₀ values for free C₁₆-ceramide and C₁₆-cer/DSPC/Chol liposomes were both greater than 100 μ M, C₁₆-cer/CHEMS liposomes had an IC₅₀ value of 36.1 μ M. This approximates the cytotoxicity of free C₆-ceramide in these cells (14.4 μ M), and was

demonstrated to be a ceramide-specific effect since control DPPC/CHEMS liposomes were inactive. Correlation of these results with cellular uptake studies confirmed internalization of both the liposome and ceramide lipid components, both of which approached 50% after 24 hours.

These results were very promising, as they demonstrated for the first time the successful formulation of a physiologically relevant, natural ceramide lipid into a liposome-based carrier system. Furthermore, whereas C₁₆-ceramide was inactive when administered in its free form, this work demonstrated that its activity could be significantly enhanced by incorporation into a liposomal delivery vehicle. Taken together, these results provide an increased understanding of the basis for the differences in the cytotoxicity of exogenous short- and long-chain ceramide lipids, and demonstrate that successful intracellular delivery of exogenous, C₁₆-ceramide can be used to trigger apoptosis. This suggests the potential for developing therapeutic strategies based on controlled ceramide delivery. The next step, then, was to develop these systems for *in vivo* applications and to evaluate their pro-apoptotic activity in an animal model. These goals formed the basis of Chapters 4 and 5 which follow.

CHAPTER 4

DEVELOPMENT OF AN IN VITRO EXCHANGE ASSAY TO ACCURATELY PREDICT THE LIPID AND DRUG RETENTION PROPERTIES OF LIPOSOME-BASED DELIVERY SYSTEMS*

4.1 INTRODUCTION AND RATIONALE

The results presented in Chapter 3 demonstrated the importance of intracellular delivery for the development and application of exogenous ceramide lipids as therapeutically active inducers of apoptosis. Although cell-permeable C₆-ceramide showed activity when applied free in solution, the development of C₆-ceramide-containing liposomes for controlled ceramide delivery was limited by the apparent rapid ceramide exchange from the liposomal carrier into cellular lipid membranes. The ability of liposome-based systems to improve the therapeutic activity of bioactive lipids such as ceramide requires that the active lipid component be retained in the liposome bilayer throughout the delivery process. While the occurrence of rapid lipid exchange during cell culture experiments is certainly a frustration, this behaviour becomes even more problematic when such observations are made during the subsequent phase of *in vivo* characterizations in animal models, which are more costly and labor intensive than evaluations using cell culture systems. Both of the C₁₆-ceramide containing formulations described in Chapter 3 appeared to retain the ceramide lipid for the duration of exposure to cells *in vitro*. However, our laboratory has observed that *in vitro* release of liposome contents is often not representative of *in vivo* release characteristics (201, 272). Consequently, before moving any ceramide liposomes forward for development and

*Adapted from: JA Shabbits, GN Chiu and LD Mayer (2002). *Development of an in vitro exchange assay that accurately predicts in vivo drug retention for liposome-based delivery systems*. Journal of Controlled Release, 84(3): 161-70.

evaluation in animal models it was necessary to develop an *in vitro* assay to predict the C₁₆-ceramide retention properties that should be observed *in vivo*.

The use of liposomes to deliver therapeutic lipids is a relatively recent application of liposome technology, and ceramide-based formulations designed for therapeutic applications have not been previously described in the literature. However, there are many well-characterized liposome formulations containing conventional anticancer agents that have already been developed for *in vivo* applications, and observations regarding the release of encapsulated drug contents from these systems can be applied to the development of the lipid exchange assay described here.

Conventional liposomal drug formulations undergo extensive *in vitro* optimization in order to achieve prolonged drug retention and stability before being moved forward to more advanced stages of testing. However, it is often the case that *in vitro* based assays do not accurately predict the liposomal drug retention properties actually observed *in vivo*. In fact, it is not uncommon for formulations to exhibit excellent drug retention properties *in vitro*, but to display almost complete drug release within minutes following systemic administration to animals (201). For example, cyclosporins incorporated into liposomes for the intended purpose of MDR modulation are rapidly released from the lipid carrier in the circulation, resulting in drug pharmacokinetic properties comparable to unencapsulated drug (273, 274). This calls into question the usefulness of current *in vitro* pre-clinical drug release assays, and highlights the need for more accurate predictors of true *in vivo* performance.

Although several *in vitro* drug release assays have been developed (275-277), one of the most commonly used methods of measuring encapsulated drug release relies on

dialyzing the liposomal formulation against large volumes of buffer at physiological temperatures. The excess extravesicular buffer is intended to serve as a driving force to promote drug leakage from the liposome. Upon release from the liposomal carrier, free drug crosses the dialysis membrane and accumulates in the buffer system. Serum is frequently added to the dialysis buffer to more closely mimic the physiological environment (proteins and lipid constituents) that liposomes encounter *in vivo*. However, despite these efforts the drug leakage properties observed using dialysis-based systems often show a poor correlation with actual *in vivo* results. It is believed that this discrepancy is due to the inability of dialysis-based assays to mimic the large cellular membrane pool (lipid "sink") that exists in the physiological setting, comprising blood cells and tissues into which hydrophobic and amphipathic drugs can distribute after *in vivo* administration. Upon systemic administration, rapid drug leakage from liposomes may be observed as encapsulated hydrophobic or amphipathic drugs diffuse across the liposome bilayer and incorporate into these membranes. A similar scenario may be envisioned to occur for the exchange of lipid bilayer components such as ceramides. In order to study this latter scenario, an *in vitro* release assay was developed in which an excess of multilamellar vesicles were used as membrane "acceptors" for ceramide lipid exchange from "donor" liposomes. It is believed that the excess MLVs will mimic the physiological lipid membrane pool and, therefore, should more closely reflect the true *in vivo* retention properties of liposomes. This chapter describes the development and validation of the assay procedure and demonstrates its utility in predicting *in vivo* ceramide lipid retention properties. Results demonstrating the application of this assay to

the evaluation of drug release from conventional drug encapsulated liposomes are also presented.

4.2 HYPOTHESIS

The hypothesis underlying the research presented in this chapter is that the development of an *in vitro* drug release assay that uses large, multilamellar acceptor vesicles to simulate the physiological tissue and membrane lipid "sink" will allow for the lipid exchange characteristics of ceramide-based liposomes observed *in vivo* to be predicted *in vitro*, thereby facilitating the characterization and development of ceramide-based liposomes for *in vivo* applications.

4.3 MATERIALS AND METHODS

4.3.1 Materials

All lipids were purchased from Avanti Polar Lipids (Alabaster, AL). Cholesterol and Sephadex G-50 were obtained from the Sigma Chemical Company (St. Louis, MO). [^3H]CHE was purchased from Perkin Elmer (Boston, MA), and [^{14}C]CHE and [^3H]verapamil were purchased from NEN (Boston, MA). [^{14}C]C₆- and [^{14}C]C₁₆-ceramide were purchased from American Radiolabeled Chemicals Inc. (St. Louis, MO). [^{14}C]doxorubicin-HCl was purchased from Amersham International (Buckinghamshire, UK). Non-radiolabeled doxorubicin-HCl and verapamil were obtained from Faulding (Montreal, QC, Canada) and Sabex Inc. (Boucherville, QC, Canada), respectively. Spectra/Por dialysis tubing was purchased from Spectrum Laboratories (Rancho Dominguez, CA). Fetal bovine serum was obtained from Hyclone (Logan, UT). Pico-

fluor 40 scintillation cocktail was purchased from Packard Biosciences (Groningen, The Netherlands). Female SCID/Rag-2 mice were bred in-house at the BC Cancer Agency animal facility (Vancouver, BC, Canada).

4.3.2 Preparation of Donor Large Unilamellar Vesicles (LUVs)

Lipid films were prepared as previously described in Chapter 3, with radiolabels incorporated as indicated. All lipid ratios are specified on a mole:mole ratio unless otherwise indicated. Lipid films containing ceramide or prepared for use as empty (non-drug encapsulated) liposomes were hydrated in 1 ml Hepes buffered saline (HBS; 20 mM Hepes/150 mM NaCl, pH 7.4) with heat and vortexing. Films to be used for conventional drug encapsulation were hydrated in 300 mM citrate buffer, pH 4.0 with heat and vortexing, followed by five freeze-thaw cycles (5 minutes liquid nitrogen freeze, 5 minutes 65°C water bath thaw). Homogenously sized liposomes were then produced following extrusion as previously described. Liposome/ceramide lipid concentrations were determined by liquid scintillation counting.

4.3.3 Preparation of Acceptor Multilamellar Vesicles (MLVs)

Egg phosphatidylcholine and cholesterol lipids were weighed and combined at a 55:45 ratio as described above. [^3H] or [^{14}C]CHE was incorporated as indicated in order to distinguish between the MLV and LUV populations. Lipids films were hydrated in 1 ml warm 300 mM sucrose with vortexing to yield MLVs, which were transferred to a 1.5 ml Eppendorf tube. The suspension was centrifuged at 4200 rpm for 10 minutes, after which the MLVs appeared as a supernatant layer with the sucrose buffer below. An 18

guage needle syringe was passed through the MLV layer to withdraw the sucrose. The MLVs were resuspended in 0.5 ml HBS with vortexing and centrifuged again at 4200 rpm for 10 minutes, after which the MLVs appeared as a pellet. The HBS supernatant was withdrawn and the pellet was washed twice (two cycles of 0.5 ml HBS/vortex/centrifuge) before being resuspended in fresh HBS and stored at 4°C until needed.

4.3.4 Separation of LUV and MLV Populations

Donor [^3H]-LUVs (0.1 μmoles) and 10 μmoles of [^{14}C]-acceptor MLVs were combined in a 1.5 ml Eppendorf tube to yield a 100-fold molar excess of acceptor vesicles, and HBS was added to bring the final volume to 0.5 ml. All samples were run in triplicate, and control samples consisting of LUV or MLV populations alone were included. Samples were vortexed and centrifuged at 4200 rpm for 10 minutes to pellet the MLVs. The LUV-containing supernatant was collected into a scintillation vial. The MLV-containing pellet was then washed twice with 250 μl additions of fresh HBS followed by vortexing and centrifuging as above. Both washes were combined into a second scintillation vial. The pellet was then resuspended in 500 μl HBS and transferred to a third scintillation vial. The amount of radioactivity in each fraction was measured by liquid scintillation counting. Radioactivity associated with the supernatant and washes was combined to give an overall supernatant count, and the degree of cross-over contamination between populations was determined. Radioactivity in the combined washes was less than 10% of the supernatant-associated radioactivity.

4.3.5 Liposomal Encapsulation of Doxorubicin

Liposomes radiolabeled with [^3H]CHE were prepared in 300 mM citrate buffer, pH 4.0. After extrusion the liposomes were passed down a Sephadex G-50 HBS (pH 7.4) column to exchange the external buffer and establish a pH gradient across the liposome membrane (inside acidic). Four milligrams of doxorubicin in saline and 20 mg of liposomes were aliquoted into separate glass test tubes and heated for 5 minutes in a 65°C waterbath. [^{14}C]doxorubicin was incorporated at 0.5 $\mu\text{Ci}/\text{mg}$ to facilitate drug quantitation. Doxorubicin was added to the liposomes while vortexing to achieve a final drug:lipid ratio of 0.2:1 (wt:wt). The liposomes were heated at 65°C with occasional vortexing for 10 minutes, cooled to room temperature and passed down a fresh Sephadex G-50 HBS column to remove any unencapsulated doxorubicin. Doxorubicin and liposome concentrations were determined by liquid scintillation counting.

4.3.6 Liposomal Encapsulation of Verapamil

Sphingomyelin:cholesterol (55:45) liposomes labeled with [^{14}C]CHE were prepared in 300 mM citrate buffer, pH 4.0. One milligram of verapamil in saline was added to 10 mg of liposomes in a 5 mL glass vial to yield a 0.1:1 (wt:wt) drug to lipid ratio. [^3H]verapamil was incorporated at 1 $\mu\text{Ci}/\text{mg}$ to facilitate drug quantitation. The vial was capped, inverted 5 times to mix and the external pH was adjusted to pH 7.4 by the addition of 1 ml of 0.5 M Na_2HPO_4 . The vial was inverted 5 times to mix and placed in a 56°C waterbath for 5 minutes, after which the vial was mixed again and heated for an additional 5 minutes. Liposomes were then passed down a fresh Sephadex G-50 HBS

column to remove unencapsulated verapamil. Verapamil and liposome concentrations were determined by liquid scintillation counting.

4.3.7 Ceramide Lipid/Drug Release from Liposomes Using Dialysis Assays

A 750 µl aliquot of donor liposomes was placed into a 4 inch piece of Spectra/Por dialysis tubing (molecular weight cut off of 12-14 kDa) sealed at both ends with clips. The dialysis tubing was placed into a beaker containing a 1000-fold excess of HBS with or without 30% FBS. Liposomes were incubated with stirring for 24 hours at 37°C. At various timepoints 50 µl aliquots were withdrawn from the tubing for drug analysis. Ceramide, doxorubicin and verapamil were quantitated by liquid scintillation counting.

4.3.8 Ceramide Lipid/Drug Release from Liposomes Using the MLV-Based Release Assay

Various ceramide containing or drug-encapsulated donor LUVs and EPC/Chol (55:45) acceptor MLVs were individually combined at a 1:100 mole ratio and incubated for the indicated times at 37°C in a revolving rack. The LUV and MLV populations were separated by centrifugation and washed as described above. The amount of ceramide lipid/drug in the pellet and supernatant fractions was then measured by liquid scintillation counting. Controls consisting of LUVs or MLVs alone were also run. The percent ceramide lipid/drug retained was determined as:

$$[(\text{amt. ceramide or drug in supernatant})/(\text{total amt. ceramide or drug at } t=0)] \times 100.$$

4.3.9 In Vivo Ceramide Lipid/Drug Release

All animal studies were conducted according to procedures approved by the University of British Columbia's Animal Care Committee and were performed in accordance with the current guidelines established by the Canadian Council of Animal Care. Ceramide-containing or drug encapsulated liposomes were diluted with appropriate volumes of HBS so as to administer a dose of 100 mg/kg total lipid for ceramide-based liposomes, 20 mg/kg doxorubicin or 0.50 mg/kg verapamil by i.v. bolus (200 μ L, tail vein) to female SCID/Rag2 mice (20 gram average weight; n=3/time point). At 1, 4, and 24 hours post-administration the mice were sacrificed with CO₂ and blood was drawn by cardiac puncture. The blood was collected in microtainer tubes (EDTA anticoagulant) and centrifuged at 2200 rpm for 10 minutes to isolate the plasma, which was analyzed for drug and lipid content by scintillation counting.

4.4 RESULTS

4.4.1 Design of the MLV-Based Exchange Assay Procedure

Figure 4.1 depicts a schematic of the overall ceramide lipid exchange assay procedure. Ceramide-containing donor LUVs of 100 nm average diameter were incubated in Eppendorf tubes with a 100-fold molar excess of MLVs, which served as a lipid sink to mimic the physiological membrane pool. At time zero, all ceramide lipid is associated with the LUVs. Over the course of incubation, however, ceramide lipid can exchange from the LUV population and associate with the acceptor MLV membranes based on mass action equilibrium. These two populations can then be isolated by centrifugation and the amount of ceramide in each fraction is measured. The LUV and

MLV populations are not drawn to scale, and for illustrative purposes the ceramide is represented as a disproportionately large lipid.

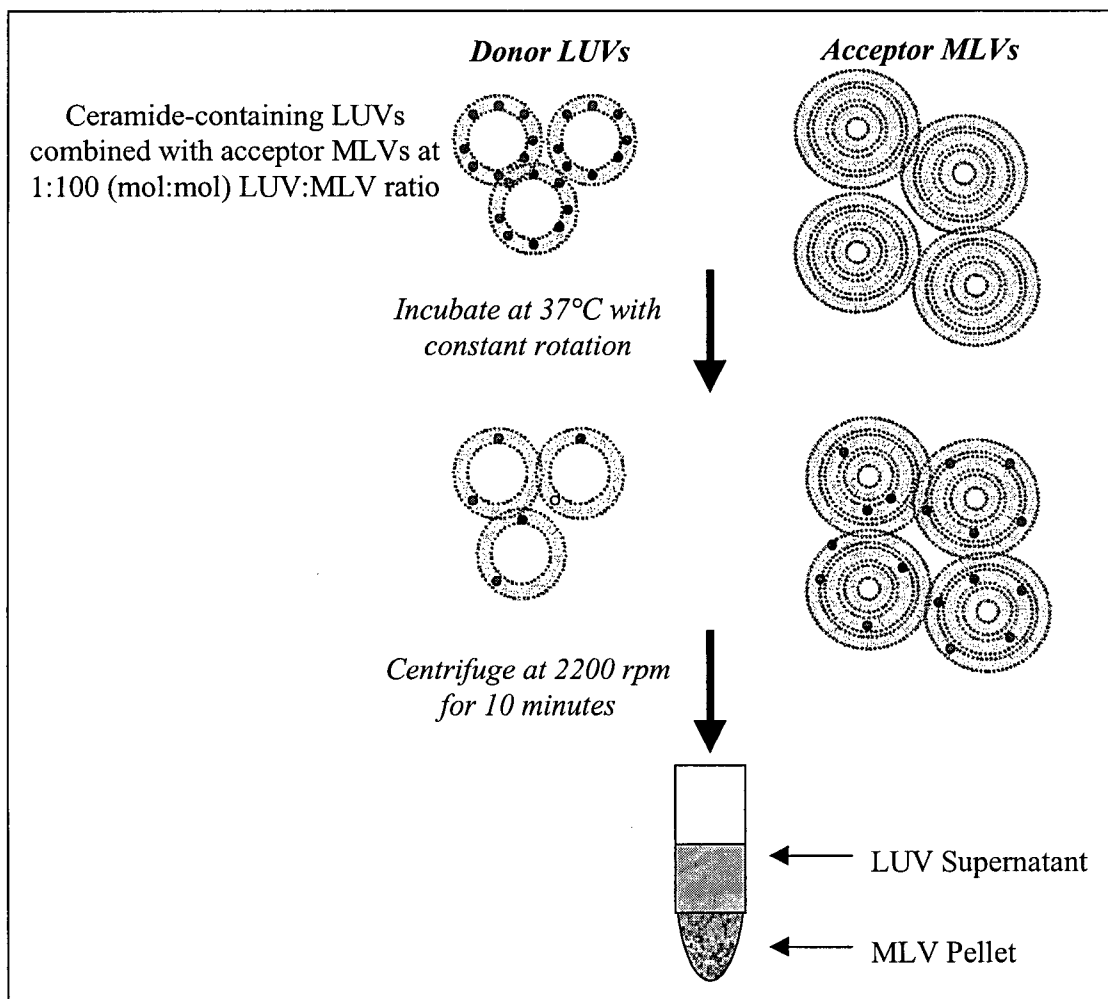


Figure 4.1 A schematic illustration of the overall *in vitro* MLV-based assay. At time zero all ceramide lipid (represented as dark circles in the liposome bilayer) was associated with donor LUVs, which were combined with acceptor MLVs at a 1:100 (mole:mole) ratio and incubated at 37°C in a revolving rack. At various timepoints selected samples were centrifuged at 4200 rpm for 10 minutes. The MLVs formed a distinct pellet and the LUVs remained in the supernatant. Separation was >85% efficient. The two populations were assayed for ceramide lipid or drug content in order to measure the extent of donor to acceptor exchange.

4.4.2 Separation of Control and Ceramide-Containing Donor LUV and Acceptor MLV Populations

In order to demonstrate the validity of this assay it was first necessary to verify that various donor LUV formulations could be efficiently separated from acceptor MLVs by centrifugation. Centrifugation at 4200 rpm for 10 minutes resulted in the formation of a distinct MLV pellet while the LUVs remained in the supernatant. The composition of EPC/Chol (55:45) was chosen as the universal MLV acceptor since it represents an unsaturated and uncharged bilayer that is similar to many physiological membranes. A number of different donor LUV formulations were evaluated, however, in order to demonstrate that separation of the two vesicle populations by this technique was not highly dependent on lipid composition. Formulations that represent a broad range of membrane/bilayer properties were investigated: unsaturated (EPC/Chol, 55:45), saturated (DSPC/Chol, 55:45), sterically stabilized (DSPC/Chol/PEG₂₀₀₀-DSPE, 50:45:5), sphingolipid-based (SM/Chol, 55:45), cationic (DOTAP/DOPC/Chol, 10:45:45), anionic (DOPS/DSPC/Chol, 10:45:45), pH sensitive (DPPC/CHEMS, 50:50), short-chain ceramide (C₆-cer/DSPC/Chol, 45:10:45), and long-chain ceramide (C₁₆-cer/CHEMS, 50:50). Regardless of the LUV composition, the efficiency of separation of LUV and MLV populations was consistently greater than 90%, with the exception of SM/Chol liposomes which was 89%. In all cases greater than 89% of the LUVs and less than 0.7% of the MLVs were recovered in the supernatant fraction, and less than 10% of the LUVs and greater than 96% of the MLVs were recovered in the pellet (Table 4.1). This indicated that the separation procedure was effective and could potentially be applied to a variety of liposome formulations.

Table 4.1

Separation of Empty [³H]-LUV Donor and [¹⁴C]-MLV Acceptor Vesicles By Centrifugation (mean ± SD)^a

LUV Formulation	% Recovery in Supernatant		% Recovery in Pellet	
	LUV	MLV	LUV	MLV
EPC/Chol (55:45)	93.56 ± 4.72	0.54 ± 0.16	6.23 ± 0.90	104.47 ± 1.08
DSPC/Chol (55:45)	97.08 ± 7.14	0.50 ± 0.01	7.58 ± 0.18	103.89 ± 2.41
DSPC/Chol/PEG ₂₀₀₀ -DSPE (55:45:5)	96.99 ± 0.50	0.30 ± 0.01	5.55 ± 4.50	105.18 ± 2.10
SM/Chol (55:45)	89.90 ± 0.42	0.47 ± 0.06	9.84 ± 0.44	102.64 ± 0.90
DOTAP/DOPC/Chol (10:45:45)	96.08 ± 0.06	0.40 ± 0.00	9.70 ± 3.07	97.88 ± 2.68
DOPS/DSPC/Chol (10:45:45)	100	0.41 ± 0.03	0	99.59 ± 0.03
DPPC/CHEMS (50:50)	93.23 ± 1.07	0.62 ± 0.04	6.08 ± 1.02	96.87 ± 0.27
C ₆ -cer/DSPC/Chol (45:10:45)	96.01 ± 4.11	0.43 ± 0.07	5.13 ± 3.27	106.87 ± 0.84
C ₁₆ -cer/CHEMS (50:50)	96.88 ± 2.29	0.42 ± 0.07	3.87 ± 1.26	100.87 ± 1.25

^aLUV and MLV populations were mixed at a 1:100 LUV:MLV (mole:mole) ratio and separated by centrifugation at 2200 rpm for 10 minutes. The MLV pellet was washed twice and combined with the supernatant fraction. The results represent the percent LUVs and MLVs in the supernatant and pellet after centrifugation as measured by liquid scintillation counting. Data represents the mean of two independent experiments conducted in triplicate.

4.4.3 Evaluation of C₆-Ceramide Retention Using Conventional *In Vitro* Dialysis Assays

Figure 4.2 shows the profile of C₆-ceramide release from C₆-cer/DSPC/Chol/PEG₂₀₀₀-DSPE (45:10:40:5) LUVs following dialysis against a 1000-fold excess of HBS (closed symbols) or HBS + 30% FBS (open symbols) at 37°C. A sterically stabilized liposome formulation containing PEG₂₀₀₀-DSPE was used in order to allow for direct comparisons between *in vitro* and later *in vivo* lipid exchange to be made. At 1, 4 and 24 hours three 50 µL aliquots were withdrawn from the dialysis bag and analyzed for [¹⁴C]C₆-ceramide content. The results demonstrated extensive C₆-ceramide exchange from the LUVs over the dialysis period. The exchange followed a biphasic pattern with a rapid loss of greater than 50% of the ceramide lipid in the first 4 hours, followed by a more gradual exchange over the 4-24 hour time period. After 24 hours only 23.6% and 21% of the ceramide lipid remained associated with the liposomes under the HBS and HBS + 30% FBS dialysis conditions, respectively.

4.4.4 Evaluation of C₆-Ceramide Retention Following I.V. Bolus Administration

The dialysis-based C₆-ceramide exchange rates were correlated with actual *in vivo* ceramide exchange following i.v. administration of the same liposomes to mice. Figure 4.3 shows the plasma C₆-ceramide circulation profile for C₆-cer/DSPC/Chol/PEG₂₀₀₀-DSPE (45:10:40:5) liposomes administered by i.v. bolus at a total lipid dose of 100 mg/kg. Rapid ceramide exchange was observed, with less than 1% of the total administered dose detectable in the plasma after 24 hours. The percent C₆-ceramide remaining in circulation after 1, 4, and 24 hours was 7.46%, 1.67% and 0.56% respectively. In order to confirm that loss of plasma-associated ceramide lipid was not

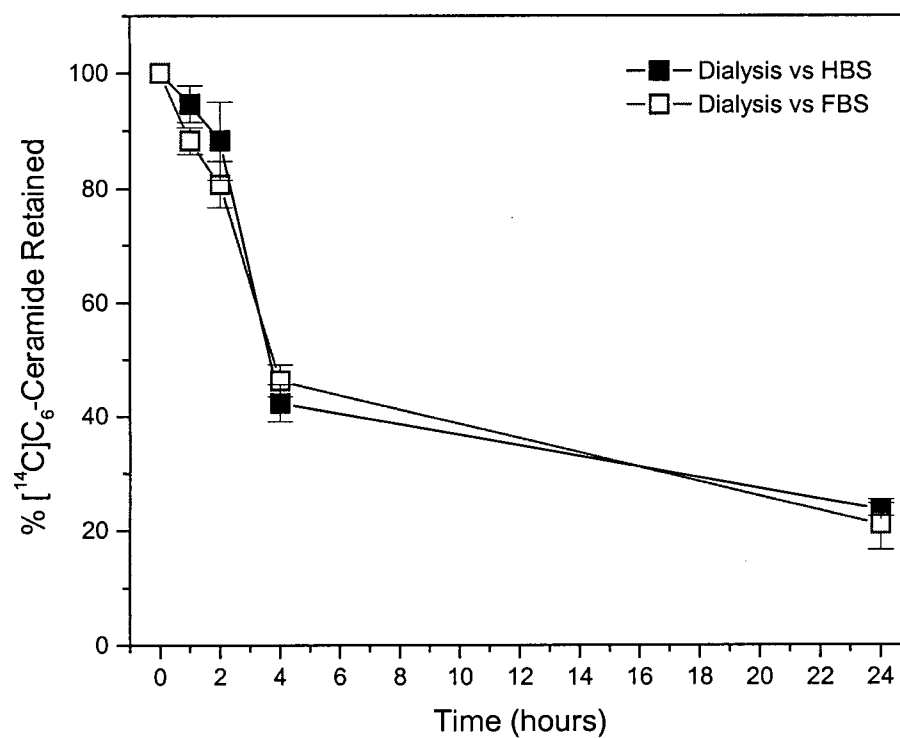


Figure 4.2 Profile of C₆-ceramide release from C₆-cer/DSPC/Chol/PEG₂₀₀₀-DSPE (15:10:40:5) donor LUVs following dialysis against HBS (open symbols) or HBS + 30% FBS (closed symbols) for 24 hours at 37°C. Each value represents the mean from three independent experiments conducted in triplicate; bars, SD.

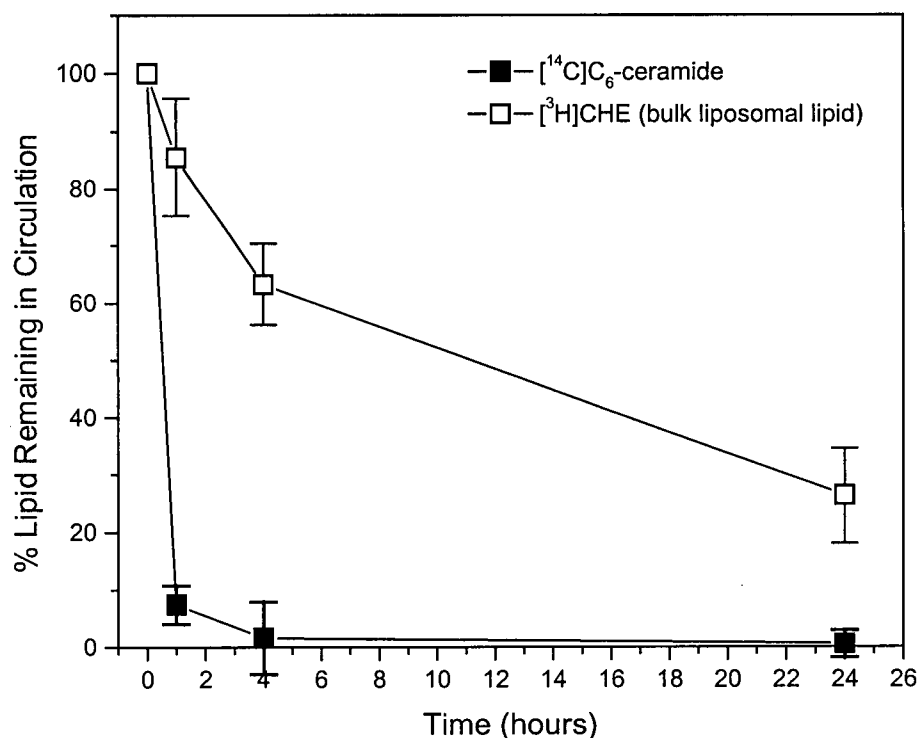


Figure 4.3 Circulation profile of $\text{C}_6\text{-ceramide}$ (closed symbols) and bulk liposomal lipid (open symbols) following i.v. bolus administration (tail vein) of $\text{C}_6\text{-cer/DSPC/Chol/PEG}_{2000}\text{-DSPE}$ (15:10:40:5) liposomes to female Balb/c mice. A 100 mg/kg total lipid dose was administered by i.v. bolus in a 200 μl injection volume. At 1, 4 and 24 hours three mice were sacrificed with CO_2 and blood was drawn by cardiac puncture. The blood was collected in microtainer tubes (EDTA anticoagulant) and centrifuged at 2200 rpm for 10 minutes to isolate the plasma, which was analyzed for $[^{14}\text{C}]\text{C}_6\text{-ceramide}$ and $[^3\text{H}]\text{CHE}$ bulk liposomal lipid by scintillation counting. Each value represents the mean from two independent experiments; bars, SD.

attributed to overall elimination of the liposomes from the circulation, the bulk liposomal lipid marker [^3H]CHE was also monitored. These results confirmed that the liposomes remained in circulation over the 24 hour period while the ceramide lipid component did not (85.47%, 63.25% and 26.34% liposomal lipid remaining at 1, 4 and 24 hours, respectively). The *in vivo* ceramide exchange results demonstrated a faster and more extensive rate of ceramide exchange from the liposomes than was predicted by the dialysis assay system ($r=0.776$ and $r=0.839$ for HBS and HBS + 30% FBS, respectively). This confirmed the need for a better *in vitro* predictor of *in vivo* behaviour.

4.4.5. Evaluation of C₆-Ceramide Retention Using the MLV-Based *In Vitro* Assay

In order to test the *in vivo* predictive accuracy of the MLV-based assay, the C₆-cer/DSPC/Chol/PEG₂₀₀₀-DSPE (45:10:40:5) liposomes were used as donor LUVs and incubated with acceptor MLVs according to the assay procedure described above. Figure 4.4 shows the profile of [^{14}C]C₆-ceramide release using this assay. In contrast to the release profiles predicted by dialysis-based assays, the drug release rates predicted by the MLV-based assay show a much better correlation with the behavior of these formulations *in vivo* ($r=0.990$). Specifically, 9.65%, 3.67% and 1.62% C₆-ceramide was retained after 1, 4 and 24 hours respectively using the MLV exchange assay. These results suggest that the MLV acceptor population more accurately mimics the physiological environment that the liposomes encounter following systemic administration than dialysis against buffer or serum. Correlation coefficients for the comparisons made between the various assays are summarized in Table 4.2.

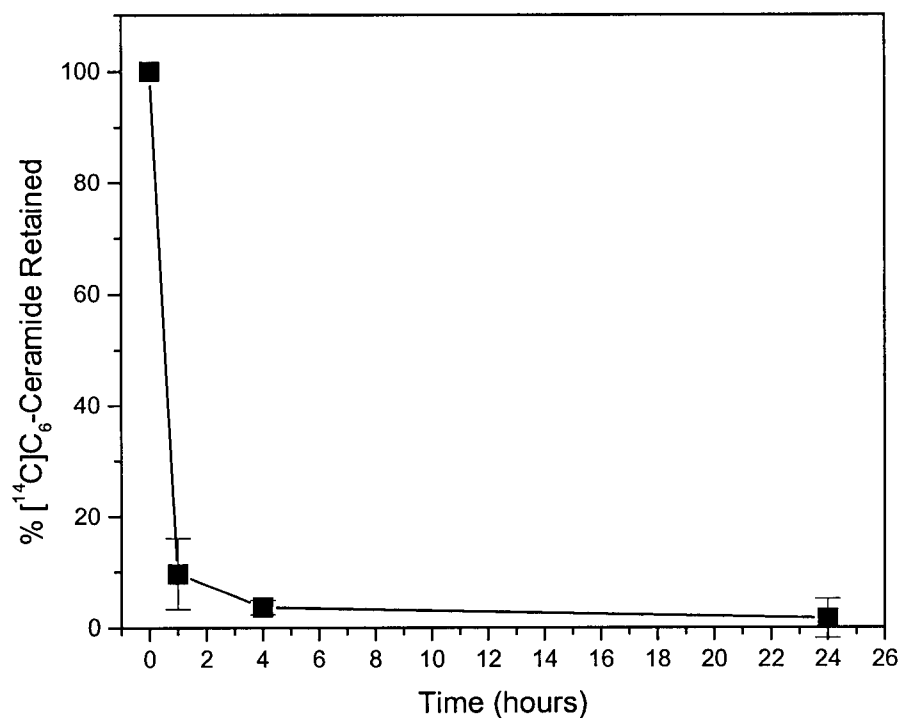


Figure 4.4 Profile of C₆-ceramide release from C₆-cer/DSPC/Chol/PEG₂₀₀₀-DSPE (15:10:40:5) donor LUVs using the MLV-based exchange assay. Ceramide-containing donor LUVs were incubated with acceptor MLVs for 24 hours at 37°C with constant mixing. At 1, 4 and 24 hours the samples were centrifuged for 10 minutes at 4200 rpm to separate the LUV and MLV populations. The MLV pellet was washed twice and combined with the supernatant fraction. The MLV and LUV fractions were analyzed for [¹⁴C]C₆-ceramide content by liquid scintillation counting. Each value represents the mean from three independent experiments conducted in triplicate; bars, SD.

Table 4.2

Correlation Coefficient (r) and Coefficient of Determination (r²) for Ceramide Lipid, Doxorubicin or Verapamil Release from Liposomes as Measured by the Dialysis and MLV-Based Assays Relative to Actual *In Vivo* Results^a

	Dialysis with HBS	Dialysis with FBS	MLV-based Assay	<i>In vivo</i>
C ₆ -ceramide	r = 0.776 r ² = 0.602	r = 0.839 r ² = 0.704	r = 0.990* r ² = 0.980*	r = 1.000 r ² = 1.000
DSPC/Chol/PEG ₂₀₀₀ -DSPE/Dox	r = 0.608 r ² = 0.370	r = 0.673 r ² = 0.453	r = 1.000* r ² = 1.000*	r = 1.000 r ² = 1.000
SM/Chol/Verapamil	r = 0.291 r ² = 0.085	r = 0.361 r ² = 0.130	r = 0.864 r ² = 0.746	r = 1.000 r ² = 1.000

^a The correlation coefficient was calculated as:

$$r = [n(\sum xy) - (\sum x)(\sum y)] / \sqrt{\{[n(\sum x^2) - (\sum x)^2][n(\sum y^2) - (\sum y)^2]\}}$$

* Statistically significant from zero (p<0.05)

4.4.6. Evaluation of C₁₆-Ceramide Retention Using the MLV-Based *In Vitro* Assay

Given the high correlation between *in vivo* and *in vitro* release for the C₆-ceramide formulation using the MLV-based exchange assay, the next step was to evaluate ceramide exchange from the C₁₆-cer/CHEMS (50:50) formulation that showed promising *in vitro* cytotoxicity. Results presented in Figure 4.5 demonstrate that C₁₆-ceramide retention in these liposomes was very high, with 90.47%, 70.56% and 32.83% of the ceramide lipid remaining liposome-associated after 1, 4 and 24 hours, respectively. This is also in agreement with previously published results demonstrating that the rate of exchange of [¹⁴C]C₁₆-ceramide between lipid vesicles was on the order of days (278). These encouraging results suggested that these liposomes should retain the bioactive ceramide lipid component *in vivo* and would be a suitable candidate to carry forward for *in vivo* evaluation.

4.4.7 Evaluation of the MLV-Based Assay as a Measure of Liposomally Encapsulated Conventional Drug Release

Additional experiments were completed to evaluate whether the utility of this new assay could be extended beyond the exchange of liposome-associated lipids to assess the release of conventional drugs encapsulated within the aqueous liposome core. Two conventional drugs were chosen for this evaluation: doxorubicin encapsulated into DSPC/Chol/PEG₂₀₀₀-DSPE (55:40:5) liposomes, which represents a well-characterized formulation known to retain the encapsulated drug for extended periods (>24 hours) post i.v. administration, and verapamil encapsulated into SM/Chol (55:45) liposomes, which represents a liposome formulation that appears to retain the drug following *in vitro* dialysis but that releases >90% of the encapsulated contents within one hour post i.v.

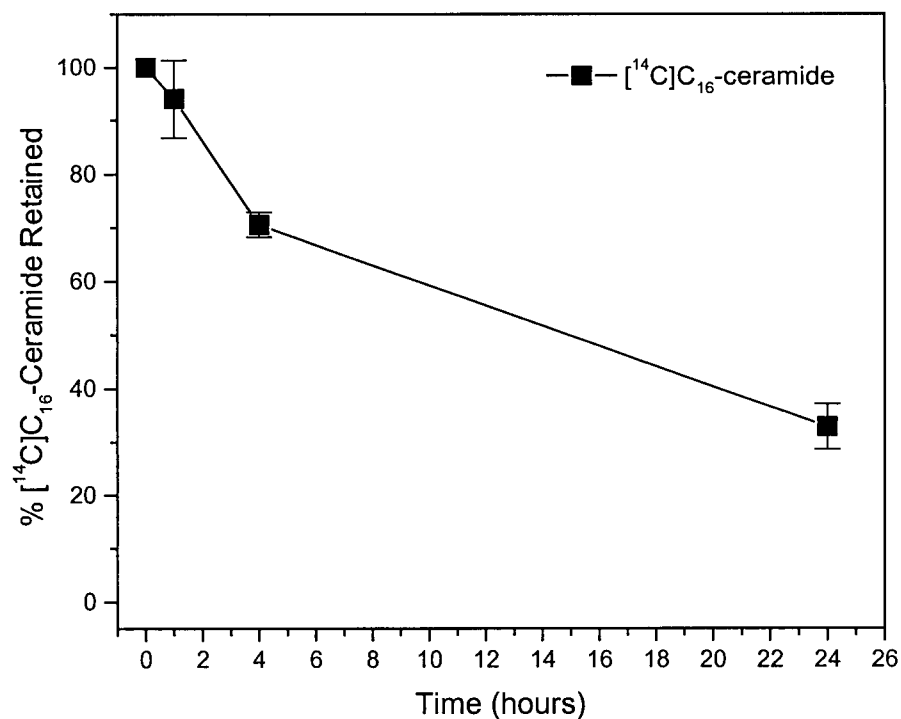


Figure 4.5 Profile of C₁₆-ceramide release from C₁₆-cer/CHEMS (50:50) donor LUVs using the MLV-based exchange assay. Ceramide-containing donor LUVs were incubated with acceptor MLVs for 24 hours at 37°C with constant mixing. At the timepoints indicated samples were centrifuged for 10 minutes at 4200 rpm to separate the LUV and MLV populations. The MLV pellet was washed twice and combined with the supernatant fraction. The MLV and LUV fractions were analyzed for [^{14}C]C₁₆-ceramide content by liquid scintillation counting. Each value represents the mean from three independent experiments conducted in triplicate; bars, SD.

administration. The results presented in Table 4.3 demonstrate that separation efficiencies of more than 90% were achieved for the drug-loaded LUV and acceptor MLV populations. This indicated that the encapsulation of drug into LUVs did not adversely affect the ability to separate the donor and acceptor vesicle populations by centrifugation. The release of doxorubicin and verapamil from their respective liposome formulations was then measured as previously described by dialysis against HBS or HBS + 30% FBS, using the MLV-based release assay, or by analysis of plasma following i.v. bolus administration.

For the evaluation of doxorubicin release (Figure 4.6A), monophasic release kinetics were observed and greater than 85% of the encapsulated drug was retained by the liposomes over the 24 hour incubation period following dialysis against HBS or HBS + 30% FBS. The MLV-based assay demonstrated biphasic doxorubicin release with 72% of the doxorubicin remaining liposome-associated after 4 hours and 58% remaining after 24 hours. In this case the MLV-based assay predicted more rapid doxorubicin release in the first 4 hours than was actually observed *in vivo*. Specifically, whereas the MLV-based assay predicted 72% and 64% doxorubicin retention after 1 and 4 hours, respectively, the actual *in vivo* results predicted 98% and 75% retention at 1 and 4 hours. However, the final 24 hour doxorubicin retention result of 58% predicted by the MLV-based assay corresponded well to the actual *in vivo* retention value of 55%, and the MLV-based assay also demonstrated more accurate biphasic release characteristics than the monophasic dialysis-based assays.

For the evaluation of verapamil release (Figure 4.6B), rapid triphasic drug release was observed following dialysis against HBS or HBS + 30% FBS, with approximately

35%, 18% and 4% retained after 1, 4 and 24 hours, respectively. However, these results did not reflect the true extent of verapamil exchange observed *in vivo*. The MLV-based assay was more predictive, although the correlation did not reach statistical significance ($p=0.33$ for the MLV-based assay versus $p=0.81$ and $p=0.76$ for dialysis versus HBS and FBS, respectively). Both the MLV-based assay and the *in vivo* results showed extensive drug loss that displayed biphasic release characteristics. The *in vivo* retention results of 5%, 4.5% and 0% at 1, 4 and 24 hours, respectively, were closely predicted by the MLV-based assay which demonstrated 11%, 6% and 3% retention at the same time points.

The doxorubicin and verapamil release results, which are summarized in Figure 4.6, indicate that for both formulations the MLV-based assay showed a higher correlation with *in vivo* drug release than the dialysis-based systems, indicating again that it serves as a better predictor of true *in vivo* performance. Table 4.2 provides a summary of the correlation coefficients for each of the assay methods.

Table 4.3

Separation of Doxorubicin or Verapamil-Loaded [^3H]-LUV Donor and [^{14}C]-MLV Acceptor Populations by Centrifugation (mean \pm SD)^a

LUV Formulation	% Recovery in Supernatant		% Recovery in Pellet	
	LUV	MLV	LUV	MLV
DSPC/Chol/PEG ₂₀₀₀ -DSPE/Dox	90.58 \pm 1.82	0.33 \pm 0.08	7.98 \pm 0.35	106.17 \pm 0.83
SM/Chol/Verapamil	94.75 \pm 0.26	0.87 \pm 0.13	3.29 \pm 0.44	101.36 \pm 0.90

^aDoxorubicin was encapsulated at a 0.2:1 drug:lipid (wt:wt) ratio and verapamil at a 0.1:1 (wt:wt) ratio. LUV and MLV populations were mixed at a 1:100 LUV:MLV (mole:mole) ratio and separated by centrifugation at 2200 rpm for 10 minutes. The results represent the percent LUVs and MLVs found in the supernatant and pellet after centrifugation as measured by liquid scintillation counting.

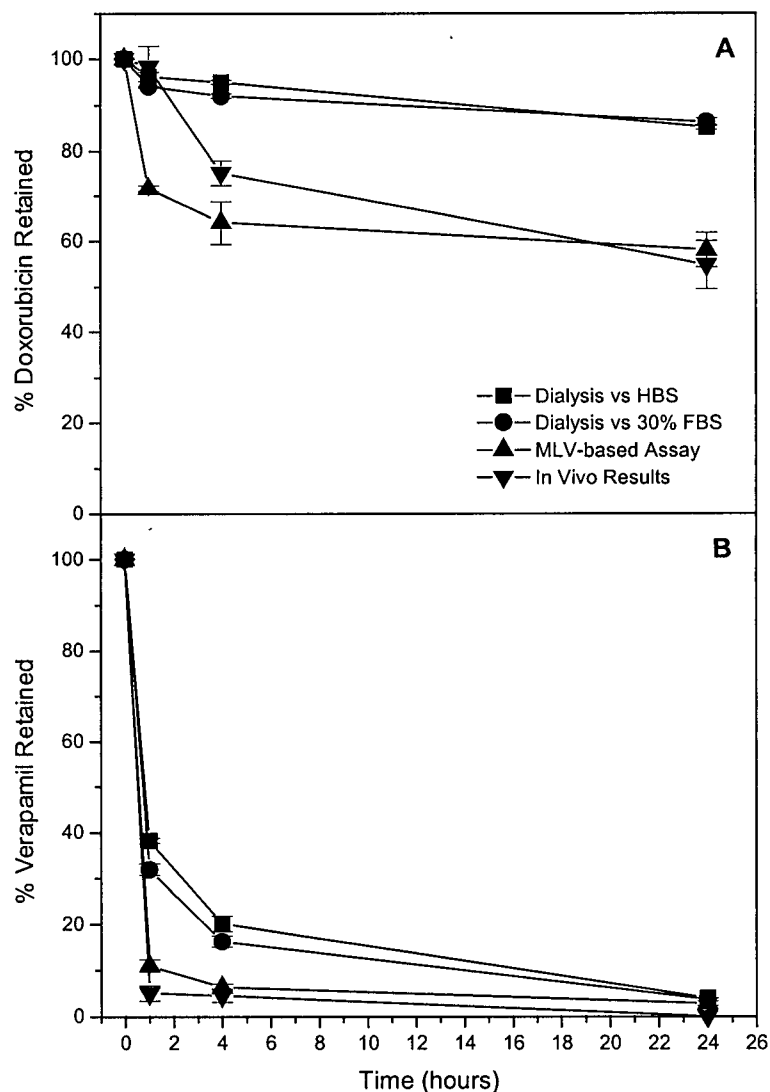


Figure 4.6 Release profiles of doxorubicin (A) and verapamil (B) from liposomes as measured by dialysis assays, the *in vitro* MLV-based assay, or from plasma collected following i.v. bolus liposome administration. Each value represents the mean from two independent experiments conducted in triplicate; bars, SD.

4.5 DISCUSSION

Liposomes are well known as delivery vehicles for many conventional drugs such as chemotherapeutic agents and antifungals (see references cited in Chapter 1). However, their utility as delivery systems for bioactive lipids incorporated into the liposome membrane is just beginning to be realized. An important step in the development of liposomes for either application is the evaluation of drug/lipid retention by the liposomal carrier. This is essential for utilizing the liposome as a delivery vehicle and for capitalizing on the inherent advantages of site-specific localization, mass-action delivery of contents and reduced drug toxicities described in Chapter 1. If the drug or bioactive lipid component is not adequately retained then the liposome can offer no delivery advantage, as was observed with the *in vitro* evaluation of the C₆-ceramide formulation in Chapter 3. Although the ultimate goal of developing liposomal formulations is to optimize them for *in vivo* applications (ultimately in humans through clinical trials, but also in animal models for pre-clinical screening), it is first necessary to characterize their properties at the level of *in vitro* testing. As conventional drug encapsulated liposomal formulations were developed, so too were *in vitro* drug release assays based on methods such as dialysis (275-277). Although commonly used, this screening process is limited by its frequent inability to accurately predict actual *in vivo* liposome behaviour. This is likely due to its inability to mimic the extensive membrane lipid pool that exists in the physiological setting. The objective of this chapter, therefore, was to develop a more reliable *in vitro* system with which to evaluate the release characteristics of ceramide-based liposomes before moving them forward to more extensive *in vivo* evaluations. A large excess of MLVs was used as an acceptor lipid "sink" to promote exchange of

ceramide lipid from donor LUVs. The results presented in this chapter demonstrate that sucrose-containing MLVs can be separated from 100 nm LUVs with ~90% efficiency, irrespective of LUV composition or the presence of encapsulated drug.

Using the C₆-cer/DSPC/Chol/PEG₂₀₀₀-DSPE liposomes from Chapter 3 as a model system, it was observed that the MLV-based assay demonstrated C₆-ceramide exchange properties consistent with the C₆-ceramide *in vitro* uptake results observed in Chapter 3 (loss of C₆-ceramide from the liposomal carrier). Although the 24 hour C₆-ceramide exchange measured by the dialysis assay was consistent with the uptake results, the rate of release predicted by dialysis was much slower than that which was observed *in vivo*. This was resolved by the fact that the MLV-based assay showed a better correlation with *in vivo* C₆-ceramide exchange than the dialysis systems ($r=0.99$ versus ~ 0.80).

The MLV-based assay was then used to evaluate C₁₆-ceramide retention in the C₁₆-cer/CHEMS (50:50) liposome bilayer. Since this formulation demonstrated superior cytotoxicity in the J774 cell line *in vitro*, it became the lead candidate for further evaluation. Results from the MLV-based assay predicted that C₁₆-ceramide should remain associated with the membrane over 24 hours. This suggested that it was a suitable formulation for the next stage of *in vivo* analysis, which was the focus of Chapter 5.

Given the apparent utility of this system for evaluating lipid exchange, its application to the release of encapsulated conventional drugs was also investigated. The results demonstrated that this MLV-based assay was a better predictor of both doxorubicin and verapamil release from liposomal carriers than dialysis-based systems, and showed a high correlation with the extent of observed *in vivo* release ($r=1.0$ and 0.86 for doxorubicin and verapamil, respectively). Therefore, not only is this system useful

for developing ceramide-based liposomes, it also has potential applications for the development of numerous liposomal systems based on other bioactive lipids or encapsulated agents.

CHAPTER 5

PHARMACOKINETIC EVALUATION AND ANTITUMOR ACTIVITY OF HIGH CERAMIDE CONTENT LIPOSOMES*

5.1 INTRODUCTION AND RATIONALE

The ability of liposomes to overcome the difficulties associated with solubilization and intracellular delivery of long-chain (natural) C₁₆-ceramide *in vitro* was demonstrated in Chapter 3 by the development of high content ceramide liposomes composed of C₁₆-cer/CHEMS (50:50). Whereas free C₁₆-ceramide showed no cytotoxicity when added to cells in culture, when delivered to cells in a liposomal formulation that was effectively internalized by macrophage-derived J774 cells, significant ceramide-specific cytotoxicity was observed. This implicated the utility of ceramide-based liposomes as a novel and biologically active ceramide delivery vehicle. However, in order to translate these *in vitro* observations into an *in vivo* model, it was first necessary to characterize the *in vivo* pharmacokinetic behavior of these formulations.

Lessons learned from the development of therapeutically active liposomes with conventional drugs and small molecules encapsulated in the aqueous core have highlighted the importance of characterizing the drug retention properties of liposome-based formulations. The same evaluation process is necessary for ceramide-based liposomes in order to ensure that the biologically active lipid component remains liposome-associated for the duration of the delivery process. The exchange assay described in Chapter 4 provided an effective preliminary *in vitro* screening mechanism to predict how these formulations would behave *in vivo*. Characterization of the C₁₆-cer/CHEMS (50:50) formulation using the MLV-based assay indicated that the liposomes

*Adapted from: JA Shabbits and LD Mayer. *Antitumor activity of ceramide liposomes* (in preparation).

should retain the bioactive lipid component over 24 hours following systemic administration. This level of stability was sufficient to warrant more extensive characterization in animal models. Therefore, the objectives of this thesis chapter were to characterize the *in vivo* behavior of these liposomes using pharmacokinetic analysis following i.v. bolus administration, and to evaluate the antitumor activity of this formulation in the J774 ascites tumor model.

5.2 HYPOTHESIS

The hypothesis underlying the research presented in this chapter is that high content ceramide liposomes with stability *in vivo* will exhibit antitumor activity against J774 cells growing as an ascites tumor in syngenic mice.

5.3 MATERIALS AND METHODS

5.3.1 Materials

All lipids and cell culture materials were obtained as previously described in Chapters 2 and 3. Female Balb/c mice were bred in-house at the BC Cancer Agency animal facility (Vancouver, BC, Canada).

5.3.2 Cell Line and Culture

J774 murine macrophage cells were obtained and cultured as previously described in Chapter 3.

5.3.3 Preparation of Liposomes

Liposomes were prepared as previously described in Chapters 3 and 4.

5.3.4 Pharmacokinetic Analysis of Control and Ceramide Liposomes

Pharmacokinetic studies were conducted in order to determine the *in vivo* circulation longevity and ceramide retention properties of high C₁₆-ceramide-content liposomes. All animal studies were conducted according to procedures approved by the University of British Columbia's Animal Care Committee and in accordance with the current guidelines established by the Canadian Council of Animal Care. Control (DPPC/CHEMS/PEG₂₀₀₀-DSPE, 47.5:47.5:5) liposomes containing the [³H]CHE radiolabel, and ceramide-based (C₁₆-cer/CHEMS/PEG₂₀₀₀-DSPE, 47.5:47.5:5) liposomes containing both [³H]CHE and [¹⁴C]C₁₆-ceramide radiolabels were administered by i.v. bolus (200 µl, tail vein) over approximately 5 seconds into female Balb/c mice (20 gram average weight) at a total lipid dose of 100 mg/kg. At 0.5, 1, 2, 4, 8, 12 and 24 hours three mice per time point were sacrificed with CO₂ and blood was drawn by cardiac puncture. The blood was collected in microtainer tubes (EDTA anticoagulant) and centrifuged at 2200 rpm for 10 minutes to isolate the plasma, which was analyzed for bulk liposomal lipid ([³H]CHE) and [¹⁴C]C₁₆-ceramide lipid by liquid scintillation counting.

Prior to obtaining the plasma pharmacokinetic parameters, the log plasma lipid concentration versus time data were fitted to one- and two-compartment models using WinNonlin Version 1.1 (Pharsight Corp., Mountain View, CA). The appropriate model was selected on the basis of goodness of fit for each model tested using the Akaike

Information Criterion (AIC). The AIC values of 72.5, 72.3 and 53.5 obtained for the control liposomes, ceramide liposomes (total lipid) and ceramide liposomes (ceramide lipid), respectively, using a one-compartment model were not improved by using a two-compartment model so the one-compartment model was used for subsequent pharmacokinetic analysis. The observed and predicted log plasma lipid concentration versus time graph shown in Figure 5.1 was also in agreement with the one-compartment model. WinNonlin Version 1.1 software was then used to calculate the following parameters:

elimination half-life ($t_{1/2}$) = $\ln 2/k$ (where $k = -2.303 \times$ slope of the log conc. vs time graph)

area under the curve ($AUC_{0 \rightarrow \infty}$) was calculated using the trapezoidal rule

plasma clearance (CL_p) = $Dose_{i.v.}/AUC_{0 \rightarrow \infty}$

volume of distribution (V_d) = CL_p/k

5.3.5 Establishment of the J774 Ascites Tumor Model

Cell suspensions were prepared in Hank's Balanced Salt Solution at a concentration of 2×10^6 cells/ml and were inoculated i.p. into female Balb/c mice in an injection volume of 0.5 ml. Animals were weighed daily and observed for morbidity and mortality. In particular, signs of ill health based on body weight gain due to ascitic tumor growth, altered gait and distension of the abdomen were monitored. Animals were terminated by CO₂ asphyxiation when significant tumor-related illness requiring euthanasia was observed.

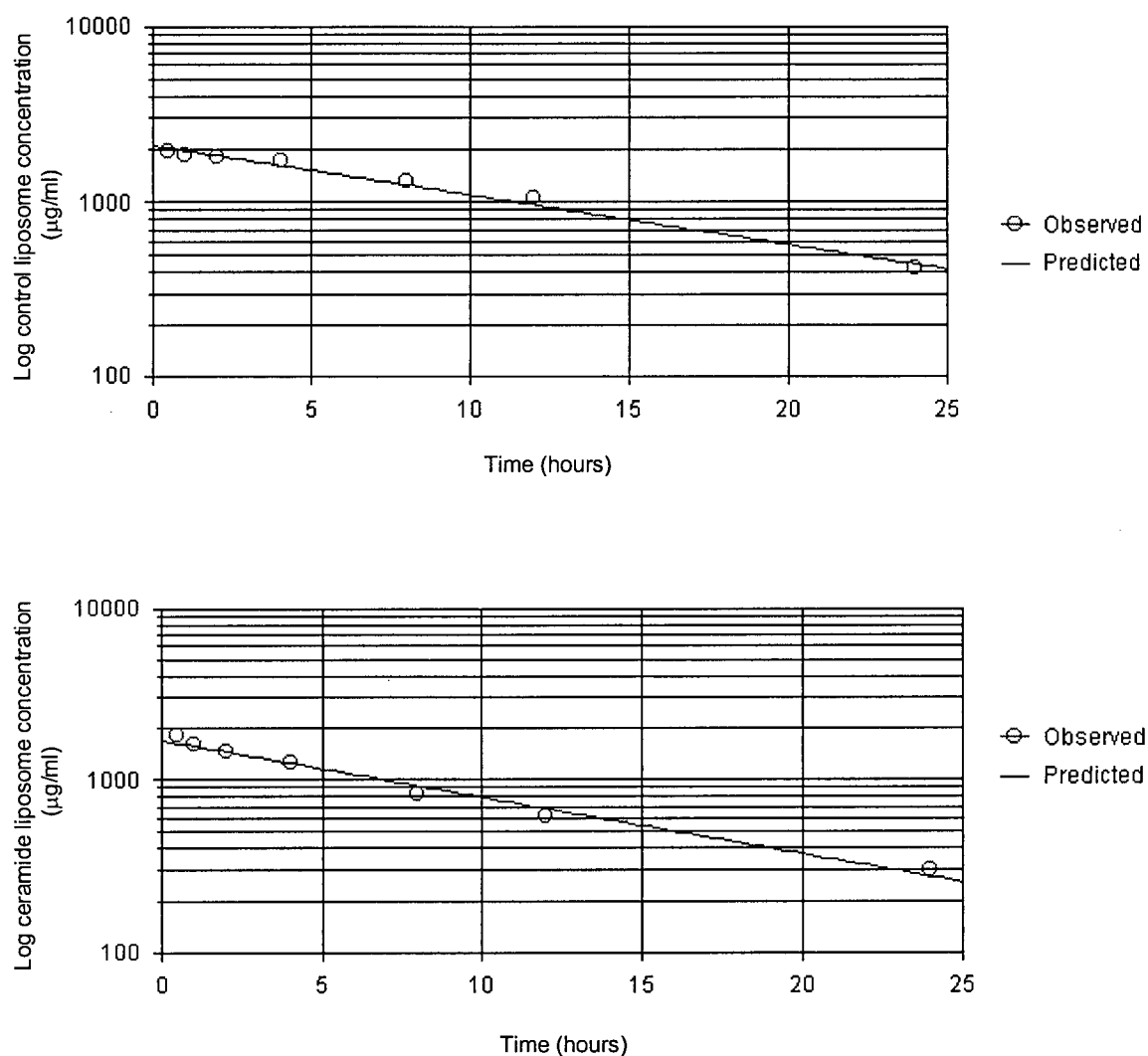


Figure 5.1 Correlation plots comparing observed and predicted log plasma lipid concentration versus time graphs for control and ceramide liposomes modeled with WinNonlin 1.1 using a one-compartment i.v. bolus dosing model.

5.3.6 Evaluation of Antitumor Activity

On day 0, 1×10^6 cells/0.5 ml were injected i.p. into the mice. A total of four mice/group were treated with saline, control liposomes or ceramide-based liposomes on day 1 (single-dose study) or days 1, 5, 9 (multi-dose studies). Animals were monitored as described above. Antitumor activity was measured as % Increase in Lifespan (%ILS) which was defined as:

$$[(\text{Median Survival}_{\text{treated}}) - (\text{Median Survival}_{\text{control}})] / [\text{Median Survival}_{\text{control}}] \times 100.$$

5.3.7 Statistical Analysis

Statistical analysis was performed using one way analysis of variance (ANOVA) followed by Student-Newman-Keuls analysis with InStat Version 3.0 for Windows (GraphPad Software, Inc., San Diego, CA). Mean differences with a p value < 0.05 were considered statistically significant.

5.4 RESULTS

5.4.1 Pharmacokinetic Analysis of Control and Ceramide Liposomes Following I.V. Bolus Administration

Although an estimated prediction of the *in vivo* behaviour of C₁₆-ceramide liposomes with respect to ceramide lipid retention was obtained using the MLV-based assay described in Chapter 4, it was necessary to confirm these retention properties following systemic administration and to fully establish the pharmacokinetic parameters associated with these liposomes *in vivo*. Formulations composed of C₁₆-cer/CHEMS/PEG₂₀₀₀-DSPE (47.5:47.5:5) and DPPC/CHEMS/PEG₂₀₀₀-DSPE (47.5:47.5:5) were compared. Control and ceramide-based liposomes were administered

to mice by i.v. bolus and plasma collected at 0.5, 1, 2, 4, 8, 12 and 24 hours was analyzed by scintillation counting to determine the percent injected lipid dose remaining in the circulation.

The pharmacokinetic behaviour of the control formulation was evaluated by following the radioactive [^3H]CHE liposomal lipid marker. Results presented in Figure 5.2 demonstrated that the control liposomes were stable in the circulation over a 24 hour time period. The liposomes were gradually eliminated from the plasma with an elimination half-life of 10.7 hours, and 21.1% of the total lipid dose administered remained in the plasma after 24 hours. A plasma clearance value of 0.061 ml/hr and a plasma AUC of 32.43 mg*hr/ml were obtained. A volume of distribution of 0.96 ml indicates that the liposomes are confined primarily to the blood/plasma, as the plasma volume of a mouse is approximately 1 ml. These pharmacokinetic parameters are summarized in Table 5.1.

The pharmacokinetic behaviour of ceramide-based liposomes was evaluated from two perspectives. As with the control formulation, the behaviour of the liposome as a whole was monitored using the [^3H]CHE lipid marker (Figure 5.2). These results demonstrated that the ceramide-containing liposomes were also stable in the circulation over 24 hours, although they displayed somewhat more rapid plasma elimination than control liposomes. This was evidenced by a shorter elimination half-life of 9.2 hours and a more rapid plasma clearance of 0.09 ml/hr. This was also confirmed by a smaller plasma AUC value of 22.28 mg*hr/ml. A volume of distribution of 1.2 ml is again consistent with the liposomes remaining in the blood/plasma (Table 5.1). Although the plasma elimination behaviour of the ceramide-containing formulations was more rapid

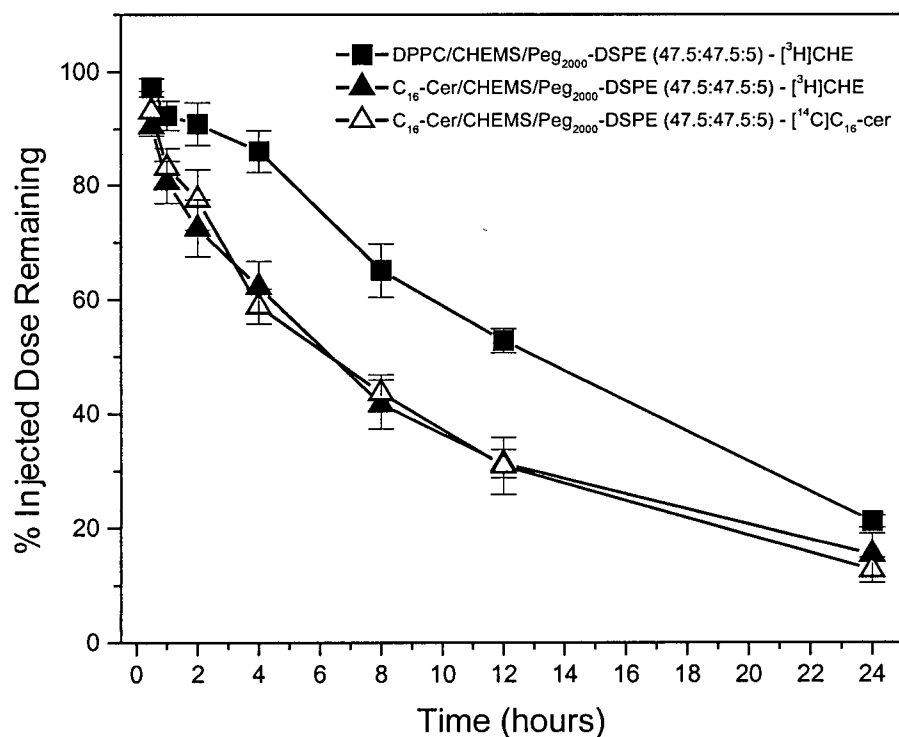


Figure 5.2 Plasma elimination profile of control (DPPC/CHEMS/PEG₂₀₀₀-DSPE, 47.5:47.5:5) and ceramide-based (C₁₆-cer/CHEMS/PEG₂₀₀₀-DSPE, 47.5:47.5:5) liposomes following i.v. bolus administration to female Balb/c mice. Bulk liposomal lipid was radiolabeled with [³H]CHE and ceramide lipid was radiolabeled with [¹⁴C]C₁₆-ceramide. Mice were sacrificed at 0.5, 1, 2, 4, 8, 12 and 24 hours and plasma was analyzed for lipid as previously described. Data are means (n=3); bars, SD.

Table 5.1

Summary of Plasma Pharmacokinetic Parameters^{a,b} for Control and C₁₆-Ceramide Containing Liposomes Following I.V. Bolus Administration at a Dose of 100 mg/kg Total Lipid

	Dose (mg)	t_{1/2} (hr)	AUC_{0→∞} (mg*hr/ml)	CL_p (ml/hr)	V_d (ml)
Control liposomes^c [³ H]CHE label	2.0	10.74 ± 0.50	32.43 ± 1.12	0.061 ± 0.002	0.96 ± 0.03
Ceramide liposomes^d [³ H]CHE label	2.0	9.19 ± 0.58	22.28 ± 0.99	0.090 ± 0.004	1.19 ± 0.06
Ceramide liposomes^d [¹⁴ C]Cer label	0.816	8.26 ± 0.33	8.62 ± 0.25	0.095 ± 0.003	1.13 ± 0.04

^aelimination half-life ($t_{1/2}$) = $\ln 2/k$, where $k = -2.303 \times$ slope of the log conc. vs time graph; area under the curve (AUC_{0→∞}) was calculated using the trapezoidal rule; plasma clearance (CL_p) = Dose_{i.v.}/AUC_{0→∞}; volume of distribution (V_d) = CL_p/k

^bData shown are mean ± SEM, n=3/group

^cDPPC/CHEMS/PEG₂₀₀₀-DSPE (47.5:47.5:5, mole:mole)

^dC₁₆-cer/CHEMS/PEG₂₀₀₀-DSPE (47.5:47.5:5, mole:mole)

than control liposomes, 15.3% of the administered lipid dose remained in the plasma after 24 hours, indicating that the formulation was still stable in the circulation.

In addition to monitoring the behaviour of the ceramide-containing liposomes as a whole, the behaviour of the ceramide lipid bilayer component itself was also measured by following the [^{14}C]C₁₆-ceramide radiolabel. A comparison of the [^3H]CHE and [^{14}C]C₁₆-ceramide radiolabels associated with the ceramide containing liposomes revealed virtually identical plasma circulation profiles over the 24 hour period (Figure 5.2). This was an important observation because it confirmed that the bioactive C₁₆-ceramide lipid remained associated with the liposome bilayer in the plasma. This observation was supported by a ceramide plasma elimination half-life of 8.26 hr and a plasma ceramide clearance of 0.95 ml/hr, both of which were similar to those obtained for the ceramide-containing liposome as measured by [^3H]CHE behaviour (Table 5.1). A plasma AUC value of 8.62 mg*hr/ml was also obtained. This value cannot be directly compared with the AUC value obtained using the [^3H]CHE data because the lipid doses for each are necessarily different [0.82 mg C₁₆-ceramide lipid versus 2.0 mg total lipid (ceramide + non-ceramide) in the formulation].

5.4.2 Evaluation of Antitumor Activity of Ceramide Liposomes in the J774 Ascites Tumor Model

The efficacy of ceramide-based liposomes compared to controls was evaluated following single and multiple dosing schedules in the J774 ascites tumor model. The first efficacy study employed a multiple dosing regimen (day 1, 5 and 9; cell inoculation day 0) for control or ceramide liposomes administered by i.v. bolus at a dose of 200 mg/kg total lipid. Under these treatment conditions the saline and liposome control groups

displayed median survival times of 23 days, while the C₁₆-ceramide containing liposome treatment group had a median survival time of 27 days. This corresponded to an ILS of 17.4% (Figure 5.3). All control animals were terminated on day 23 in accordance with the animal welfare guidelines. Since there was no standard deviation associated with the treatment group survival times it was not possible to calculate the statistical significance of the results.

Given the importance of intracellular delivery of the ceramide component of the liposomes, subsequent studies were initiated to investigate whether direct i.p. administration of the formulation to the site of the ascites tumor cells might improve the therapeutic response beyond that observed following i.v. bolus administration. This was done on the basis that maximizing the liposome contact with the target J774 cells would improve the likelihood of liposome endocytosis. The first of these studies compared control liposomes at 200 mg/kg total lipid with ceramide-containing liposomes at 100 mg/kg and 200 mg/kg total lipid doses administered i.p. one day after cell inoculation. The survival curves presented in Figure 5.4 indicate that groups treated with saline or control liposomes at 200 mg/kg total lipid had a median survival time of 24 days. The group treated i.p. with ceramide-liposomes at a dose of 100 mg/kg total lipid showed a median survival time of 26 days, which corresponded to an 8.3% ILS. Again, all treatment group animals were terminated on day 26 so the statistical significance of the 100 mg/kg treatment regimen could not be determined. Animals in the 200 mg/kg dosing group showed a median survival time of 27.5 days, which corresponded to a 14.6% ILS. Animals in this group showed survival to days 23, 25 and 30 (2 mice). Although these

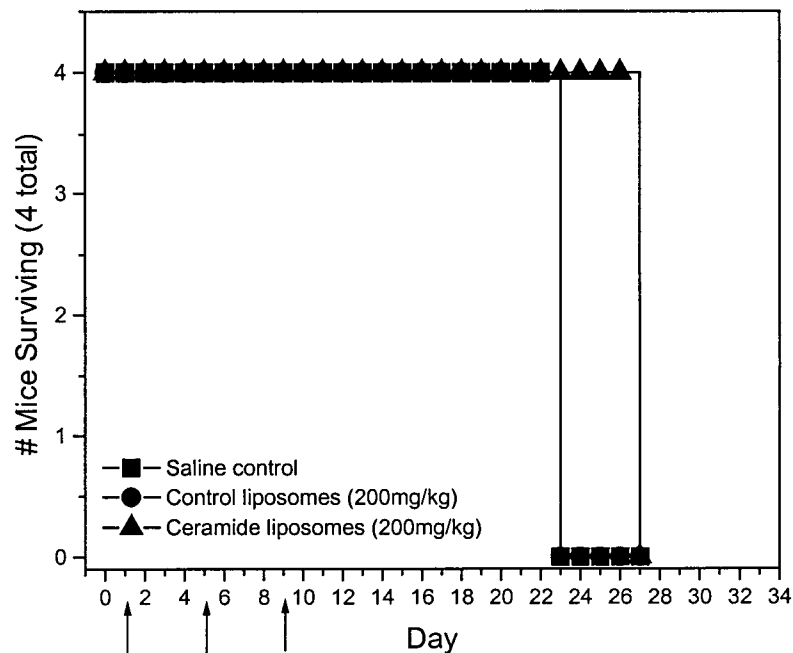


Figure 5.3 Evaluation of antitumor activity of C₁₆-cer/CHEMS/PEG₂₀₀₀-DSPE (47.5:47.5:5) versus DPPC/CHEMS/PEG₂₀₀₀-DSPE (47.5:47.5:5) liposomes in the J774 ascites tumor model. On day zero, 1×10^6 cells were inoculated i.p. into female Balb/c mice (4 mice/group) and saline, control liposomes or ceramide liposomes were administered by i.v. bolus on days 1, 5, and 9 at the lipid concentrations indicated. Arrows indicate the days of treatment administration. Animals were weighed and monitored daily for survival.

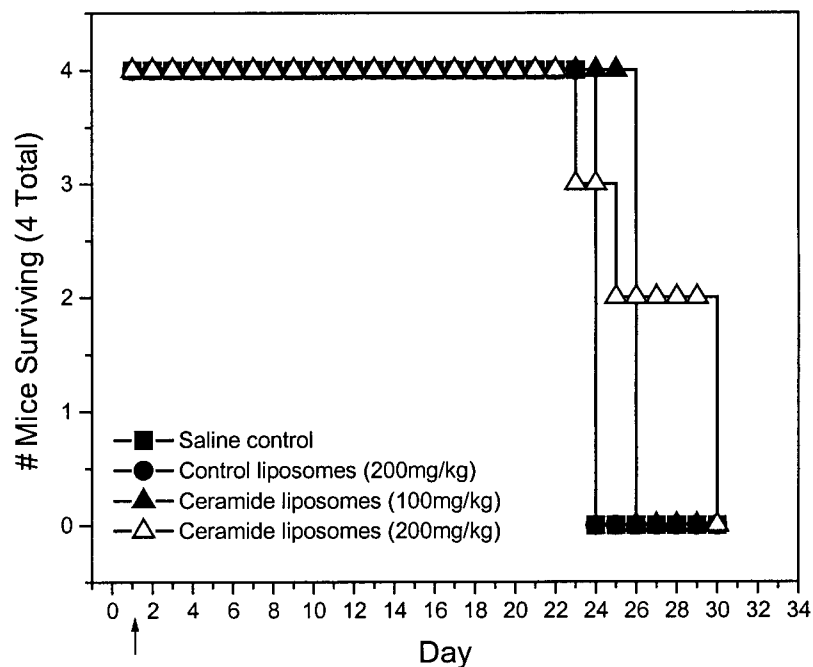


Figure 5.4 Evaluation of antitumor activity of C₁₆-cer/CHEMS/PEG₂₀₀₀-DSPE (47.5:47.5:5) versus DPPC/CHEMS/PEG₂₀₀₀-DSPE (47.5:47.5:5) liposomes in the J774 ascites tumor model. On day zero 1x10⁶ cells were innoculated i.p. into female Balb/c mice (4 mice/group) and saline, control liposomes or ceramide liposomes were administered i.p. on day 1 at the lipid concentrations indicated. The arrow indicates the day of treatment administration. Animals were weighed and monitored daily for survival.

results did not reach statistical significance ($p=0.190$), the %ILS values suggest a trend toward an increased response at the higher dose.

On the basis of these results a follow-up study using a multiple-dosing schedule with i.p. treatments at 200 mg/kg total lipid administered on days 1, 5 and 9 was then investigated. Using this regimen the saline and 200 mg/kg control liposome groups showed median survival times of 23 days, whereas the C₁₆-ceramide containing liposome group at a dose of 200 mg/kg total lipid showed a median survival time of 33 days (Figure 5.5). This corresponded to an ILS of 43.5%, which was determined to be statistically significant ($p=0.028$).

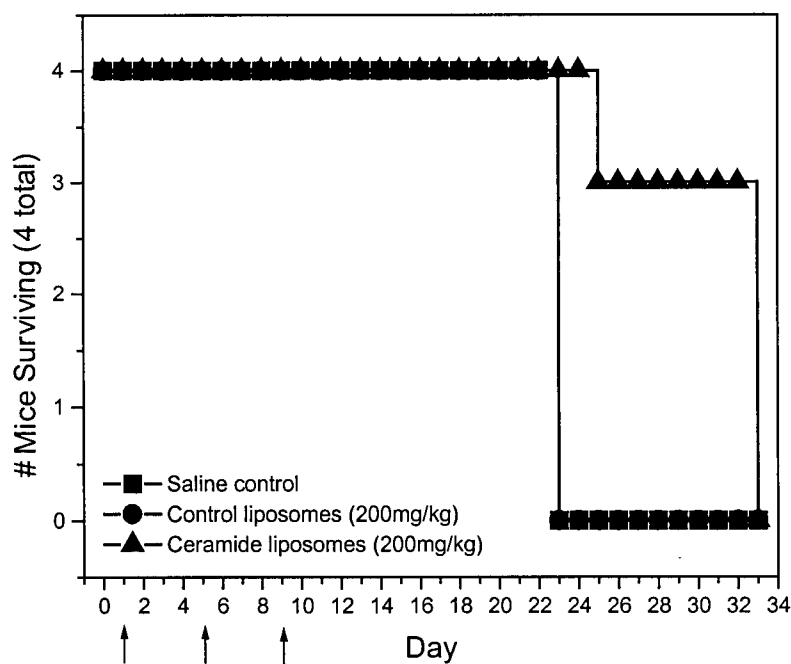


Figure 5.5 Evaluation of antitumor activity of C₁₆-cer/CHEMS/PEG₂₀₀₀-DSPE (47.5:47.5:5) versus DPPC/CHEMS/PEG₂₀₀₀-DSPE (47.5:47.5:5) liposomes in the J774 ascites tumor model. On day zero 1×10^6 cells were inoculated i.p. into female Balb/c mice (4 mice/group) and saline, control liposomes or ceramide liposomes were administered i.p. on days 1, 5, and 9 at the lipid concentrations indicated. Arrows indicate the days of treatment administration. Animals were weighed and monitored daily for survival.

5.5 DISCUSSION

The increasing attention being paid to the intracellular signaling and pro-apoptotic properties of ceramide lipids has made them an exciting new target for therapeutic manipulation. Dysregulation of ceramide production and/or metabolism has been implicated in a number of disease states including atherosclerosis, insulin resistance, diabetes, cancer and multidrug resistance to chemotherapy (61, 279-284). Consequently, the ability to successfully modulate intracellular ceramide levels in a controlled and precise manner holds great therapeutic promise. Most of the efforts directed toward this goal thus far have utilized short-chain ceramide lipids. Two recent pre-clinical studies demonstrated the utility of synthetic, cell-permeable ceramides as potential therapeutic agents with anti-proliferative effects. Charles *et al.* showed that C₆-ceramide coated balloon catheters prevent neointimal hyperplasia in rabbit carotid arteries (284), and Furuya *et al.* demonstrated that systemic administration of cell-permeable C₈-ceramide significantly reduced focal cerebral ischemia in spontaneously hypertensive rats (285). However, due to difficulties associated with effectively solubilizing and delivering the more physiologically relevant long-chain ceramides, approaches aimed at investigating the therapeutic effects of natural ceramide have primarily focused on indirect modulation of ceramide levels, either via enhanced ceramide production through increased metabolism of precursor sphingolipids (126, 127), or by using inhibitors of ceramide metabolism (132-134). Research presented in the preceding chapters demonstrated that these solubility obstacles could be overcome by formulating C₁₆-ceramide into liposome-based carrier systems. The encouraging cytotoxicity and cellular uptake data obtained following exposure of these liposomes to J774 cells *in vitro* led to the *in vivo* studies

presented in this chapter, which were aimed at translating the *in vitro* observations to an animal model.

Initial studies examined the pharmacokinetic parameters of control and ceramide-based liposomes following i.v. bolus administration to Balb/c mice. This was done in order to confirm the stability of the liposomes and lipid components in the circulation. Control liposomes were labeled with the bulk lipid marker [^3H]CHE, and the behavior of ceramide-containing liposomes was monitored using both [^3H]CHE and [^{14}C]C₁₆-ceramide radiolabels. This dual labeling approach allowed the behavior of the liposomes in general, and the ceramide lipid component in particular, to be simultaneously evaluated. Control and ceramide liposomes were administered at a total lipid dose of 100 mg/kg, which corresponded to a lipid dose of 2 mg total lipid per mouse for both formulations, and 0.816 mg C₁₆-ceramide lipid for the ceramide-based formulation. Data were modeled in WinNonlin Version 1.1 using a one-compartment i.v. bolus dosing model.

The pharmacokinetic parameters and liposome circulation longevity graph obtained from these studies revealed two key observations. First, although the ceramide-based liposomes showed more rapid plasma clearance than control liposomes ($\text{CL}_p=0.09$ ml/hr ceramide versus 0.061 ml/hr control), the ceramide-based formulation was still stable in the circulation over the 24 hour period investigated. Second, the plasma clearance parameters for [^3H]CHE and [^{14}C]C₁₆-ceramide were comparable (0.090 ml/hr and 0.095 ml/hr, respectively). This was an important observation because it indicated that the C₁₆-ceramide remained associated with the liposomal carrier, thereby confirming the ceramide retention properties predicted by the MLV-based assay in Chapter 4, and it

also confirmed that the liposomes were indeed acting as a carrier system for the ceramide lipid.

In light of these encouraging stability results, the next studies were aimed at evaluating the efficacy of these formulations with respect to antitumor activity. The J774 cells that were used for *in vitro* studies were established as an ascites tumor model following i.p. inoculation. Using a multi-dose treatment regimen, liposomes were administered by i.v. bolus on days 1, 5 and 9 post cell inoculation. Mice treated with ceramide-based liposomes survived to day 27 whereas mice treated with control liposomes survived only until day 23. Although encouraging, this corresponded to a modest 17.4% ILS.

It was then speculated that perhaps the liposomes would be more efficacious if their interaction with the target tumor cells was maximized by administering the liposomes directly into the tumor site (i.p.). Both single-dose (day 1) and multi-dose (days 1, 5, 9) treatment regimens were evaluated. In the single-dose study there was trend toward increased response related to increased dose (8.3% ILS at 100 mg/kg and 14.6% ILS at 200 mg/kg ceramide liposomes) compared to control liposomes. However, the effect of using the single dose i.p. approach was not superior to the multiple dose i.v. regimen. Therefore, a multiple dosing regimen was investigated for i.p. treatment administration. These results demonstrated statistically significant antitumor activity in mice treated with ceramide liposomes at 200 mg/kg compared to controls, and this corresponded to a 43.5% ILS ($p=0.028$).

The results presented in this chapter demonstrate that endogenous ceramides can be formulated into liposomes that display pharmacokinetic parameters suitable for *in vivo*

applications. Furthermore, this work demonstrates that ceramide delivered in appropriately designed liposomal carriers can inhibit tumor growth in animal models. These results are very promising and provide proof-of-principle data that delivery of exogenous natural ceramide can provide therapeutic antitumor activity *in vivo*.

CHAPTER 6

SUMMARY OF RESULTS AND FUTURE DIRECTIONS

The field of ceramide biology has received significant attention over the past decade as roles for this family of bioactive lipids in such diverse cellular responses as inflammation, proliferation, differentiation, senescence and apoptosis have emerged. Dysregulation of ceramide production and/or metabolism has been implicated in numerous disease states including diabetes, atherosclerosis, cancer and multidrug resistance to chemotherapy. Although the mechanisms by which ceramide mediates these effects are not fully understood, studies designed to understand the specific involvement of ceramides in these responses have begun to reveal many opportunities for exploiting these lipids in order to achieve specific therapeutic objectives.

The work presented in this thesis comprised a series of experiments designed to test the hypothesis that modulating intracellular ceramide levels can be used as a therapeutic approach to achieve chemosensitization of multidrug resistant tumors and induce apoptosis. Studies employing both indirect and direct approaches to ceramide modulation yielded results that supported this hypothesis.

Observations that cellular apoptosis is preceded by increases in intracellular ceramide, combined with evidence to suggest that multidrug resistance can arise due to overexpression of the ceramide metabolizing enzyme GCS, prompted studies to evaluate the effect of indirect ceramide modulation on the chemosensitivity of multidrug resistant tumor cells. The results presented in Chapter 2 demonstrated that PDMP-induced inhibition of pro-apoptotic ceramide metabolism to non-cytotoxic GlcCer resulted in significant chemosensitization of two MDR human breast cancer cell lines to Taxol[®] and

vincristine. Interestingly, chemosensitization to the non-tubulin binding drugs doxorubicin and cisplatin was not observed. Although this aspect of the results was not investigated further, it would be interesting to pursue the possible involvement of intracellular ceramide and ceramide metabolite transport via the vesicular trafficking pathway in the context of drug resistance and chemosensitization in light of these results. The successful chemosensitization results obtained with Taxol[®] and vincristine provided preliminary evidence that therapeutic approaches aimed at increasing endogenous ceramide levels should enhance apoptosis.

This conclusion, combined with research demonstrating that cell-permeable ceramides induce apoptosis when added to tumor cells *in vitro*, led to the experiments described in Chapter 3, which investigated the effect of direct ceramide modulation using exogenously applied synthetic ceramides. By comparing the cytotoxicity and cellular uptake of synthetic ceramides with varying acyl chain lengths it was determined that the short-chain, cell-permeable C₆-ceramide was internalized and cytotoxic to cells whereas the longer chain C₁₆-ceramide was not internalized and therefore did not induce apoptosis. This difference established the importance of achieving intracellular ceramide delivery as a pre-requisite to apoptosis induction.

The well established ability of liposomes to facilitate localized delivery of large amounts of carrier-associated agents to target cells prompted the subsequent formulation and development of a novel class of ceramide-based liposomes for this purpose. Although liposomes containing up to 45 mole percent C₆-ceramide were successfully formulated into DSPC/Chol-based liposomes, these systems did not retain the ceramide lipid in the liposome bilayer when added to the breast cancer cells in culture. Rather, the

amphipathic nature of C₆-ceramide allowed it to exchange from the liposome membrane into the cells where it exhibited cytotoxicity independent of the liposomal carrier, which was not internalized.

Although the limited stability of these liposomes with respect to ceramide retention excluded them from further development in the context of this thesis, the successful incorporation of such a large amount of biologically active ceramide lipid into the liposome bilayer is in itself significant enough to warrant further investigation from a formulation perspective. For example, it may be possible to improve the ceramide retention properties by employing novel strategies to complex the ceramide lipids to other liposome bilayer components or to metals present in the intra-liposomal buffer. Successful formulation of stable C₆-ceramide liposomes may provide yet another avenue from which ceramide delivery may be pursued.

Returning to the research focus of this thesis, given the apparent rapid exchange of C₆-ceramide from the bilayer, it was reasoned that this problem could potentially be avoided by focusing on the more hydrophobic C₁₆-ceramide form. This approach offered the additional advantage of employing a more physiologically relevant and naturally occurring ceramide. However, the unique physico-chemical properties of this longer-chain ceramide limited its stable incorporation into DSPC/Chol-based liposomes to a maximum of 15 mole percent. Consistent with the prediction of increased stability, however, the liposome formulation containing C₁₆-ceramide did not demonstrate appreciable ceramide exchange from the liposome bilayer upon addition to cells. However, because of limited internalization of liposomes by the breast cancer cells, the ceramide was not delivered intracellularly and minimal cytotoxicity was observed.

Although beyond the scope of this thesis, one potential solution to this problem may be to employ active liposome targeting techniques to facilitate liposome internalization. Liposome targeting using antibodies or ligands that bind to receptors known to be overexpressed and internalized by tumor cells could be investigated to promote endocytosis of ceramide-based liposomes.

The approaches used in this thesis to address the problem of reduced liposome internalization involved making changes to the non-ceramide liposome bilayer components and the target cell population. Relatively recent developments in the liposome field in the areas of triggered drug release, pH sensitive liposomes and fusogenic vesicles prompted an investigation of the cholesterol derivative CHEMS as an alternate non-ceramide lipid bilayer component. Cholesteryl hemisuccinate was demonstrated to dramatically increase the limit of stable C₁₆-ceramide incorporation from 15 to 50 mole percent, presumably by virtue of its lipid molecular shape. Cholesteryl hemisuccinate should also provide the added benefit of acid-induced liposome destabilization upon intracellular delivery to endosomes, where natural ceramide is known to be endogenously generated. Although the negatively charged CHEMS lipid appeared to increase liposome association with the breast cancer cell lines somewhat, this alone was not sufficient to achieve adequate intracellular delivery. However, when the macrophage-derived J774 cells were used as target cells the C₁₆-cer/CHEMS (50:50) liposomes were extensively endocytosed and the previously non-cytotoxic C₁₆-ceramide became active. These results collectively confirmed the importance of intracellular delivery and demonstrated that, once achieved, exogenously administered natural ceramide could be used to induce apoptosis.

Although these studies moved away from chemosensitization strategies aimed at improving cellular response to conventional chemotherapy drugs, these results were significant because they demonstrated the utility of exogenous ceramide delivery as a therapeutic agent itself. Furthermore, the successful formulation of liposomes containing such a large amount of natural ceramide in the bilayer has not been previously described and presents a novel strategy for controlled ceramide delivery.

The next step was to determine whether the encouraging *in vitro* activity could be translated into *in vivo* antitumor activity. It was apparent from the C₆-ceramide exchange results that C₁₆-ceramide must remain liposome-associated *in vivo* in order to be utilized for controlled ceramide delivery purposes. Although the *in vitro* studies suggested that the longer chain C₁₆-ceramide should remain associated with its liposomal carrier, it is often the case that liposome behaviour observed *in vitro* is not predictive of *in vivo* performance. Therefore, before moving the C₁₆-ceramide-based formulations forward to studies in animal models it was necessary to develop an *in vitro* release assay to accurately predict the *in vivo* ceramide retention properties of these novel liposomes.

Previous studies using various methods to evaluate the release of conventional drugs encapsulated within the liposome core have demonstrated that the drug retention parameters obtained using *in vitro* assays do not accurately reflect *in vivo* retention properties. This is likely attributed to the fact that current *in vitro* methods do not adequately simulate the extensive lipid environment comprising cellular membranes into which drugs can distribute following systemic administration. Presumably the same scenario would apply to the exchange of ceramide lipids from liposome bilayers *in vivo*. Therefore, the work presented in Chapter 4 described the development and validation of a

novel *in vitro* exchange assay that employed an excess of acceptor MLVs to mimic the physiological lipid membrane pool. This assay was used to evaluate the ceramide retention properties of ceramide-based liposomes and confirmed the observations of extensive C₆- and minimal C₁₆-ceramide lipid exchange obtained in Chapter 3. This supported the decision to further investigate the behavior of C₁₆-cer/CHEMS liposomes in an animal model.

Although liposomes containing encapsulated chemotherapy drugs were not utilized for testing the hypothesis set out at the beginning of this thesis, the potential application of the MLV-based assay described in Chapter 4 to the improved evaluation of such conventional liposomal formulations was also demonstrated using doxorubicin and verapamil as model systems. In addition, as a new generation of multifunctional liposomes that incorporate features such as targeting ligands, exchangeable PEG lipids and other novel bioactive lipids are developed, it will become increasingly important to accurately measure the retention of these components in the liposome bilayer. It is anticipated that the *in vitro* assay described in Chapter 4 will be of value to the liposome community as a whole since it appears to be applicable to a diverse range of liposomal systems.

On the basis of the encouraging *in vitro* results presented in Chapters 3 and 4, the objective of the research comprising Chapter 5 was to evaluate the pharmacokinetic behavior and antitumor activity of the C₁₆-cer/CHEMS formulation *in vivo*. Pharmacokinetic studies demonstrated *in vivo* stability over 24 hours of both the ceramide-based liposomes in general and the ceramide-lipid component in particular. The antitumor activity of these systems was then evaluating using the J774 ascites tumor

model. Optimal antitumor activity was observed following a multi-dosing (days 1, 5, 9) regimen with i.p. liposome administration at 200 mg/kg. This corresponded to a statistically significant increase in animal survival (43.5% ILS) over non-ceramide based control formulations.

In summary, this thesis demonstrates that modulation of intracellular ceramide can be used to chemosensitize resistant tumor cells and induce apoptosis *in vitro*, and provides proof-of-principle evidence that delivery of exogenous natural ceramide can provide therapeutic antitumor activity *in vivo*. Although this work is preliminary in nature, it provides evidence for the rational design of ceramide-based liposomes to enhance intracellular delivery of exogenous ceramide lipids, and demonstrates that this approach holds therapeutic promise as a novel strategy for cancer chemotherapy. It is anticipated that future developments, both in the field of ceramide-based therapeutics and targeted liposomal delivery systems, will facilitate the translation of these observations to even more effective systemic tumor treatments. As well, the application of ceramide-based systems may expand to include other therapeutic agents encapsulated within the aqueous core of ceramide-containing liposomes. Given the ability of ceramide lipids to directly induce apoptosis and sensitize tumor cells to chemotherapy, such formulations may have important therapeutic potential in combination chemotherapy approaches. Given the multifaceted nature of apoptosis and drug resistance, this approach may offer a significant treatment advantage over current individual therapies.

REFERENCES

1. Jemal A, Thomas A, Murray T, Thun M: Cancer statistics, 2002. *CA Cancer J Clin* 52: 23-47, 2002.
2. Broxterman H, G J, SC L, J L: The Impact of Transport-Associated Resistance in Anticancer Chemotherapy. In NH G (ed), *Drug Transport in Antimicrobial and Anticancer Chemotherapy*. New York, Marcel Dekker, 1995, 21-62.
3. Tan B, Piwnica-Worms D, Ratner L: Multidrug resistance transporters and modulation. *Curr Opin Oncol* 12: 450-8, 2000.
4. Gros P, Ben Neriah YB, Croop JM, Housman DE: Isolation and expression of a complementary DNA that confers multidrug resistance. *Nature* 323: 728-31, 1986.
5. Ueda K, Cardarelli C, Gottesman MM, Pastan I: Expression of a full-length cDNA for the human MDR1 gene confers resistance to colchicine, doxorubicin, and vinblastine. *Proc Natl Acad Sci USA* 84: 3004-8, 1987.
6. Ling V, Thompson LH: Reduced permeability in CHO cells as a mechanism of resistance to colchicine. *J Cell Physiol* 83: 103-16, 1974.
7. Juliano RL, Ling V: A surface glycoprotein modulating drug permeability in Chinese hamster ovary cell mutants. *Biochim Biophys Acta* 455: 152-62, 1976.
8. Chen CJ, Chin JE, Ueda K, Clark DP, Pastan I, Gottesman MM, Roninson IB: Internal duplication and homology with bacterial transport proteins in the *mdr1* (P-glycoprotein) gene from multidrug-resistant human cells. *Cell* 47: 381-9, 1986.
9. Higgins CF, Gottesman MM: Is the multidrug transporter a flippase? *Trends Biochem Sci* 17: 18-21, 1992.
10. Gottesman MM, Pastan I: Biochemistry of multidrug resistance mediated by the multidrug transporter. *Annu Rev Biochem* 62: 385-427, 1993.
11. Sikic BI: Modulation of multidrug resistance: a paradigm for translational clinical research. *Oncology (Huntingt)* 13: 183-7, 1999.
12. Horio M, Gottesman MM, Pastan I: ATP-dependent transport of vinblastine in vesicles from human multidrug-resistant cells. *Proc Natl Acad Sci USA* 85: 3580-4, 1988.
13. Robert J: Resistance to anticancer drugs: are we ready to use biologic information for the treatment of patients with cancer? *Ther Drug Monit* 20: 581-7, 1998.
14. Campos L, Guyotat D, Archimbaud E, Calmard-Oriol P, Tsuruo T, Troncy J, Treille D, Fiere D: Clinical significance of multidrug resistance P-glycoprotein expression on acute nonlymphoblastic leukemia cells at diagnosis. *Blood* 79: 473-6, 1992.
15. Chan HS, Thorner PS, Haddad G, Ling V: Immunohistochemical detection of P-glycoprotein: prognostic correlation in soft tissue sarcoma of childhood. *J Clin Oncol* 8: 689-704, 1990.
16. Chan HS, Haddad G, Thorner PS, DeBoer G, Lin YP, Ondrusek N, Yeager H, Ling V: P-glycoprotein expression as a predictor of the outcome of therapy for neuroblastoma. *N Engl J Med* 325: 1608-14, 1991.
17. Cole SP, Bhardwaj G, Gerlach JH, Mackie JE, Grant CE, Almquist KC, Stewart AJ, Kurz EU, Duncan AM, Deeley RG: Overexpression of a transporter gene in a multidrug-resistant human lung cancer cell line. *Science* 258: 1650-4, 1992.

18. Kast C, Gros P: Epitope insertion favors a six transmembrane domain model for the carboxy-terminal portion of the multidrug resistance-associated protein. *Biochemistry* 37: 2305-13, 1998.
19. Keppler D, Leier I, Jedlitschky G, Konig J: ATP-dependent transport of glutathione S-conjugates by the multidrug resistance protein MRP1 and its apical isoform MRP2. *Chem Biol Interact* 111-112: 153-61, 1998.
20. Stavrovskaya AA: Cellular mechanisms of multidrug resistance of tumor cells. *Biochemistry (Mosc)* 65: 95-106, 2000.
21. Zaman GJ, Versantvoort CH, Smit JJ, Eijdemans EW, de Haas M, Smith AJ, Broxterman HJ, Mulder NH, de Vries EG, Baas F, et al.: Analysis of the expression of MRP, the gene for a new putative transmembrane drug transporter, in human multidrug resistant lung cancer cell lines. *Cancer Res* 53: 1747-50, 1993.
22. Oshika Y, Nakamura M, Tokunaga T, Fukushima Y, Abe Y, Ozeki Y, Yamazaki H, Tamaoki N, Ueyama Y: Multidrug resistance-associated protein and mutant p53 protein expression in non-small cell lung cancer. *Mod Pathol* 11: 1059-63, 1998.
23. Broxterman HJ, Schuurhuis GJ: Transport proteins in drug resistance: detection and prognostic significance in acute myeloid leukemia. *J Intern Med Suppl* 740: 147-51, 1997.
24. Wright SR, Boag AH, Valdimarsson G, Hipfner DR, Campling BG, Cole SP, Deeley RG: Immunohistochemical detection of multidrug resistance protein in human lung cancer and normal lung. *Clin Cancer Res* 4: 2279-89, 1998.
25. Beck J, Niethammer D, Gekeler V: High *mdr1*- and *mrp*-, but low topoisomerase II α -gene expression in B-cell chronic lymphocytic leukaemias. *Cancer Lett* 86: 135-42, 1994.
26. Chu G: Cellular responses to cisplatin. The roles of DNA-binding proteins and DNA repair. *J Biol Chem* 269: 787-90, 1994.
27. Johnson SW, Perez RP, Godwin AK, Yeung AT, Handel LM, Ozols RF, Hamilton TC: Role of platinum-DNA adduct formation and removal in cisplatin resistance in human ovarian cancer cell lines. *Biochem Pharmacol* 47: 689-97, 1994.
28. Bodell WJ, Tokuda K, Ludlum DB: Differences in DNA alkylation products formed in sensitive and resistant human glioma cells treated with N-(2-chloroethyl)-N-nitrosourea. *Cancer Res* 48: 4489-92, 1988.
29. Pegg AE: Mammalian O6-alkylguanine-DNA alkyltransferase: regulation and importance in response to alkylating carcinogenic and therapeutic agents. *Cancer Res* 50: 6119-29, 1990.
30. Link Jr. CJ, Bohr VA: DNA repair in drug resistance: Studies on the repair process at the level of the gene. In Ozols RF (ed), *Molecular and Clinical Advances in Anticancer Drug Resistance*. Boston, Kluwer Academic Publishers, 1991.
31. Hao XY, Bergh J, Brodin O, Hellman U, Mannervik B: Acquired resistance to cisplatin and doxorubicin in a small cell lung cancer cell line is correlated to elevated expression of glutathione-linked detoxification enzymes. *Carcinogenesis* 15: 1167-73, 1994.

32. Tew KD: Glutathione-associated enzymes in anticancer drug resistance. *Cancer Res* 54: 4313-20, 1994.
33. Wang JC: Recent studies of DNA topoisomerases. *Biochim Biophys Acta* 909: 1-9, 1987.
34. Teicher BAE: *Drug Resistance in Oncology*. New York, Marcel Dekker, Inc., 1993.
35. Jain RK: Transport of molecules in the tumor interstitium: a review. *Cancer Res* 47: 3039-51, 1987.
36. Jain RK: Determinants of tumor blood flow: a review. *Cancer Res* 48: 2641-58, 1988.
37. Teicher BA: Hypoxia and drug resistance. *Cancer Metastasis Rev* 13: 139-68, 1994.
38. Tannock IF: Tumor physiology and drug resistance. *Cancer Metastasis Rev* 20: 123-32, 2001.
39. Smets LA: Programmed cell death (apoptosis) and response to anti-cancer drugs. *Anticancer Drugs* 5: 3-9, 1994.
40. Hannun YA: Apoptosis and the dilemma of cancer chemotherapy. *Blood* 89: 1845-53, 1997.
41. Reed JC: Regulation of apoptosis by bcl-2 family proteins and its role in cancer and chemoresistance. *Curr Opin Oncol* 7: 541-6, 1995.
42. Hickman JA: Apoptosis and chemotherapy resistance. *Eur J Cancer* 32A: 921-6, 1996.
43. Hermine O, Haioun C, Lepage E, d'Agay MF, Briere J, Lavignac C, Fillet G, Salles G, Marolleau JP, Diebold J, Reyas F, Gaulard P: Prognostic significance of bcl-2 protein expression in aggressive non-Hodgkin's lymphoma. *Groupe d'Etude des Lymphomes de l'Adulte (GELA)*. *Blood* 87: 265-72, 1996.
44. Minn AJ, Rudin CM, Boise LH, Thompson CB: Expression of bcl-xL can confer a multidrug resistance phenotype. *Blood* 86: 1903-10, 1995.
45. Ito K, Watanabe K, Nasim S, Sasano H, Sato S, Yajima A, Silverberg SG, Garrett CT: Prognostic significance of p53 overexpression in endometrial cancer. *Cancer Res* 54: 4667-70, 1994.
46. Wilson JW, Booth C, Potten CS: *Apoptosis Genes*. Boston, Kulwer Academic Publishers, 1998.
47. Ryan KM, Vousden KH: Regulation of cell growth and death by p53. In Gutkind JS (ed), *Signaling Networks and Cell Cycle Control*. New Jersey, Humana Press, 2000.
48. Kuerbitz SJ, Plunkett BS, Walsh WV, Kastan MB: Wild-type p53 is a cell cycle checkpoint determinant following irradiation. *Proc Natl Acad Sci USA* 89: 7491-5, 1992.
49. Lane DP: Cancer. p53, guardian of the genome. *Nature* 358: 15-6, 1992.
50. Dbaibo GS, Pushkareva MY, Rachid RA, Alter N, Smyth MJ, Obeid LM, Hannun YA: p53-dependent ceramide response to genotoxic stress. *J Clin Invest* 102: 329-39, 1998.
51. Crook NE, Clem RJ, Miller LK: An apoptosis-inhibiting baculovirus gene with a zinc finger-like motif. *J Virol* 67: 2168-74, 1993.

52. Deveraux QL, Reed JC: IAP family proteins--suppressors of apoptosis. *Genes Dev* 13: 239-52, 1999.
53. Deveraux QL, Takahashi R, Salvesen GS, Reed JC: X-linked IAP is a direct inhibitor of cell-death proteases. *Nature* 388: 300-4, 1997.
54. Roy N, Deveraux QL, Takahashi R, Salvesen GS, Reed JC: The c-IAP-1 and c-IAP-2 proteins are direct inhibitors of specific caspases. *Embo J* 16: 6914-25, 1997.
55. LaCasse EC, Baird S, Korneluk RG, MacKenzie AE: The inhibitors of apoptosis (IAPs) and their emerging role in cancer. *Oncogene* 17: 3247-59, 1998.
56. Tamm I, Kornblau SM, Segall H, Krajewski S, Welsh K, Kitada S, Scudiero DA, Tudor G, Qui YH, Monks A, Andreeff M, Reed JC: Expression and prognostic significance of IAP-family genes in human cancers and myeloid leukemias. *Clin Cancer Res* 6: 1796-803, 2000.
57. Hannun YA: Functions of ceramide in coordinating cellular responses to stress. *Science* 274: 1855-1859, 1996.
58. Senchenkov A, Litvak DA, Cabot MC: Targeting ceramide metabolism--a strategy for overcoming drug resistance. *J Natl Cancer Inst* 93: 347-57, 2001.
59. Haimovitz-Friedman A, Kan CC, Ehleiter D, Persaud RS, McLoughlin M, Fuks Z, Kolesnick RN: Ionizing radiation acts on cellular membranes to generate ceramide and initiate apoptosis. *J. Exp. Med.* 180: 525-35, 1994.
60. Levade T, Malagarie-Cazenave S, Gouaze V, Segui B, Tardy C, Betito S, Andrieu-Abadie N, Cuvillier O: Ceramide in apoptosis: a revisited role. *Neurochem Res* 27: 601-7, 2002.
61. Lavie Y, Cao H, Bursten SL, Giuliano AE, Cabot MC: Accumulation of glucosylceramides in multidrug-resistant cancer cells. *J. Biol. Chem.* 271: 19530-6, 1996.
62. Lucci A, Giuliano AE, Han TY, Dinur T, Liu YY, Senchenkov A, Cabot MC: Ceramide toxicity and metabolism differ in wild-type and multidrug-resistant cancer cells. *Int. J. Oncol.* 15: 535-40, 1999.
63. Liu YY, Han TY, Giuliano AE, Ichikawa S, Hirabayashi Y, Cabot MC: Glycosylation of ceramide potentiates cellular resistance to tumor necrosis factor- α -induced apoptosis. *Exp Cell Res* 252: 464-70, 1999.
64. Kok JW, Veldman RJ, Klappe K, Koning H, Filipescu CM, Muller M: Differential expression of sphingolipids in MRP1 overexpressing HT29 cells. *Int J Cancer* 87: 172-8, 2000.
65. Liu YY, Han TY, Giuliano AE, Cabot MC: Ceramide glycosylation potentiates cellular multidrug resistance. *Faseb J.* 15: 719-30, 2001.
66. Lucci A, Cho WI, Han TY, Giuliano AE, Morton DL, Cabot MC: Glucosylceramide: a marker for multiple-drug resistant cancers. *Anticancer Res.* 18: 475-80, 1998.
67. Liu YY, Han TY, Giuliano AE, Cabot MC: Expression of glucosylceramide synthase, converting ceramide to glucosylceramide, confers adriamycin resistance in human breast cancer cells. *J. Biol. Chem.* 274: 1140-6, 1999.
68. Tsuruo T, Iida H, Tsukagoshi S, Sakurai Y: Overcoming of vincristine resistance in P388 leukemia in vivo and in vitro through enhanced cytotoxicity of vincristine and vinblastine by verapamil. *Cancer Res* 41: 1967-72, 1981.

69. Ganapathi R, Grabowski D, Turinic R, Valenzuela R: Correlation between potency of calmodulin inhibitors and effects on cellular levels and cytotoxic activity of doxorubicin (adriamycin) in resistant P388 mouse leukemia cells. *Eur J Cancer Clin Oncol* 20: 799-806, 1984.
70. Ford JM, Hait WN: Pharmacology of drugs that alter multidrug resistance in cancer. *Pharmacol Rev* 42: 155-99, 1990.
71. Ford JM, Hait WN: Pharmacologic circumvention of multidrug resistance. *Cytotechnology* 12: 171-212, 1993.
72. Bartlett NL, Lum BL, Fisher GA, Brophy NA, Ehsan MN, Halsey J, Sikic BI: Phase I trial of doxorubicin with cyclosporine as a modulator of multidrug resistance. *J Clin Oncol* 12: 835-42, 1994.
73. Anderson P, Bondesson U, Sylven C, Astrom H: Plasma concentration--response relationship of verapamil in the treatment of angina pectoris. *J Cardiovasc Pharmacol* 4: 609-14, 1982.
74. Pirker R, Keilhauer G, Raschack M, Lechner C, Ludwig H: Reversal of multidrug resistance in human KB cell lines by structural analogs of verapamil. *Int J Cancer* 45: 916-9, 1990.
75. Krishna R, Mayer LD: Multidrug resistance (MDR) in cancer. Mechanisms, reversal using modulators of MDR and the role of MDR modulators in influencing the pharmacokinetics of anticancer drugs. *Eur J Pharm Sci* 11: 265-83, 2000.
76. Advani R, Saba HI, Tallman MS, Rowe JM, Wiernik PH, Ramek J, Dugan K, Lum B, Villena J, Davis E, Paietta E, Litchman M, Sikic BI, Greenberg PL: Treatment of refractory and relapsed acute myelogenous leukemia with combination chemotherapy plus the multidrug resistance modulator PSC 833 (Valspodar). *Blood* 93: 787-95, 1999.
77. Advani R, Fisher GA, Lum BL, Hausdorff J, Halsey J, Litchman M, Sikic BI: A phase I trial of doxorubicin, paclitaxel, and valspodar (PSC 833), a modulator of multidrug resistance. *Clin Cancer Res* 7: 1221-9, 2001.
78. Chauncey TR, Rankin C, Anderson JE, Chen I, Kopecky KJ, Godwin JE, Kalaycio ME, Moore DF, Shurafa MS, Petersdorf SH, Kraut EH, Leith CP, Head DR, Luthardt FW, Willman CL, Appelbaum FR: A phase I study of induction chemotherapy for older patients with newly diagnosed acute myeloid leukemia (AML) using mitoxantrone, etoposide, and the MDR modulator PSC 833: a southwest oncology group study 9617. *Leuk Res* 24: 567-74, 2000.
79. Visani G, Milligan D, Leoni F, Chang J, Kelsey S, Marcus R, Powles R, Schey S, Covelli A, Isidori A, Litchman M, Piccaluga PP, Mayer H, Malagola M, Pfister C: Combined action of PSC 833 (Valspodar), a novel MDR reversing agent, with mitoxantrone, etoposide and cytarabine in poor-prognosis acute myeloid leukemia. *Leukemia* 15: 764-71, 2001.
80. Lum BL, Gosland MP: MDR expression in normal tissues. Pharmacologic implications for the clinical use of P-glycoprotein inhibitors. *Hematol Oncol Clin North Am* 9: 319-36, 1995.
81. Krishna R, St-Louis M, Mayer LD: Increased intracellular drug accumulation and complete chemosensitization achieved in multidrug-resistant solid tumors by co-

- administering valspodar (PSC 833) with sterically stabilized liposomal doxorubicin. *Int J Cancer* 85: 131-41, 2000.
82. Nooter K, Oostrum R, Deurloo J: Effects of verapamil on the pharmacokinetics of daunomycin in the rat. *Cancer Chemother Pharmacol* 20: 176-8, 1987.
 83. Horton JK, Thimmaiah KN, Houghton JA, Horowitz ME, Houghton PJ: Modulation by verapamil of vincristine pharmacokinetics and toxicity in mice bearing human tumor xenografts. *Biochem Pharmacol* 38: 1727-36, 1989.
 84. Krishna R, Mayer LD: Liposomal doxorubicin circumvents PSC 833-free drug interactions, resulting in effective therapy of multidrug-resistant solid tumors. *Cancer Res* 57: 5246-53, 1997.
 85. Dantzig AH, Shepard RL, Cao J, Law KL, Ehlhardt WJ, Baughman TM, Bumol TF, Starling JJ: Reversal of P-glycoprotein-mediated multidrug resistance by a potent cyclopropyldibenzosuberane modulator, LY335979. *Cancer Res* 56: 4171-9, 1996.
 86. Mistry P, Stewart AJ, Dangerfield W, Okiji S, Liddle C, Bootle D, Plumb JA, Templeton D, Charlton P: In vitro and in vivo reversal of P-glycoprotein-mediated multidrug resistance by a novel potent modulator, XR9576. *Cancer Res* 61: 749-58, 2001.
 87. Thomas H, Steiner JA, Mould GP, Mellows G, Stewart A, Norris DB: A Phase IIA pharmacokinetic study of the P-glycoprotein inhibitor, XR9576 in combination with paclitaxel in patients with ovarian cancer. *American Society of Clinical Oncology*, Vol. Abstract #288. San Francisco, CA, 2001
 88. Newman MJ, Rodarte JC, Benbatoul KD, Romano SJ, Zhang C, Krane S, Moran EJ, Uyeda RT, Dixon R, Guns ES, Mayer LD: Discovery and characterization of OC144-093, a novel inhibitor of P- glycoprotein-mediated multidrug resistance. *Cancer Res* 60: 2964-72, 2000.
 89. Sparreboom A, Planting AS, Jewell RC, van der Burg ME, van der Gaast A, de Bruijn P, Loos WJ, Nooter K, Chandler LH, Paul EM, Wissel PS, Verweij J: Clinical pharmacokinetics of doxorubicin in combination with GF120918, a potent inhibitor of MDR1 P-glycoprotein. *Anticancer Drugs* 10: 719-28, 1999.
 90. Hyafil F, Vergely C, Du Vignaud P, Grand-Perret T: In vitro and in vivo reversal of multidrug resistance by GF120918, an acridonecarboxamide derivative. *Cancer Res* 53: 4595-602, 1993.
 91. Germann UA, Shlyakhter D, Mason VS, Zelle RE, Duffy JP, Galullo V, Armistead DM, Saunders JO, Boger J, Harding MW: Cellular and biochemical characterization of VX-710 as a chemosensitizer: reversal of P-glycoprotein-mediated multidrug resistance in vitro. *Anticancer Drugs* 8: 125-40, 1997.
 92. Rowinsky EK, Smith L, Wang YM, Chaturvedi P, Villalona M, Campbell E, Aylesworth C, Eckhardt SG, Hammond L, Kraynak M, Drengler R, Stephenson J, Jr., Harding MW, Von Hoff DD: Phase I and pharmacokinetic study of paclitaxel in combination with biricodar, a novel agent that reverses multidrug resistance conferred by overexpression of both MDR1 and MRP. *J Clin Oncol* 16: 2964-76, 1998.
 93. Peck RA, Hewett J, Harding MW, Wang YM, Chaturvedi PR, Bhatnagar A, Ziessman H, Atkins F, Hawkins MJ: Phase I and pharmacokinetic study of the

- novel MDR1 and MRP1 inhibitor biricodar administered alone and in combination with doxorubicin. *J Clin Oncol* 19: 3130-41, 2001.
94. Blatt NB, Glick GD: Signaling pathways and effector mechanisms pre-programmed cell death. *Bioorg Med Chem* 9: 1371-84, 2001.
 95. Desagher S, Martinou JC: Mitochondria as the central control point of apoptosis. *Trends Cell Biol* 10: 369-77, 2000.
 96. Earnshaw WC, Martins LM, Kaufmann SH: Mammalian caspases: structure, activation, substrates, and functions during apoptosis. *Annu Rev Biochem* 68: 383-424, 1999.
 97. Budihardjo I, Oliver H, Lutter M, Luo X, Wang X: Biochemical pathways of caspase activation during apoptosis. *Annu Rev Cell Dev Biol* 15: 269-90, 1999.
 98. Kinloch RA, Treherne JM, Furness LM, Hajimohamadreza I: The pharmacology of apoptosis. *Trends Pharmacol Sci* 20: 35-42, 1999.
 99. Herr I, Debatin KM: Cellular stress response and apoptosis in cancer therapy. *Blood* 98: 2603-14, 2001.
 100. Salvesen GS, Dixit VM: Caspase activation: the induced-proximity model. *Proc Natl Acad Sci USA* 96: 10964-7, 1999.
 101. Scaffidi C, Fulda S, Srinivasan A, Friesen C, Li F, Tomaselli KJ, Debatin KM, Krammer PH, Peter ME: Two CD95 (APO-1/Fas) signaling pathways. *Embo J* 17: 1675-87, 1998.
 102. Mow BM, Blajeski AL, Chandra J, Kaufmann SH: Apoptosis and the response to anticancer therapy. *Curr Opin Oncol* 13: 453-62, 2001.
 103. Crompton M: The mitochondrial permeability transition pore and its role in cell death. *Biochem J* 341: 233-49, 1999.
 104. Richter C, Ghafourifar P: Ceramide induces cytochrome c release from isolated mitochondria. *Biochem Soc Symp* 66: 27-31, 1999.
 105. Siskind LJ, Colombini M: The lipids C2- and C16-ceramide form large stable channels. Implications for apoptosis. *J Biol Chem* 275: 38640-4, 2000.
 106. Siskind LJ, Kolesnick RN, Colombini M: Ceramide channels increase the permeability of the mitochondrial outer membrane to small proteins. *J Biol Chem* 277: 26796-803, 2002.
 107. Zou H, Henzel WJ, Liu X, Lutschg A, Wang X: Apaf-1, a human protein homologous to *C. elegans* CED-4, participates in cytochrome c-dependent activation of caspase-3. *Cell* 90: 405-13, 1997.
 108. Li P, Nijhawan D, Budihardjo I, Srinivasula SM, Ahmad M, Alnemri ES, Wang X: Cytochrome c and dATP-dependent formation of Apaf-1/caspase-9 complex initiates an apoptotic protease cascade. *Cell* 91: 479-89, 1997.
 109. Susin SA, Zamzami N, Castedo M, Hirsch T, Marchetti P, Macho A, Daugas E, Geuskens M, Kroemer G: Bcl-2 inhibits the mitochondrial release of an apoptogenic protease. *J Exp Med* 184: 1331-41, 1996.
 110. Joza N, Susin SA, Daugas E, Stanford WL, Cho SK, Li CY, Sasaki T, Elia AJ, Cheng HY, Ravagnan L, Ferri KF, Zamzami N, Wakeham A, Hakem R, Yoshida H, Kong YY, Mak TW, Zuniga-Pflucker JC, Kroemer G, Penninger JM: Essential role of the mitochondrial apoptosis-inducing factor in programmed cell death. *Nature* 410: 549-54, 2001.

111. Wilson MR: Apoptotic signal transduction: emerging pathways. *Biochem Cell Biol* 76: 573-82, 1998.
112. Ekert PG, Silke J, Hawkins CJ, Verhagen AM, Vaux DL: DIABLO promotes apoptosis by removing MIHA/XIAP from processed caspase 9. *J Cell Biol* 152: 483-90, 2001.
113. Green DR: Apoptosis and Sphingomyelin Hydrolysis: The Flip Side. *Journal of cell biology* 150: F5-F7, 2000.
114. Liu X, Zou H, Slaughter C, Wang X: DFF, a heterodimeric protein that functions downstream of caspase-3 to trigger DNA fragmentation during apoptosis. *Cell* 89: 175-84, 1997.
115. Webb A, Cunningham D, Cotter F, Clarke PA, di Stefano F, Ross P, Corbo M, Dziewanowska Z: BCL-2 antisense therapy in patients with non-Hodgkin lymphoma. *Lancet* 349: 1137-41, 1997.
116. Ziegler A, Luedke GH, Fabbro D, Altmann KH, Stahel RA, Zangemeister-Wittke U: Induction of apoptosis in small-cell lung cancer cells by an antisense oligodeoxynucleotide targeting the Bcl-2 coding sequence. *J Natl Cancer Inst* 89: 1027-36, 1997.
117. Lopes D, Mayer LD: Pharmacokinetics of Bcl-2 antisense oligonucleotide (G3139) combined with doxorubicin in SCID mice bearing human breast cancer solid tumor xenografts. *Cancer Chemother Pharmacol* 49: 57-68, 2002.
118. Klasa RJ, Bally MB, Ng R, Goldie JH, Gascoyne RD, Wong FM: Eradication of human non-Hodgkin's lymphoma in SCID mice by BCL-2 antisense oligonucleotides combined with low-dose cyclophosphamide. *Clin Cancer Res* 6: 2492-500, 2000.
119. Jansen B, Wacheck V, Heere-Ress E, Schlagbauer-Wadl H, Hoeller C, Lucas T, Hoermann M, Hollenstein U, Wolff K, Pehamberger H: Chemosensitisation of malignant melanoma by BCL2 antisense therapy. *Lancet* 356: 1728-33, 2000.
120. Sasaki H, Sheng Y, Kotsuji F, Tsang BK: Down-regulation of X-linked inhibitor of apoptosis protein induces apoptosis in chemoresistant human ovarian cancer cells. *Cancer Res* 60: 5659-66, 2000.
121. Zhou M, Gu L, Li F, Zhu Y, Woods WG, Findley HW: DNA damage induces a novel p53-survivin signaling pathway regulating cell cycle and apoptosis in acute lymphoblastic leukemia cells. *J Pharmacol Exp Ther* 303: 124-31, 2002.
122. Kanwar JR, Shen WP, Kanwar RK, Berg RW, Krissansen GW: Effects of survivin antagonists on growth of established tumors and B7-1 immunogene therapy. *J Natl Cancer Inst* 93: 1541-52, 2001.
123. Merritt JA, Roth JA, Logothetis CJ: Clinical evaluation of adenoviral-mediated p53 gene transfer: review of INGN 201 studies. *Semin Oncol* 28: 105-14, 2001.
124. Roth JA, Grammer SF, Swisher SG, Komaki R, Nemunaitis J, Merritt J, Meyn RE: P53 gene replacement for cancer--interactions with DNA damaging agents. *Acta Oncol* 40: 739-44, 2001.
125. Myrick D, Blackinton D, Klostergaard J, Kouttab N, Maizel A, Wanebo H, Mehta S: Paclitaxel-induced apoptosis in Jurkat, a leukemic T cell line, is enhanced by ceramide. *Leuk Res* 23: 569-78, 1999.

126. Modrak DE, Lew W, Goldenberg DM, Blumenthal R: Sphingomyelin potentiates chemotherapy of human cancer xenografts. *Biochem Biophys Res Commun* 268: 603-6, 2000.
127. Modrak DE, Rodriguez MD, Goldenberg DM, Lew W, Blumenthal RD: Sphingomyelin enhances chemotherapy efficacy and increases apoptosis in human colonic tumor xenografts. *Int J Oncol* 20: 379-84, 2002.
128. Liu YY, Han TY, Giuliano AE, Hansen N, Cabot MC: Uncoupling ceramide glycosylation by transfection of glucosylceramide synthase antisense reverses adriamycin resistance. *J Biol Chem* 275: 7138-43, 2000.
129. Abe A, Radin NS, Shayman JA, Wotring LL, Zipkin RE, Sivakumar R, Ruggieri JM, Carson KG, Ganem B: Structural and stereochemical studies of potent inhibitors of glucosylceramide synthase and tumor cell growth. *J Lipid Res* 36: 611-21, 1995.
130. Radin NS, Shayman JA, Inokuchi J: Metabolic effects of inhibiting glucosylceramide synthesis with PDMP and other substances. *Adv. Lipid. Res.* 26: 183-213, 1993.
131. Radin NS: Rationales for cancer chemotherapy with PDMP, a specific inhibitor of glucosylceramide synthase. *Mol Chem Neuropathol* 21: 111-27, 1994.
132. Sietsma H, Veldman RJ, Kolk D, Ausema B, Nijhof W, Kamps W, Vellenga E, Kok JW: 1-phenyl-2-decanoylamino-3-morpholino-1-propanol chemosensitizes neuroblastoma cells for taxol and vincristine. *Clin. Cancer Res.* 6: 942-8, 2000.
133. Shabbits JA, Mayer LD: P-glycoprotein modulates ceramide-mediated sensitivity of human breast cancer cells to tubulin-binding anticancer drugs. *Molecular Cancer Therapeutics* 1: 205-213, 2002.
134. Nicholson KM, Quinn DM, Kellett GL, Warr JR: Preferential killing of multidrug-resistant KB cells by inhibitors of glucosylceramide synthase. *Br J Cancer* 81: 423-30, 1999.
135. Maurer BJ, Melton L, Billups C, Cabot MC, Reynolds CP: Synergistic cytotoxicity in solid tumor cell lines between N-(4- hydroxyphenyl)retinamide and modulators of ceramide metabolism. *J Natl Cancer Inst* 92: 1897-909, 2000.
136. Strelow A, Bernardo K, Adam-Klages S, Linke T, Sandhoff K, Kronke M, Adam D: Overexpression of acid ceramidase protects from tumor necrosis factor-induced cell death. *J Exp Med* 192: 601-12, 2000.
137. Selzner M, Bielawska A, Morse MA, Rudiger HA, Sindram D, Hannun YA, Clavien PA: Induction of apoptotic cell death and prevention of tumor growth by ceramide analogues in metastatic human colon cancer. *Cancer Res* 61: 1233-40, 2001.
138. Bielawska A, Perry DK, Hannun YA: Determination of ceramides and diglycerides by the diglyceride kinase assay. *Anal Biochem* 298: 141-50, 2001.
139. Mimeault M: New advances on structural and biological functions of ceramide in apoptotic/necrotic cell death and cancer. *FEBS Lett* 530: 9, 2002.
140. Yardley HJ, Summerly R: Lipid composition and metabolism in normal and diseased epidermis. *Pharmacol Ther* 13: 357-83, 1981.
141. Claus R, Russwurm S, Meisner M, Kinscherf R, Deigner HP: Modulation of the ceramide level, a novel therapeutic concept? *Curr Drug Targets* 1: 185-205, 2000.

142. Birbes H, Bawab SE, Obeid LM, Hannun YA: Mitochondria and ceramide: intertwined roles in regulation of apoptosis. *Adv Enzyme Regul* 42: 113-29, 2002.
143. Kolesnick RN: Sphingomyelin and derivatives as cellular signals. *Prog Lipid Res* 30: 1-38, 1991.
144. Liu P, Anderson RG: Compartmentalized production of ceramide at the cell surface. *J Biol Chem* 270: 27179-85, 1995.
145. Schissel SL, Schuchman EH, Williams KJ, Tabas I: Zn²⁺-stimulated sphingomyelinase is secreted by many cell types and is a product of the acid sphingomyelinase gene. *J Biol Chem* 271: 18431-6, 1996.
146. Okazaki T, Bielawska A, Domae N, Bell RM, Hannun YA: Characteristics and partial purification of a novel cytosolic, magnesium-independent, neutral sphingomyelinase activated in the early signal transduction of 1 α 2,5-dihydroxyvitamin D₃-induced HL-60 cell differentiation. *J Biol Chem* 269: 4070-7, 1994.
147. Kolesnick R, Hannun YA: Ceramide and apoptosis. *Trends Biochem Sci* 24: 224-5; discussion 227, 1999.
148. Duan RD, Nyberg L, Nilsson A: Alkaline sphingomyelinase activity in rat gastrointestinal tract: distribution and characteristics. *Biochim Biophys Acta* 1259: 49-55, 1995.
149. Koch J, Gartner S, Li CM, Quintern LE, Bernardo K, Levran O, Schnabel D, Desnick RJ, Schuchman EH, Sandhoff K: Molecular cloning and characterization of a full-length complementary DNA encoding human acid ceramidase. Identification Of the first molecular lesion causing Farber disease. *J Biol Chem* 271: 33110-5, 1996.
150. El Bawab S, Roddy P, Qian T, Bielawska A, Lemasters JJ, Hannun YA: Molecular cloning and characterization of a human mitochondrial ceramidase. *J Biol Chem* 275: 21508-13, 2000.
151. Mao C, Xu R, Szulc ZM, Bielawska A, Galadari SH, Obeid LM: Cloning and characterization of a novel human alkaline ceramidase. A mammalian enzyme that hydrolyzes phytoceramide. *J Biol Chem* 276: 26577-88, 2001.
152. Cuvillier O, Pirianov G, Kleuser B, Vanek PG, Coso OA, Gutkind S, Spiegel S: Suppression of ceramide-mediated programmed cell death by sphingosine-1-phosphate. *Nature* 381: 800-3, 1996.
153. Jarvis WD, Kolesnick RN, Fornari FA, Traylor RS, Gewirtz DA, Grant S: Induction of apoptotic DNA damage and cell death by activation of the sphingomyelin pathway. *Proc Natl Acad Sci USA* 91: 73-7, 1994.
154. Obeid LM, Linardic CM, Karolak LA, Hannun YA: Programmed cell death induced by ceramide. *Science* 259: 1769-71, 1993.
155. Tepper CG, Jayadev S, Liu B, Bielawska A, Wolff R, Yonehara S, Hannun YA, Seldin MF: Role for ceramide as an endogenous mediator of Fas-induced cytotoxicity. *Proc. Natl. Acad. Sci. USA* 92: 8443-7, 1995.
156. Haimovitz-Friedman A, Kolesnick RN, Fuks Z: Ceramide signaling in apoptosis. *Br Med Bull* 53:539-53, 1997.
157. Cifone MG, De Maria R, Roncaioli P, Rippon MR, Azuma M, Lanier LL, Santoni A, Testi R: Apoptotic signaling through CD95 (Fas/Apo-1) activates an acidic sphingomyelinase. *J. Exp. Med.* 180: 1547-52, 1994.

158. Herr I, Wilhelm D, Bohler T, Angel P, Debatin KM: Activation of CD95 (APO-1/Fas) signaling by ceramide mediates cancer therapy-induced apoptosis. *Embo J* 16: 6200-8, 1997.
159. Santana P, Pena LA, Haimovitz-Friedman A, Martin S, Green D, McLoughlin M, Cordon-Cardo C, Schuchman EH, Fuks Z, Kolesnick R: Acid sphingomyelinase-deficient human lymphoblasts and mice are defective in radiation-induced apoptosis. *Cell* 86: 189-99, 1996.
160. Kirschnek S, Paris F, Weller M, Grassme H, Ferlinz K, Riehle A, Fuks Z, Kolesnick R, Gulbins E: CD95-mediated apoptosis in vivo involves acid sphingomyelinase. *J Biol Chem* 275: 27316-23, 2000.
161. Thomas RL, Jr., Matsko CM, Lotze MT, Amoscato AA: Mass spectrometric identification of increased C16 ceramide levels during apoptosis. *J Biol Chem* 274: 30580-8, 1999.
162. Bose R, Verheij M, Haimovitz-Friedman A, Scotto K, Fuks Z, Kolesnick R: Ceramide synthase mediates daunorubicin-induced apoptosis: an alternative mechanism for generating death signals. *Cell* 82: 405-14, 1995.
163. Bielawska A, Linardic CM, Hannun YA: Ceramide-mediated biology. Determination of structural and stereospecific requirements through the use of N-acyl-phenylaminoalcohol analogs. *J Biol Chem* 267: 18493-7, 1992.
164. Ruvolo PP, Deng X, Ito T, Carr BK, May WS: Ceramide induces Bcl2 dephosphorylation via a mechanism involving mitochondrial PP2A. *J Biol Chem* 274: 20296-300, 1999.
165. Ruvolo PP: Ceramide regulates cellular homeostasis via diverse stress signaling pathways. *Leukemia* 15: 1153-60, 2001.
166. Gulbins E, Kolesnick R: Acid sphingomyelinase-derived ceramide signaling in apoptosis. *Subcell Biochem* 36: 229-44, 2002.
167. Heinrich M, Wickel M, Schneider-Brachert W, Sandberg C, Gahr J, Schwandner R, Weber T, Saftig P, Peters C, Brunner J, Kronke M, Schutze S: Cathepsin D targeted by acid sphingomyelinase-derived ceramide. *Embo J* 18: 5252-63, 1999.
168. Heinrich M, Wickel M, Winoto-Morbach S, Schneider-Brachert W, Weber T, Brunner J, Saftig P, Peters C, Kronke M, Schutze S: Ceramide as an activator lipid of cathepsin D. *Adv Exp Med Biol* 477: 305-15, 2000.
169. Petak I, Houghton JA: Shared pathways: death receptors and cytotoxic drugs in cancer therapy. *Pathol Oncol Res* 7: 95-106, 2001.
170. Smyth MJ, Perry DK, Zhang J, Poirier GG, Hannun YA, Obeid LM: p132: a downstream target for ceramide-induced apoptosis and for the inhibitory action of Bcl-2. *Biochem J* 316: 25-8, 1996.
171. Hearps AC, Burrows J, Connor CE, Woods GM, Lowenthal RM, Ragg SJ: Mitochondrial cytochrome c release precedes transmembrane depolarisation and caspase-3 activation during ceramide-induced apoptosis of Jurkat T cells. *Apoptosis* 7: 387-94, 2002.
172. Ardail D, Popa I, Alcantara K, Pons A, Zanetta JP, Louisot P, Thomas L, Portoukalian J: Occurrence of ceramides and neutral glycolipids with unusual long-chain base composition in purified rat liver mitochondria. *FEBS Lett* 488: 160-4, 2001.

173. Birbes H, El Bawab S, Hannun YA, Obeid LM: Selective hydrolysis of a mitochondrial pool of sphingomyelin induces apoptosis. *Faseb J* 15: 2669-79, 2001.
174. Zhang J, Alter N, Reed JC, Borner C, Obeid LM, Hannun YA: Bcl-2 interrupts the ceramide-mediated pathway of cell death. *Proc. Natl. Acad. Sci. USA* 93: 5325-8, 1996.
175. Brown DA, London E: Structure and origin of ordered lipid domains in biological membranes. *J Membr Biol* 164: 103-14, 1998.
176. Grassme H, Jekle A, Riehle A, Schwarz H, Berger J, Sandhoff K, Kolesnick R, Gulbins E: CD95 Signaling Via ceramide rich membrane rafts. *J Biol Chem* 276: 20589-20596, 2001.
177. Cremesti A, Paris F, Grassme H, Holler N, Tschopp J, Fuks Z, Gulbins E, Kolesnick R: Ceramide enables Fas to cap and kill. *J Biol Chem* 276: 23954-61, 2001.
178. ten Grotenhuis E, Demel RA, Ponc M, Boer DR, van Miltenburg JC, Bouwstra JA: Phase behavior of stratum corneum lipids in mixed Langmuir-Blodgett monolayers. *Biophys J* 71: 1389-99, 1996.
179. Veiga MP, Arrondo JL, Goni FM, Alonso A: Ceramides in phospholipid membranes: effects on bilayer stability and transition to nonlamellar phases. *Biophys J* 76: 342-50, 1999.
180. Holopainen JM, Subramanian M, Kinnunen PK: Sphingomyelinase induces lipid microdomain formation in a fluid phosphatidylcholine/sphingomyelin membrane. *Biochemistry* 37: 17562-70, 1998.
181. Grassme H, Schwarz H, Gulbins E: Molecular mechanisms of ceramide-mediated CD95 clustering. *Biochem Biophys Res Commun* 284: 1016-30, 2001.
182. Bangham AD, Standish MM, Watkins JC: Diffusion of univalent ions across the lamellae of swollen phospholipids. *J Mol Biol* 13: 238-52, 1965.
183. Sessa G, Weissmann G: Phospholipid spherules (liposomes) as a model for biological membranes. *J Lipid Res* 9: 310-8, 1968.
184. Chu CJ, Dijkstra J, Lai MZ, Hong K, Szoka FC: Efficiency of cytoplasmic delivery by pH-sensitive liposomes to cells in culture. *Pharm Res* 7: 824-34, 1990.
185. Connor J, Yatvin MB, Huang L: pH-sensitive liposomes: acid-induced liposome fusion. *Proc Natl Acad Sci USA* 81: 1715-8, 1984.
186. Anyarambhatla GR, Needham D: Enhancement of the phase transition permeability of DPPC liposomes by incorporation of MPPC: a new temperature-sensitive liposome for use with mild hyperthermia. *J Liposome Res.* 9: 491-506, 1999.
187. Rahman A, Treat J, Roh JK, Potkul LA, Alvord WG, Forst D, Woolley PV: A phase I clinical trial and pharmacokinetic evaluation of liposome- encapsulated doxorubicin. *J Clin Oncol* 8: 1093-100, 1990.
188. Cowens JW, Creaven PJ, Greco WR, Brenner DE, Tung Y, Ostro M, Pilkievicz F, Ginsberg R, Petrelli N: Initial clinical (phase I) trial of TLC D-99 (doxorubicin encapsulated in liposomes). *Cancer Res* 53: 2796-802, 1993.
189. Mayer LD, Tai LC, Ko DS, Masin D, Ginsberg RS, Cullis PR, Bally MB: Influence of vesicle size, lipid composition, and drug-to-lipid ratio on the

- biological activity of liposomal doxorubicin in mice. *Cancer Res* 49: 5922-30, 1989.
190. Mayer LD: Future developments in the selectivity of anticancer agents: drug delivery and molecular target strategies. *Cancer Metastasis Rev* 17: 211-8, 1998.
 191. Gill PS, Espina BM, Muggia F, Cabriaes S, Tulpule A, Esplin JA, Liebman HA, Forssen E, Ross ME, Levine AM: Phase I/II clinical and pharmacokinetic evaluation of liposomal daunorubicin. *J Clin Oncol* 13: 996-1003, 1995.
 192. Mayer LD, Masin D, Nayar R, Boman NL, Bally MB: Pharmacology of liposomal vincristine in mice bearing L1210 ascitic and B16/BL6 solid tumours. *Br J Cancer* 71: 482-8, 1995.
 193. Webb MS, Harasym TO, Masin D, Bally MB, Mayer LD: Sphingomyelin-cholesterol liposomes significantly enhance the pharmacokinetic and therapeutic properties of vincristine in murine and human tumour models. *Br J Cancer* 72: 896-904, 1995.
 194. Lopez-Berestein G: Liposomes as carriers of antimicrobial agents. *Antimicrob Agents Chemother* 31: 675-8, 1987.
 195. Moribe K, Maruyama K: Pharmaceutical design of the liposomal antimicrobial agents for infectious disease. *Curr Pharm Des* 8: 441-54, 2002.
 196. Schiffelers RM, Storm G, ten Kate MT, Stearne-Cullen LE, den Hollander JG, Verbrugh HA, Bakker-Woudenberg IA: In vivo synergistic interaction of liposome-coencapsulated gentamicin and ceftazidime. *J Pharmacol Exp Ther* 298: 369-75, 2001.
 197. Cao YJ, Shibata T, Rainov NG: Liposome-mediated transfer of the bcl-2 gene results in neuroprotection after in vivo transient focal cerebral ischemia in an animal model. *Gene Ther* 9: 415-9, 2002.
 198. Hu Q, Shew CR, Bally MB, Madden TD: Programmable fusogenic vesicles for intracellular delivery of antisense oligodeoxynucleotides: enhanced cellular uptake and biological effects. *Biochim Biophys Acta* 1514: 1-13, 2001.
 199. Pastorino F, Stuart D, Ponzoni M, Allen TM: Targeted delivery of antisense oligonucleotides in cancer. *J Control Release* 74: 69-75, 2001.
 200. Ponnappa BC, Dey I, Tu GC, Zhou F, Aini M, Cao QN, Israel Y: In vivo delivery of antisense oligonucleotides in pH-sensitive liposomes inhibits lipopolysaccharide-induced production of tumor necrosis factor-alpha in rats. *J Pharmacol Exp Ther* 297: 1129-36, 2001.
 201. Tardi P, Ickenstein L, Bally M, Mayer L: The Development of Liposomes for Enhanced Delivery of Chemotherapeutics to Tumors. In Page M (ed), *Cancer Drug Discovery and Development: Tumor Targeting in Cancer Therapy*. Totowa, NJ, Humana Press Inc., 2001
 202. O'Sullivan MM, Powell N, French AP, Williams KE, Morgan JR, Williams BD: Inflammatory joint disease: a comparison of liposome scanning, bone scanning, and radiography. *Ann Rheum Dis* 47: 485-91, 1988.
 203. Bakker-Woudenberg IA, Lokerse AF, ten Kate MT, Storm G: Enhanced localization of liposomes with prolonged blood circulation time in infected lung tissue. *Biochim Biophys Acta* 1138: 318-26, 1992.

204. Richardson VJ, Ryman BE, Jewkes RF, Jeyasingh K, Tattersall MN, Newlands ES, Kaye SB: Tissue distribution and tumour localization of 99m-technetium-labelled liposomes in cancer patients. *Br J Cancer* 40: 35-43, 1979.
205. Gabizon A, Papahadjopoulos D: Liposome formulations with prolonged circulation time in blood and enhanced uptake by tumors. *Proc Natl Acad Sci USA* 85: 6949-53, 1988.
206. Hobbs SK, Monsky WL, Yuan F, Roberts WG, Griffith L, Torchilin VP, Jain RK: Regulation of transport pathways in tumor vessels: role of tumor type and microenvironment. *Proc Natl Acad Sci USA* 95: 4607-12, 1998.
207. Rahman YE, Cerny EA, Patel KR, Lau EH, Wright BJ: Differential uptake of liposomes varying in size and lipid composition by parenchymal and kupffer cells of mouse liver. *Life Sci* 31: 2061-71, 1982.
208. Szoka F, Olson F, Heath T, Vail W, Mayhew E, Papahadjopoulos D: Preparation of unilamellar liposomes of intermediate size (0.1-0.2 μ mol) by a combination of reverse phase evaporation and extrusion through polycarbonate membranes. *Biochim Biophys Acta* 601: 559-71, 1980.
209. Mayer LD, Hope MJ, Cullis PR: Vesicles of variable sizes produced by a rapid extrusion procedure. *Biochim Biophys Acta* 858: 161-8, 1986.
210. Ostro MJ, Cullis PR: Use of liposomes as injectable-drug delivery systems. *Am J Hosp Pharm* 46: 1576-87, 1989.
211. Even-Chen S, Barenholz Y: DOTAP cationic liposomes prefer relaxed over supercoiled plasmids. *Biochim Biophys Acta* 1509: 176-88, 2000.
212. Crook K, Stevenson BJ, Dubouchet M, Porteous DJ: Inclusion of cholesterol in DOTAP transfection complexes increases the delivery of DNA to cells in vitro in the presence of serum. *Gene Ther* 5: 137-43, 1998.
213. Scherphof G, Morselt H, Regts J, Wilschut JC: The involvement of the lipid phase transition in the plasma-induced dissolution of multilamellar phosphatidylcholine vesicles. *Biochim Biophys Acta* 556: 196-207, 1979.
214. Kirby C, Clarke J, Gregoriadis G: Effect of the cholesterol content of small unilamellar liposomes on their stability in vivo and in vitro. *Biochem J* 186: 591-8, 1980.
215. Kirby C, Clarke J, Gregoriadis G: Cholesterol content of small unilamellar liposomes controls phospholipid loss to high density lipoproteins in the presence of serum. *FEBS Lett* 111: 324-8, 1980.
216. Moghimi SM, Patel HM: Tissue specific opsonins for phagocytic cells and their different affinity for cholesterol-rich liposomes. *FEBS Lett* 233: 143-7, 1988.
217. Hafez IM, Cullis PR: Cholesteryl hemisuccinate exhibits pH sensitive polymorphic phase behavior. *Biochim Biophys Acta* 1463: 107-14, 2000.
218. Hafez IM, Ansell S, Cullis PR: Tunable pH-sensitive liposomes composed of mixtures of cationic and anionic lipids. *Biophys J* 79: 1438-46, 2000.
219. Allen TM, Hansen C: Pharmacokinetics of stealth versus conventional liposomes: effect of dose. *Biochim Biophys Acta* 1068: 133-41, 1991.
220. Allen TM, Hansen C, Martin F, Redemann C, Yau-Young A: Liposomes containing synthetic lipid derivatives of poly(ethylene glycol) show prolonged circulation half-lives in vivo. *Biochim Biophys Acta* 1066: 29-36, 1991.

221. Allen TM, Austin GA, Chonn A, Lin L, Lee KC: Uptake of liposomes by cultured mouse bone marrow macrophages: influence of liposome composition and size. *Biochim Biophys Acta* 1061: 56-64, 1991.
222. Papahadjopoulos D, Allen TM, Gabizon A, Mayhew E, Matthay K, Huang SK, Lee KD, Woodle MC, Lasic DD, Redemann C, et al.: Sterically stabilized liposomes: improvements in pharmacokinetics and antitumor therapeutic efficacy. *Proc Natl Acad Sci USA* 88: 11460-4, 1991.
223. Woodle MC, Newman MS, Cohen JA: Sterically stabilized liposomes: physical and biological properties. *J Drug Target* 2: 397-403, 1994.
224. Vertut-Doi A, Ishiwata H, Miyajima K: Binding and uptake of liposomes containing a poly(ethylene glycol) derivative of cholesterol (stealth liposomes) by the macrophage cell line J774: influence of PEG content and its molecular weight. *Biochim Biophys Acta* 1278: 19-28, 1996.
225. Allen TM: Long-circulating (sterically stabilized) liposomes for targeted drug delivery. *Trends Pharmacol Sci* 15: 215-20, 1994.
226. Cullis P, Fenske D, Hope M: Physical properties and functional roles of lipids in membranes. In Vance DVaJ (ed), *Biochemistry of lipids, lipoproteins and membranes*, Elsevier Science BV, 1996, 1-33.
227. Carrer DC, Maggio B: Transduction to self-assembly of molecular geometry and local interactions in mixtures of ceramides and ganglioside GM1. *Biochim Biophys Acta* 1514: 87-99, 2001.
228. Madden TD, Janoff AS, Cullis PR: Incorporation of amphotericin B into large unilamellar vesicles composed of phosphatidylcholine and phosphatidylglycerol. *Chem Phys Lipids* 52: 189-98, 1990.
229. Mayer LD, Hope MJ, Cullis PR, Janoff AS: Solute distributions and trapping efficiencies observed in freeze- thawed multilamellar vesicles. *Biochim Biophys Acta* 817: 193-6, 1985.
230. Juliano RL, Stamp D, McCullough N: Pharmacokinetics of liposome-encapsulated antitumor drugs and implications for therapy. *Ann N Y Acad Sci* 308: 411-25, 1978.
231. Madden TD, Harrigan PR, Tai LC, Bally MB, Mayer LD, Redelmeier TE, Loughrey HC, Tilcock CP, Reinish LW, Cullis PR: The accumulation of drugs within large unilamellar vesicles exhibiting a proton gradient: a survey. *Chem Phys Lipids* 53: 37-46, 1990.
232. Boman NL, Mayer LD, Cullis PR: Optimization of the retention properties of vincristine in liposomal systems. *Biochim Biophys Acta* 1152:253-8, 1993.
233. Dedhar S, Hannigan GE, Rak J, Kerbel RS: The extracellular environment in cancer. In Tannock IF, Hill RP (eds), *The Basic Science of Oncology*, 3rd Edition. New York, McGraw-Hill, 1998, 198-218.
234. Gabizon AA: Selective tumor localization and improved therapeutic index of anthracyclines encapsulated in long-circulating liposomes. *Cancer Res* 52: 891-6, 1992.
235. Huang SK, Mayhew E, Gilani S, Lasic DD, Martin FJ, Papahadjopoulos D: Pharmacokinetics and therapeutics of sterically stabilized liposomes in mice bearing C-26 colon carcinoma. *Cancer Res* 52: 6774-81, 1992.

236. Hu YP, Henry-Toulme N, Robert J: Failure of liposomal encapsulation of doxorubicin to circumvent multidrug resistance in an in vitro model of rat glioblastoma cells. *Eur J Cancer* 31A: 389-94, 1995.
237. Kong G, Anyarambhatla G, Petros WP, Braun RD, Colvin OM, Needham D, Dewhirst MW: Efficacy of liposomes and hyperthermia in a human tumor xenograft model: importance of triggered drug release. *Cancer Res* 60: 6950-7, 2000.
238. Needham D, Anyarambhatla G, Kong G, Dewhirst MW: A new temperature-sensitive liposome for use with mild hyperthermia: characterization and testing in a human tumor xenograft model. *Cancer Res* 60: 1197-201, 2000.
239. Chiu GN, Bally MB, Mayer LD: Selective protein interactions with phosphatidylserine containing liposomes alter the steric stabilization properties of poly(ethylene glycol). *Biochim Biophys Acta* 1510: 56-69, 2001.
240. Chiu GN, Bally MB, Mayer LD: Effects of phosphatidylserine on membrane incorporation and surface protection properties of exchangeable poly(ethylene glycol)-conjugated lipids. *Biochim Biophys Acta* 1560: 37-50, 2002.
241. van Helvoort A, Smith AJ, Sprong H, Fritzsche I, Schinkel AH, Borst P, van Meer G: MDR1 P-glycoprotein is a lipid translocase of broad specificity, while MDR3 P-glycoprotein specifically translocates phosphatidylcholine. *Cell* 87: 507-17, 1996.
242. van Helvoort A, Giudici ML, Thielemans M, van Meer G: Transport of sphingomyelin to the cell surface is inhibited by brefeldin A and in mitosis, where C6-NBD-sphingomyelin is translocated across the plasma membrane by a multidrug transporter activity. *J. Cell Sci.* 110: 75-83, 1997.
243. Smyth MJ, Krasovskis E, Sutton VR, Johnstone RW: The drug efflux protein, P-glycoprotein, additionally protects drug-resistant tumor cells from multiple forms of caspase-dependent apoptosis. *Proc. Natl. Acad. Sci. USA* 95: 7024-9, 1998.
244. Li R, Blanchette-Mackie EJ, Ladisch S: Induction of endocytic vesicles by exogenous C(6)-ceramide. *J. Biol. Chem.* 274: 21121-7, 1999.
245. Lucci A, Han TY, Liu YY, Giuliano AE, Cabot MC: Multidrug resistance modulators and doxorubicin synergize to elevate ceramide levels and elicit apoptosis in drug-resistant cancer cells. *Cancer* 86: 300-11, 1999.
246. Charles AG, Han TY, Liu YY, Hansen N, Giuliano AE, Cabot MC: Taxol-induced ceramide generation and apoptosis in human breast cancer cells. *Cancer Chemother. Pharmacol.* 47: 444-50, 2001.
247. Lavie Y, Cao H, Volner A, Lucci A, Han TY, Geffen V, Giuliano AE, Cabot MC: Agents that reverse multidrug resistance, tamoxifen, verapamil, and cyclosporin A, block glycosphingolipid metabolism by inhibiting ceramide glycosylation in human cancer cells. *J. Biol. Chem.* 272: 1682-7, 1997.
248. Jeckel D, Karrenbauer A, Burger KN, van Meer G, Wieland F: Glucosylceramide is synthesized at the cytosolic surface of various Golgi subfractions. *J. Cell. Biol.* 117: 259-67, 1992.
249. Trinchera M, Fabbri M, Ghidoni R: Topography of glycosyltransferases involved in the initial glycosylations of gangliosides. *J. Biol. Chem.* 266: 20907-12, 1991.

250. Molinari A, Calcabrini A, Meschini S, Stringaro A, Del Bufalo D, Cianfriglia M, Arancia G: Detection of P-glycoprotein in the Golgi apparatus of drug-untreated human melanoma cells. *Int. J. Cancer* 75: 885-93, 1998.
251. Molinari A, Cianfriglia M, Meschini S, Calcabrini A, Arancia G: P-glycoprotein expression in the Golgi apparatus of multidrug-resistant cells. *Int. J. Cancer* 59: 789-95, 1994.
252. Bour-Dill C, Gramain MP, Merlin JL, Marchal S, Guillemin F: Determination of intracellular organelles implicated in daunorubicin cytoplasmic sequestration in multidrug-resistant MCF-7 cells using fluorescence microscopy image analysis. *Cytometry* 39: 16-25, 2000.
253. Shapiro AB, Fox K, Lee P, Yang YD, Ling V: Functional intracellular P-glycoprotein. *Int J Cancer* 76: 857-64, 1998.
254. Labroille G, Belloc F, Bilhou-Nabera C, Bonnefille S, Bascans E, Boisseau MR, Bernard P, Lacombe F: Cytometric study of intracellular P-gp expression and reversal of drug resistance. *Cytometry* 32: 86-94, 1998.
255. Lannert H, Bunning C, Jeckel D, Wieland FT: Lactosylceramide is synthesized in the lumen of the Golgi apparatus. *FEBS Lett.* 342: 91-6, 1994.
256. Lannert H, Gorgas K, Meissner I, Wieland FT, Jeckel D: Functional organization of the Golgi apparatus in glycosphingolipid biosynthesis. Lactosylceramide and subsequent glycosphingolipids are formed in the lumen of the late Golgi. *J. Biol. Chem.* 273: 2939-46, 1998.
257. van Echten G, Sandhoff K: Ganglioside metabolism. *Enzymology, Topology, and regulation.* *J. Biol. Chem.* 268: 5341-4, 1993.
258. Derksen JT, Morselt HW, Scherphof GL: Processing of different liposome markers after in vitro uptake of immunoglobulin-coated liposomes by rat liver macrophages. *Biochim Biophys Acta* 931: 33-40, 1987.
259. Almgren M, Edwards K, Karlsson G: Cryo transmission electron microscopy of liposomes and related structures. *Colloids and Surfaces* 174: 3-21, 2000.
260. Szoka F, Papahadjopoulos D: Liposomes: preparation and characterization. In Knight CG (ed), *Liposomes, from physical structure to therapeutic applications.* New York, Elsevier/North-Holland Biomedical Press, 1981, 52-82.
261. Cullis PR, Hope MJ, Bally MB, Madden TD, Mayer LD, Janoff AS: Liposomes as Pharmaceuticals. In Ostro MJ (ed), *Liposomes: From Biophysics to Therapeutics.* New York, Marcel Dekker, Inc., 1987, 39-72.
262. Paris F, Grassme H, Cremesti A, Zager J, Fong Y, Haimovitz-Friedman A, Fuks Z, Gulbins E, Kolesnick R: Natural ceramide reverses Fas resistance of acid sphingomyelinase(-/-) hepatocytes. *J Biol Chem* 276: 8297-305, 2001.
263. Allan D, Shawyer A, Taylor A: Mechanisms by which short-chain ceramides cause apoptosis. *Biochem Soc Trans* 27: 428-32, 1999.
264. Radin NS: Killing cancer cells by poly-drug elevation of ceramide levels: a hypothesis whose time has come? *Eur J Biochem* 268: 193-204, 2001.
265. Kim JH, Han JS, Yoon YD: Biochemical and morphological identification of ceramide-induced cell cycle arrest and apoptosis in cultured granulosa cells. *Tissue Cell* 31: 531-9, 1999.
266. Spinedi A, Bartolomeo SD, Piacentini M: Apoptosis induced by N-hexanoylsphingosine in CHP-100 cells associates with accumulation of

- endogenous ceramide and is potentiated by inhibition of glucocerebroside synthesis. *Cell Death Differ* 5: 785-91, 1998.
267. Ogretmen B, Pettus BJ, Rossi MJ, Wood R, Usta J, Szulc Z, Bielawska A, Obeid LM, Hannun YA: Biochemical mechanisms of the generation of endogenous long chain ceramide in response to exogenous short chain ceramide in the A549 human lung adenocarcinoma cell line. Role for endogenous ceramide in mediating the action of exogenous ceramide. *J Biol Chem* 277: 12960-9, 2002.
 268. Payne SG, Brindley DN, Guilbert LJ: Epidermal growth factor inhibits ceramide-induced apoptosis and lowers ceramide levels in primary placental trophoblasts. *J Cell Physiol* 180: 263-70, 1999.
 269. O'Byrne D, Sansom D: Lack of costimulation by both sphingomyelinase and C2 ceramide in resting human T cells. *Immunology* 100: 225-30, 2000.
 270. Bielawska A, Crane HM, Liotta D, Obeid LM, Hannun YA: Selectivity of ceramide-mediated biology. Lack of activity of erythro-dihydroceramide. *J Biol Chem* 268: 26226-32, 1993.
 271. Holopainen JM, Lehtonen JY, Kinnunen PK: Lipid microdomains in dimyristoylphosphatidylcholine-ceramide liposomes. *Chem Phys Lipids* 88: 1-13, 1997.
 272. Shabbits JA, Chiu GN, Mayer LD: Development of an in vitro drug release assay that accurately predicts in vivo drug retention for liposome-based delivery systems. *J Control Release* 84: 161-70, 2002.
 273. Ouyang C, Choice E, Holland J, Meloche M, Madden TD: Liposomal cyclosporine. Characterization of drug incorporation and interbilayer exchange. *Transplantation* 60: 999-1006, 1995.
 274. Choice E, Masin D, Bally MB, Meloche M, Madden TD: Liposomal cyclosporine. Comparison of drug and lipid carrier pharmacokinetics and biodistribution. *Transplantation* 60: 1006-11, 1995.
 275. Peschka R, Dennehy C, Szoka FC, Jr.: A simple in vitro model to study the release kinetics of liposome encapsulated material. *J Control Release* 56: 41-51, 1998.
 276. Allen TM, Cleland LG: Serum-induced leakage of liposome contents. *Biochim Biophys Acta* 597: 418-26, 1980.
 277. De Cuyper M, Valtonen S: Investigation of the spontaneous transferability of a phospholipid-poly(ethylene glycol)-biotin derivative from small unilamellar phospholipid vesicles to magnetoliposomes. *Journal of magnetism and magnetic materials* 225: 89-94, 2001.
 278. Simon CG, Jr., Holloway PW, Gear AR: Exchange of C(16)-ceramide between phospholipid vesicles. *Biochemistry* 38: 14676-82, 1999.
 279. Kinnunen PK, Holopainen JM: Sphingomyelinase activity of LDL: a link between atherosclerosis, ceramide, and apoptosis? *Trends Cardiovasc Med* 12: 37-42, 2002.
 280. Feuerstein GZ: Apoptosis in cardiac diseases--new opportunities for novel therapeutics for heart diseases. *Cardiovasc Drugs Ther* 13: 289-94, 1999.
 281. Feuerstein GZ, Young PR: Apoptosis in cardiac diseases: stress- and mitogen-activated signaling pathways. *Cardiovasc Res* 45: 560-9, 2000.

282. Levade T, Auge N, Veldman RJ, Cuvillier O, Negre-Salvayre A, Salvayre R: Sphingolipid mediators in cardiovascular cell biology and pathology. *Circ Res* 89: 957-68, 2001.
283. Listenberger LL, Schaffer JE: Mechanisms of lipoapoptosis: implications for human heart disease. *Trends Cardiovasc Med* 12: 134-8, 2002.
284. Charles R, Sandirasegarane L, Yun J, Bourbon N, Wilson R, Rothstein RP, Levison SW, Kester M: Ceramide-coated balloon catheters limit neointimal hyperplasia after stretch injury in carotid arteries. *Circ Res* 87: 282-8, 2000.
285. Furuya K, Ginis I, Takeda H, Chen Y, Hallenbeck JM: Cell permeable exogenous ceramide reduces infarct size in spontaneously hypertensive rats supporting in vitro studies that have implicated ceramide in induction of tolerance to ischemia. *Journal of Cerebral Blood Flow and Metabolism* 21: 226-232, 2001.